



Durham E-Theses

The extent and an analysis of shallow failures on the slopes of highway earthworks

Perry, John

How to cite:

Perry, John (1991) *The extent and an analysis of shallow failures on the slopes of highway earthworks*, Durham theses, Durham University. Available at Durham E-Theses Online:
<http://etheses.dur.ac.uk/6062/>

Use policy

The full-text may be used and/or reproduced, and given to third parties in any format or medium, without prior permission or charge, for personal research or study, educational, or not-for-profit purposes provided that:

- a full bibliographic reference is made to the original source
- a [link](#) is made to the metadata record in Durham E-Theses
- the full-text is not changed in any way

The full-text must not be sold in any format or medium without the formal permission of the copyright holders.

Please consult the [full Durham E-Theses policy](#) for further details.

The extent and an analysis of shallow failures
on the slopes of highway earthworks

by

Mr. John Perry

being

a Thesis submitted to the University of Durham
in partial fulfilment of the requirements for
the degree of Doctor of Philosophy.

School of Engineering and Applied
Science
March 1991



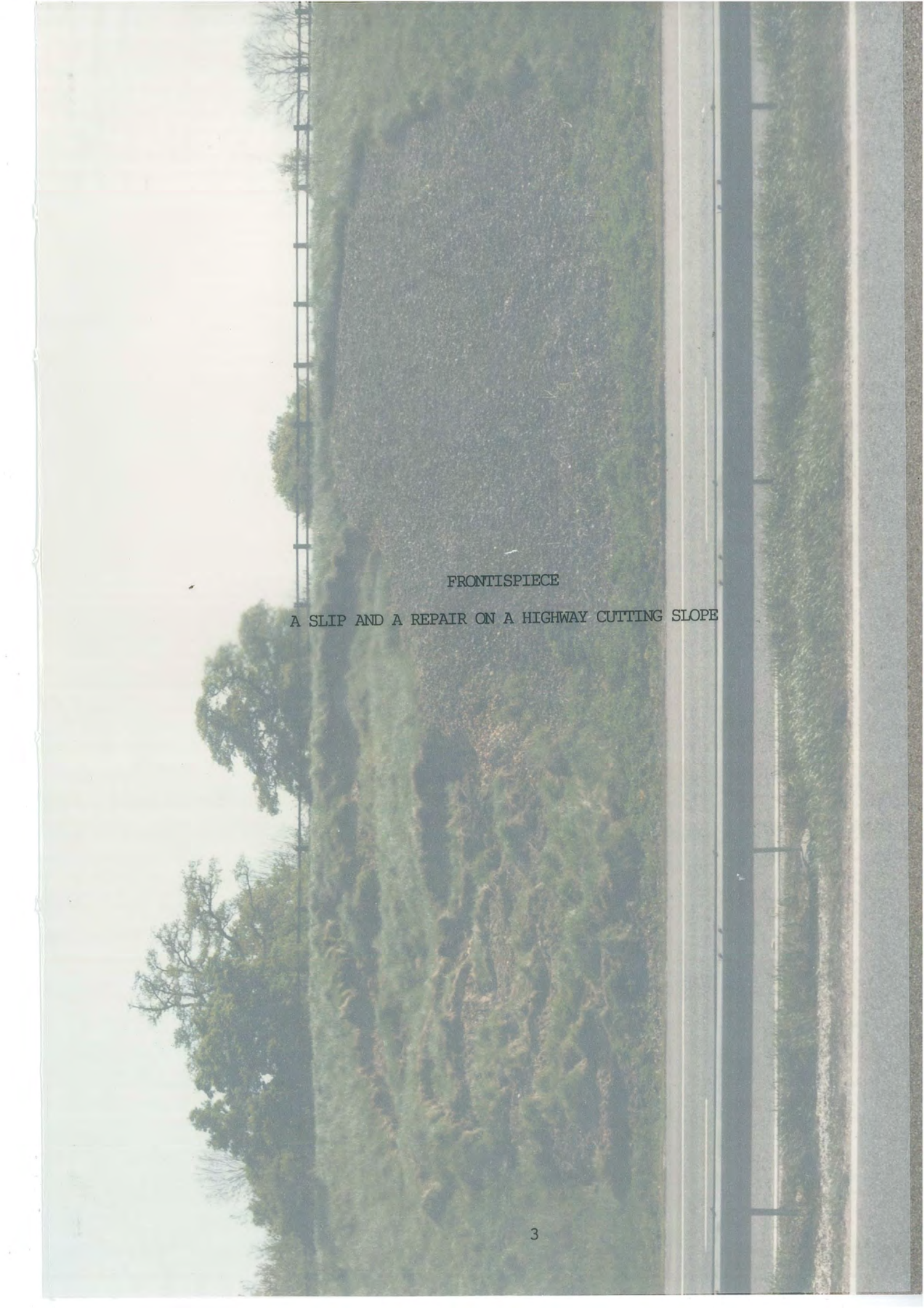
14 MAY 1992

'In every case they made the ground to
suit the plan and not the plan to
suit the ground'

Sir Marc Isambard Brunel

(1769 - 1849)





FRONTISPIECE

A SLIP AND A REPAIR ON A HIGHWAY CUTTING SLOPE

Mr J. Perry

The extent and an analysis of shallow failures
on the slopes of highway earthworks/PhD/1991

ABSTRACT

The reported incidences of shallow failures on the slopes of highway earthworks has increased in recent years. This Thesis includes a study of the extent of this problem, the likely factors contributing to failure, and presents the results of empirical design and the analysis of the likely mechanism of failure.

A survey was conducted, covering a total length of 570km of selected lengths of motorway in England and Wales, which included the principal geologies encountered on the British motorway system, in particular, areas where over-consolidated clays predominate. From the survey, the basic factors that have contributed to shallow failures on the side slopes of embankments and cuttings can be deduced, and attempts are made to quantify any long-term problems. The results show a high incidence of failure associated with the major influences of geology, age of earthworks and geometry of slope, with many more failures occurring on embankments than on cuttings. The slope angles recommended are empirically derived and can be used both in the design of new earthwork side slopes and to identify slopes at risk of failure in existing earthworks. An estimate is made of the extent of failures in the future which suggests that three times as many slopes are likely to fail than have failed so far.

To study the mechanisms of failure and the behaviour of over-consolidated clays at extremely low effective stresses, an analytical method is developed which includes a detailed study of non-linear failure envelopes and the fitting of the most representative curve to peak strength data. Also a new rigorous slope stability analysis method is developed which incorporates this type of failure envelope. Back-analyses are conducted for several embankment slopes from which samples have been tested in the laboratory. Results indicate that the critical state strength rather than the peak strength governs the formation of shallow failures.

ACKNOWLEDGEMENTS

The work presented in this Thesis forms part of the research programme of the Department of Transport and has been carried out in association with the University of Durham. The author expresses his gratitude to his supervisors, the late Dr R K Taylor and Dr D Toll, University of Durham and Dr M P O'Reilly, Head of Ground Engineering Division, Transport and Road Research Laboratory.

The assistance of Mr A W Parsons and Dr R D Andrews with the survey work is also acknowledged. The help given by Mr G Crabb with the computer programming is appreciated. The author is grateful for the many forms of assistance provided by the Department of Transport.

The author would like to thank the Consulting Engineers and County Highway Authorities concerned with the maintenance and original construction of the lengths of motorway studied for their co-operation. The soil testing was carried out under contract to TRRL by City University and their contribution is fully acknowledged.

TABLE OF CONTENTS

	Page
Abstract.....	4
Acknowledgements.....	5
Table of Contents.....	6
List of Tables.....	10
List of Figures.....	14
List of Plates.....	19
List of Appendices.....	19
Chapter 1. Introduction and literature review.....	20
1.1 Introduction.....	20
1.2 Literature review of British sources.....	24
1.3 Literature review of foreign sources.....	30
Chapter 2. A survey of slope instability.....	37
2.1 Extent of survey.....	37
2.2 Preparatory work.....	40
2.3 The survey.....	40
2.4 Processing the data.....	45
2.5 Factors studied in the analysis of slopes.....	46
Chapter 3. Drift deposits.....	56
3.1 Geology.....	56
3.2 Age of earthworks.....	59
3.3 Geometry of slope.....	59
3.4 Type of drainage.....	61
3.5 Orientation of slope.....	62
3.6 Design of side slopes in new construction.....	63
Chapter 4. Solid deposits.....	75
4.1 Geology.....	75
4.1.1 Eocene and Cretaceous deposits.....	75
4.1.2 Jurassic and Triassic deposits.....	76
4.1.3 Carboniferous and Old Red Sandstone deposits.....	77
4.2 Age of earthworks.....	79
4.2.1 Eocene and Cretaceous deposits.....	79
4.2.2 Jurassic and Triassic deposits.....	79
4.2.3 Carboniferous and Old Red Sandstone deposits.....	80

4.3	Geometry of slope.....	80
4.3.1	Eocene and Cretaceous deposits.....	80
4.3.2	Jurassic and Triassic deposits.....	82
4.3.3	Carboniferous and Old Red Sandstone deposits.....	83
4.4	Type of drainage.....	84
4.4.1	Eocene and Cretaceous deposits.....	84
4.4.2	Jurassic and Triassic deposits.....	86
4.4.3	Carboniferous and Old Red Sandstone deposits.....	88
4.5	Orientation of slope.....	89
4.6	Design of side slopes in new construction.....	89
4.6.1	Eocene and Cretaceous deposits.....	89
4.6.2	Jurassic and Triassic deposits.....	91
4.6.3	Carboniferous and Old Red Sandstone deposits.....	92
Chapter 5.	General results for all the motorways surveyed.....	116
5.1	Description of slope failures.....	116
5.2	Variation of design parameters.....	119
Chapter 6.	Testing of soils for detailed investigation...	125
6.1	Location of sampling sites.....	125
6.2	Types of test conducted.....	126
6.3	Results of tests.....	129
Chapter 7.	Linear failure envelopes at low effective stresses.....	163
7.1	Introduction.....	163
7.2	The Mohr circle diagram and Mohr-Coulomb failure criteria.....	163
7.3	Techniques for fitting the Mohr-Coulomb failure envelope to experimental data.....	167
7.4	Results from test data using techniques for fitting linear failures envelopes.....	181
Chapter 8.	Non-linear shear strength envelopes at low effective stresses.....	190
8.1	Types of non-linear shear strength envelope...	190

8.2	Techniques for fitting a power curve to Mohr circles.....	192
8.2.1	Free-hand method for fitting a power curve to Mohr circles (Method 1)....	193
8.2.2	Top point construction (Method 2)...	193
8.2.3	Method requiring an approximation of the failure stresses using a tangent through the origin (Method 3).....	194
8.2.4	Method using a power curve or straight line between two Mohr circles to determine the failure stresses (Method 4).....	195
8.2.5	Using Mohr circles in logarithmic space (Method 5).....	198
8.2.6	Method for determining the 'best fit' of a power curve to a series of Mohr circles (Method 6-least sum of squares method).....	199
8.3	Results and accuracies of methods developed...	203
Chapter 9	A slope stability method of analysis for soils with a non-linear strength envelope.....	221
9.1	Introduction.....	221
9.2	A suitable existing method for conversion....	221
9.3	The Janbu generalised procedure of slices....	226
9.4	A limit equilibrium slope analysis method for soils exhibiting a non-linear shear strength..	226
9.5	A computer program using a rigorous solution and non-linear failure envelope.....	228
9.6	Effect of varying the position of the line of thrust.....	231
9.7	Effect of soil parameters on the factor of safety.....	232
9.8	Applications of the computer program.....	234
9.9	The method of Charles and Soares.....	234
9.10	Methods used for rock fill and closely jointed rock.....	236
Chapter 10	Back-analyses of shallow failures.....	245
10.1	General.....	245
10.2	Characteristics of slopes and soil properties.	245

10.3	Pore water pressures.....	247
10.4	Results of back-analyses.....	248
Chapter 11	Discussion.....	258
Chapter 12	Conclusion.....	274
	References.....	279
	Appendices.....	289

The copyright of this Thesis rests with the author. No quotation from it should be published without his prior written consent and information derived from it should be acknowledged.

LIST OF TABLES

Table	Title	Page
3/1	Drift deposits encountered in the survey, with a total length of slope in excess of 1.0km - embankments.....	65
3/2	Drift deposits encountered in the survey, with a total length of slope in excess of 1.0km - cuttings.....	66
3/3	The percentages of failure of Boulder Clay in different parts of England and Wales with a slope angle of 1:2 and a height greater than 5.0m.....	67
3/4	Comparisons of the percentages of failure in embankments of different ages for given combinations of Drift deposits and geometry.....	68
3/5	Comparisons of the percentages of failure in cuttings of different ages for given combinations of Drift deposits and geometry.....	69
3/6	Maximum slope angles allowable to restrict the percentages of failure to below 1 per cent within 25 years of construction as indicated by the results of the survey - embankments of Drift deposits.....	70
3/7	Maximum slope angles allowable to restrict the percentages of failure to below 1 per cent within 25 years of construction as indicated by the results of the survey - cuttings in Drift deposits.....	71
3/8	Types of drainage and maximum slope angles allowable to restrict the percentages of failure to below 1 per cent within 25 years of construction as indicated by the results of the survey - Drift deposits.....	72
4/1	Eocene and Cretaceous deposits encountered in the survey, with a total length of slope in excess of 1.0km - embankments.....	93
4/2	Eocene and Cretaceous deposits encountered in the survey, with a total length of slope in excess of 1.0km - cuttings.....	94
4/3	Jurassic and Triassic deposits encountered in the survey, with a total length of slope in excess of 1.0km - embankments.....	95
4/4	Jurassic and Triassic deposits encountered in the	

	survey, with a total length of slope in excess of 1.0km - cuttings.....	96
4/5	Carboniferous and Old Red Sandstone deposits encountered in the survey, with a total length of slope in excess of 1.0km - embankments.....	97
4/6	Carboniferous and Old Red Sandstone deposits encountered in the survey, with a total length of slope in excess of 1.0km - cuttings.....	98
4/7	Comparisons of the percentages of failure in embankments and cuttings of different ages for given Eocene and Cretaceous deposits and geometry....	99
4/8	Comparisons of the percentages of failure in embankments and cuttings of different ages for given Jurassic and Triassic deposits and geometry....	100
4/9	Comparisons of the percentages of failure in embankments and cuttings of different ages for given Carboniferous and Old Red Sandstone deposits and geometry.....	101
4/10	The effect of slope drains on the percentages of failure in cuttings of Reading Beds (cohesive) at a slope angle of 1:3 (10 years old).....	102
4/11	Effect of slope orientation on the percentages of failure of Reading Beds (cohesive) embankment and cutting slopes (10 years old).....	102
4/12	Maximum slope angles allowable to restrict the percentages of failure to below 1 per cent within 22 years of construction as indicated by the results of the survey - embankments of Eocene and Cretaceous deposits.....	103
4/13	Maximum slope angles allowable to restrict the percentages of failure to below 1 per cent within 22 years of construction as indicated by the results of the survey - cuttings in Eocene and Cretaceous deposits.....	104
4/14	Types of drainage and maximum slope angles allowable to restrict the percentages of failure to below 1 per cent within 22 years of construction as indicated by the results of the survey - Eocene and Cretaceous deposits.....	105

4/15	Maximum slope angles allowable to restrict the percentages of failure to below 1 per cent within 25 years of construction as indicated by the results of the survey - embankments of Jurassic and Triassic deposits.....	106
4/16	Maximum slope angles allowable to restrict the percentages of failure to below 1 per cent within 25 years of construction as indicated by the results of the survey - cuttings in Jurassic and Triassic deposits.....	107
4/17	Types of drainage and maximum slope angles allowable to restrict the percentages of failure to below 1 per cent within 25 years of construction as indicated by the results of the survey - Jurassic and Triassic deposits.....	108
4/18	Maximum slope angles allowable to restrict the percentages of failure to below 1 per cent within 23 years of construction as indicated by the results of the survey - embankments of Carboniferous and Old Red Sandstone deposits.....	109
4/19	Maximum slope angles allowable to restrict the percentages of failure to below 1 per cent within 23 years of construction as indicated by the results of the survey - cuttings in Carboniferous and Old Red Sandstone deposits.....	110
5/1	Percentage of slips with different depths of failure.....	123
5/2	Distribution of drainage at the bottom of embankments and the top of cuttings.....	123
6/1	Sampling locations.....	131
6/2	Effective stresses at the peak strength for undisturbed samples.....	132
6/3	Effective stresses at 'ultimate' condition of undisturbed samples.....	132
6/4	Effective stresses at the critical state strength using reconstituted samples.....	133
7/1	Linear strength parameters at the peak strength for undisturbed samples.....	184
7/2	Critical state strength parameters.....	184

7/3	'Ultimate' strength parameters.....	185
8/1	Power curve parameters, A and b, for curved failure envelopes at the peak strength of undisturbed samples, using methods developed.....	206
8/2	Non-linear strength parameters at peak strength of undisturbed samples.....	207
8/3	Non-linear strength parameters at test's ultimate condition for undisturbed samples.....	207
9/1	An example of the computations involved in the determination of a factor of safety using the rigorous method of slices with a non-linear failure envelope.....	237
9/2	Effect of the position of the line of thrust on the factor of safety.....	238
10/1	Slope characteristics and soil bulk density.....	253
10/2	Factors of safety from back-analysis using a non-linear failure envelope and peak strength for undisturbed samples (phreatic surface at surface of slope).....	253
10/3	Factors of safety from back-analysis using a non-linear failure envelope and 'ultimate' strength for undisturbed samples (phreatic surface at surface of slope).....	254
10/4	Factors of safety from back-analysis using a conventional linear failure envelope and critical state strength from reconstituted samples (phreatic surface at surface of slope).....	254
10/5	Factors of safety from back-analysis using a conventional linear failure envelope and critical state strength from reconstituted samples (zero pore water pressures).....	254
10/6	Proportion of slope surface requiring a phreatic surface to achieve a factor of safety of unity.....	254
11/1	Geologies with a high percentage of failure.....	271
11/2	Comparison of depth of failure surface in embankments of different ages and geometries.....	272
11/3	Comparison of critical state strength friction angles and friction angles from triaxial tests at high stress levels on undisturbed samples.....	273

LIST OF FIGURES

Figure	Title	Page
2/1	A completed survey form.....	51
2/2	A typical feature.....	52
3/1	Relations between the percentage of failure of embankment slopes and geometry of slope - Drift deposits.....	73
3/2	Relations between the percentage of failure of cutting slopes and geometry of slope - Drift deposits.....	74
4/1	Relations between the percentage of failure of embankment slopes and geometry of slope - Eocene and Cretaceous deposits.....	111
4/2	Relations between the percentage of failure of cutting slopes and geometry of slope - Eocene and Cretaceous deposits.....	112
4/3	Relations between the percentage of failure of embankment slopes and geometry of slope - Jurassic and Triassic deposits.....	112
4/4	Relations between the percentage of failure of cutting slopes and geometry of slope - Jurassic and Triassic deposits.....	113
4/5	Relations between the percentage of failure of cutting slopes and geometry of slope - Carboniferous and Old Red sandstone deposits.....	114
4/6	The variation of slope angle with time for first-time slides in London Clay cuttings (Tavenas and Leroueil, 1981).....	115
5/1	Failure and repair of soil in rock cavities.....	124
5/2	The distribution of height and slope angle for embankments and cuttings encountered in the survey..	124
6/1	Plot of Mohr circles at low effective stresses - Dunton Gault.....	134
6/2	Plot of Mohr circles at low effective stresses - Nepicar Gault.....	135
6/3	Plot of Mohr circles at low effective stresses - Kimmeridge Clay.....	136
6/4	Plot of Mohr circles at low effective stresses - London Clay.....	137

6/5	Plot of Mohr circles at low effective stresses - Oxford Clay.....	138
6/6	Plot of Mohr circles at low effective stresses - Reading Beds clay.....	139
6/7	Plot of Mohr circles at low effective stresses - Weald Clay.....	140
6/8	Plot of effective deviator stress, q' , against mean normal effective stress, p' , showing stress paths to the peak strength and 'ultimate' strength - Gault Clay.....	141
6/9	Plot of effective deviator stress, q' , against mean normal effective stress, p' , showing stress paths to the peak strength and 'ultimate' strength - London Clay and Reading Beds clay.....	142
6/10	Plot of effective deviator stress, q' , against mean normal effective stress, p' , showing stress paths to the peak strength and 'ultimate' strength - Weald Clay and Kimmeridge Clay.....	143
6/11	Plot of effective deviator stress, q' , against mean normal effective stress, p' , showing stress paths to the peak strength and 'ultimate' strength - Oxford Clay.....	144
6/12	Plot of normal effective stress, p' , against volumetric strain, ϵ_v , for increasing pore water pressure tests on undisturbed samples - Gault Clay - Nepicar.....	145
6/13	Plot of normal effective stress, p' , against volumetric strain, ϵ_v , for increasing pore water pressure tests on undisturbed samples - Gault Clay - Dunton Green.....	146
6/14	Plot of effective deviator stress, q' , against strain, ϵ , for drained tests on undisturbed samples - Gault Clay.....	147
6/15	Plot of normal effective stress, p' , against volumetric strain, ϵ_v , for increasing pore water pressure tests on undisturbed samples - London Clay.....	148
6/16	Plot of normal effective stress, p' , against volumetric strain, ϵ_v , for increasing pore water pressure tests on undisturbed samples - Reading Beds clay.....	149

6/17	Plot of effective deviator stress, q' , against strain, ϵ , for drained tests on undisturbed samples - London Clay and Reading Beds clay.....	150
6/18	Plot of normal effective stress, p' , against volumetric strain, ϵ_v , for increasing pore water pressure tests on undisturbed samples - Weald Clay.....	151
6/19	Plot of normal effective stress, p' , against volumetric strain, ϵ_v , for increasing pore water pressure tests on undisturbed samples - Kimmeridge Clay.....	152
6/20	Plot of effective deviator stress, q' , against strain, ϵ , for drained tests on undisturbed samples - Weald Clay and Kimmeridge Clay.....	153
6/21	Plot of normal effective stress, p' , against volumetric strain, ϵ_v , for increasing pore water pressure tests on undisturbed samples - Oxford Clay.....	154
6/22	Plot of effective deviator stress, q' , against strain, ϵ , for drained tests on undisturbed samples - Oxford Clay.....	155
6/23	Plot of effective deviator stress, q' , against mean normal effective stress, p' , at the critical state condition for reconstituted samples.....	156
6/24	Plot of effective deviator stress, q' , against strain, ϵ , for undrained tests on reconstituted samples - Gault Clay - Nepicar.....	157
6/25	Plot of effective deviator stress, q' , against strain, ϵ , for undrained tests on reconstituted samples - London Clay.....	158
6/26	Plot of effective deviator stress, q' , against strain, ϵ , for undrained tests on reconstituted samples - Reading Beds clay.....	159
6/27	Plot of effective deviator stress, q' , against strain, ϵ , for undrained tests on reconstituted samples - Weald Clay.....	160
6/28	Plot of effective deviator stress, q' , against strain, ϵ , for undrained tests on reconstituted samples - Kimmeridge Clay.....	161
6/29	Plot of effective deviator stress, q' , against strain, ϵ , for undrained tests on reconstituted samples - Oxford Clay.....	162

7/1	Stress conditions in a soil during compression.....	186
7/2	The Mohr circle diagram.....	186
7/3	The modified Mohr - Coulomb relation.....	187
7/4	Top point of a Mohr circle.....	187
7/5	The relation between the least square fit line through the maximum shear stresses and the failure envelope.....	188
7/6	Minimizing the distances between Mohr circles and the failure envelope using the method of Lisle and Strom.....	188
7/7	Using Bland's method to minimize the perpendicular distance between Mohr circles and the failure envelope.....	189
7/8	Minimizing the error for a top point construction...	189
8/1	Nature of power functions.....	208
8/2	Curve fitting using Method 1.....	209
8/3	Determination of failure stresses using Method 3....	210
8/4	Curve fitting using Method 4 assuming a power curve between Mohr circles.....	211
8/5	Curve fitting using Method 4 assuming a straight line between Mohr circles.....	211
8/6	Taking the logarithms of Mohr circles in order to determine the failure envelope.....	212
8/7	Least square of the error of a curved failure envelope.....	213
8/8	Best fit power curve to peak strengths - Dunton Gault.....	214
8/9	Best fit power curve to peak strengths - Nepicar Gault.....	215
8/10	Best fit power curve to peak strengths - Kimmeridge Clay.....	216
8/11	Best fit power curve to peak strengths - London Clay.....	217
8/12	Best fit power curve to peak strengths - Oxford Clay.....	218
8/13	Best fit power curve to peak strengths - Reading Beds clay.....	219
8/14	Best fit power curve to peak strengths - Weald Clay.....	220

9/1	Forces acting on a slice.....	239
9/2	Flow diagram describing a computer program using a non-linear failure envelope for arbitrary shaped failure surfaces.....	240
9/3	Input data required for analysis of shallow slab failures.....	242
9/4	Input data required for analysis of deep circular failures.....	243
9/5	The variation of factor of safety with different parameters.....	244
10/1	The slope and failure surface profiles used in the back-analyses, with the likely positions of the phreatic surface at failure.....	255
10/2	A45 Cambridge by-pass slope failure investigation...	256
10/3	The relation between peak strength, critical state strength and residual strength.....	257
11/1	Maximum recommended slope angles for less than 1 per cent failure on slopes greater than 5.0m high.....	273

LIST OF PLATES

Plate	Title	Page
Frontispiece	A slip and a repair on a highway cutting slope.....	3
1/1	Shallow failure adjacent to motorway hardshoulder.....	35
1/2	Slickensiding on a planar failure surface.....	36
2/1	Shallow failure on a highway embankment...	53
2/2	An embankment which has been repaired over most of its length.....	54
2/3	Seepage and erosion at the interface of sand and clay strata.....	55

LIST OF APPENDICES

Appendix	Title	Page
A	Glossary of terms.....	289
B	Details of motorways surveyed.....	290
C	Membrane correction for triaxial tests at low effective stresses.....	311
D	Computer program for 'best fit' power curve.....	313
E	Computer program for slope stability analyses using a non-linear failure envelope.....	327

THE EXTENT AND AN ANALYSIS OF SHALLOW FAILURES
ON THE SLOPES OF HIGHWAY EARTHWORKS

Chapter 1

Introduction and literature review

1.1 Introduction

Shallow failures on the slopes of highway earthworks are undesirable (Plate 1/1). They can undermine the road structure, damage drainage, cabling and crash barriers, and in some cases obstruct the motorway hard shoulder. They are usually only locally reported and documented, but they can constitute a large maintenance expense item in Highway Authority budgeting. A single shallow failure is usually not extensive, normally only about 300m³ of slip material is involved, but the frequency of occurrence means the number of slopes requiring repair is considerable.

Shallow failures do not constitute a threat to the integrity of the embankment or cutting as a whole, provided they are repaired before regression occurs further into the slope where critical areas can be undermined. Also the danger to the travelling public is minimal provided embankments are repaired before the road pavement is damaged or failed material in

cuttings is 'coned off' and subsequently removed from the motorway hard shoulder.

The construction of the motorway system in Great Britain began over thirty years ago and, over considerable lengths of the system, a sufficient time has elapsed to allow a useful study to be made of the performance of the earthwork side slopes. A survey was therefore undertaken (Perry, 1989) to determine the scale of deterioration of earthworks, attempt to quantify their long-term performance and, if possible, identify the factors observed during the survey, for example geology, geometry and associated soil properties, that have contributed to slope instability. Further slope failures are inevitably going to occur on the motorway system, and this Thesis describes the opening phases of this continuing process. An in-depth study of the failure mechanism and investigations of the behaviour of soils at low effective stresses provides an understanding of the fundamental causes of shallow failures.

In this Thesis, 'shallow failures' refers to failures on the slopes of cuttings and embankments at a vertical depth not greater than 2.5m with movement usually being translational although rotational movement may occur. Failure surfaces are usually slickensided (Plate 1/2). In terms of the classification of landslides by Skempton and Hutchinson (1969) this type of failure falls into the categories of 'slab slide - translational slides' and 'shallow slide - rotational slides'.

Most text books and courses will highlight the need to design man-made slopes, but usually only deep-seated failures are considered. Cuttings in over-consolidated clays have long been recognized as becoming more unstable with time (Vaughan, 1973; Chandler and Skempton, 1974; Chandler, 1984) and slope design has usually attempted to take this into account. Embankments on the other hand have usually been designed in the short-term when undrained conditions prevail. This is based on experience of failures which have occurred soon after construction due to the presence of weak foundation soils, the generation of excessive pore water pressures or movement along pre-existing shear planes. Consequently the opinion has been that if an embankment is seen to be stable shortly after completion then a design life is not always considered as the embankment is certain to last longer than the 120 year design life of associated structures such as bridges and reinforced earth retaining walls (Greenwood, Holt and Herrick, 1985). This may generally be true for deep-seated failures associated with the foundation soil but consideration needs to be given to shallow failures. To design an earthwork with this consideration is likely to become more common in the future as our man-made structures age and the possibility of further shallow failures increases. This Thesis will show that failures of embankments can occur well after the construction period and that failures in cuttings occur in a similar way. In order to give an indication of the performance of modern and past design and construction methods, consideration is given to earthworks which have been constructed at different times.

The early chapters of this Thesis describe a survey into the extent of shallow failures in England and Wales and investigates how certain factors have contributed to failure. Empirical designs are then presented based on the angles and heights of slopes where failures have and have not occurred. In order to study the mechanisms of failure, a number of drained triaxial tests is presented to illustrate the properties of six different over-consolidated soils from embankments where failures have occurred. To determine the strength characteristics of these soils, the shape of the failure envelope in shear and normal stress space is discussed, and six methods are developed and considered as possible ways of fitting a non-linear failure envelope to a series of Mohr circles. The peak strength parameters of the soils are then calculated using the most accurate method. A slope stability method of analysis is then developed that uses the strength parameters from the non-linear failure criteria. Back-analyses of the failed slopes are then conducted using the peak, 'ultimate' and critical strengths with various pore water regimes. In the discussion, the results of this approach to low effective stress analysis of slopes is considered and areas of further work highlighted.

Terms are used which have specific meanings, and a list of definitions is given in Appendix A.

1.2 Literature review of British sources.

The first reference found to shallow failures as a specific engineering phenomenon separate from deeper seated failures is in the all-embracing volume by Newman (1890). He incorporates a considerable amount of experience in his book, and it must have been the most comprehensive document on 'earthwork slips and subsidences' in its time. The earthworks he describes are in connection with railways, canals, and roads. Today it can still be a useful collection of empirical data and further reference is made to it in Chapter 11.

Glossop and Wilson (1953) recognized the problems associated with shallow failures on highways. They explained that shallow failures can cause transverse tilting or longitudinal cracking of a concrete pavement or local depressions in a flexible pavement. At that time slope drainage systems were only employed on embankments where 'surface failure is apparent' rather than as a preventative measure. The function of the drain was to remove water flowing down the slope to reduce softening of clay soils.

In the discussion to this paper, Bradbeer (1953) stressed the high cost of repairing the 'innumerable day-to-day instances' of shallow failures for the county of Worcestershire. He described their undramatic nature, as compared to the more spectacular deep seated failures that have occurred, but explained that due to the frequency of the shallow failures

their total cost was considerable.

Skempton (1953) continued on this theme and explained that the types of failure that occurred at depth, on a circular surface, and shallow failures were completely distinct and there were, no doubt, two entirely different mechanisms involved. In the first type of failure the ratio of the depth of the slip, D , to the length, L , measured up the slope lay between the limits 0.15 and 0.28. The ratio of D to L in the shallow failures lay between the limits 0.03 and 0.06. Two different methods of stabilization would be required for the two types of failure. Stabilizing a deep seated failure by reducing the disturbing moment, either by removing soil from the top of the slope or adding weight to the bottom, or both, would not improve the stability significantly for a shallow failure where drainage of the slope is the preferred method.

In 1970 a study was conducted using questionnaires (Symons, 1970) to estimate the magnitude and cost of shallow failures. This study was limited to particular lengths of the M1, M10, M45 and M6 motorways, and sections of the A1 trunk road. In order to determine the most economic long-term design, the study recommended that the estimated repair costs for failures on steep slopes should be compared to the costs of the additional land required for less steep and more stable slopes. It also reported that the maintenance expenditure on slope repairs appeared to be very low. Although failures were noted the problem was not considered to be extensive.

The first extensive detailed study of shallow failures was by Parsons and Perry (1985). This work highlighted the extent of failures on highway earthworks and published the results for the first stage of a survey of major earthworks constructed of a variety of materials. A further publication by Perry (1985) gave results of studies of Lower Lias and Weald Clay. TRRL Report RR199 (Perry, 1989), written as part of this Thesis, included all stages of the survey and produced a large collection of empirical information on slopes and shallow failures. This Thesis also expands on this information, and develops and applies possible failure mechanisms.

Shallow failures in Gault Clay are described by Greenwood, Holt and Herrick (1985). The type of failure is the same as described by Perry when surveying motorways. Descriptions are given of the various repairs available for these types of failure in Greenwood et al, and by Johnson (1985) who also describes the relative costs of the repairs.

Further investigations of the Gault Clay on the M20, M25 and M26 motorways are given by Garrett and Wale (1985). Both Greenwood et al, and Garrett and Wale have investigated the properties and behaviour of Gault Clay and show the difficulty of using or re-using Gault Clay in highway construction.

Again on the M25, a major shallow failure occurred in a cutting of Gault Clay but in this particular case it was during

construction (Horner, 1985). Failure occurred along shear planes within soliflucted and cryoturbated material. Since failure occurred during construction along extensive pre-existing shear planes, the mechanism is likely to be different from that of a first-time failure some time after construction. Also the extent of the failure reflects the nature of the glacially affected Gault Clay. This extent of failure is not usually found for shallow failures which also occur later in the earthwork's life.

Research by Andrews (1990) shows the rate at which failures occur has increased in recent years. This would explain why, when Symons conducted his study in the late 1960's, failures were of limited concern. It also agrees with the increasing number of observed reports of shallow failures in the past few years.

Earth embankment dams would seem to be a useful source of information. The most relevant reference is that of Charles and Boden (1985) who conducted a desk study of the failure of earth embankment dams in the United Kingdom. Almost all earth embankment dams were built before the beginning of the 20th Century before the science of soil mechanics was established and so few records exist of fill properties or a detailed description of the fill. Most failures occurred as a result of overtopping of the impounded water or internal erosion. Until 35 years ago, dams of this sort were constructed with a puddle clay core with surrounding zoned fill ranging from clay to more

granular material on the slopes. The slope angle upstream tended to be 1:3 and 1:2.5 downstream. Since 1925, there has only been one recorded problem with the long-term performance of these dams and generally it appears that the possibility of slips occurring is reducing with the increasing age of the dam system. This is the reverse of the process for highway earthworks and probably reflects the different methods of construction and the rate at which construction takes place. With earth dams very little compaction of the fill occurred, the rate of construction was slow and material was handled in smaller quantities. This would provide a greater opportunity for negative pore water pressures to reach equilibration, that is absorb water, and reduce the number of long-term failures. Consequently any instability of the fill would occur early in the life of the structure for the slope geometries used. This has indeed proved the case with most failures unrelated to the impounded water, that is shear failures or slips, occurring during or soon after construction. The weak puddle clay itself may be a destabilising agent as its strength at construction was as low as 10kN/m^2 . Charles and Boden found only one case where a shallow slip was recorded. If more shallow slips did occur they presumably were not such a major problem as on highways. Possible explanations for this are that shallow slips do not effect the safety of the dam and that the possibility of failure is reduced since dams are relatively short although high structures in comparison with the length of the motorway system in the United Kingdom.

Records which give details of the construction of earth embankment dams and their types of materials are very rarely available; cohesion and internal friction parameters for soils were not even conceived at the time most earth dams were constructed. Also since pore water pressure equilibrium in dams appears to be achieved in a relatively short period of time the mechanism of failure is totally different from that of highway earthworks. From the reference of Charles and Boden and the above discussion it is doubtful if a detailed survey of slips on the slopes of earth dams would be fruitful at this time.

The railway system would also seem to be a useful source of information for shallow slips on ageing earthworks. Although extensive literature searches were conducted, very little seems to have been written on this particular subject given that many shallow and deep failures have occurred (Ayres 1990, personal communication). Apart from Newman (1890) mentioned earlier, only two other references were found. Gardner (1921) stresses the need for adequate slope drainage and presents slope angles at which earthworks will stand under ordinary conditions. Ayres (1985) includes two case histories where slab failures occurred after many years of movement. Stabilization in these cases involved the use of grouts.

Since most railway earthworks and earth embankment dams were constructed in about the same period of time, the type and pace

of construction is likely to be the same. The construction method may therefore have the same effect on the stability of railway embankments as on earth embankment dams.

If a detailed survey of the sort described in this Thesis were to be undertaken for railway earthworks, there may be a problem locating failures which occurred in the distant past due to lack of records and masking of slips and repairs by erosion, vegetation and ballast. However, the extent of recent failures could be established in a survey or, if less detail were required, a study of aerial photographs could be considered. This would provide information on the amount of failure that could occur on highway earthworks within a short period in the future. Results for railway cuttings are likely to be relevant to highway cuttings but embankment comparisons are unlikely to be appropriate due to differing methods of construction.

1.3 Literature review of foreign sources.

The United Kingdom's motorway system is not unique in suffering from shallow failures. Similar earthworks failures can be seen elsewhere in the world. In the United States of America several states have reported shallow failures on embankment slopes which have been used in different applications. Shallow failures on cutting slopes have also been reported. North Carolina has been 'plagued' with numerous shallow failures on both cutting and embankment highway slopes (Sotir and Gray, 1989). Similar failures are recorded on Missouri highways

(Missouri Highway and Transportation Department, 1984) and one of the conclusions reached is that 'the incidence of all forms of distress increased with increasing plasticity as well as with increasing slope height'. A slope survey was conducted in this state similar to that described in this Thesis, although there was greater detailed investigation of the type of vegetation.

The conclusions of an examination of earth slope failures in Texas, explained that shallow failures represented the most significant type of slope stability problem examined in the study (Stauffer and Wright, 1984). Failures in embankments, studied in some detail as they occurred most frequently, were generally observed in soils where the liquid limit was in excess of 50, and plasticity indices were more than 30. Such soils are prone to swelling and shrinkage. Similar extensive numbers of failures are reported on Alabama and Arkansas highways (Blacklock and Wright, 1986).

According to Templeton, Sills and Cooley (1984), shallow failures have been occurring along the mainline Mississippi River Levées for the past 40 years. Although failures do not threaten the integrity of the levées, they pose a recurring maintenance problem as is the case for highways in England and Wales. The depth of failure varied from 1 to 2 metres and failures occurred in high plasticity clays after periods of dry weather followed by rainfall.

In Southern California 'surficial failures have become commonplace' and frequently occur after prolonged periods of rain (Day and Axten, 1989). Failures are generally 1.2m deep and occur in clay slopes.

Failures in weathered shale material in Oklahoma (Laguros, Kumar and Medhani, 1982) are recorded for cuttings where the failure surfaces were 3.0m deep. Failures occurred only one or three years after construction. This highlights the rapid loss of strength of the outer layer of the cutting in this weathered shale material after heavy rainfall.

At Notch Hill in Canada, shallow failures have occurred on both sides of a railway embankment several years after completion (Krahn, Fredlund and Klassen, 1989). Failure occurred over several kilometres of embankment constructed of a lacustrine silt. The maximum depth of failure of the slips was between 1m and 2m.

In the Regina area of Saskatchewan, numerous cutting and embankment slopes have failed 4 to 6 years after construction (Widger and Fredlund, 1979). The failures are shallow, occurring at depths between 2.1m and 2.4m.

Suzuki and Matsuo (1988) explained that 24 cases had been reported of failures in cutting along the Chuo Expressway in Japan between 1983 and 1985. The depth of failure ranged from 1.0m to 2.0m, however the material type was sand and gravel,

not materials usually associated with shallow failures. Also in Japan, Kobashi (1971) carried out several laboratory investigations into shallow failures using a number of experimental models simulating sandy soils. He was able to classify shallow failures as those caused by piping phenomenon, and those failing in the manner of a soil flow. In the first case the pore water head rose higher than the slope surface, washing out the surface material, and in the second case movement occurred as soon as the soil became saturated with the pore water pressure increasing until the slope failed in a rapid manner. Kobashi identifies the main source of water as being from rainfall.

The survey of slope condition described in this Thesis is very similar to the CHASE research project adopted for studying failures on earthworks in Hong Kong (Brand and Hudson, 1982). The only major differences are that with CHASE only cuttings were surveyed, the number of failures was measured rather than the length of failures, the geologies studied were very different and encompassed volcanic rocks, granite and residual soils, and the slopes were considerably steeper and higher. The survey method involved studies on foot and the same measurement and descriptive techniques as used for the motorway survey. Data sheets were used and arranged in a suitable way for entering on to a computer. The similar approaches adopted for gathering empirical slope information indicates the suitability of these procedures for a variety of situations. Also it indicates the acceptance of such methods for

determining slope designs.

The literature review highlights the problem of shallow failures internationally and reveals that most failures are of embankments rather than cuttings. There may be some evidence to suggest that the problem has increased in recent times as a result of modern practice of relatively quick construction and the need to reduce settlement by good compaction. This process effectively 'locks in' negative pore water pressures, allowing slopes to be constructed at initially stable angles. These angles, however, prove to be too severe in the longer term as the negative pore water pressures reduce or become positive and result in failure of the weakened soil.

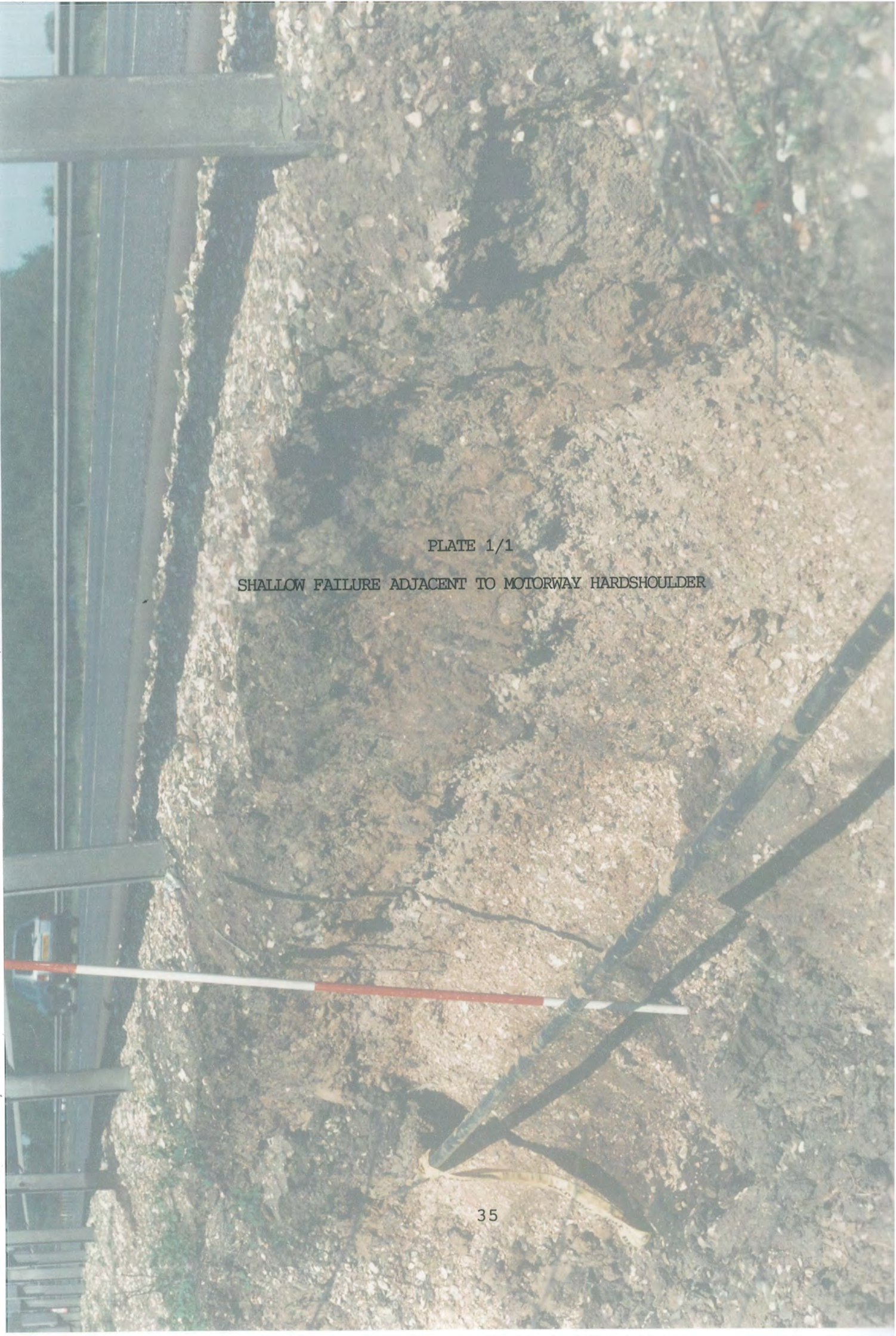
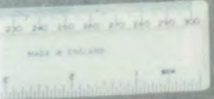


PLATE 1/1

SHALLOW FAILURE ADJACENT TO MOTORWAY HARD SHOULDER

PLATE 1/2

SLICKENSIDING ON A PLANAR SURFACE



Chapter 2

A survey of slope instability

2.1 Extent of survey

In 1987 there were over 2700km of motorway in England and Wales (Department of Transport, 1988). A survey covering 570km, 21 per cent of the motorway system, was undertaken to study the extent of shallow failures, attempt to quantify the long-term performance of earthworks and identify factors contributing to failure. Figure B1 of Appendix B, shows the extent of the survey with respect to the current motorway system. Although some large earthworks occur on other major highways, motorways were chosen because of their high and extensive earthworks which are necessary to restrict the longitudinal gradient to an absolute maximum of 4 per cent (Department of Transport, 1981).

Although Drift deposits were of interest, the choice of length of motorway was primarily governed by the Solid deposits present as more failures in these materials occurred, as reported in the literature review and as described by County Council and Department of Transport sources. Consequently, motorways in Scotland were not included since most of these had been constructed in Drift deposits and few failures were reported prior to the beginning of the survey. However, the reports of shallow failures in Scotland have increased since the completion of the survey (Scottish Development Department sources). As geology is one of the major factors affecting

stability, the survey covered the principal geologies encountered on motorways in England and Wales from the Old Red Sandstone Series to Recent deposits (Figures B2 to B18). Greater attention was paid to heavily over-consolidated clay soils where failures are likely to occur more frequently. The survey included a variety of motorways with earthworks of differing age, geometries, orientations and types of drainage. Table B1 of Appendix B, gives details of the motorways that were covered in the survey. Motorways were chosen, in seventeen counties of England and Wales, which would incorporate large lengths of a variety of geologies and cover several ages since construction.

For convenience, the motorway lengths were bounded by the maintenance limits of a county or the interchanges between which the geology occurred. These lengths, in some cases, were subsequently split into construction contracts. The age of a motorway within a county can vary due to different opening dates for each construction contract. The ages of sections of motorway included in the survey ranged from 1 year to 25 years with about 75 per cent of the lengths surveyed being 10 years and older, and 6 per cent of the younger ages being improvements, such as earthwork widening on existing motorways, which were included as part of the main motorway survey.

Not all the geologies in England and Wales were encountered in the survey for the following reasons:

- (a) there are no motorways on some geologies.

(b) the geology is only present as a foundation material and is not present on the slope.

(c) the survey did not cover some materials which are known to have relatively stable slopes, such as granites and basalts.

The survey included the main carriageway, interchanges and the side road diversions built at the same time as the motorway; of the total length surveyed, each constituted 75 per cent, 11 per cent and 14 per cent respectively. Of the 1500km of slope surveyed 850km was embankment slope and 650km was cutting slope. (The length of slope is greater than the length of motorway because the slope length includes all slopes on both sides of the motorway and slopes associated with side roads and interchanges.)

The survey procedure described here may be used for studying any length of highway where information is required for a particular area with significant earthworks. The survey was mostly carried out on foot although an aerial study was considered. Although an aerial survey may have been quicker, detail would not have been observed and many overgrown slips and cracks on the slope would have been missed. Also measurement of slope characteristics such as measurements of slope angle and height, and descriptions of soil type and drainage are more accurately found on the ground. An aerial survey would, however, be worth while in the future as a means of updating the results of this survey.

2.2 Preparatory work

Before the on-site survey could begin an investigation was necessary of the likely site conditions. This involved obtaining plans of the lengths of motorway to be surveyed, usually at a scale of 1:2500, and superimposing the Solid and Drift geology likely to be encountered on the site. The geology was acquired from geological survey maps and site investigation reports. Borehole logs were particularly useful in establishing the depth of Drift in cutting slopes. The materials in embankments were established as accurately as possible from mass-haul data prepared during construction, from records made by supervisory staff of day-to-day earthmoving operations, progress photographs or from 'as constructed' motorway plans. Most of the information regarding materials in embankments was obtained from the Consulting Engineers or County Highway Authorities who supervised the motorway construction.

Using longitudinal sections, earthworks on the plans were split into three height bands 0-2.5m, 2.5-5.0m and greater than 5.0m. This would assist in the graded investigation followed during the survey.

2.3 The survey

The purpose of the survey was to investigate, in detail, motorway slopes that had failed, slopes with problems that

might lead to instability and slopes that were behaving satisfactorily at the time of survey.

The survey involved inspecting on foot all earthworks delineated on the prepared plans as being greater than 2.5m high. Those areas of earthwork less than 2.5m high were observed from a slow moving vehicle operating on the hard shoulder of the motorway.

The types of instability encountered and the problems that might affect stability comprised

- (a) slope failures, generally known as slips (Plate 2/1)
- (b) slips that have been repaired (Plate 2/2)
- (c) tension cracks near the top of the slope, where a slip has begun to form, and shrinkage cracks all over the slope, promoting failure by allowing water to enter the slope
- (d) settlement emanating either within the fill or in the subsoil
- (e) seepage of water onto the slope (Plate 2/3)
- (f) erosion of material at the bottom of the slope (toe erosion).

Of the above problems, the most difficult to identify were the slopes where cracking had occurred and those areas where repaired slips had been topsoiled and seeded. Any omissions due to these difficulties are considered to be low in number as thorough on-site investigations were made and only two counties had a policy of topsoiling repaired failures. Also, since

slopes where cracking had occurred were not included in the failed slope category, any omission of slopes with cracking does not affect the total length of failed slope. If any omission did occur it would have resulted in an small underestimate of the problems.

For those areas of earthworks with heights greater than 5.0m and those slopes with a problem whatever the height of slope, full details of the characteristics of the slope and of the problem were noted on a specially designed survey form. It was recognised at an early stage that every slope on the motorways chosen could not be measured. If they were measured, the loss in time and resources would be such as to render a wide investigation of materials impractical. By concentrating more on slopes above 5.0m high the major earthworks were covered with the caveat that a slope be measured if it had a problem whatever the height. Slopes above 5.0m were identified by Symons (1970) as having the greatest number of failures.

Figure 2/1 shows an example of a completed survey form. Several slips and repairs can be entered on a single form with descriptions of slip type, for example slab or circular, and shape of area affected. The type of failure was identified by studying the inclination of both the failed material's surface and tension crack profile. With slab type failures the angle of the surface of the slipped material remains similar to the rest of the stable slope and the tension crack is usually vertical (Plate 1/2). Rotational failures exhibit heave at the

toe and near vertical downward motion at the crest (Plate 1/1), and, if there is sufficient movement, an observed tension crack which is curved in profile. The vertical depth to the failure surface is fairly constant for slab type failures and so measurements of depth of slipped material were made at the tension crack. For rotational failures, the depth varies of course, as the failure surface is curved concave upwards and so the depth of slip was taken to be the maximum vertical distance from the original slope to the failure surface. In most cases of rotational failure, the depth of failure had to be judged due to insufficient movement of the slipped material. This depth assessment was made by studying the inclination of the tension crack profile, the amount of slope effected and assuming a circular failure surface.

The condition of slip repairs, such as satisfactory, bulging or complete failure beneath the material used in the repair, can also be recorded.

Measurements of slope angle were taken using an optical prismatic clinometer or an Abney level, mounted on a ranging rod sighted along the slope to a marker at the same height on another ranging rod. The ranging rods were positioned at the top and bottom of a slope. Other methods of measuring slope angle are available (Stauffer and Wright, 1984; Francis, 1987) but this method was considered the most appropriate. The instruments were accurate to 0.5 degrees and including operator error the maximum error is 1.0 degree. The advantage of this

method is that minor local changes in slope profile did not influence the slope angle. This allowed a representative slope angle to be measured and at a reasonable speed. Where a change of slope angle occurred at a higher point on an earthwork, the slope angles were measured independently. With benched slopes, each slope was measured separately and a measure taken of the width of the bench. The length of slope was measured with a 30m tape or with a 100m tape on exceptionally large earthworks. In the exceptional cases where access was not possible, optical range finders were used. The height of the slope was calculated from measurements of the slope angle and the distance between the top and bottom of the slope. The slope bearing is the direction the slope faces, ie the bearing of a normal away from the slope. Other major characteristics noted were the drainage at the top and bottom of the slope and the drainage on the slope itself. A photographic record was also kept of failures and problems of interest.

Generally one survey form would cover the length of slope of a single earthwork unless the earthwork was split by bridges, contract demarcations or retaining walls, when a corresponding number of sheets would be completed.

A description of the soil or rock was made by observing any exposed material, for example on a failure surface, and by using a simple probe made from 6mm steel reinforcing rod. The feel of the probe as it was pushed into the slope indicated how granular, cohesive or rocky the material was. A visual

inspection could be made from the material adhering to the probe when it was withdrawn. As well as being useful for identifying construction materials, the probe could identify repaired areas beneath topsoils. In these cases the contrast in materials detected and the shape of the area in which they were found, were good indications as to when a repair was present.

2.4 Processing the data

Information from the completed survey forms and the prepared plans was used to describe the motorways as a series of 'features' as defined in Appendix A. These were entered and analysed on the TRRL CDC Cyber mainframe computer with the aid of an appropriate computer program. The program was outlined by the author and required his geotechnical input but was written by TRRL, partly in Fortran 5 (a CDC extension of Fortran77) and partly in Cyber Control Language (CCL). Using the program, the length of slope with any given combination of characteristics could be extracted by summing those features with the characteristics required. Interpolation within a feature was necessary for restrictions on slope angle and height. An example of a feature and the type information it contains is given in Figure 2/2. The feature connection type defines if the slope is continuous, splits into a number of slopes or a number of slopes converge to become a single slope.

2.5 Factors studied in the analysis of slopes

It was considered that the principal factors having an influence on the extent of failures were the geology, the age of the earthworks and their geometry. (These criteria are based on evidence given in the literature and common engineering practice.) The effects of these factors have therefore been studied in detail. Also considered to be worthy of examination was the type of drainage used (at the bottom of embankment slopes and the top of cutting slopes) and the orientation of the slope, as these could effect the pore water pressure regime within slopes, by either removing water or providing a micro-climate for slopes facing in certain directions. For example, slopes facing south may be drier than north facing slopes and as a result be more susceptible to cracking; this could allow water to enter deep into the slope.

Geology was the first slope characteristic to be examined and variation in age and geometry was not taken into account at that stage. Initially this Thesis considers the effect of geology in two Sections, beginning with the youngest materials, Drift deposits, and going on to Solid deposits. Chapter 5 covers the overall problem of failure. Single and combinations of two geologies were studied. The proportional effect of each geology in combination with others was difficult to quantify. Where mixtures of geologies occur in an earthwork, they are considered in the Section where the youngest geology appears. Similarly in the tables of results, the youngest geologies

appear first (as they would in a geological log of a borehole) and where there is a combination of materials the younger geology governs its position.

Analyses have been made, for given ranges of height and slope angle, of the variation of percentage of failure for geologies on different motorways, or on different lengths of the same motorway, which cover a number of ages. Percentage of failure is defined as the length of failed slope expressed as a percentage of the total length of slope involved. The necessity to compare different ages, each with failures in the same geology, restricts the number for comparison and consequently any trends are limited. Height bands of 0-2.5m, 2.5-5.0m and more than 5.0m were used in this instance.

In order to determine the effect of age on the performance of earthworks for each individual motorway, dates of occurrence of slope failures are required over a long time- scale. Unfortunately, such information was not readily available during the survey from the Authorities responsible for the maintenance of the particular lengths of motorway. Andrews (1990) has, however, determined the effect of age on specific lengths of motorway by studying aerial photographs taken in the lifetime of the earthworks as explained early in the literature review. Locations were selected where high percentages of failure have been observed during the survey presented in this Thesis.

Although surveyed, failures which occurred during motorway construction have not, for the purposes of analysis, been included in the length of failed slope. The survey was primarily concerned with the performance of slopes since construction.

In general, the slope angles of the earthworks tended to be designed as fairly uniform for any given age, especially for embankments, although sufficient variability occurred in practice to provide some indication of the effect of slope angle on the occurrence of failures. The height bands used in the Sections relating to the effect of geometry are in 2.5m steps.

The effect on the percentage of failure of three types of drainage at the bottom of embankments and the top of cuttings is considered. The drainage in both locations has been categorized as follows: none, where no drainage was seen; open ditch, where a simple steep sided, lined or unlined ditch occurred; and French drain, which appeared as parallel sided, aggregate filled trenches with a pipe at the bottom. Comparisons of the effect of the types of drainage are made and in each case earthworks of the same geology, age and geometry are considered.

A study has been made to find the effect of slope drains on the percentage of failure. This is discussed in the Section on Jurassic and Triassic deposits for embankment slopes and in the

Section on Eocene and Cretaceous deposits for cutting slopes. A slope drain appears as an aggregate filled trench running up the slope in a straight line or in a pattern such as herringbone. Slope drains were very rarely seen on embankments and were more commonly seen on cuttings in areas of seepage.

To show the effect of orientation on the percentage of failures, combinations of geology, age and geometry were classified in 90 degree quadrants averaging north, east, south and west facing directions.

From the geometry data, maximum slope angles are derived for given ranges of heights, which minimize the risk of shallow failures within the maximum life span of the motorways studied. (Data from the survey only apply to a maximum age of 25 years, with many results only being applicable to younger ages.) In most cases these recommended slope angles are based on results where no failures occurred. For the remaining cases a percentage of failure of up to 1 per cent is assumed to be acceptable in order to exclude single slips less than 10m wide, which have occurred because of local effects. Also the cost of repairing such small lengths of failure is acceptable when compared to the greater landtake required to prevent them. Similarly, the effect of the various types of drainage at the top and bottom of slopes on the above recommended slope angles has been studied. The percentage of failure is again restricted to 1 per cent or less within 25 years of construction as indicated by the results of the survey. It

should be noted that the provision of drainage at the top and bottom of a slope may be unavoidable even if shallow failures occur as a result. For example, drains may be needed to drain the foundation, provide a cut-off for water flow on the natural ground surface or provide continuity for the whole scheme's drainage system.

County Road Sheet **3263**
 Recent weather Personnel **JP** Date **1-6-85**

Setting: embankment

1. Soil and/or rock description including rock discontinuity information	Observed <i>Grey/brown/red mottled clay</i>		From geol survey <i>Reading Beds</i>															
2. Vegetation type	<i>Grass, small trees gorse</i>																	
3. Slip, minor slip and incipient slip descrip.	Prop. aff.	1	2	3	4	5	Sound above	1	2	3	4	5	Depth of slip	1	2	3	4	5
<i>1 Slab type, N-shape, chalk layer 40 cm thick at top, striated, exposed gully down pipe.</i>		<i>0.5</i>	<i>0.5</i>	<i>0.5</i>				<i>0.2</i>	<i>0</i>	<i>0</i>				<i>2</i>	<i>2</i>	<i>1.5</i>		
<i>2 Slab type, chalk layer, again striated N-shape of slip</i>																		
<i>3 Slab type, striated N-shape of slip</i>																		
4. Pavement problems ?	1 <i>NONE</i>					2					1. ch.		2. ch.					
5. Water present ?	Prop. aff.		Location			6. Profile change ?					7. Seepage and/or erosion							
On failure plane	<input checked="" type="checkbox"/>	<i>1 0.5 2 0.3 3 0.3</i>	<i>0.2 0</i>	<i>All slips</i>			<i>Crack with scarp at top of slips and debris at base</i>					Prop. aff.		1	2	3		
Saturating soil	<input checked="" type="checkbox"/>	<i>1.0</i>	<i>0</i>	<i>Everywhere</i>								Sound ab.		1	2	3		
As springs	<input checked="" type="checkbox"/>																	
Ponding	<input checked="" type="checkbox"/>	<i>1 0.5 2 0.3 3 0.3</i>	<i>0.2 0</i>	<i>All slips</i>														
8. Description of repair	Prop. aff.		1	2	3	4	5	Sound above		1	2	3	4	5	Age <i>All overgrown. Old</i>			
			<i>1.0</i>	<i>1.0</i>	<i>1.0</i>					<i>0</i>	<i>0</i>	<i>0</i>						
	Material		<i>Gravel, limestone, concrete in all cases</i>											Other				
	Top soil ?		<i>No</i>		Condition <i>sound</i>													
9. Drainage, type and condition	T <i>Gully breaking up</i>			Loc. <i>all</i>			S		Sp. Loc.		B <i>Open ditch sound</i>					Loc. <i>all</i>		
10.	Chainage	Description					Slope angle	Slope length	Slope height	Slope bearing								
	<i>78.270</i>	<i>Highest point and east end of slip No 1 20 m of slip No 1</i>					<i>25</i>	<i>33.3</i>	<i>14.1</i>	<i>40</i>								
	<i>78.290</i>	<i>West of slip No. 1, east of Remedial No. 1 30 m of Remedial No. 1</i>					<i>25</i>	<i>33.7</i>	<i>14.2</i>	<i>40</i>								
	<i>78.320</i>	<i>West of Remedial No. 1, east of slip No. 2 15 m of slip No. 2 5 m of Remedial No. 2 10 m of slip No. 3</i>					<i>24</i>	<i>34.0</i>	<i>13.8</i>	<i>40</i>								
	<i>78.350</i>	<i>West of slip No 3, east of Remedial No 3 170 m of Remedial No 3</i>					<i>25</i>	<i>34.0</i>	<i>14.4</i>	<i>40</i>								
	<i>78.520</i>	<i>West of Remedial No 3</i>					<i>18</i>	<i>9.4</i>	<i>2.9</i>	<i>40</i>								
11. Classify problem	<i>Slips, remedials</i>																	
12. Photos	<i>No. 4, 5</i>			(Space overleaf)											(Delete as necessary)			

Fig 2/1 A completed survey form

OUTPUT FROM PROGRAM SLEX 89/09/20. 14.30.24.
DATA HELD IN FILE M4C5C7

M4 BERKSHIRE/CONTRACT5+CONTRACT7(A329(M))/CH.54.07-73.800

AGE AT TIME OF SURVEY = 10. YEARS

CONSTRAINTS ON FEATURE NUMBER

NO. OF RESTRAINTS ; 1 NULL ELEMENT ; 0
163 INCLUDED SINGLE VALUE.

FEATURE NO.	; 163
J11 A33 SOUTH WEST SIDE B10	
NOMINAL CHAINAGE	; 65.800
LENGTH OF FEATURE	; 15 METRES
JUNCTION NON-MAINLINE	
FEATURE CONNECTION TYPE	; 0 = THROUGH
NO OF PRECEDING PRIMARY FEATURE	; 162
NO OF FOLLOWING PRIMARY FEATURE	; 164
FEATURE TYPE	; 20 = EMBANKMENT
NUMBER OF FEATURE GROUP	; 10
OBSERVED MATERIAL	; 4 = STONY CLAY
CONSTRUCTION MATERIAL	; 29 = LONDON CLAY
FOUNDATION GEOLOGY	; 29 = LONDON CLAY
INFERRED HEIGHT & SLOPE AT START	; 8.1 METRES ; 24.9 DEGREES
OBSERVED HEIGHT & SLOPE AT END	; 8.2 METRES ; 24.0 DEGREES
ORIENTATION OF NORMAL TO SLOPE	; 250 DEGREES
VEGETATION TYPES	; 1 = GRASS
	; 4 = TREES
DRAINAGE AT TOP OF SLOPE	; GULLEY DRAIN
DRAINAGE ON SLOPE	; NONE
DRAINAGE AT BASE OF SLOPE	; OPEN DITCH
SLOPE CONDITION	; 5 = SLIP-NO REMEDIAL
DEPTH OF SLIP .5 METRES	
EXTENT OF FAILURE	; 1.0 OF SLOPE
PAVEMENT SOUND	

CONTRIBUTION FROM THIS FEATURE IS 15. METRES.

Fig 2/2 A typical feature



PLATE 2/1

SHALLOW FAILURE ON A HIGHWAY EMBANKMENT

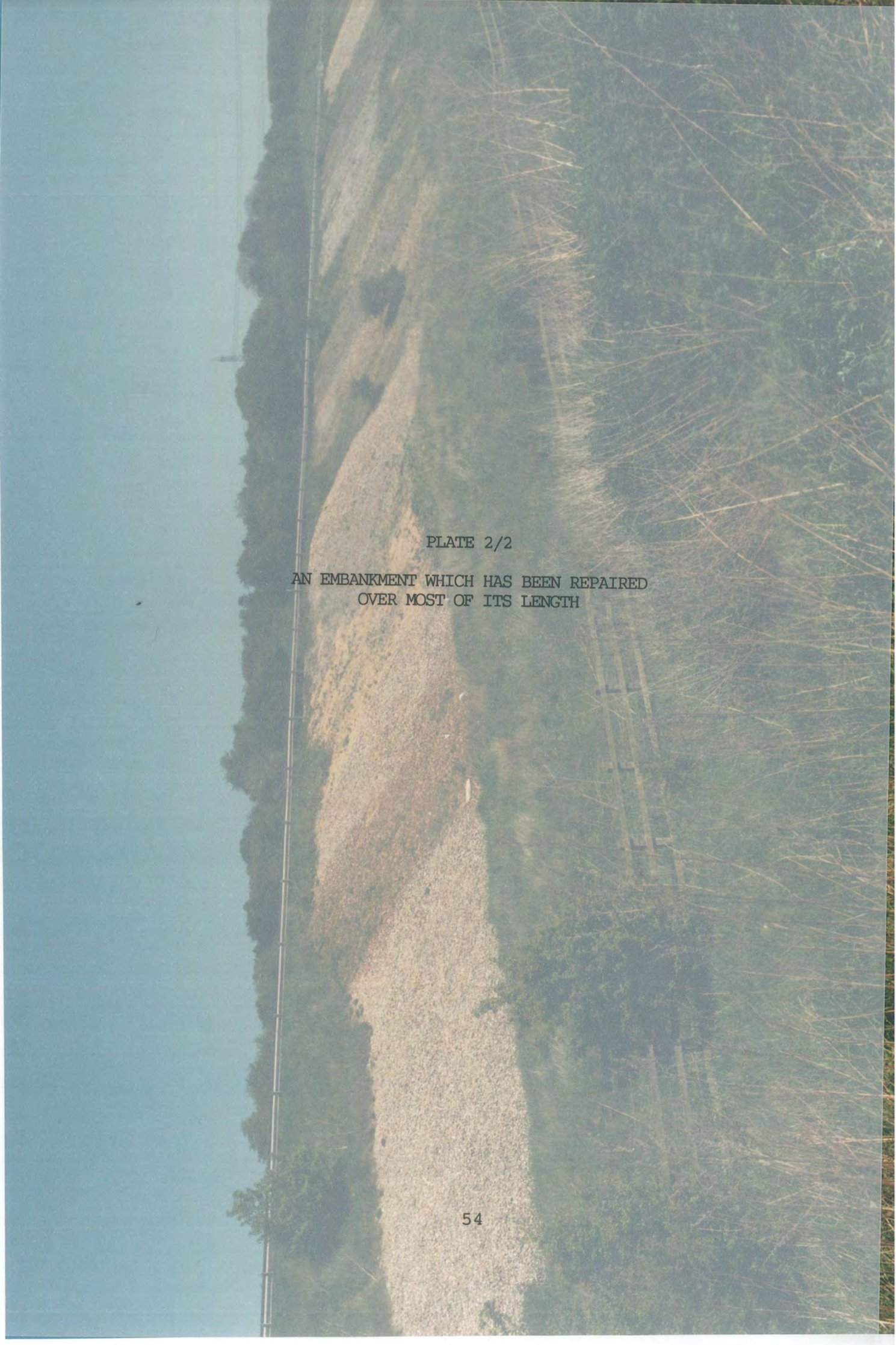
A photograph showing a riverbank. The left side of the image is a calm, blue-grey body of water. A metal fence runs along the top edge of the frame. The right side of the image shows a grassy bank with a large, light-colored gravel area that has been laid down for repair. The text is centered over the gravel area.

PLATE 2/2

AN EMBANKMENT WHICH HAS BEEN REPAIRED
OVER MOST OF ITS LENGTH

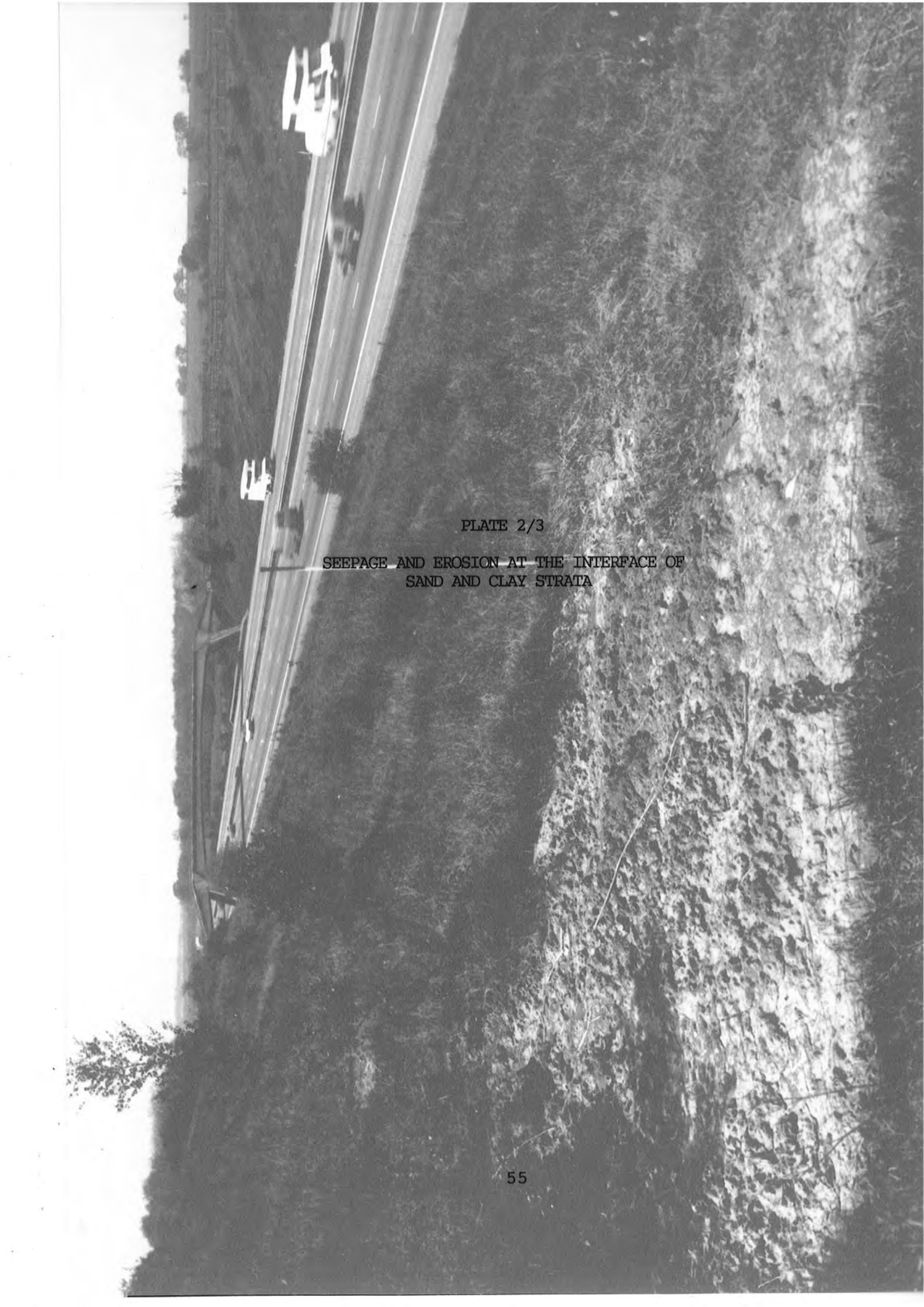


PLATE 2/3

SEEPAGE AND EROSION AT THE INTERFACE OF
SAND AND CLAY STRATA

Chapter 3
Drift deposits

3.1 Geology

Drift deposits are extremely heterogeneous and allowance must be made for this in the following analyses. In addition, the geological name as shown on the geological survey maps may not describe the material accurately in an engineering sense, for example some of the named gravels have a high clay content. The Drift titles used in this Thesis are general terms for similar types of material and consequently may encompass several geologies.

Tables 3/1 and 3/2 give the overall results for single Drift deposits and for combinations of two geologies where at least one geology is a Drift deposit, for total lengths of cutting and embankment slope in excess of 1.0 km. Drift deposits do not always occur at one particular geological age, so the order of geologies given in the Tables is only a guide.

Considering embankment slopes of a single geology, River Gravel has the highest percentage of failure of 2.8 per cent and shows the steepest predominant slope angle of 1:1.5. The other geologies have much smaller percentages of failure of less than 1 per cent and a slope angle of 1:2 is most commonly used.

Plateau Gravel is the only single material in cutting slopes

with a percentage of failure greater than 1 per cent and the predominant slope angle is 1:3.

Comparing single geologies in embankments and cuttings shows higher percentages of failure in River Gravel and Clay-with-flints embankments, however Glacial Gravel and Boulder Clay have the opposite trend. Cuttings show a greater variety of predominant slope angle varying from 1:3 to 1:2 whereas embankments are generally steeper varying from 1:2 to 1:1.5.

Glacial Gravel with Middle Lias (Silts and Clays) in embankments has a very high percentage of failure of 11.0 per cent. Boulder Clay with Enville Beds also has a high percentage of failure of 6.6 per cent. Concentrating on the over-consolidated clays, London Clay when combined with three differing Drift deposits, consistently had percentages of failure in a range from 2 to 6 per cent. There were no failures in River Gravel with Oxford Clay and Clay-with-flints with Reading Beds, but Boulder Clay mixed with Gault Clay has a percentage of failure of 1.4 per cent. The combinations of Glacial head with Lower Lias or Keuper Marl have a percentage of failure of 5.8 per cent and 2.8 per cent respectively but Boulder Clay with Keuper Marl slopes are stable. Clay-with-flints with Reading Beds shows no sign of failure.

Boulder Clay with Enville Beds has the highest percentage of failure in cuttings with a value of 8.1 per cent. The percentages of failure in other combinations of geologies range

from 0 to 3.3 per cent.

Compared with embankments, cuttings of Boulder Clay with London Clay and Glacial Gravel with Carboniferous Limestone Series (Carbonate) or Lower Old Red Sandstone - St Maughan's Group show lower percentages of failure. Cuttings of Boulder Clay with Enville Beds, Clay-with-flints with Upper Chalk and Glacial Gravel with Boulder Clay have higher percentages of failure than the same combinations in embankments. The range of predominant slope angle in cuttings is greater than in embankments with extremes of slope of 1:3.5 and 1:1.25.

Boulder Clay, the most extensive material surveyed, behaves differently depending on the area where the slope occurs as shown in Table 3/3. Southern England (M1 Hertfordshire, Bedfordshire, Buckinghamshire and M11 Essex) has the highest percentage of failure, North-West England (M6 Cumbria) has a low percentage of failure or none at all and South Wales (M4) is between the two. There was only a short length of embankment surveyed in the Midlands (M45 Northamptonshire). It would appear from these results that the properties of Boulder Clay, with respect to slope stability, deteriorate to the south and east. It should also be remembered that 'Boulder Clay' exhibits considerable variation in its engineering properties and is found commonly on geological survey maps with reference to its origin rather than specific material type.

Many of the Drift deposits encountered in the survey, over

significant lengths of cutting and embankment slopes, exhibited percentages of failure of less than 1 per cent or had no failures at all.

3.2 Age of earthworks

The ages of the earthworks in Drift deposits are included in Tables 3/1 and 3/2 and range from 2 to 25 years. Tables 3/4 and 3/5 show the results of an analysis to compare percentages of failure of similar earthworks which cover a number of ages. Failures begin at a variety of ages depending on the geology and the geometry. The general trend in embankments is for the percentage of failed slope to increase with the age of the earthwork, as would be expected, although one of the results for Boulder Clay is inconsistent. Cuttings show a less clear trend with some geometries behaving very erratically. The variability of these results, especially for Boulder Clay, may reflect the heterogeneous nature of the materials. Four out of the seven cases where failure occurred, however, show an increase in the percentage of failure with time.

3.3 Geometry of slope

Results of the effect of geometry on the percentage of failure are given in Figures 3/1 and 3/2 for those combinations of geology and age that had a percentage of failure greater than 1 per cent and a total length of slope in excess of 2.5km. These Figures illustrate the high percentages of failed slope that

have occurred with certain combinations of geology, age and geometry. Boulder Clay with London Clay (6 years old), Plateau Gravel with London Clay (10 years old) and Glacial Head with Lower Lias (13 years old) are cases where more than 50 per cent of embankment slopes have failed for particular geometries. In cuttings the percentages of failure are generally lower; the highest percentage being Boulder Clay with London Clay (7 years old) which has approximately 25 per cent of slopes failing. It is worth noting again the poor performance of London Clay in combination with more granular materials.

For both embankments and cuttings there is clear evidence that the height of slope has an effect on the percentage of failure. In the majority of cases an increase in height for constant slope angle is accompanied by an increase in the percentage of failure.

The effect of slope angle on embankments and cuttings is not so clear and in some instances flatter or intermediate slope angles have yielded higher percentages of failure. This is most pronounced for embankments of River Gravel (10 years old), River Gravel with London Clay (10 years old), Glacial Head with Lower Lias (13 years old) and Glacial Head with Keuper Marl (23 years old). A similar effect is shown by cuttings of Boulder Clay with London Clay (7 years old) and Clay-with-flints with Upper Chalk (10 years old). Embankments of Glacial Gravel with Lower Old Red Sandstone - St Maughan's Group show an increase in the percentage of failure with increasing slope angle at two

different ages. In cuttings of Clay-with-flints with Upper Chalk, there is a similar behaviour for both the ages studied at the steeper slope angles. At the flatter slope angles both ages may show a similar trend but a comparison has not been possible as there were no 22 year old slopes, in these materials, encountered in the survey.

3.4 Type of drainage

For embankments there were no cases where all three types of drainage at the bottom of the slope could be compared. Comparing the cases where two types occurred, in six out of eleven cases distinctly higher percentages of failed slope occurred where no drainage was provided; slopes with open ditches had the smallest percentage of failure in five of these six cases. There were two cases where slopes with open ditches had a higher percentage of failure than when drainage was not provided. In the eleven examples studied the ranges of percentages of failure are as follows:

None	0 - 58 per cent
French drain	0 - 13 per cent
Open ditch	0 - 4 per cent

With cutting slopes there were three cases where all three types of drainage occurred at the top of the slope and in every case the greatest percentage of failure occurred with no drainage. Where there were two types of drainage to compare,

slopes with French drains showed distinctly higher percentages of failure in three cases, two of which were greater than where no drainage was provided, however, in the third case the slopes with no drainage produced the higher percentage of failure. Slopes with open ditches had no failures or a very small amount in the four cases where they occurred. In the seven examples studied the ranges of percentages of failure are,

None	0 - 35 per cent
French drain	0 - 13 per cent
Open ditch	0 - 5 per cent

These ranges are similar to those for embankments and it would appear that drainage at the bottom of embankment slopes and at the top of cuttings produces, in the majority of cases, the least percentages of failure for earthworks constructed of Drift material or mixtures of Drift and Solid material. The presence of an open ditch or French drain at the top of cuttings indicates that the need for a cut-off drain was recognized during design and the results show this arrangement performs satisfactorily.

3.5 Orientation of slope

Variations occurred between the percentages of failure of embankment and cutting slopes of differing orientations, but there was no consistent pattern of behaviour over the range of geologies studied. No evidence has been obtained to indicate

whether or not the climatic influence of orientation has any effect.

3.6 Design of side slopes in new construction

Tables 3/6 and 3/7 give the results of an analysis of the maximum slope angles allowable to minimize failure in the height ranges of 0-2.5m, 2.5-5.0m and greater than 5.0m. The geologies are given in the same order as Tables 3/1 and 3/2 so that comparisons can be made between the maximum recommended slope angle and the actual predominant slope angle. For example embankments of Glacial Gravel with Middle Lias (Silts and Clays) are constructed at a predominant slope angle of 1:2, but a slope angle of 1:3 would reduce the percentage of failure from 11 per cent to less than 1 per cent based on the results of the survey. In the North-West of England, engineers have independently, over the years since construction of the M5 Preston Northern By-Pass, reduced the slope angle used for Boulder Clay cuttings to 1:2.5 (Arrowsmith 1987, personal communication). This slope angle is exactly the same as the maximum recommended slope angle found in the survey.

The effect of drainage on the maximum recommended slope angles of certain geologies is given in Table 3/8. This Table shows the types of drainage and geometry that restrict failures to less than 1 per cent within 25 years of construction as indicated by the results of the survey. Steeper slope angles can be used for slopes with open ditches in most of the cases

where Drift deposits are present, and French drains also affect two of the remaining geologies. Only River Gravel with London Clay in embankment slopes exhibits a greater percentage of failure when drainage is provided. The results for both this Section and Section 3.4 indicate that open ditches are more effective than French drains at reducing slope failures. Open ditches are also less expensive and simpler to construct than French drains although in the longer term they may require more maintenance.

TABLE 3/1

Drift deposits encountered in the survey, with a total length of slope in excess of 1.0km.

	Age of earthworks when surveyed (years)	Total length (km)	Percentage of failure	Predominant measured slope angle all heights (v:h)
<u>EMBANKMENTS</u>				
SINGLE GEOLOGIES				
River Gravel	10, 19	2.8	2.8	1:1.5
Glacial Gravel	6.5, 9.5, 22	9.6	0.4	1:2
Boulder Clay	3, 6, 7, 9.5, 16, 17, 18, 22, 23, 25	49.4	0.3	1:2
Clay-with-flints	10, 22	12.7	0.7	1:2
COMBINATIONS OF TWO GEOLOGIES				
River Gravel with				
London Clay	10	2.8	2.2	1:2
Upper Chalk	10, 22	1.7	0	1:2
Lower Chalk	22	2.5	0	1:2
Oxford Clay	22	2.2	0	1:2.5
Plateau Gravel with				
London Clay	10	4.7	6.0	1:2
Glacial Gravel with				
Boulder Clay	3, 18, 22	3.0	0	1:2
Pebbly Clay and Sand	22	1.5	0	1:2.5
Upper Chalk	22	3.1	0.3	1:2
Middle Lias	25	2.1	11.0	1:2
(Silts and Clays)				
Keuper Marl	23	4.2	0	1:2
Carboniferous Limestone Series (Carbonate)	9.5	4.2	1.4	1:2
Lower Old Red Sandstone - St. Maughan's Group	6.5, 9.5, 20	10.8	2.3	1:2
Lower Old Red Sandstone - Raglan Marl Group	6.5, 20	1.4	0	1:2
Boulder Clay with				
Glacial Silt and Varved Clay	18	2.6	0.6	1:2
London Clay	6, 7	3.9	4.6	1:3
Upper Chalk	3	6.9	0	1:2
Gault Clay	22	3.3	1.4	1:2.5
Lower Greensand	22	2.2	0	1:2
Keuper Marl	23	2.7	0	1:2
Enville Beds	19.5	3.7	6.6	1:2
Carboniferous Limestone Series (Carbonate)	16, 17	10.6	0	1:2
Carboniferous Limestone Series (Arenaceous)	16	1.9	0	1:2
Glacial Head with				
Lower Lias	13	11.5	5.8	1:2
Keuper Marl	23	3.3	2.8	1:1.5
Clay-with-flints with				
Reading Beds	10	1.8	0	1:2
Upper Chalk	10, 22	22.5	0.1	1:2

TABLE 3/2

Drift deposits encountered in the survey, with a total length of slope in excess of 1.0km.

	Age of earthworks when surveyed (years)	Total length (km)	Percentage of failure	Predominant measured slope angle all heights (v:h)
<u>CUTTINGS</u>				
SINGLE GEOLOGIES				
River Gravel	10,20,22	4.7	0.2	1:2.5
Plateau Gravel	6,10	2.6	1.1	1:3
Glacial Gravel	3,6.5,7,9.5,20,22,23,25	36.4	0.6	1:2
Boulder Clay	2,3,4.5,6,7,9.5,14,16,17,18,22,23,25	97.2	0.8	1:2
Glacial Head	6,13,23	4.4	0	1:3
Clay-with-flints	10,22	29.4	0.2	1:3
Pebbly Clay and Sand	22	1.0	0.5	1:2
COMBINATIONS OF TWO GEOLOGIES				
Glacial Gravel with				
Boulder Clay	3,18,25	2.0	1.7	1:2
Carboniferous Limestone Series (Carbonate)	9.5	4.7	0.1	1:2
Lower Old Red Sandstone - St.Maughan's Group	6.5,9.5,20	6.9	1.4	1:2
Boulder Clay with				
London Clay	0,6,7	2.6	3.3	1:3.5
Upper Chalk	3	3.3	0	1:2
Lower Greensand	22	2.9	0	1:2
Oxford Clay	22	1.0	0	1:2
Keuper Conglomerate	2,4.5,9.5	1.8	1.5	1:2.5
Enville Beds	19.5	2.0	8.1	1:2.5
Carboniferous Limestone Series (Carbonate)	4.5,9.5,16	3.1	0	1:2
Clay-with-flints with				
Reading Beds	22	1.1	0	1:3
Upper Chalk	9,10,22	10.5	2.1	1:1.25

TABLE 3/3

The percentages of failure of Boulder Clay in different parts of England and Wales with a slope angle of 1:2 and a height greater than 5.0m

Area	Age of earthworks when surveyed (years)	Total length (m)	Percentage of failure
<u>Embankments</u>			
Southern England	6, 7, 22	1418	8.8
South Wales	9.5	546	2.7
North-West England	16, 18	1296	0
<u>Cuttings</u>			
Southern England	22	1033	18.1
South Wales	9.5	648	11.6
Midlands	25	690	5.5
North-West England	16, 17, 18	3089	3.9

TABLE 3/4

Comparisons of the percentages of failure in embankments of different ages for given combinations of Drift deposits and geometry

Geology	Slope angle (v:h)	Height (m)	Age (years)	Total length (m)	Percentage of failure	
<u>Embankments</u>	1:2.5	0-2.5	7	1155	0	
			22	287	0.7	
	Boulder Clay	2.5-5.0	7	1307	0	
			16	392	0	
			22	311	1.5	
		1:2	0-2.5	3 to 22	4572	0
				2.5-5.0	3 to 18	2483
					22	2075
	more than 5.0	6,7	748	8.7		
		9.5	546	2.7		
16		316	0			
18		980	0			
22		670	8.9			
Glacial Gravel with Lower Old Red Sandstone - St Maughan's Group		0-2.5	6.5	590	0	
			9.5	724	0	
	1:2	2.5-5.0	6.5	712	0	
			9.5	830	0	
	more than 5.0	6.5	1179	7.5		
		9.5	636	12.9		
	Clay-with-flints with Upper Chalk		0-2.5	10	1749	0
				22	1108	0
1:2		2.5-5.0	10	1823	0	
			22	957	0	
more than 5.0		10	3339	0		
		22	216	13.9		

TABLE 3/5
 Comparisons of the percentages of failure in cuttings of different
 ages for given combinations of Drift deposits and geometry.

Geology	Slope angle (v:h)	Height (m)	Age (years)	Total length (m)	Percentage of failure
<u>Cuttings</u>					
Boulder Clay	1:2.5	0-2.5	3 to 22	4744	0
		2.5-5.0	3 to 18	4142	0
			22	204	20.5
	more than 5.0	3	1634	2.4	
		7	2558	0	
		9.5	502	7.0	
		16	567	0	
	1:2	0-2.5	3 to 7	746	0
			9.5	803	0.2
			16 to 23	6665	0
			25	898	1.7
		2.5-5.0	7 to 17	3291	0
			18	1750	1.0
			22	2319	3.7
			25	463	5.8
more than 5.0		9.5	648	11.6	
		16 to 17	1064	0	
		18	2025	5.9	
		22	1033	18.1	
	25	690	5.5		
Glacial Gravel with Lower Old Red Sandstone- St Maughan's Group	1:2	0-2.5	6.5	202	0
			9.5	472	0
	2.5-5.0	6.5	629	0	
		9.5	274	0	
	more than 5.0	6.5	1994	2.6	
		9.5	987	0	
Clay-with-flints with Upper Chalk	1:2	2.5-5.0	9	202	0
			22	290	1.7

TABLE 3/6

Maximum slope angles allowable to restrict the percentages of failure to below 1 per cent within 25 years of construction as indicated by the results of the survey

DRIFT DEPOSITS

Maximum slope angle (v:h)

	Height		
	0 - 2.5m	: 2.5 - 5.0m	: More than 5.0m
<u>EMBANKMENTS</u>			
<u>SINGLE GEOLOGIES</u>			
River Gravel	1:1.5	1:1.75	1:1.75*
Glacial Gravel	1:1.75	1:2.5	1:2.5*
Boulder Clay	South 1:2	1:3	1:3
	West 1:2	1:2	1:2.5*
	North-West 1:1.75	1:1.75	1:1.75
Clay-with-flints	1:2	1:3	1:3.5*
<u>COMBINATIONS OF TWO GEOLOGIES</u>			
River Gravel with			
London Clay	1:2	1:3*	1:3*
Upper Chalk	1:2	1:2	-
Lower Chalk	1:1.75	1:1.75	-
Oxford Clay	1:2.5	1:2.5	-
Plateau Gravel with			
London Clay	1:2	1:3*	1:3.5*
Glacial Gravel with			
Boulder Clay	1:2	1:2	-
Pebbly Clay and Sand	1:2	1:2	-
Upper Chalk	1:2	1:2	1:2
Middle Lias	1:3*	1:3*	1:3*
(Silts and Clays)			
Keuper Marl	1:2	1:2*	1:2*
Carboniferous Limestone	1:1.75	1:1.75	1:2
Series (Carbonate)			
Lower Old Red Sandstone	1:1.75	1:2	1:3
- St. Maughan's Group			
Lower Old Red Sandstone	1:2	-	-
- Raglan Marl Group			
Boulder Clay with			
Glacial Silt + Varv. Cl.	1:2.5*	1:2.5*	1:2.5*
London Clay	1:2	1:2	1:3
Upper Chalk	1:1.75	1:1.75	1:1.75
Gault Clay	1:2.5	1:3.5*	-
Lower Greensand	1:2	1:2	-
Keuper Marl	1:2	1:2	1:2
Enville Beds	1:2	1:3	1:3.5*
Carboniferous Limestone	1:2	1:2	1:2
Series (Carbonate)			
Carboniferous Limestone	1:2	1:2	1:2
Series (Arenaceous)			
Glacial Head with			
Lower Lias	1:2	1:3.5	1:3.5
Keuper Marl	1:1.5	1:2	1:2
Clay-with-flints with			
Reading Beds	1:2	1:2	1:2
Upper Chalk	1:1.75	1:1.75	1:2.5

* Extrapolated result.

TABLE 3/7

Maximum slope angles allowable to restrict the percentages of failure to below 1 per cent within 25 years of construction as indicated by the results of the survey

<u>DRIFT DEPOSITS</u>	Maximum slope angle (v:h)		
	0 - 2.5m	Height : 2.5 - 5.0m	: More than 5.0m
<u>CUTTINGS</u>	<u>SINGLE GEOLOGIES</u>		
River Gravel	1:2.5	1:2.5	1:2.5
Plateau Gravel	1:2.5	1:2.5	1:3.5*
Glacial Gravel	1:1.5	1:1.75	1:2
Boulder Clay South	1:1.75	1:3.5	1:3.5
West	1:1.75	1:2	1:3*
Midlands	1:2.5	1:2.5	1:2.5*
North-West	1:1.75	1:2	1:2.5
Glacial Head	1:2.5	-	-
Clay-with-flints	1:2.5	1:2.5	1:2.5
	<u>COMBINATIONS OF TWO GEOLOGIES</u>		
Glacial Gravel with			
Carboniferous Limestone Series (Carbonate)	1:1.75	1:1.75	1:1.75
Lower Old Red Sandstone - St Maughan's Group	1:2	1:2	1:2.5
Boulder Clay with			
London Clay	1:2.5	1:2.5	1:4*
Upper Chalk	1:2	1:2	1:2
Lower Greensand	1:2	1:2	1:2
Oxford Clay	1:2	1:2	-
Keuper Conglomerate	1:2	1:2	-
Enville Beds	1:2	1:3	1:3
Carboniferous Limestone Series (Carbonate)	1:2	1:2	-
Clay-with-flints with			
Upper Chalk	1:2	1:3.5	1:3.5*

* Extrapolated result.

TABLE 3/8

Types of drainage and maximum slope angles allowable to restrict the percentages of failure to below 1 per cent within 25 years of construction as indicated by the results of the survey

<u>DRIIFT DEPOSITS</u>	Type of drainage	Maximum slope angle (v:h)		
		Height		
		0 - 2.5m	2.5 - 5.0m	More than 5.0m
<u>EMBANKMENTS</u>				
COMBINATIONS OF TWO GEOLOGIES				
River Gravel with London Clay	None	1:2	1:2	1:2
Plateau Gravel with London Clay	Open ditch	1:2	1:2	-
Glacial Gravel with Carboniferous Limestone Series (Carbonate)	Open ditch	1:1.75	1:1.75	1:1.75
Lower Old Red Sandstone - St Maughan's Group	French drain	1:1.75	1:2	1:2
Glacial Head with Lower Lias	Open ditch	1:2	1:2	1:2
Keuper Marl	Open ditch	1:1.5	1:1.5	1:1.5
<u>CUTTINGS</u>				
SINGLE GEOLOGIES				
Plateau Gravel	French drain	1:2.5	1:2.5	1:3
COMBINATIONS OF TWO GEOLOGIES				
Clay-with-flints with Upper Chalk	Open ditch	1:1.25	1:1.25	-

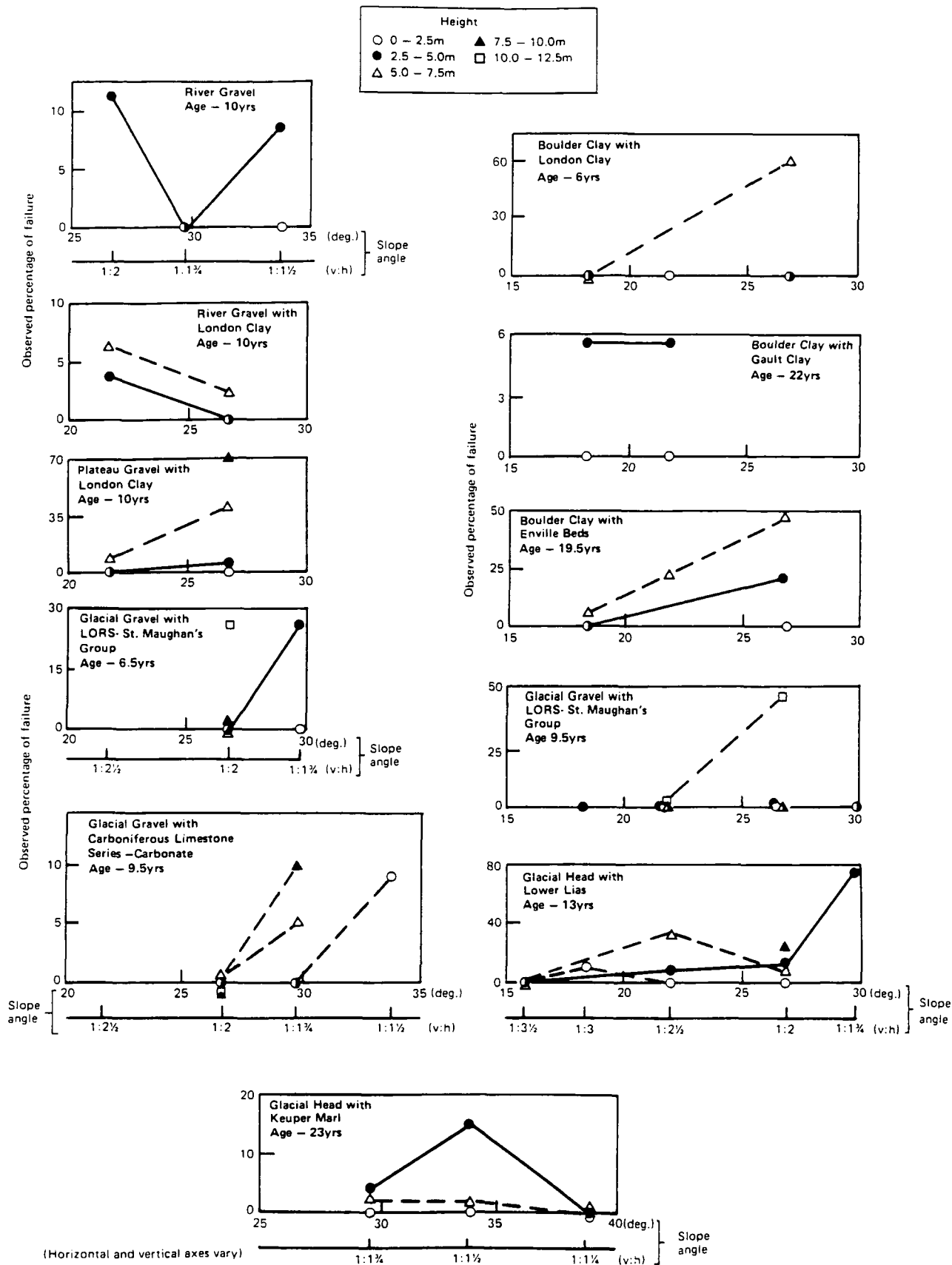


Fig 3/1 Relations between the percentage of failure of embankment slopes and geometry of slope - Drift deposits

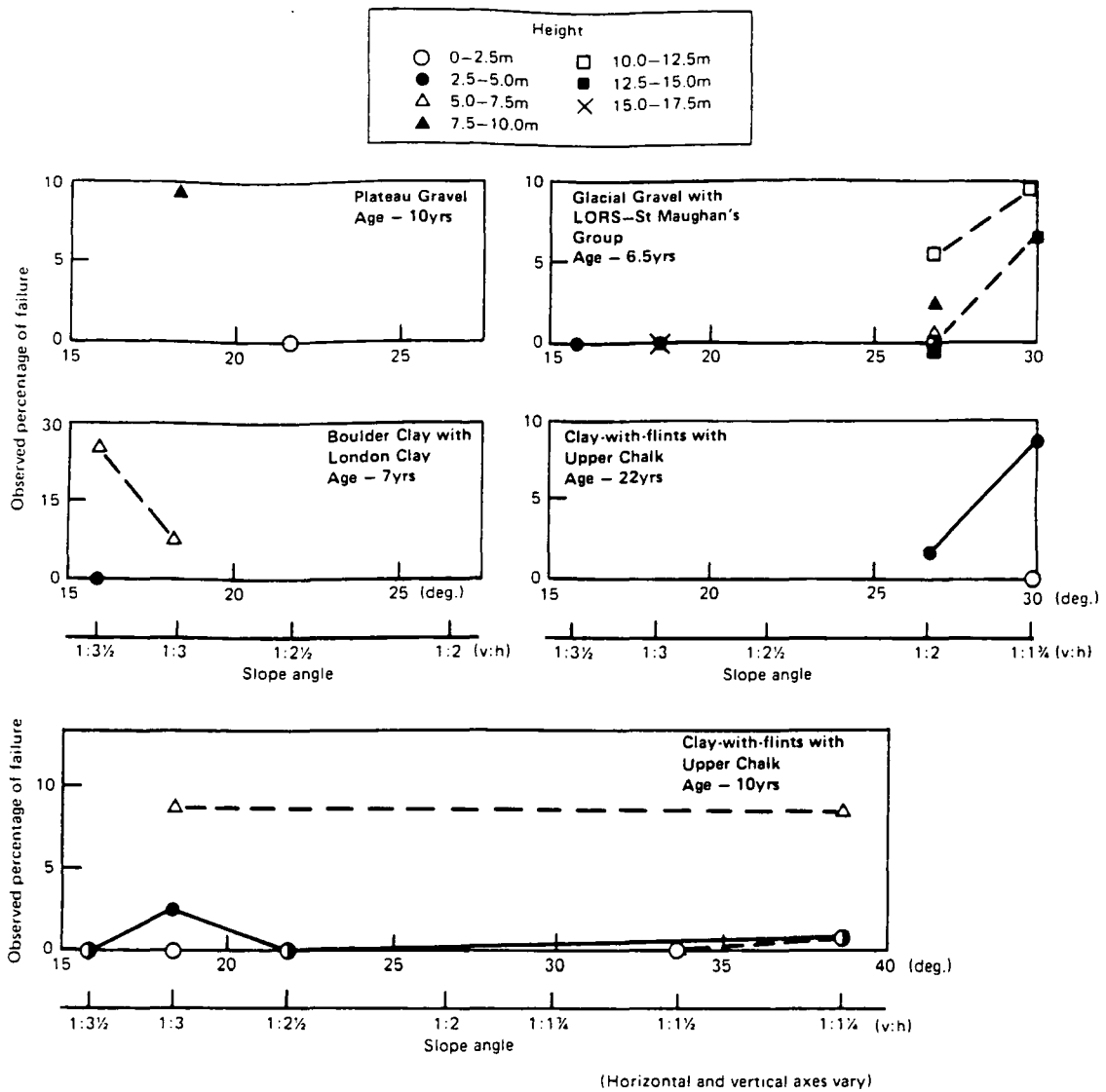


Fig 3/2 Relations between the percentage of failure of cutting slopes and geometry of slope - Drift deposits

Chapter 4
Solid deposits

4.1 Geology

4.1.1 Eocene and Cretaceous deposits

Tables 4/1 and 4/2 show the overall results of single Eocene and Cretaceous deposits and combinations of two geologies, provided they are not associated with younger deposits where they will have appeared previously in Chapter 3. Again only total lengths of slope greater than 1.0km have been considered.

For embankments, Gault Clay, Reading Beds, Reading Beds with Upper Chalk, London Clay with Reading Beds and London Clay have, in descending order, high percentages of failure ranging from 8.2 to 4.4 per cent. The remaining deposits have percentages of failure of 1.6 per cent or less. Overall 1:2 is the most common and steepest predominant slope angle but slope angles as flat as 1:2.5 and 1:3 do occur.

Gault Clay shows a high percentage of failure of 9.6 per cent in cuttings and a predominant slope angle of 1:2.5. Reading Beds have a percentage of failure of 2.9 per cent and the other geologies have percentages of failure of 1.2 per cent or less. Cutting slopes show a greater variety of predominant slope angle than embankments and vary from 1:3 to 1:1.25.

Cutting slopes of Gault Clay had 1.4 per cent more failure than embankment slopes with the predominant slope angle being 1:2.5 in each case. The slopes of Reading Beds and those of London Clay have a much higher percentage of failure in embankments than in cuttings which may be due to the predominant slope angle, for both geologies, being much steeper in embankments.

There are a number of Eocene and Cretaceous deposits that exhibited percentages of failure of less than 1 per cent or had no failures at all.

4.1.2 Jurassic and Triassic deposits

The overall results for Jurassic and Triassic deposits, with total lengths of slope greater than 1.0km, are given in Tables 4/3 and 4/4. Results for combinations of these geologies with a younger deposit are given earlier in Chapter 3 or Section 4.1.1.

Kimmeridge Clay and Oxford Clay are the geologies with the highest percentages of failure in embankment slopes, with values of 6.1 per cent and 5.7 per cent respectively. Lower Keuper Sandstone slopes have a predominant slope angle of 1:1.5 and a percentage of failure of 4.9 per cent. Of these failures, 62 per cent were failures of the topsoil at its junction with the more rocky material within the fill. It would appear, therefore, that although the rock fill is stable, for most slopes of Lower Keuper Sandstone, the topsoil fails at

such steep slope angles. These slips were overgrown at the time of the survey indicating failure at an earlier stage in the motorway's life. Lower Lias and Oxford Clay with Kellaways Beds both have percentages of failure of 3.5 per cent. All other geologies have percentages of failure of 1.2 per cent or less, with some having no failures at all. The commonest predominant slope angle overall is 1:2 with other slope angles ranging from 1:2 up to 1:1.5.

Middle Lias (Silts and Clays) with Lower Lias cutting slopes show a very high percentage of failure of 13.1 per cent. Oxford Clay and Bunter Pebble Beds show percentages of failure of 3.2 and 2.3 per cent respectively. All other geologies have percentages of 1.0 per cent or less. The predominant slope angles for all the cuttings in these geologies range from 1:4 to 1:1.5 with 1:2 being the most frequent.

Oxford Clay and Lower Lias slopes failed in both cuttings and embankments but Oxford Clay with Kellaways Beds failed in embankments only which may reflect the flatter predominant slope angle in cuttings.

4.1.3 Carboniferous and Old Red Sandstone deposits

Tables 4/5 and 4/6 show the overall results for single geologies and combinations of two geologies for Carboniferous and Old Red Sandstone deposits with total lengths of slope greater than 1.0km. Where these deposits are combined with

younger materials they appear earlier in Chapter 3, Section 4.1.1 or Section 4.1.2. The Coal Measures and Millstone Grit Series are divided into argillaceous and arenaceous lithologies, using information from geological survey maps and observations made during the survey. These divisions were necessary as the stability of each lithology varied.

There is no percentage of failure greater than 0.8 per cent for embankments constructed from these geologies and the failures that do occur are in geologies with some argillaceous material present. These failures appear to be a result of weathering of the shale or mudstone at the surface of the fill beneath the topsoil. The predominant slope angle in all cases is 1:2.

Cutting slopes of Enville Beds have 5.8 per cent failure; other materials have 1.7 per cent or less and some have none at all. Cutting slopes of Carboniferous Limestone Series (Carbonate) have 1.1 per cent failure. This is due to failure of the soil which infills cavities within the limestone as explained in more detail in Chapter 5. The commonest predominant slope angle is 1:2 with a range from 1:2.5 to 1:1.25.

A meaningful comparison cannot be made between the performance of Enville Beds in cuttings and its performance in embankments. Although 3.3km of cutting slope were surveyed in this material, there was only a total length of 75m of embankment slope which is not considered sufficient to be representative.

4.2 Age of earthworks

4.2.1 Eocene and Cretaceous deposits

Tables 4/1 and 4/2 show that the ages of earthworks constructed of Eocene and Cretaceous deposits range from 0 to 22 years. The results of an analysis of the effect of age on the percentage of failure is given in Table 4/7.

There is a clear trend for embankments constructed of London Clay and London Clay with Reading Beds, which shows that slopes of particular geometries on younger earthworks are exhibiting higher percentages of failure than the slopes of older earthworks. A similar trend can be seen in embankments of Oxford Clay in Section 4.2.2. Variations of soil properties, motorway specifications and construction practices are likely explanations of this behaviour. Cutting slopes in London Clay and Gault Clay, exhibit higher percentages of failure as the age of earthworks increases.

4.2.2 Jurassic and Triassic deposits

The ages of the earthworks surveyed in these deposits range from 1 to 25 years. The effect of age on the percentage of failure was analysed and the results are given in Table 4/8. Oxford Clay embankment slopes show a similar trend to the Eocene deposits in Section 4.2.1 where the percentage of failure decreases as the age of the earthworks increases.

However, Lower Lias over a similar range of ages shows the opposite trend in both embankments and cuttings.

4.2.3 Carboniferous and Old Red Sandstone deposits

Tables 4/5 and 4/6 show that the ages of earthworks studied range from 4.5 to 23 years. An analysis of the effect of age on the percentage of failure is shown in Table 4/9. Embankment slopes and cutting slopes show a similar trend, with higher percentages of failure occurring on the older motorways. There is one exception to this trend in Lower Old Red Sandstone - St. Maughan's Group, where 5 year old slopes with a geometry of 1:2 slope angle and a height of more than 5.0m show a higher percentage of failure than slopes of 6.5 years, 9.5 years and 20 years of age at the same geometry. This erratic behaviour may reflect the differences in the proportions of strong and weak rock that occur in this formation.

4.3 Geometry of slope

4.3.1 Eocene and Cretaceous deposits

Figures 4/1 and 4/2 show the results of the effect of various combinations of geology, age and geometry on the percentage of failure, for slopes of total length in excess of 2.5km with a percentage of failure greater than 1 per cent.

It was recognized during the survey that Reading Beds contained

two extensive soil types, one that was granular and the other cohesive, occurring in two distinct areas. The cohesive beds contained the majority of failures and consequently are analysed in detail.

Total failure has occurred in embankment slopes of Reading Beds (cohesive) which have a slope angle of 1:2 and heights in the range of 12.5m to 15.0m. Although embankments within this height range in an over-consolidated clay are uncommon, Reading Beds (cohesive) showed high percentages of failure for all heights above 2.5m at 1:2. Similarly, Gault Clay (22 years old) has a high percentage of failure of nearly 50 per cent at 1:2.5 and over 25 per cent at 1:2 for heights between 5.0m and 7.5m. Greenwood, Holt and Herrick (1985) also report a large number of failures in this material on the A45 trunk-road at a slope angle of 1:2. Reading Beds (cohesive), Reading Beds with Upper Chalk, London Clay with Reading Beds (cohesive) and Gault Clay all show a reduction in the percentage of failure with increasing slope angle. (Upper Tunbridge Wells Sand shows a gradual increase and then a reduction in the percentage of failure for one particular height band but the percentages are small.) London Clay, as a single geology, and Weald Clay show the opposite trend.

In cuttings, the two geologies represented show high percentages of failure. Twenty-two year old Gault Clay slopes at 1:3 between 5.0m and 7.5m high have a percentage of failure in excess of 50 per cent. The 10 year old slopes in Gault Clay

show an increase in the percentage of failure with an increase in slope angle while the 22 year old slopes show a maximum percentage of failure at a slope angle of 1:3. It is reasonable to assume that the older Gault Clay slopes would behave similarly to the 10 year old slopes, with the percentage of failure increasing, if slopes with angles steeper than 1:2 had been found.

There is a clear indication, with both embankments and cuttings, that the percentage of failure increases as the height of slope increases.

4.3.2. Jurassic and Triassic deposits

The effect of geometry on the percentage of failure is illustrated in Figures 4/3 and 4/4 for Jurassic and Triassic deposits with total lengths of slope in excess of 2.5km and a percentage of failure of greater than 1 per cent. Embankment slopes of Oxford Clay, Kimmeridge Clay and Lower Lias and cutting slopes in Oxford Clay show percentages of failure of 50 per cent or more for certain combinations of geometry. Bunter Pebble Beds and Lower Keuper Sandstone embankment slopes, and Bunter Pebble Beds and Keuper Conglomerate cutting slopes exhibit lower percentages of failure. The results for each height band do not always cover more than one slope angle.

In the 10 year old Oxford Clay embankments there is a strong trend for the percentage of failure to decrease as slope angle

increases. However, the 22 year old Oxford Clay embankments, covering the same range of slope angle, show the opposite trend for one height band, the same trend for another and a constant percentage of failure for 2.5-5.0m. Lower Lias embankments (25 years old) show a similar pattern to that seen with other geologies, where there is an increase in the percentage of failure as the slope angle increases at the lower end of the range, then a reduction occurs at steeper slope angles.

Presumably the percentage of failure would have again increased if slopes with steeper angles had been encountered.

Kimmeridge Clay shows a reduction in the percentage of failure with an increase in slope angle.

In cuttings, the 22 year old Oxford Clay slopes show an increase in the percentage of failure at steeper slope angles.

In both embankment and cutting slopes, there is evidence that as the height of slope increases so does the percentage of failure.

4.3.3 Carboniferous and Old Red Sandstone deposits

As shown in Table 4/5, no lengths of embankment slope were found, in these materials, with a percentage of failure greater than 1 per cent. The geometry of these slopes has proved to be sufficient to prevent most failures from occurring.

Consequently an analysis of the effect of geometry on the percentage of failure, for these lengths of embankment slope,

is not possible.

Figure 4/5 shows the results of the effect of geometry on the percentages of failure for cutting slopes. Only geologies with a total length of slope greater than 2.5km and a percentage of failure greater than 1 per cent were considered. Enville Beds have a trend of increasing percentage of failure with increasing slope angle for two bands of height, and Raglan Marl Group (6.5 years old) shows the same trend for one band of height. St. Maughan's Group (5.0 years old) has one band of height with increasing percentage of failure, and another with decreasing percentage, as the slope angle is steepened.

In most cases the percentage of failure increases as the height of slope increases.

4.4 Type of drainage

4.4.1 Eocene and Cretaceous deposits

At the bottom of embankment slopes there were seven cases where the effect of all three types of drainage could be compared. The types of drainage associated with the slopes having the highest percentage of failure varied in each case. French drains and no drainage were highest in two cases and open ditches were highest in three cases. Open ditches never occurred at the bottom of slopes with the least percentage of failure. Studying all the cases where more than one type of

drainage occurred, twelve out of a total of nineteen cases showed slopes with open ditches as having the highest percentage of failure. French drains accounted for three of the other cases and no drainage for the remaining four. The last two types of drainage each had some cases where the percentage of failure of the slope was greater than for a comparable slope with open ditch. Open ditches occurred with slopes having the least percentage of failure in three cases compared to eight for each of the two other types of drainage. It would appear from these results that open ditches at the bottom of embankment slopes are associated with the majority of failures. The ranges of percentages of failure found are,

French drain	0 - 46 per cent
Open ditch	0 - 45 per cent
None	0 - 22 per cent

Only five cases for comparison could be made of drainage at the top of cuttings. In the one case where all three types of drainage could be compared, the highest percentage of failure was for slopes with no drainage. These slopes also had a distinctly higher percentage of failure when compared with French drain only. There were three cases in Gault Clay where slopes with open ditches had a distinctly higher percentage of failure than slopes with no drainage. The ranges of percentages of failure found are,

Open ditch	0 - 83 per cent
------------	-----------------

None	5.8 - 37 per cent
French drain	0 - 10 per cent

There are insufficient data for cuttings to describe trends for all the geologies. In Gault Clay cuttings, however, there is a higher percentage of failure in slopes associated with open ditches at the top, rather than in slopes with no drainage.

The effect of slope drains, that is drains situated on the slope itself rather than just at the top or bottom, on the percentages of failure of cutting slopes in Reading Beds (cohesive) is given in Table 4/10 for slope angles of 1:3. These results clearly show that slope drains can prevent shallow failures from occurring with this type of material. The slopes affected by slope drains accounted for thirty per cent of the cutting slope at 1:3 in Reading beds (cohesive).

4.4.2 Jurassic and Triassic deposits

There were three cases of embankment slopes where all three types of base drainage could be compared. Each case had slopes with one of the three types of drainage associated with the highest percentage of failure. Where two or three types of drainage could be compared, fifteen out of a total of twenty-one cases had slopes with open ditches associated with the highest percentage of failure. In fourteen out of the twenty-one cases, slopes with no drainage had the least percentage of failure. The ranges of percentages of failure are,

Open ditch	0 - 62 per cent
French drain	0 - 58 per cent
None	0 - 34 per cent

In cuttings, comparing all cases including one where all three types of drainage occurred, slopes with open ditches at the top had the highest percentage of failure in four out of the total of six cases. Slopes with no drainage had the least percentage of failure in five of the cases. The performance of slopes with French drains cannot be fully established as there were only two cases for comparison. The ranges of percentages of failure are as follows:

Open ditch	6 - 52 per cent
None	0 - 20 per cent
French drain	0 - 3 per cent

Open ditches at the bottom of embankment slopes and at the top of cutting slopes appear to be associated with most of the highest percentages of failure. The lowest percentages of failure occurred with slopes which had no drainage.

In the survey, the area found to have the most slope drains on embankments was the M6 in Staffordshire on slopes of Keuper Marl. These lengths, with slope angles up to 1:1.5 and heights greater than 5.0m, had no failures of either slopes with drains on them (which accounted for twenty five per cent

of the measured length) or of slopes without drains. Other motorways, with similar slope characteristics and no slope drains only show small percentages of failure, illustrating the good performance of the existing Keuper Marl embankments up to the present time. Based on the results of the survey, slope drains in Keuper Marl embankments, under normal drainage conditions, will prevent only a small number of failures occurring within 23 years of construction. This number of failures is probably too small to warrant the cost of extensive slope drains. Although the evidence for the use of slope drains in Keuper Marl embankments is unfavourable, this certainly does not mean that other materials would not benefit from such drainage facilities. For example, outside the survey area, slope drains installed in an embankment slope of Gault Clay (Johnson, 1985) are currently stable while adjacent untreated slopes are failing; slope drains were also the least expensive of the two preventative measures considered.

4.4.3 Carboniferous and Old Red Sandstone deposits

The design and maintenance of the types of drainage used, as well as the geometry, may be further reasons for the lack of failure in most of these geologies. The slips that have occurred are in cuttings of Enville Beds and Lower Old Red Sandstone where nearly 16km of slopes were surveyed. In these materials there are insufficient data from which to draw any conclusions about the effect of drainage on slope failures.

4.5 Orientation of slope

Out of all the geologies studied, Reading Beds (cohesive) was the only geology which showed any distinct trend toward a particular slope orientation having an effect on the percentage of failure. In this material, the majority of slope angle and height combinations with the highest percentages of failure in embankments, and all the highest percentages in cuttings, faced toward the north as shown in Table 4/11.

4.6 Design of side slopes in new construction

4.6.1 Eocene and Cretaceous deposits

Results of an analysis of the maximum slope angles allowable to minimize failure in the height range of 0-2.5m, 2.5-5.0m and greater than 5.0m are given in Tables 4/12 and 4/13.

Comparisons can be made, with Tables 4/1 and 4/2, between the predominant slope angle and those required for a percentage of failure of less than 1 per cent. The major over-consolidated clays would require flatter slope angles. Gault Clay, for example, in embankments and cuttings, would require a slope angle of 1:5 (for slopes greater than 5.0m high) in order to reduce percentages of failure, while their current predominant slope angle is 1:2.5 in both cases.

A considerable amount of data exists concerning the stability of cutting slopes in London Clay as reviewed by Skempton

(1977). Vaughan and Walbancke (1973), Leonards (1979) and subsequently Tavenas and Leroueil (1981) used this data and, based on the relation between the pore pressure parameter r_u and time, produced a graph of slope angle against time (Figure 4/6). The recommended slope angle from the survey was 1:3.5, indicating that failures were occurring at 1:3, and the maximum age for this recommendation was 10 years. Figure 4/6, however, indicates that 1:3 cutting slopes should fail at 45 years. A possible reason for this is that Skempton's original back-analyses was of deep-seated failures and pore water pressures were only measured at depths greater than those associated with shallow failures. Although pore water pressure equilibration is described as being a slow process at depth, nearer the surface equilibration appears to be achieved much more rapidly. Shallow failures might also have occurred on these slopes nearer the time of construction. Time will tell as to whether deeper failures will occur on cutting slopes at 1:3 on the present motorway system and the survey computer database will be a valuable source for fulfilling this purpose. Based on the results of both sets of data a slope angle of 1:3.5 is recommended for London Clay cutting slopes; this slope angle should prevent shallow failures for at least 10 years after construction and prevent deeper failures for at least 120 years after construction.

Table 4/14 shows how the use of particular types of drainage located at the bottom of embankments and the top of cuttings can result in a steepening of the recommended slope angle for a

number of geologies. Open ditches are associated with most of the highest percentages of failure, as shown in Section 4.4, and so they are not a recommended type of drainage for most of the geologies shown.

For cuttings in Reading Beds (cohesive), the recommended slope angle can be altered by taking into account the slope's orientation (Table 4/11). On those slopes up to 5.0m high which face east, south or west, with any type of drainage, the recommended slope angle can be steepened to 1:3.5. For slopes facing south with a French drain at the top, further steepening to a slope angle of 1:3 is possible while still keeping failures to a minimum.

4.6.2 Jurassic and Triassic deposits

Tables 4/15 and 4/16 show the results of an analysis of the maximum slope angles allowable to minimize failure in the height ranges 0-2.5m, 2.5- 5.0m and greater than 5.0m. Comparisons with the predominant slope angles in Tables 4/3 and 4/4 can be made. Oxford Clay, for example in embankments and cuttings, was commonly constructed at a slope angle of 1:2 but a percentage of failure of less than 1 per cent would have been achieved on slopes more than 5.0m high if, based on the results of the survey, a slope angle of 1:3.5 had been used.

Table 4/17 shows how the recommended slope angle for Oxford Clay embankments and Bunter Pebble Beds cuttings can be

steepened if a particular type of drainage is used.

4.6.3 Carboniferous and Old Red Sandstone deposits

Tables 4/18 and 4/19 show the results of an analysis of the maximum slope angles allowable to minimize failure in the height ranges of 0-2.5m, 2.5-5.0m and greater than 5.0m. Comparisons can be made, with Tables 4/5 and 4/6, between the predominant slope angles and those required for percentages of failure of less than 1 per cent. In embankments, for a large number of geologies, the predominant slope angle is the same as the maximum allowable to minimize failures on slopes more than 5.0m high. This indicates that, for these materials, the original design has proved to be correct for the majority of slopes and conservative for the shorter lengths of slope at a flatter slope angle than the predominant. The exceptions which would require flatter slope angles are Middle Coal Measures (Argillaceous), Middle Coal Measures (Argillaceous with Arenaceous) and Lower Coal Measures (Argillaceous with Arenaceous). The only geology which is stable at a steeper slope angle than the predominant is Millstone Grit Series (Argillaceous with Arenaceous). For cuttings, there is some evidence that for certain geologies a steeper slope angle than the predominant one would still produce a percentage of failure of less than 1 per cent. Some geologies, particularly Enville Beds, show percentages of failure in excess of 1 per cent and would require flatter slope angles to reduce the amount of failure.

TABLE 4/1

Eocene and Cretaceous deposits encountered in the survey, with a total length of slope in excess of 1.0km.

	Age of earthworks when surveyed (years)	Total length (km)	Percentage of measured failure	Predominant slope angle all heights (v:h)
<u>EMBANKMENTS</u>				
<u>EOCENE DEPOSITS</u>				
	SINGLE GEOLOGIES			
London Clay	5,6,10	60.9	4.4	1:2
Reading Beds	3,10	40.7	7.6	1:2
	COMBINATIONS OF TWO GEOLOGIES			
Bagshot Beds with London Clay	5	1.6	0	-
London Clay with Reading Beds	10,14	10.7	5.0	1:2
Reading Beds with Upper Chalk	10	4.1	5.9	1:2
<u>CRETACEOUS DEPOSITS</u>				
	SINGLE GEOLOGIES			
Upper Chalk	10,19,22	11.1	0.1	1:2
Middle Chalk	3,22	5.3	0	1:2
Lower Chalk	10,22	7.7	<0.1	1:2
Gault Clay	9,22	5.3	8.2	1:2.5
Lower Greensand	22	4.1	0.1	1:2.5
Weald Clay	9	12.0	1.6	1:2.5
Folkestone Beds	9	1.2	0	1:3
Upper Tunbridge Wells Sand	9	14.2	1.0	1:2
	COMBINATIONS OF TWO GEOLOGIES			
Upper Chalk with Lower Chalk	10	3.7	0	1:2
Lower Chalk with Upper Greensand	10	4.3	0	1:2
Upper Greensand and Gault Clay	10	1.6	0	1:2
Weald Clay with Upper Tunbridge Wells Sands	8,9	4.0	0.4	1:2
Folkestone Beds with Sandgate Beds	9	1.3	0	1:3

TABLE 4/2

Eocene and Cretaceous deposits encountered in the survey, with a total length of slope in excess of 1.0km.

	Age of earthworks when surveyed (years)	Total length (km)	Percentage of measured failure	Predominant slope angle all heights (v:h)
<u>CUTTINGS</u>				
<u>EOCENE DEPOSITS</u>				
	SINGLE GEOLOGIES			
Bagshot Beds	5	1.5	0	-
London Clay	0,3,5,6,7,10	20.2	0.3	1:3
Reading Beds	10	20.0	2.9	1:3
<u>CRETACEOUS DEPOSITS</u>				
	SINGLE GEOLOGIES			
Upper Chalk	3,10,14,22	28.4	0	1:2
Middle Chalk	3,9,10,22	10.6	0	1:2
Lower Chalk	9,10,22	13.8	0.1	1:2
Gault Clay	10,22	6.5	9.6	1:2.5
Lower Greensand	10,22	2.7	0	1:1.75
Weald Clay	9	6.1	0	1:3
Folkestone Beds	9	1.7	1.2	1:1.5
Upper Tunbridge Wells Sand	9	14.9	0.4	1:2
	COMBINATIONS OF TWO GEOLOGIES			
Lower Chalk with Upper Greensand	10	1.2	0	1:1.25

TABLE 4/3

Jurassic and Triassic deposits encountered in the survey, with a total length of slope in excess of 1.0km.

	Age of earthworks when surveyed (years)	Total length (km)	Percentage of measured failure	Predominant slope angle all heights (v:h)
<u>EMBANKMENTS</u>				
<u>JURASSIC DEPOSITS</u>				
SINGLE GEOLOGIES				
Kimmeridge Clay	10	16.7	6.1	1:2
Coral Rag	10	3.6	0	1:2
Oxford Clay	10,22	33.8	5.7	1:2
Great Oolite Clay	10	7.5	0	1:1.75
Acton Turville Beds	10	1.1	0	1:2
Middle Lias (Silts and Clays)	25	2.8	0	1:2
Lower Lias	4.5,13,25	34.1	3.5	1:2
COMBINATIONS OF TWO GEOLOGIES				
Kimmeridge Clay with Coral Rag	10	1.1	0	1:1.75
Oxford Clay with Kellaways Beds	10	1.6	3.5	1:1.75
Kellaways Beds with Cornbrash	10	7.9	0.9	1:1.75
Cornbrash with Great Oolite Clay	10	1.1	0	1:1.5
<u>TRIASSIC DEPOSITS</u>				
SINGLE GEOLOGIES				
Keuper Marl	10,20,23	29.6	<0.1	1:1.5
Lower Keuper Sandstone	10,23	4.0	4.9	1:1.5
Bunter Pebble Beds	19.5,23	6.5	1.2	1:2
COMBINATIONS OF TWO GEOLOGIES				
Keuper Marl with Lower Keuper Sandstone	23	1.9	0.8	1:1.5
Bunter Pebble Beds	23	1.3	0	1:2
Lower Old Red Sandstone - St.Maughan's Group	5,20	1.8	0	1:2
Lower Keuper Sandstone with Bunter Pebble Beds	23	1.4	0	1:2
Bunter Pebble Beds with Keele Beds	23	3.1	0	1:2

TABLE 4/4

Jurassic and Triassic deposits encountered in the survey, with a total length of slope in excess of 1.0km.

	Age of earthworks when surveyed (years)	Total length (km)	Percentage of measured failure	Predominant slope angle all heights (v:h)
<u>CUTTINGS</u>				
<u>JURASSIC DEPOSITS</u>				
	SINGLE GEOLOGIES			
Kimmeridge Clay	10	4.5	0	-
Coral Rag	10	2.4	0	1:2.5
Oxford Clay	10,22	14.6	3.2	1:2
Kellaways Beds	10	6.1	0	1:4
Cornbrash	10	3.8	0	1:1.5
Great Oolite Clay	10	9.0	0	-
Acton Turville Beds	10	2.0	0	-
Great Oolite Limestone	10	2.4	0	-
Middle Lias (Marlstone Rock)	25	2.5	0	1:2
Middle Lias (Silts and Clays)	25	6.5	0.6	1:2
Lower Lias	4, 5, 13, 25	41.0	0.4	1:3
	COMBINATIONS OF TWO GEOLOGIES			
Oxford Clay with Kellaways Beds	10	1.1	0	1:3
Kellaway Beds with Cornbrash	10	1.9	0	1:2
Middle Lias (Silts and Clays) with Lower Lias	25	1.7	13.1	1:2
	SINGLE GEOLOGIES			
<u>TRIASSIC DEPOSITS</u>				
Rhaetic	4.5	4.5	<0.1	1:2
Keuper Marl	4.5, 5, 10, 20, 23	35.6	0.2	1:2
Keuper Conglomerate	2, 4.5, 9.5, 20	3.0	1.0	1:2
Lower Keuper Sandstone	10, 23	5.3	0	1:1.5
Bunter Pebble Beds	1, 19.5, 23	10.6	2.3	1:2

TABLE 4/5

Carboniferous and Old Red Sandstone deposits encountered in the survey,
with a total length of slope in excess of 1.0km.

	Age of earthworks when surveyed (years)	Total length (km)	Percentage of measured failure	Predominant slope angle all heights (v:h)
<u>EMBANKMENTS</u>				
<u>CARBONIFEROUS DEPOSITS</u>				
SINGLE GEOLOGIES				
Middle Coal measures (Argillaceous)	14,15	12.8	0.5	1:2
Lower Coal Measures (Argillaceous)	13	9.3	0.3	1:2
Lower Coal Measures (Arenaceous)	13	1.6	0	1:2
Millstone Grit Series (Argillaceous)	4.5,15	8.9	<0.1	1:2
Millstone Grit Series (Arenaceous)	4.5,15	1.8	0	1:2
Carboniferous Limestone Series (Carbonate)	9.5	10.3	0	1:2
COMBINATIONS OF TWO GEOLOGIES				
Upper Coal Meas (Arg) with Upper Coal Meas (Aren)	15	2.0	0	1:2
Middle Coal Meas (Arg) with Middle Coal Meas (Aren)	14,15	38.5	0.8	1:2
Lower Coal Meas (Arg) with Lower Coal Meas (Aren)	4.5,13,14	24.8	0.8	1:2
Mill Grit Series (Arg) with Mill Grit Series (Aren)	4.5,15	20.1	0	1:2
<u>OLD RED SANDSTONE</u>				
<u>DEPOSITS</u>				
SINGLE GEOLOGIES				
Lower Old Red Sandstone - St Maughan's Group	5,9.5,20	6.4	0	1:2
COMBINATIONS OF TWO GEOLOGIES				
Lower Old Red Sandstone - Brownstone Group with Lower Old Red Sandstone - St Maughan's Group	6.5	2.5	0	1:2

TABLE 4/6

Carboniferous and Old Red Sandstone deposits encountered in the survey,
with a total length of slope in excess of 1.0km.

	Age of earthworks when surveyed (years)	Total length (km)	Percentage of failure	Predominant measured slope angle all heights (v:h)
<u>CUTTINGS</u>				
<u>CARBONIFEROUS DEPOSITS</u>				
	SINGLE GEOLOGIES			
Enville Beds	19.5	3.3	5.8	1:2.5
Keele Beds	19.5, 23	2.6	0	1:1.75
Upper Coal Measures (Argillaceous)	15	1.1	0	1:2
Upper Coal Measures (Arenaceous)	15	4.4	0	1:2
Middle Coal Measures (Argillaceous)	14, 15	22.2	0.9	1:2
Middle Coal Measures (Arenaceous)	14, 15	3.5	0.7	1:2
Lower Coal Measures (Argillaceous)	4.5, 13, 14	11.6	0.3	1:2
Lower Coal Measures (Arenaceous)	4.5, 13	1.8	0	1:2
Millstone Grit Series (Argillaceous)	4.5, 15	3.8	0.3	1:2
Millstone Grit Series (Arenaceous)	4.5, 13, 15	13.4	0.1	1:1.25
Carboniferous Limestone Series (Carbonate)	4.5, 9.5, 16, 17	6.7	1.1	1:2
	COMBINATIONS OF TWO GEOLOGIES			
Upper Coal Meas (Arg) with Upper Coal Meas (Aren)	15	1.1	0	1:2
Middle Coal Meas (Arg) with Middle Coal Meas (Aren)	14, 15	23.3	0.4	1:2
Lower Coal Meas (Arg) with Lower Coal Meas (Aren)	13, 14	21.0	0.4	1:2
Mill Grit Series (Arg) with Mill Grit Series (Aren)	4.5, 15	13.9	<0.1	1:1.75
	SINGLE GEOLOGIES			
<u>OLD RED SANDSTONE DEPOSITS</u>				
Upper Old Red Sandstone	9.5, 20	3.7	0.5	1:2
Lower Old Red Sandstone - St. Maughan's Group	5, 6.5, 9.5, 20	9.7	1.7	1:2
Lower Old Red Sandstone - Raglan Marl Group	6.5, 7, 20	2.9	1.5	1:2

TABLE 4/7

Comparisons of the percentages of failure in embankments
and cuttings of different ages for given
Eocene and Cretaceous deposits and geometry

Geology	Slope angle (v:h)	Height (m)	Age (years)	Total length (m)	Percentage of failure
<u>Embankments</u>					
London Clay	1:2	0-2.5	5,6	551	0
			10	7426	0
		2.5-5.0	5,6	625	14.6
			10	9499	6.2
		more than 5.0	5,6	149	32.2
			10	7596	21.6
London Clay with Reading Beds	1:2	0-2.5	10	834	1.8
			14	286	0
		2.5-5.0	10	713	14.8
			14	302	3.3
		more than 5.0	10	1008	11.7
			14	429	6.2
<u>Cuttings</u>					
London Clay	1:3	0-2.5	0	424	0
			10	380	3.2
		2.5-5.0	0	390	0
			6	533	1.9
			10	543	3.2
Gault Clay	1:2.5	0-2.5	10	348	0
			22	202	0
		2.5-5.0	10	353	3.8
			22	299	4.4

TABLE 4/8

Comparisons of the percentages of failure in embankments and cuttings of different ages for given Jurassic and Triassic deposits and geometry.

Geology	Slope angle (v:h)	Height (m)	Age (years)	Total length (m)	Percentage of failure
<u>Embankments</u>					
Oxford Clay	1:2	0-2.5	10	3567	2.0
			22	1417	1.8
		2.5-5.0	10	1191	23.0
			22	1500	7.1
		more than 5.0	10	512	41.4
			22	1263	36.3
Lower Lias	1:2	0-2.5	13	3672	0
			25	654	5.5
		2.5-5.0	13	2402	1.7
			25	694	12.6
		more than 5.0	13	1726	10
			25	293	32.6
<u>Cuttings</u>					
Lower Lias	1:2	0-2.5	4.5	443	0
			25	679	6.4
		2.5-5.0	4.5	529	0
			25	894	1.4

TABLE 4/9

Comparisons of the percentages of failure in embankments and cuttings of different ages for given Carboniferous and Old Red Sandstone deposits and geometry

Geology	Slope angle (v:h)	Height (m)	Age (years)	Total length (m)	Percentage of failure
		0-2.5	4.5	373	0
			13,14	2731	0
<u>Embankments</u>					
Lower Coal Measures (Argillaceous with Arenaceous)	1:2	2.5-5.0	4.5	670	0
			13,14	3322	4.4
		more than 5.0	4.5	917	0
			13,14	3718	0.8
		0-2.5	5	392	0
			9.5	508	0
			20	223	0
<u>CUTTINGS</u>					
Lower Old Red Sandstone - St Maughan's Group	1:2	2.5-5.0	5	443	0
			9.5	570	0
			20	449	0
		more than 5.0	5	736	7.6
			6.5	382	1.0
			9.5	952	1.9
			20	742	2.0



TABLE 4/10

The effect of slope drains on the percentages of failure in cuttings of Reading Beds (cohesive) at a slope angle of 1:3 (10 years old).

Height (m)	Percentage of failure	
	Slopes without drains	Slopes with drains
0-2.5	0	0
2.5-5.0	5	0
more than 5.0	33	0

TABLE 4/11

Effect of slope orientation on the percentages of failure of Reading Beds (cohesive) embankment and cutting slopes (10 years old)

	Slope angle (v:h)	Height (m)	Percentage of failure	
			North	East, South, West
Embankments	1:2.5	0-2.5	8	0
	1:2.5	2.5-5.0	41	7
	1:2.5	5.0-7.5	60	19
	1:2	2.5-5.0	9	15
	1:2	5.0-7.5	31	27
Cuttings	1:3.5	2.5-5.0	10	0
	1:3	2.5-5.0	14	1
	1:3	5.0-7.5	41	10

TABLE 4/12

Maximum slope angles allowable to restrict the percentages of failure to below 1 per cent within 22 years of construction as indicated by the results of the survey

Maximum slope angle (v:h)

	Height		
	0 - 2.5m	2.5 - 5.0m	: More than 5.0m
<u>EMBANKMENTS</u>			
<u>EOCENE DEPOSITS</u>			
	SINGLE GEOLOGIES		
London Clay	1:2	1:3	1:3*
Reading Beds (cohesive)	1:3	1:4*	1:4*
(non-cohesive)	1:1.75	1:1.75	1:1.75
	COMBINATIONS OF TWO GEOLOGIES		
London Clay with Reading Beds	1:2.5	1:3*	1:3*
Reading Beds with Upper Chalk	1:2.5	1:3*	1:3*
<u>CRETACEOUS DEPOSITS</u>			
	SINGLE GEOLOGIES		
Upper Chalk	1:2	1:2	1:2
Middle Chalk	1:2	1:2	1:2
Lower Chalk	1:2	1:2	1:2
Gault Clay #	1:3.5*	1:4*	1:5*
Lower Greensand	1:2	1:2	-
Weald Clay	1:2.5	1:3*	1:3*
Folkestone Beds	1:3	1:3	1:3
Upper Tunbridge Wells Sand	1:2	1:2.5	1:3
	COMBINATIONS OF TWO GEOLOGIES		
Upper Chalk with Lower Chalk	1:2	1:2	1:2
Lower Chalk with Upper Greensand	1:2	1:2	1:2
Upper Greensand with Gault Clay	1:2	1:2	1:2
Weald Clay with Upper Tunbridge Wells Sand	1:2	1:2	1:2.5
Folkestone Beds with Sandgate Beds	1:3	1:3	1:3

* Extrapolated result.

These results take account of a failure on a more recently constructed motorway (M26) than those included in the survey.

TABLE 4/13

Maximum slope angles allowable to restrict the percentages of failure to below 1 per cent within 22 years of construction as indicated by the results of the survey

Maximum slope angle (v:h)

0 - 2.5m : ^{Height} 2.5 - 5.0m : More than 5.0m

CUTTINGS

EOCENE DEPOSITS

SINGLE GEOLOGIES

London Clay	1:3.5	1:3.5	1:3.5
Reading Beds (cohesive)	1:4*	1:4*	1:4*
(non-cohesive)	1:2.5	1:2.5	1:3

CRETACEOUS DEPOSITS

SINGLE GEOLOGIES

Upper Chalk	1:1.25	1:1.25	1:1.25
Middle Chalk	1:1	1:1	1:1
Lower Chalk	1:1.5	1:2	1:2
Gault Clay	1:3.5	1:4	1:5*
Lower Greensand	1:1.75	1:1.75	1:1.75
Weald Clay	1:2.5	1:2.5	1:2.5
Upper Tunbridge Wells Sand	1:2	1:2	1:2.5

COMBINATIONS OF TWO GEOLOGIES

Lower Chalk with Upper Greensand	1:1.25	1:1.25	1:1.25
-------------------------------------	--------	--------	--------

* Extrapolated result.

TABLE 4/14

Types of drainage and maximum slope angles allowable to restrict the percentages of failure to below 1 per cent within 22 years of construction as indicated by the results of the survey

	Type of drainage	Maximum slope angle (v:h)		
		Height		
		0 - 2.5m	2.5 - 5.0m	More than 5.0
<u>EMBANKMENTS</u>				
<u>EOCENE DEPOSITS</u>		SINGLE GEOLOGIES		
London Clay	None	1:2	1:2.5	-
Reading Beds (cohesive)	French drain	1:2.5	-	-
COMBINATIONS OF TWO GEOLOGIES				
London Clay with Reading Beds	French drain	1:2	1:2	-
<u>CRETACEOUS DEPOSITS</u>		SINGLE GEOLOGIES		
Weald Clay	Open ditch	1:2	1:2.5	1:2.5
Upper Tunbridge Wells Sand	None	1:2	1:2	1:2
<u>CUTTINGS</u>				
<u>EOCENE DEPOSITS</u>		SINGLE GEOLOGIES		
Reading Beds (cohesive)	French drain	1:3	1:3	-

TABLE 4/15

Maximum slope angles allowable to restrict the percentages of failure to below 1 per cent within 25 years of construction as indicated by the results of the survey

	Maximum slope angle (v:h)		
	0 - 2.5m	Height 2.5 - 5.0m	: More than 5.0m
<u>EMBANKMENTS</u>			
<u>JURASSIC DEPOSITS</u>			
	SINGLE GEOLOGIES		
Kimmeridge Clay	1:2.5	1:3.5*	1:3.5*
Coral Rag	1:2	-	-
Oxford Clay	1:3*	1:3.5*	1:3.5*
Great Oolite Clay	1:1.75	1:1.75	1:1.75
Acton Turville Beds	1:2	1:2	1:2
Middle Lias (Silts and Clays)	1:2	1:2	1:2
Lower Lias	1:5	1:5*	1:5*
	COMBINATIONS OF TWO GEOLOGIES		
Kimmeridge Clay with Coral Rag	1:1.75	1:1.75	-
Kellaways Beds with Cornbrash	1:2	1:2.5	1:3*
<u>TRIASSIC DEPOSITS</u>			
	SINGLE GEOLOGIES		
Keuper Marl	1:1.5	1:1.5	1:1.75*
Lower Keuper Sandstone	1:2*	1:2*	1:2*
Bunter Pebble Beds	1:1.75	1:1.75	1:1.75
	COMBINATIONS OF TWO GEOLOGIES		
Keuper Marl with Lower Keuper Sandstone	1:1.5	1:1.75*	1:2*
Bunter Pebble Beds	1:2	-	-
Bunter Pebble Beds with Keele Beds	1:2	1:2	1:2

* Extrapolated result.

TABLE 4/16

Maximum slope angles allowable to restrict the percentages of failure to below 1 per cent within 25 years of construction as indicated by the results of the survey

	Maximum slope angle (v:h)		
	0 - 2.5m	Height : 2.5 - 5.0m	: More than 5.0m
<u>CUTTINGS</u>			
<u>JURASSIC DEPOSITS</u>	SINGLE GEOLOGIES		
Coral Rag	1:1.25	1:1.25	-
Oxford Clay	1:2.5	1:3	1:3.5*
Kellaways Beds	1:2	1:3	1:3.5
Cornbrash	1:1.5	1:1.5	1:1.5
Middle Lias (Marlstone Rock)	1:2	1:2	1:2
Middle Lias (Silts and Clays)	1:2	1:2.5*	1:2.5*
Lower Lias	1:4	1:5*	1:5*
COMBINATIONS OF TWO GEOLOGIES			
Oxford Clay with Kellaways Beds	1:3	1:3	-
Kellaways Beds with Cornbrash	1:2	1:2	-
Middle Lias (Silts and Clays) with Lower Lias	1:2	1:2.5	1:2.5
<u>TRIASSIC DEPOSITS</u>	SINGLE GEOLOGIES		
Rhaetic	1:1.5	1:1.5	1:1.5
Keuper Marl	1:1.5	1:1.75	1:1.75
Keuper Conglomerate	1:1	-	-
Lower Keuper Sandstone	1:1.25	1:1.25	1:1.5
Bunter Pebble Beds	1:2	1:2	1:2.5

* Extrapolated result.

TABLE 4/17

Types of drainage and maximum slope angles allowable to restrict the percentages of failure to below 1 per cent within 25 years of construction as indicated by the results of the survey

Type of drainage	Maximum slope angle (v:h)			
	Height			
	0 - 2.5m	2.5 - 5.0m	More than 5.0m	

EMBANKMENTSJURASSIC DEPOSITS

SINGLE GEOLOGIES

Oxford Clay

French drain

1:2

1:2

-

CUTTINGSTRIASSIC DEPOSITS

SINGLE GEOLOGIES

Bunter Pebble Beds

None

1:2

1:2

1:2

TABLE 4/18

Maximum slope angles allowable to restrict the percentages of failure to below 1 per cent within 23 years of construction as indicated by the results of the survey

		Maximum slope angle (v:h)		
		0 - 2.5m	Height 2.5 - 5.0m	More than 5.0m
<u>EMBANKMENTS</u>				
<u>CARBONIFEROUS DEPOSITS</u>		<u>SINGLE GEOLOGIES</u>		
Middle Coal Measures (Argillaceous)	1:2.5	1:3*	1:3*	
Lower Coal Measures (Argillaceous)	1:1.75	1:2	1:2	
Lower Coal Measures (Arenaceous)	1:2	1:2	1:2	
Millstone Grit Series (Argillaceous)	1:2	1:2	1:2	
Millstone Grit Series (Arenaceous)	1:2	1:2	1:2	
Carboniferous Limestone Series (Carbonate)	1:2	1:2	1:2	
<u>COMBINATIONS OF TWO GEOLOGIES</u>				
Upper Coal Meas (Arg) with Upper Coal Meas (Aren)	1:2	1:2	-	
Middle Coal Meas (Arg) with Middle Coal Meas (Aren)	1:2	1:2.5	1:3	
Lower Coal Meas (Arg) with Lower Coal Meas (Aren)	1:2	1:2.5	1:2.5	
Mill Grit Series (Arg) with Mill Grit Series (Aren)	1:1.5	1:1.75	1:1.75	
<u>OLD RED SANDSTONE DEPOSITS</u>		<u>SINGLE GEOLOGIES</u>		
Lower Old Red Sandstone -St. Maughan's Group	1:2	1:2	1:2	
<u>COMBINATIONS OF TWO GEOLOGIES</u>				
Lower Old Red Sandstone -Brownstone Group with Lower Old Red Sandstone -St. Maughan's Group	1:1.5	1:1.75	1:2	

* Extrapolated result.

TABLE 4/19

Maximum slope angles allowable to restrict the percentages of failure to below 1 per cent within 23 years of construction as indicated by the results of the survey

Maximum slope angle (v:h)

	Height		
	0 - 2.5m	: 2.5 - 5.0m	: More than 5.0m
<u>CUTTINGS</u>			
<u>CARBONIFEROUS DEPOSITS</u>			
	SINGLE GEOLOGIES		
Enville Beds	1:2	1:2.5	1:3
Keele Beds	1:1.75	1:1.75	-
Upper Coal Measures (Argillaceous)	1:2	1:2	1:2
Upper Coal Measures (Arenaceous)	1:2	1:2	1:2
Middle Coal Measures (Argillaceous)	1:2.5	1:3	1:3.5
Middle Coal Measures (Arenaceous)	1:2	1:2	1:2.5
Lower Coal Measures (Argillaceous)	1:2	1:2	1:2
Millstone Grit Series (Argillaceous)	1:1.75	1:1.75	1:1.75
Millstone Grit Series (Arenaceous)	1:1.5	1:1.5	1:1.75
Carboniferous Limestone Series (Carbonate)	1:1	1:1.25	1:1.25
COMBINATIONS OF TWO GEOLOGIES			
Upper Coal Meas (Arg) with Upper Coal Meas (Aren)	1:2	1:2	1:2
Middle Coal Meas (Arg) with Middle Coal Meas (Aren)	1:2	1:2.5	1:2.5
Lower Coal Meas (Arg) with Lower Coal Meas (Aren)	1:1.75	1:2	1:2.5
Mill Grit Series (Arg) with Mill Grit Series (Aren)	1:1	1:1	1:1
<u>OLD RED SANDSTONE</u>			
<u>DEPOSITS</u>			
Upper Old Red Sandstone	1:1.75	1:2	1:2
Lower Old Red Sandstone -St. Maughan's Group	1:1.75	1:2	1:2.5
Lower Old Red Sandstone - Raglan Marl Group	1:2	1:2.5	1:2.5*

* Extrapolated result.

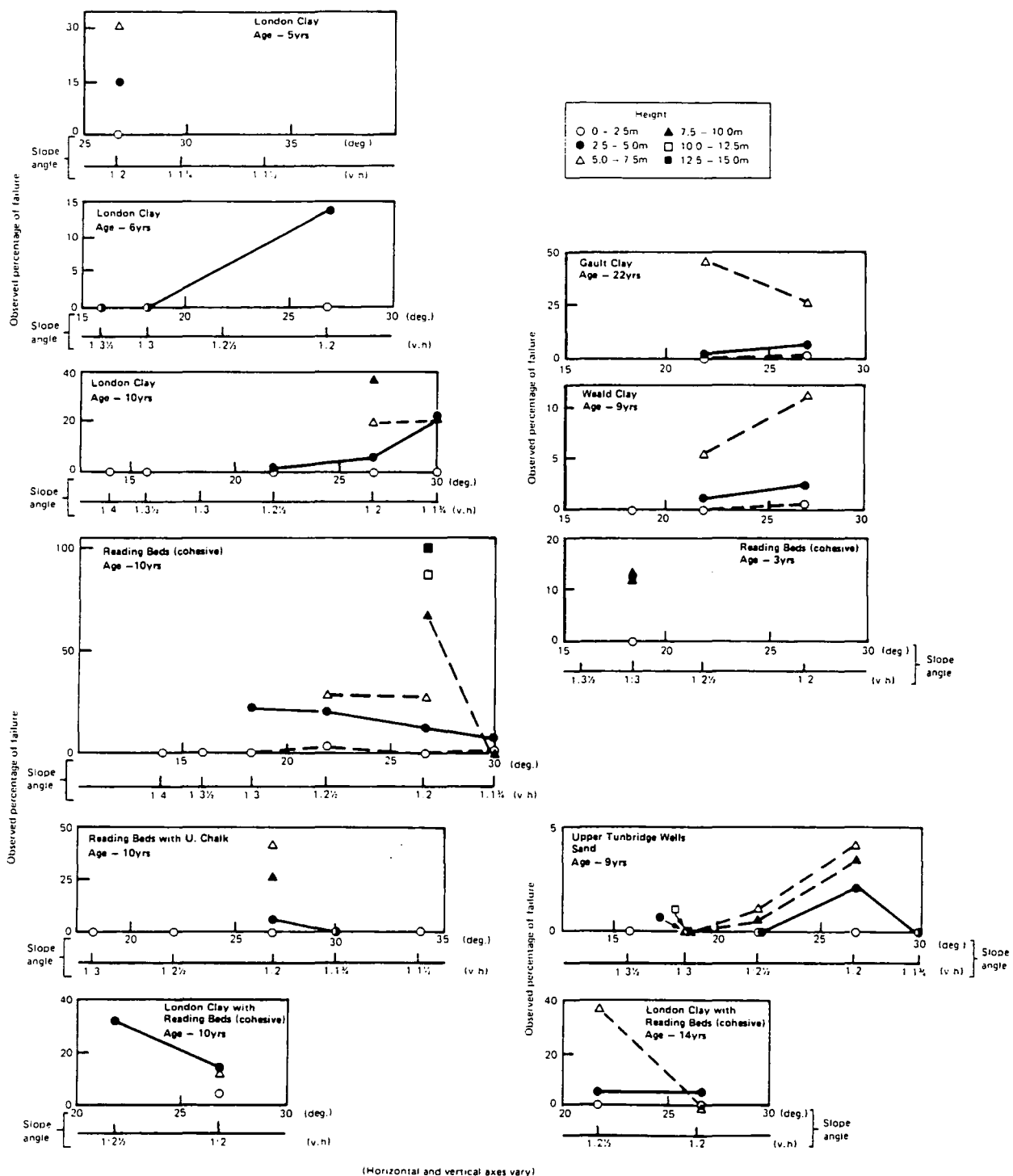


Fig 4/1 Relations between the percentage of failure of embankment slopes and geometry of slope - Eocene and Cretaceous deposits

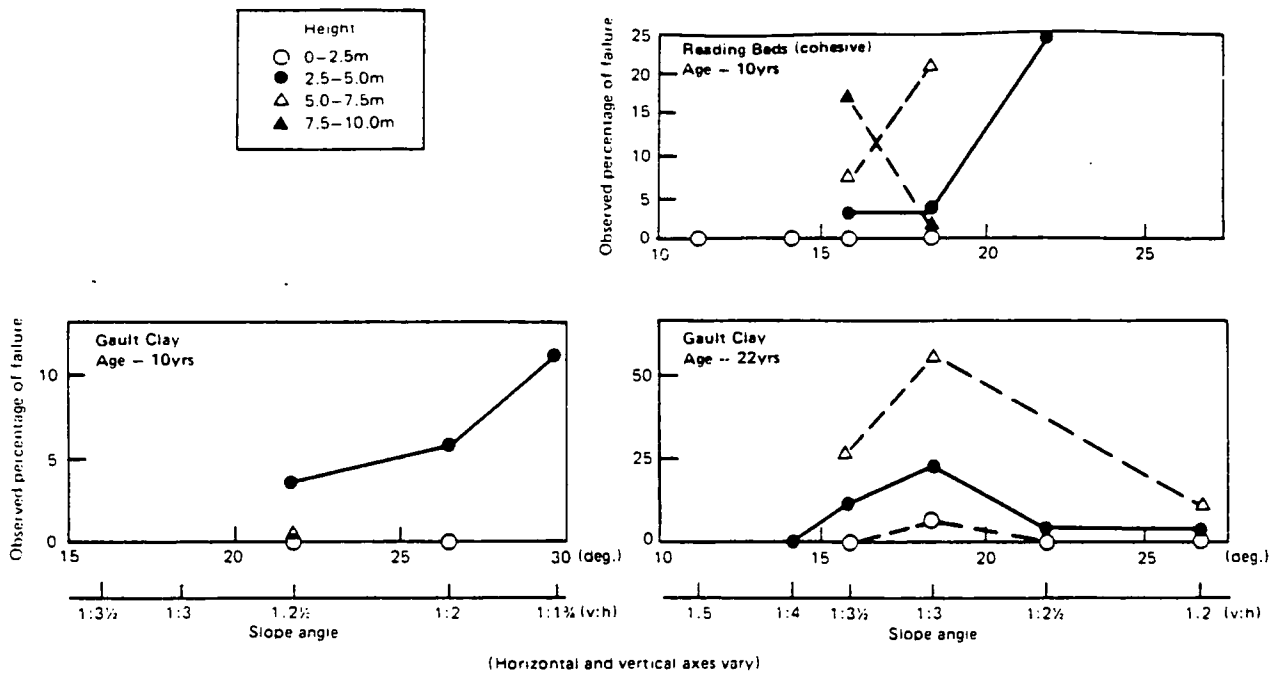


Fig 4/2 Relations between the percentage of failure of cutting slopes and geometry of slope - Eocene and Cretaceous deposits

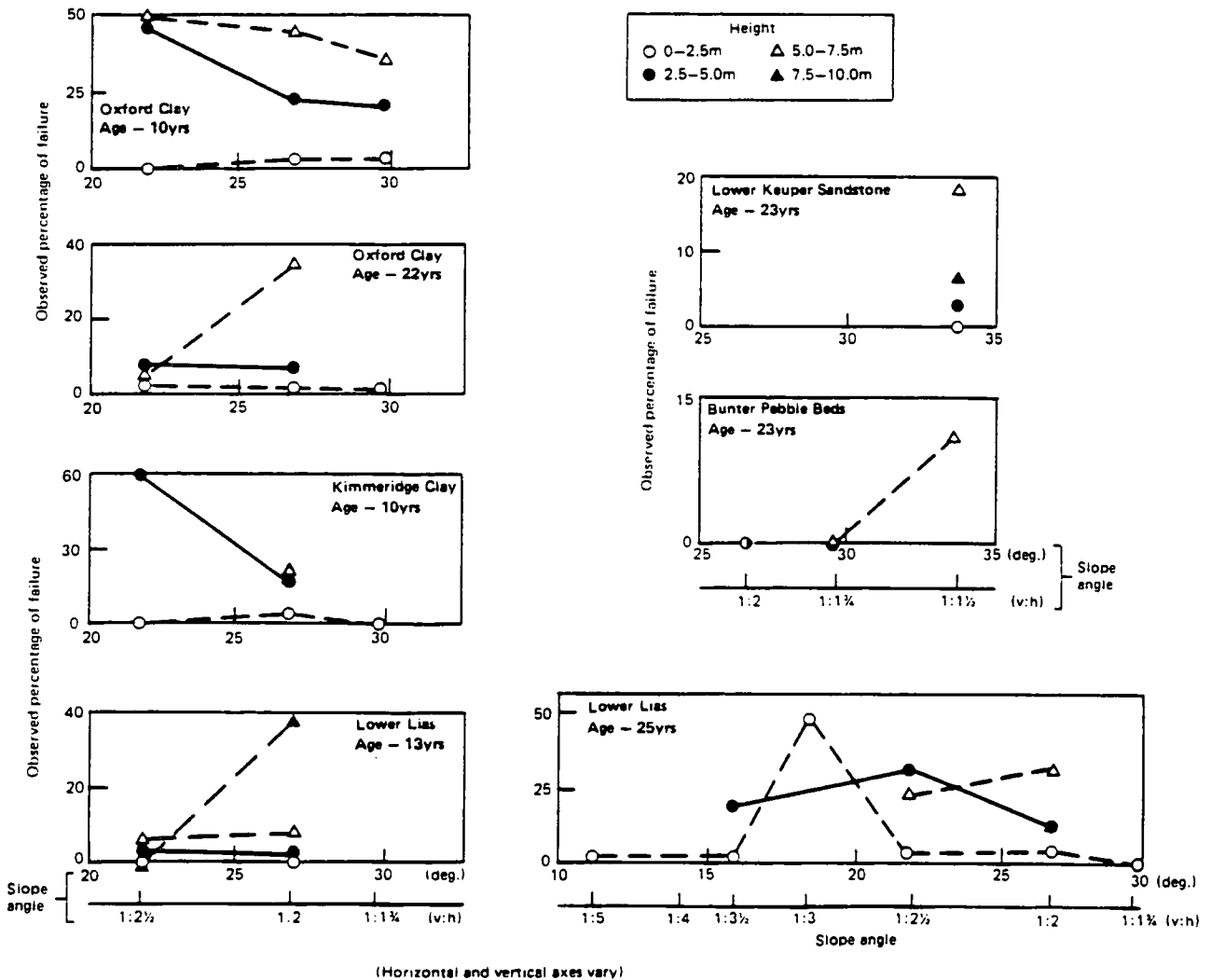


Fig 4/3 Relations between the percentage of failure of embankment slopes and geometry of slope - Jurassic and Triassic deposits

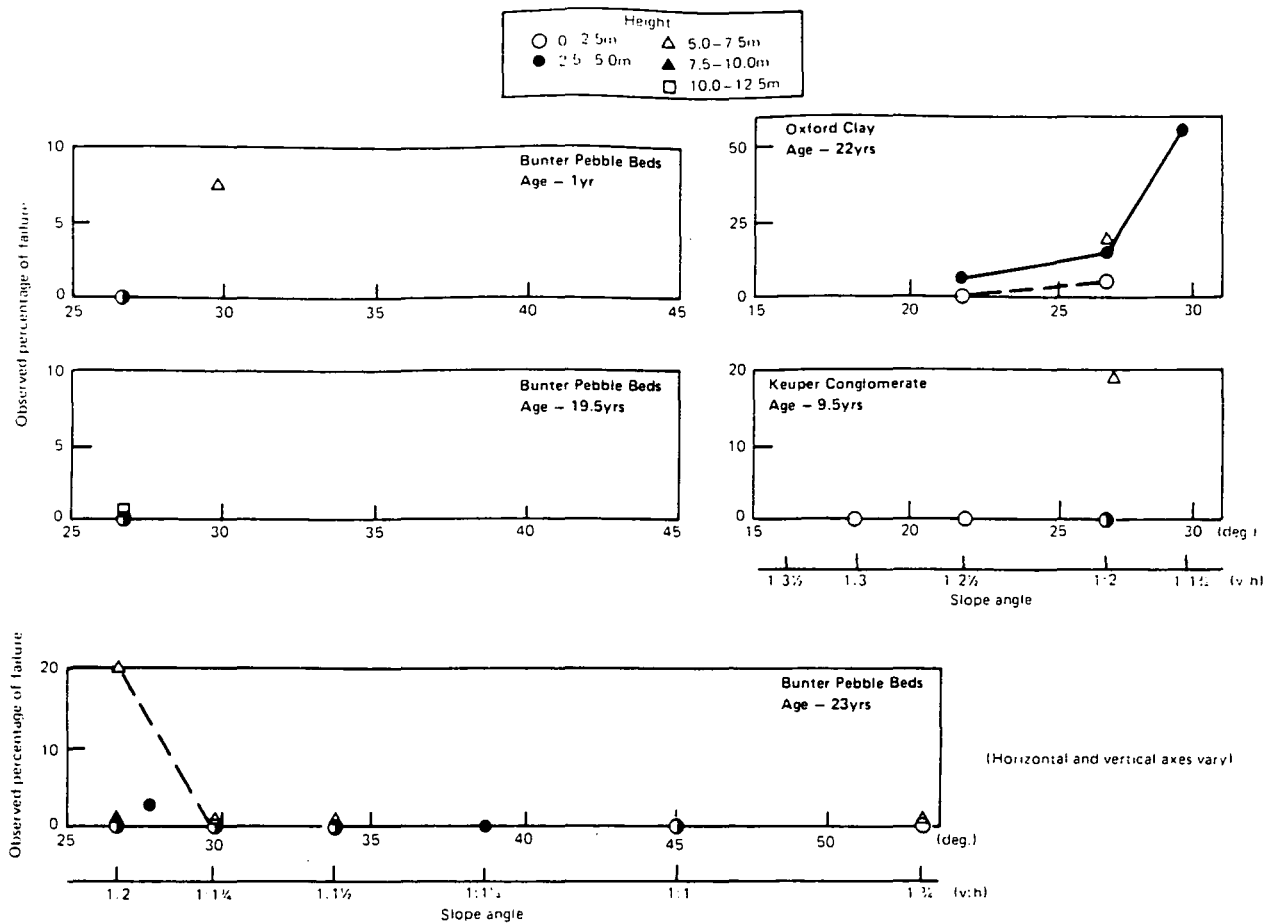


Fig 4/4 Relations between the percentage of failure of cutting slopes and geometry of slope - Jurassic and Triassic deposits

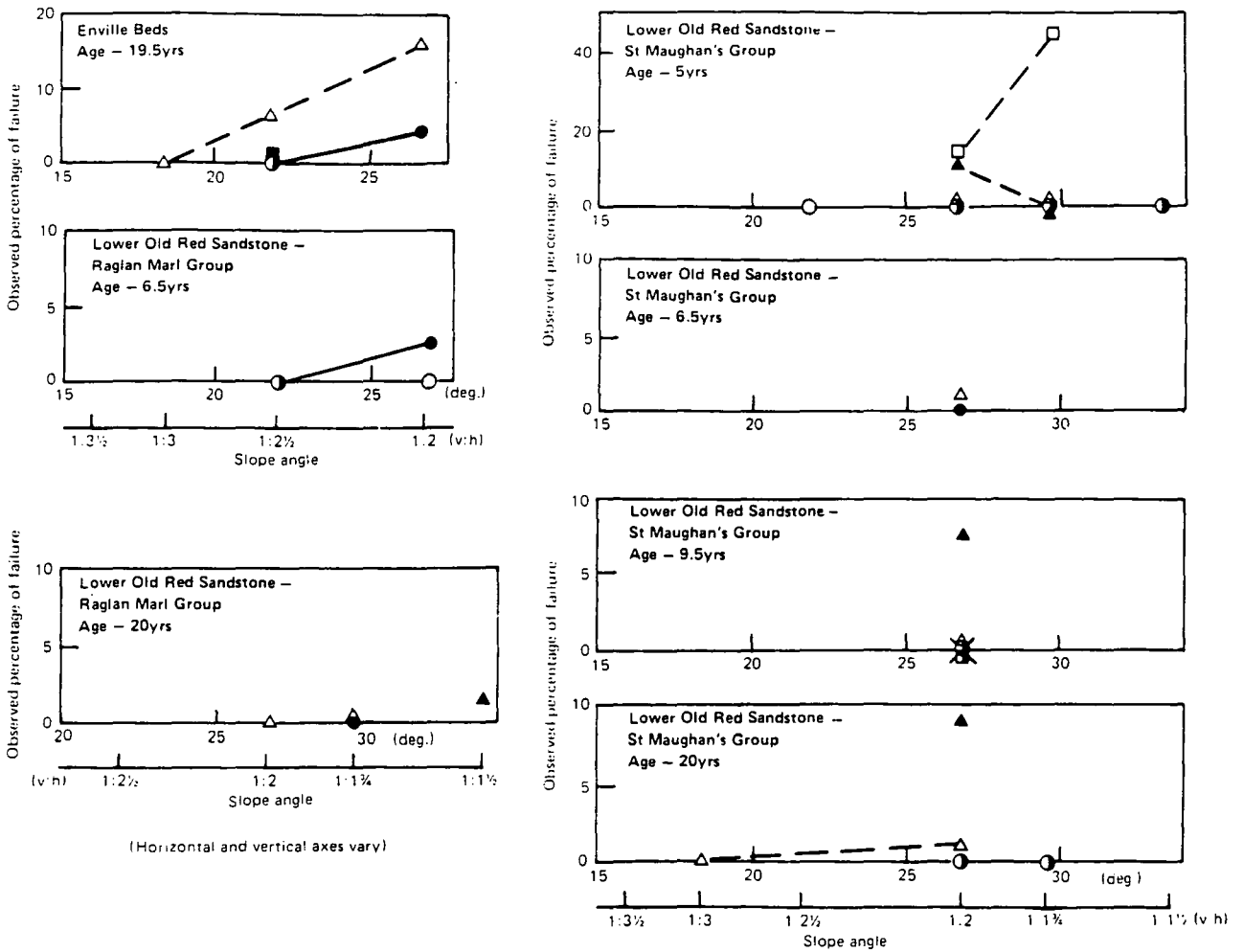
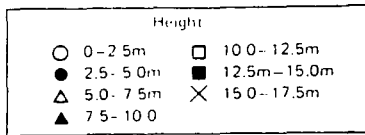


Fig 4/5 Relations between the percentage of failure of cutting slopes and geometry of slope - Carboniferous and Old Red sandstone deposits

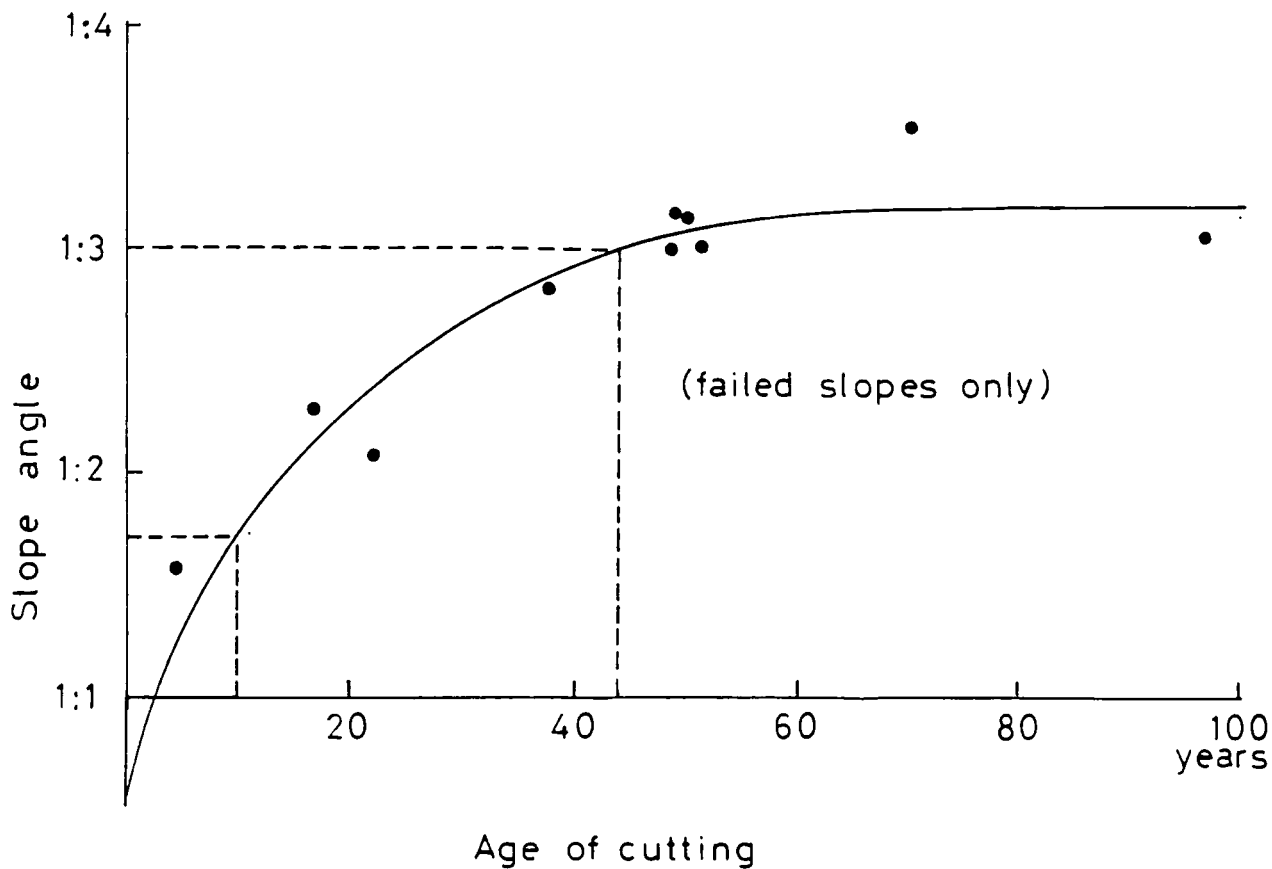


Fig 4/6 The variation of slope angle with time for first-time slides in London Clay cuttings (Tavenas and Leroueil, 1981)

Chapter 5

General results for all the motorways surveyed

5.1 Description of slope failures

The survey has revealed a significant incidence of slope failures in side slopes of both cuttings and embankments. In the 570km of motorway surveyed, accumulated lengths of over 17km of embankment slope and over 5.5km of cutting slope have failed. The type of slope failure observed varied from distinct slab type to shallow circular type but with most slips having a combination of translational and circular movement. The vertical depth of the failure surface beneath the surface of slopes unrepaired at the time of the survey rarely exceeded 1.5m with a minimum depth of 0.2m and a maximum depth of 2.5m, (Table 5/1).

Where embankments are constructed of rock and the slope angle is high, very shallow failures can develop due to failure of the topsoil on the stable rock fill beneath, for example on Lower Keuper Sandstone and Chalk. Although the slope is stable for the rock fill it cannot always retain a topsoil and when failure occurs the rock becomes exposed to weathering. In the majority of embankments constructed of soil, the failure surface extends through the topsoil into the fill to greater depths than in embankments of rock fill.

In most instances the area of failure extended from the crest

to the toe of the slope.

During the survey it was observed that, at the bottom of a small percentage of embankments and cuttings, the toe of the slope had been disturbed leaving a vertical face. This has been called 'toe erosion' and may have formed as a result of disturbance by maintenance plant or as a consequence of the motorway hard shoulder being widened. The vertical face was normally less than 0.5m high in those geologies susceptible to failure. Although failures were present on slopes affected by toe erosion, analysis indicates that usually other factors, such as geometry, contributed to these failures.

The method used for repairing failures has been similar for all areas included in the survey and involved excavating the failed material, sometimes in benches, to below the failure surface and backfilling with a granular free-draining material such as gravel, brick rubble or crushed rock. Topsoil has been added in some regions, obscuring the repair and providing a more attractive appearance. Occasionally failure of a previously repaired slope has occurred presumably because excavation did not proceed beyond the original failure surface or a new failure surface has developed deeper in the fill.

Only one fabric reinforced soil reinstatement was located in the survey area, in a cutting on the M4 in Berkshire. This was a reinstatement of a deep seated failure, rather than a shallow slip, the design and construction of which is described by

Murray, Wrightman and Burt (1982).

In cutting slopes where a soil overlies a rock, failures have occurred where the soil infilled cavities in the rock (Figure 5/1). Although the upper soil slope is generally constructed at a flatter slope angle, soil within the cavities is constructed at the steeper slope angle suitable for the rock and consequently fails. Drift material above Carboniferous Limestone Series limestone is a good example of this. Failures have also occurred in steep rock cuttings due to weathering of vulnerable sections of the exposed rock face. In both situations, rock 'dentition', where the failed soil or weathered rock is removed and the remaining material buttressed with more durable blocks of rock, has been used as a successful repair technique.

Failures that occurred during construction were usually deep seated and infrequent, compared to the number of shallow failures in later years. Repairs of these failures were completed before the motorway was open to traffic.

Slopes where cracking has occurred, have been treated in the survey as contributing to the length of stable slope. However a number of these slopes have subsequently failed. Had these slopes been treated as fully developed failures, the length of failure would have increased by a factor of about 1.8 for embankments and 2.0 for cuttings. No information is available on the time between the initial crack formation and the fully

developed failure occurring. However, when the failure does become fully developed movements can occur at a rate of 1m in 13 days (Crabb et al, 1987).

An assessment has been made as to what lengths of slope will be at risk of failure in the future. This is based on two criteria. Firstly, that an earthwork with an existing failed or cracked area will be likely to fail elsewhere in the same earthwork (with the same geology and age) but on slopes of more severe slope angle and height. Secondly, that slopes which have cracked are likely to fail in the future. The total length at risk of failure is the sum of the slopes of more severe geometry and the length of slope with cracking. Based on this premise, three times as many slopes are likely to fail in the future than have failed so far if no preventative measures are taken. This future estimate is almost certainly conservative as it is most likely that in the long-term failures will occur on slopes constructed at less severe geometries or on earthworks where no previous failures have occurred. The time-scale of future failures is, however, uncertain at this time but for some slopes it may take up to 120 years before failure occurs (Chandler and Skempton, 1974).

5.2 Variation of design parameters

The survey covered a number of motorways of differing age and geology and, as a result, included many different design parameters. Figure 5/2 illustrates the range of heights and

slope angles encountered. The distribution of height shows that 81 per cent of the embankment length and 76 per cent of the cutting length is less than 5.0m high and that only 6 per cent of the embankment length and 9 per cent of the cutting length is greater than 7.5m high. The highest embankment slope and highest cutting slope were 66.7m and 32.0m respectively. The height distribution is almost identical to that found previously by Parsons and Broad (1970). The distribution of embankment slope angle shows that over half the slopes were at 1:2. Cutting slopes were more variable and ranged up to 90 degrees for some rock slopes.

The overall drainage distribution for all the motorways surveyed is given in Table 5/2.

Open ditches are the most common type of drainage at the bottom of embankments. The majority of cutting slopes have no drainage at the top, which may reflect the fact that in cases where water movements at or near the ground surface are away from the motorway, a cut-off drain was not thought to be necessary.

The previous chapters present a catalogue of real events. Consequently the conclusions reached are not subject to the uncertainties and assumptions of the analysis and testing of soils. The values given in the tables of maximum slope angle are based on actual failures and so no assumptions have to be made and, unless the situation of the slope is exceptionally

unusual, the uncertainties have been reduced by the large lengths of motorway studied. Steeper slope angles than those recommended in the tables may be acceptable in existing and new slopes if suitable preventative measures, such as rock ribs and geomesh plus anchors, are used (Johnson, 1985). In new construction or for widening an existing highway where only a small amount of land is available, steeper slope angles may be constructed by, for example, using more stable material, such as rock fill, on the outer slope or by incorporation of geomesh or geotextile reinforcement.

Using various types of drainage can result in the recommended slope angles being steepened. Based on the analysis of differing types of drainage and its effect on the percentage of failure, tables are given in most Sections, of the steepened slope angle and most effective type of drainage. Although 570 km of motorway were surveyed, there is insufficient data to show the effect of drainage on the recommended slope angle for all of the geologies with failures.

The choice of slope angle may also be affected by other factors, outside the scope of this Thesis, such as land prices, environmental considerations and possible uses for the slope.

Observation of shallow failures during the survey provides information on the design of slope geometries based on engineering considerations. In order to take this further and study how failure occurs, information is required on the

mechanism of failure and is the subject of following chapters. An understanding of the failure mechanism will not only explain why failures occur but will provide design criteria for preventative and reinforcement methods, and allow design of slopes in materials and situations not met in the survey.

TABLE 5/1

Percentage of slips with different
depths of failure

Depth of failure surface (m)	Percentage of total slip length
0.2 - 0.4	14
0.5 - 0.9	35
1.0 - 1.5	46
1.6 - 2.0	4
2.1 - 2.5	1

TABLE 5/2

Distribution of drainage at the bottom of embankments
and the top of cuttings

Type of drainage	Embankments	Cuttings
None	26%	60%
Open ditch	46%	18%
French drain	27%	17%
Other	1%	5%

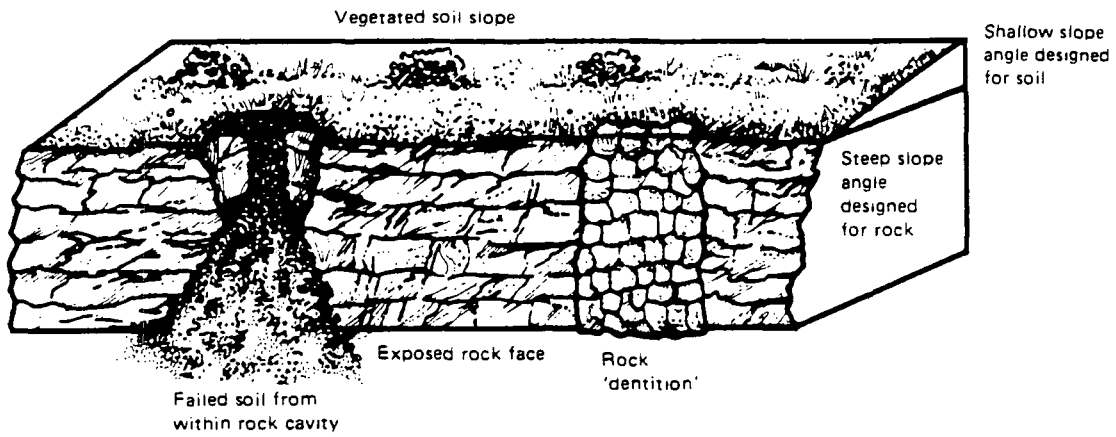


Fig 5/1 Failure and repair of soil in rock cavities

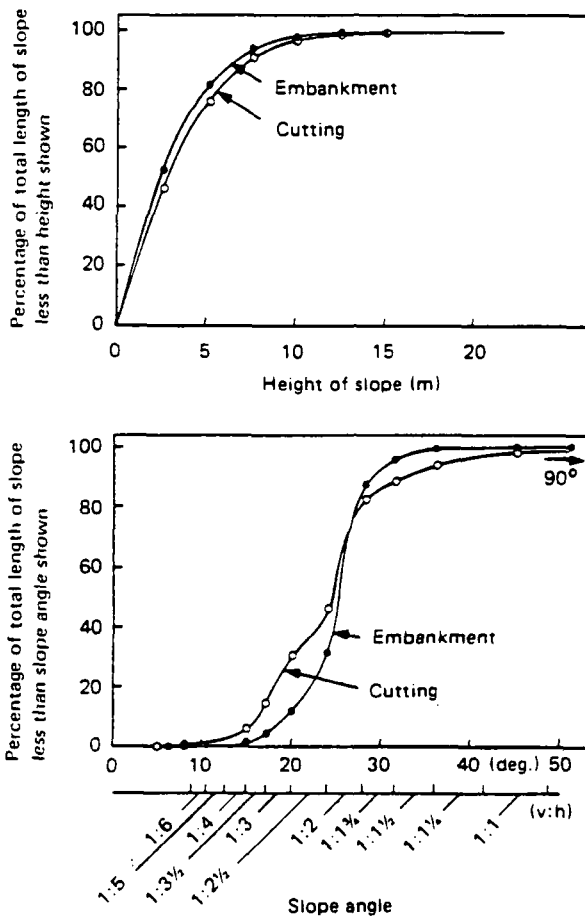


Fig 5/2 The distribution of height and slope angle for embankments and cuttings encountered in the survey

Testing of soils for detailed investigation

6.1 Location of sampling sites

In the survey, over-consolidated clays were the materials most frequently found to be susceptible to failure. Six of these clays with a high percentage of failure were chosen for investigation from six sites where failure had occurred. Undisturbed samples were taken for laboratory testing and subsequent back-analysis. A further Gault Clay site was chosen where no failure had occurred in order to extend the studies of the behaviour of soils at low effective stresses. Table 6/1 shows the geologies sampled, their location and the date the motorway was opened. Only embankments were sampled as most failures occur in this type of earthwork and very little is known of the behaviour of embankments in the long-term.

At each site, large diameter holes were manually augered to a depth of 1.5m before any sampling commenced; this depth corresponds to the most frequent depth of failure (Table 5/1). Six, and in one case seven samples were taken using thin-walled 38mm sampling tubes with a relieved bore cutting edge. The tubes were jacked into the soil on an anchored framework. Using this type of apparatus, taking the necessary care, and following this procedure keeps the disturbance of the soil to a minimum. The samples were sealed within the tubes until ready for testing as soon as possible after the samples were taken.

6.2 Types of test conducted

The effective normal stresses at the depth at which shallow failures occur are very low. In order to simulate these conditions in the laboratory, City University were contracted by TRRL to conduct a series of special tests, as well as conventional tests, at low effective stresses on the six types of clay under study. As a starting point for studying the shear strength at failure, peak strength conditions were first considered. All the soil tests were conducted in a triaxial apparatus using a hydraulic Bishop and Wesley (1975) cell with automatic control (Atkinson, Evans and Scott, 1976). The soils were saturated at a mean effective normal stress of 100kPa, and then swollen to a low all round stress. For each soil, except the Gault Clay at Nepicar, three samples were subjected to conventional drained triaxial compression tests and three were induced to failure by increasing pore water pressure at low normal stresses. The Gault Clay from Nepicar was subject to four conventional triaxial tests and three were induced to failure by increasing pore water pressure at low normal stresses. At low effective stresses it is considered most important to apply a membrane correction. For the drained compression tests the correction was applied to the peak stress and for the failure by pore water increase tests the correction was applied to a defined failure point. Appendix C describes the correction applied.

For failure by increasing pore water pressure, the definition of failure is not well defined. The failure point has therefore been defined, arbitrarily, as the instant when the ratio of the change in volumetric strain, caused by the water pumped into the sample, to the change in all round effective stress, directly related to the increase in the pore water pressure, achieved a value of 1%/kPa. This is a rate of deformation exceedingly close to catastrophic failure, but not necessarily the penultimate point especially if the record interval was very small in relation to the rate of pore water pressure increase. These types of deformation were irrecoverable leaving no opportunity to examine behaviour at higher shear strains.

The drained compression tests were however strain controlled up to and beyond their failure points (peak stresses) and permitted further examination of the soil under higher strains. For the drained compression tests, a definite maximum value of deviatoric stress was observed but in all cases the additional compression of the sample was not accompanied by the expected substantial decrease in the deviatoric stress and as a result the end point of the test does not represent the critical state strength (Schofield and Wroth, 1968; Atkinson and Bransby, 1978) or residual stress (Skempton, 1964) but was more indicative of an 'ultimate' condition for the testing. The residual strength, which is associated with the development of highly polished slip surfaces as a result of clay particles orientating in a preferred direction, requires large movements,

of the order of several metres, before developing. These amounts of movement were not observed in the field and so the residual strength is considered not to have developed before failure occurred. The critical state strength, however, requires much smaller strains and is characterized by straining at constant volume and constant effective stress. Skempton (1970) refers to this critical state strength as the fully softened strength. The reason for adopting critical state strength (or fully softened) is that for fissured clays progressive failure (associated with the fissures) reduces the mobilized strength to between peak and residual. This is not to say that the critical state strength is the actual mobilized condition but it seems to give a comparable strength to that developed due to progressive failure.

In order to study the critical state strength, further tests were carried out on remoulded samples at higher effective stresses. Unfortunately the graphs of q' versus strain or q'/p' versus strain did not become asymptotic to a horizontal line which would have indicated that the critical state strength had been achieved; p' is the mean normal effective stress $1/3.(\sigma'_a + 2\sigma'_r)$, q' is the effective deviator stress $(\sigma'_a - \sigma'_r)$, and σ'_a and σ'_r are the axial and radial effective normal stresses applied to the sample during testing. It was then considered that the best way to achieve the critical state strength was to reconstitute the over-consolidated clays to try to remove their brittle behaviour and encourage plastic deformations which should allow the critical state strength to

be achieved more easily. Reconstitution of the samples involved completely breaking down the structure of the soil by oven drying each sample and grinding it to a powder. The soil was then rebuilt as a normally consolidated soil by saturating and consolidating the sample. Hence, the final material has the same mineralogy as the original over-consolidated soil but is in a normally consolidated state. Two undrained triaxial tests with pore water measurement were then conducted at high stress levels for each soil type. Only two tests were conducted because the critical state strength requires the critical state failure envelope to intercept the origin of the effective normal stress and shear stress plot. Although these tests are at high stress levels and since the critical state failure envelope is represented by a straight line, the strength measured at high stresses is as applicable to low stresses levels as it is to high stress levels.

6.3 Results of tests

The City University test results are contained in Tables 6/2, 6/3 and 6/4, and Figures 6/8 to 6/29. The results of the low effective stress tests on undisturbed samples at the peak stresses are given in Table 6/2 and the Mohr stress circles are plotted in Figures 6/1 to 6/7. The stress paths to the peak strength and 'ultimate' strength are shown in Figures 6/8 to 6/11 and the associated stress-strain curves are given in Figures 6/12 to 6/22. By studying the Mohr circles, it can be seen that a curved failure envelope would seem to be more

appropriate than a straight line. The stress path graphs show the two types of test used and points of failure. The stress paths at the lower stresses are those of the tests where failure occurred by increasing pore water pressure and results in a fall in p' at constant q' . The higher stress tests are the drained compression tests. The 'ultimate' strengths are shown on these graphs on the same stress paths as for the peak strengths but at lower stress values. Table 6/3 shows the results for the best 'ultimate' condition possible in these tests. Table 6/4 and Figure 6/23 contain the results for the tests on the reconstituted samples at higher effective stresses in order to study the critical state strength. Figures 6/24 to 6/29 are the stress-strain curves for these results.

TABLE 6/1

Sampling locations and associated failures

Geology	Location of slip from which samples were taken	Date of opening
Gault Clay	M26 Nepicar (Kent) A20 Junction Exit Slip Road Eastbound	Nov'80
Oxford Clay	M1 J13 (Beds) S.Side of A5140 W.Approach	Nov'59
London Clay	M4/A329m J10 (Berks Westbound Approach Slip Road	Dec'71
Reading Beds Clay	M11 (Essex) N.of J8 ch.51.0	Nov'79
Kimmeridge Clay	M4 J16 (Wilts) N.Side of Roundabout	Dec'71
Weald Clay	M23 (Surrey) ch. 36.0	Dec'74

Sampling location where no failure had occurred

Gault Clay	M26 Dunton Green (Kent) ch.25.0	Nov'80
---------------	------------------------------------	--------

TABLE 6/2

Effective stresses at the peak strength for undisturbed samples

Geology	Test no.	1	2	3	4	5	6	7
Gault-Dunton	σ'_a	14.3	27.6	37.6	77.2	127.1	177.0	
	σ'_r	0.9	3.8	2.3	21.3	41.1	61.1	
Gault-Nepicar	σ'_a	14.2	31.9	51.9	97.2	90.9	149.5	173.1
	σ'_r	2.1	1.8	8.5	29.8	31.5	45.1	60.9
Kimmeridge Clay	σ'_a	17.7	31.6	53.5	56.5	101.9	126.3	
	σ'_r	3.4	4.0	14.5	15.7	30.9	45.7	
London Clay	σ'_a	15.3	27.2	37.4	48.1	84.2	101.8	
	σ'_r	0.4	0.8	3.1	6.0	16.0	26.2	
Oxford Clay	σ'_a	17.0	28.8	40.4	94.0	88.3	112.7	
	σ'_r	1.6	3.3	5.0	26.2	16.2	36.2	
Reading Beds-clay	σ'_a	19.1	29.0	40.4	55.1	80.5	94.7	
	σ'_r	3.5	3.6	5.7	15.8	25.6	35.6	
Weald Clay	σ'_a	16.6	29.1	41.6	92.4	108.0	126.5	
	σ'_r	2.6	6.6	6.1	20.8	30.7	40.9	

(All units are kPa)

TABLE 6/3

Effective stresses at 'Ultimate' condition of undisturbed samples

Geology	Test no.	1	2	3	4
Gault-Nepicar	σ'_a	81.3	93.0	143.7	160.0
	σ'_r	31.3	30.0	46.7	61.0
Kimmeridge Clay	σ'_a	52.2	87.7	109.2	
	σ'_r	15.2	29.7	45.2	
London Clay	σ'_a	30.0	66.3	93.3	
	σ'_r	4.5	14.8	25.3	
Oxford Clay	σ'_a	79.5	95.3		
	σ'_r	25.5	36.3		
Reading Beds-clay	σ'_a	54.7	75.3	87.3	
	σ'_r	14.7	25.3	37.3	
Weald Clay	σ'_a	81.7	100.0	120.7	
	σ'_r	20.7	31.0	41.7	

(All units are kPa)

TABLE 6/4

Effective stresses at the critical state strength
using reconstituted samples

Geology	Test no.	1	2
Gault-	σ'_a	140.0	298.7
Nepicar	σ'_r	59.0	129.7
Kimmeridge	σ'_a	139.3	314.7
Clay	σ'_r	62.3	136.7
London	σ'_a	161.0	312.3
Clay	σ'_r	59.0	127.3
Oxford	σ'_a	149.7	321.0
Clay	σ'_r	58.7	129.0
Reading	σ'_a	154.7	308.0
Beds-clay	σ'_r	72.7	155.0
Weald	σ'_a	164.7	322.3
Clay	σ'_r	64.7	134.3

(All units are kPa)

DUNTON GAULT

134

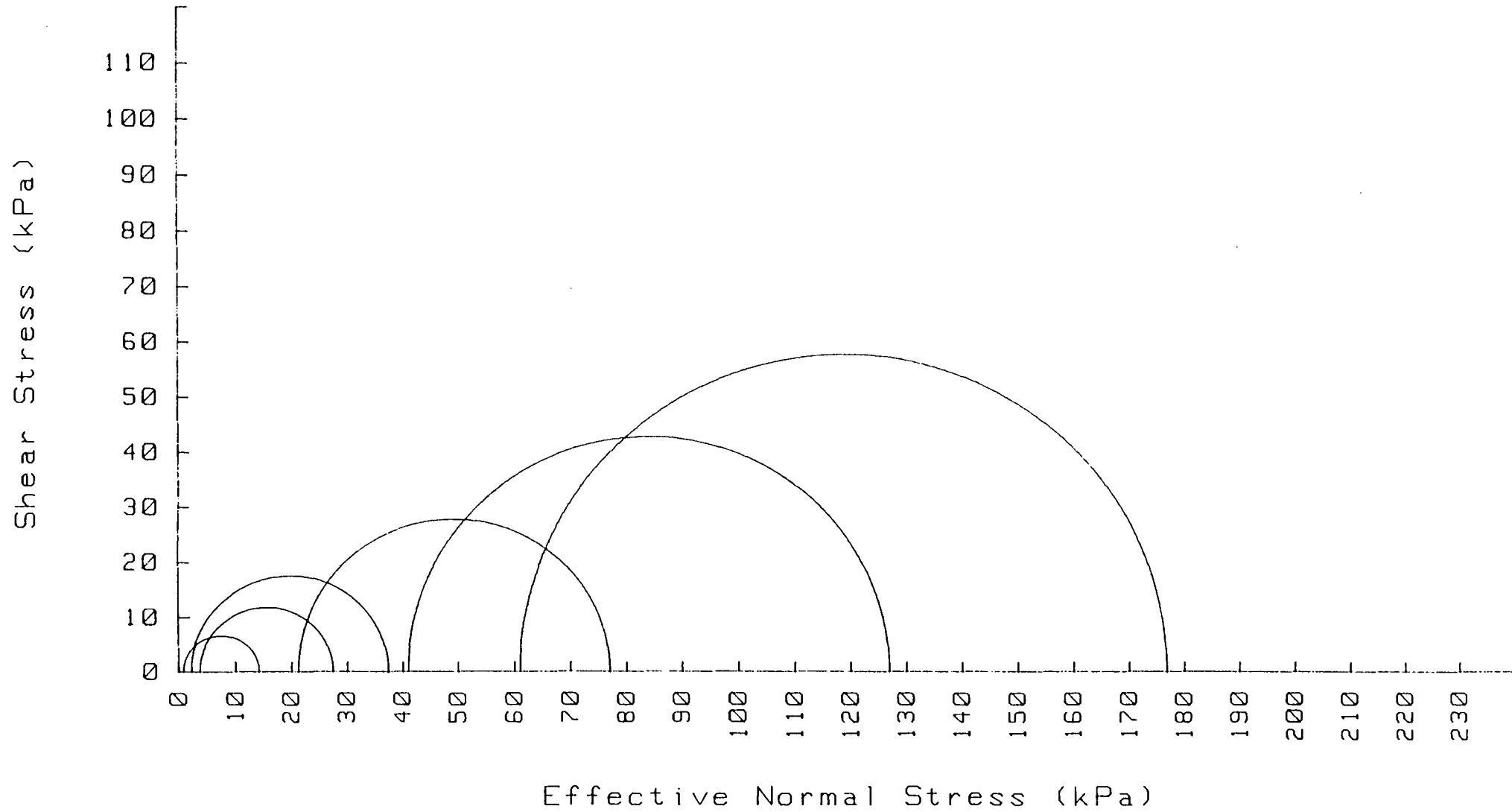


Fig 6/1 Plot of Mohr circles at low effective stresses -
Dunton Gault

NEPICAR GAULT

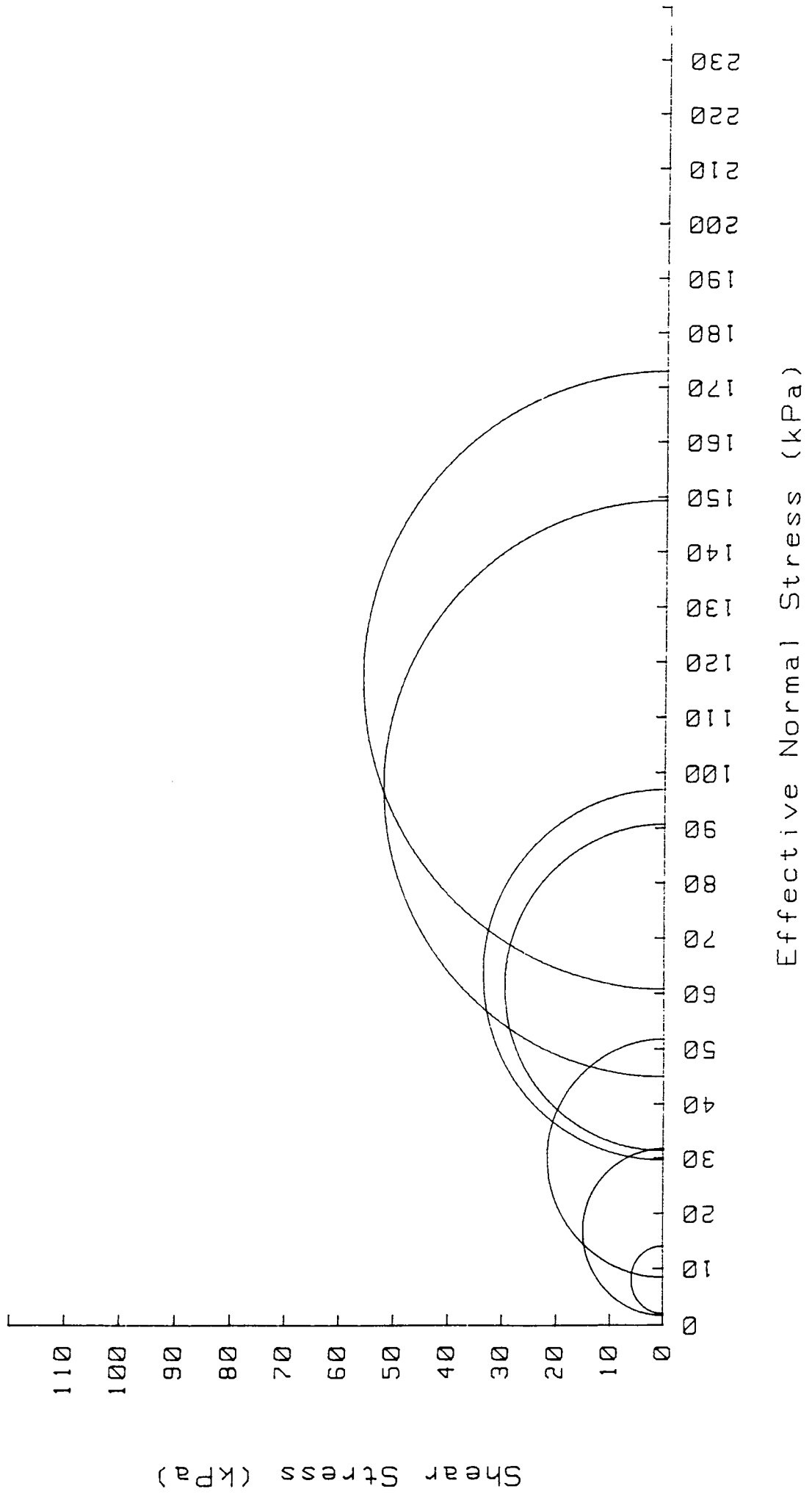


Fig 6/2 Plot of Mohr circles at low effective stresses -
Nepicar Gault

KIMMERIDGE CLAY

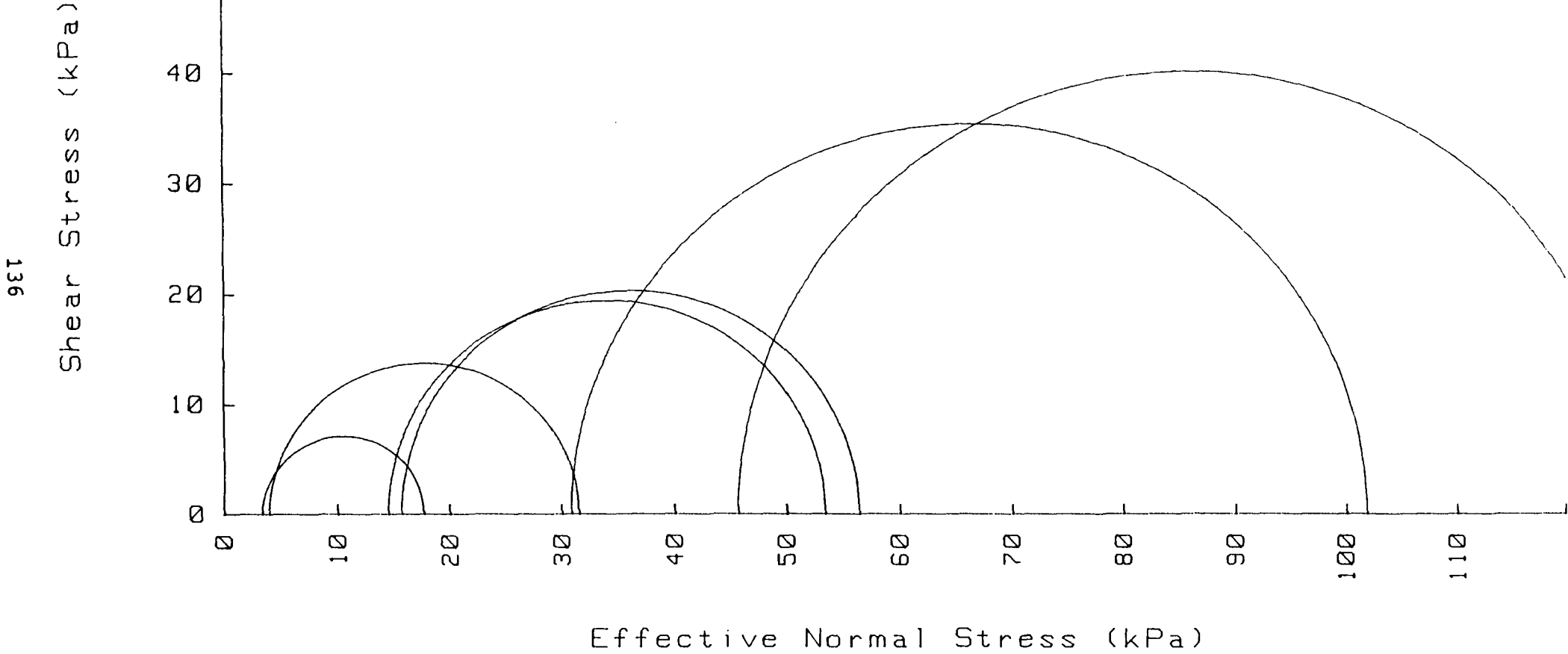


Fig 6/3 Plot of Mohr circles at low effective stresses -
Kimmeridge Clay

LONDON CLAY

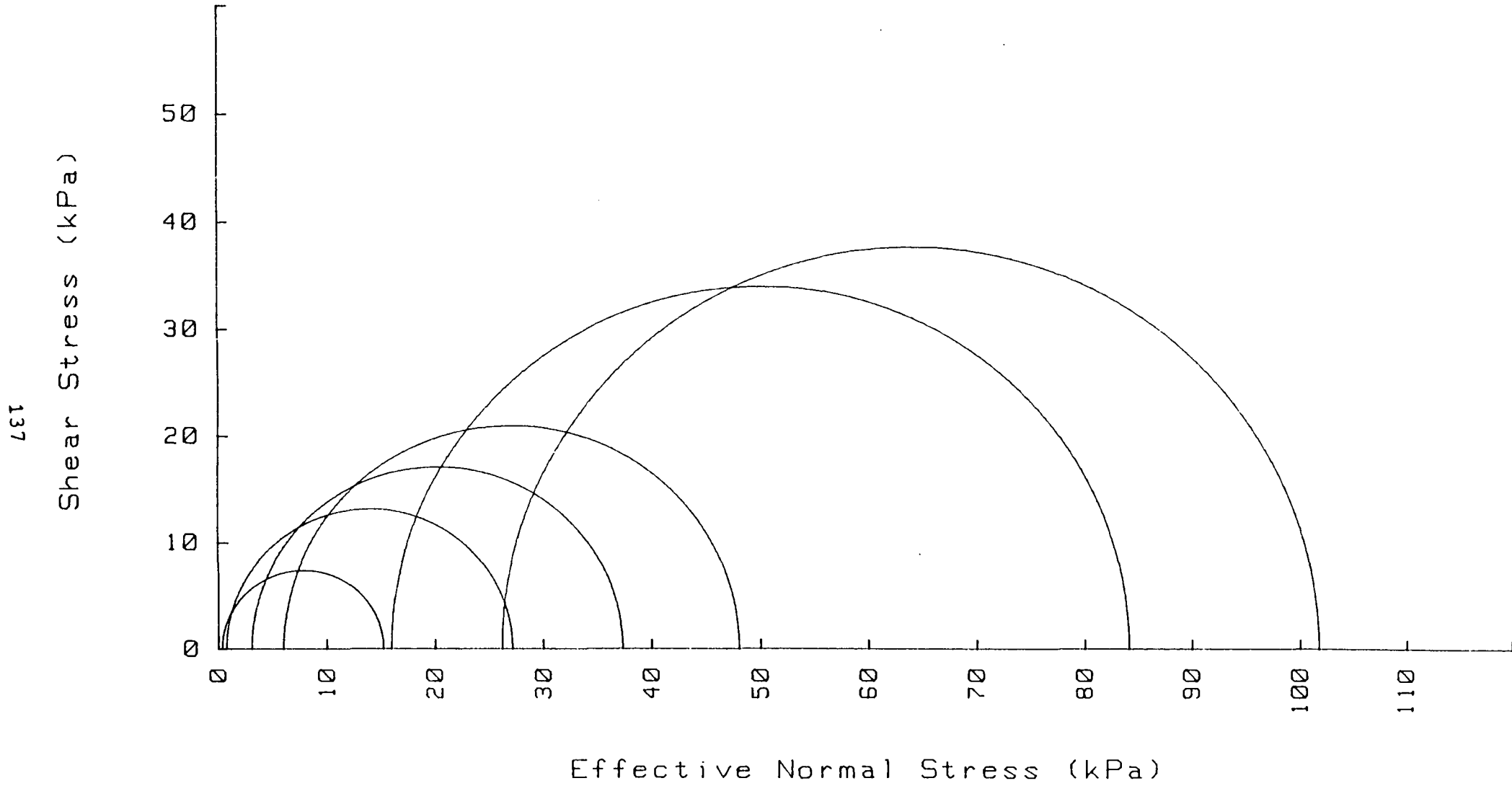


Fig 6/4 Plot of Mohr circles at low effective stresses -
London Clay

OXFORD CLAY

138

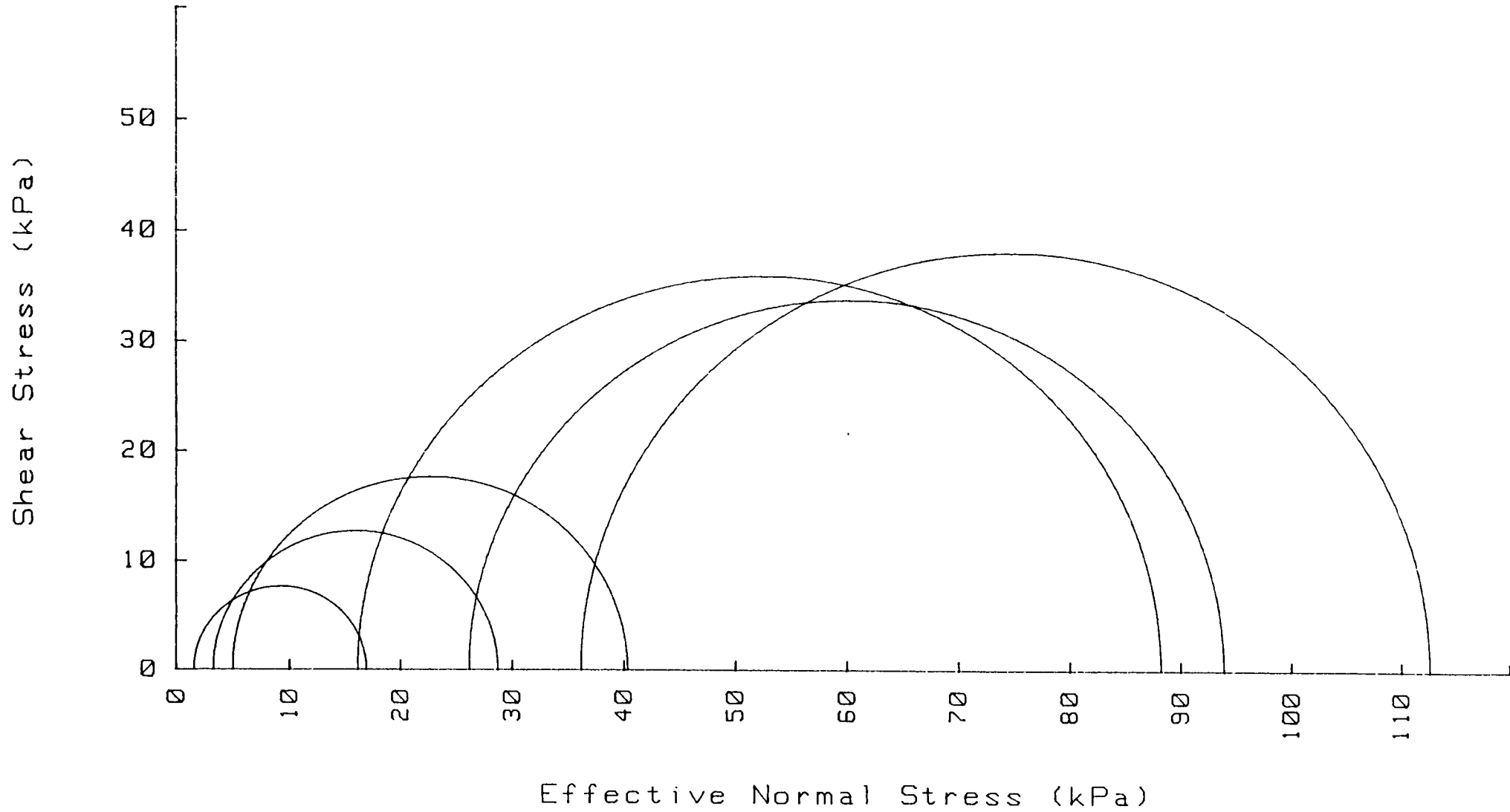


Fig 6/5 Plot of Mohr circles at low effective stresses -
Oxford Clay

READING BEDS CLAY

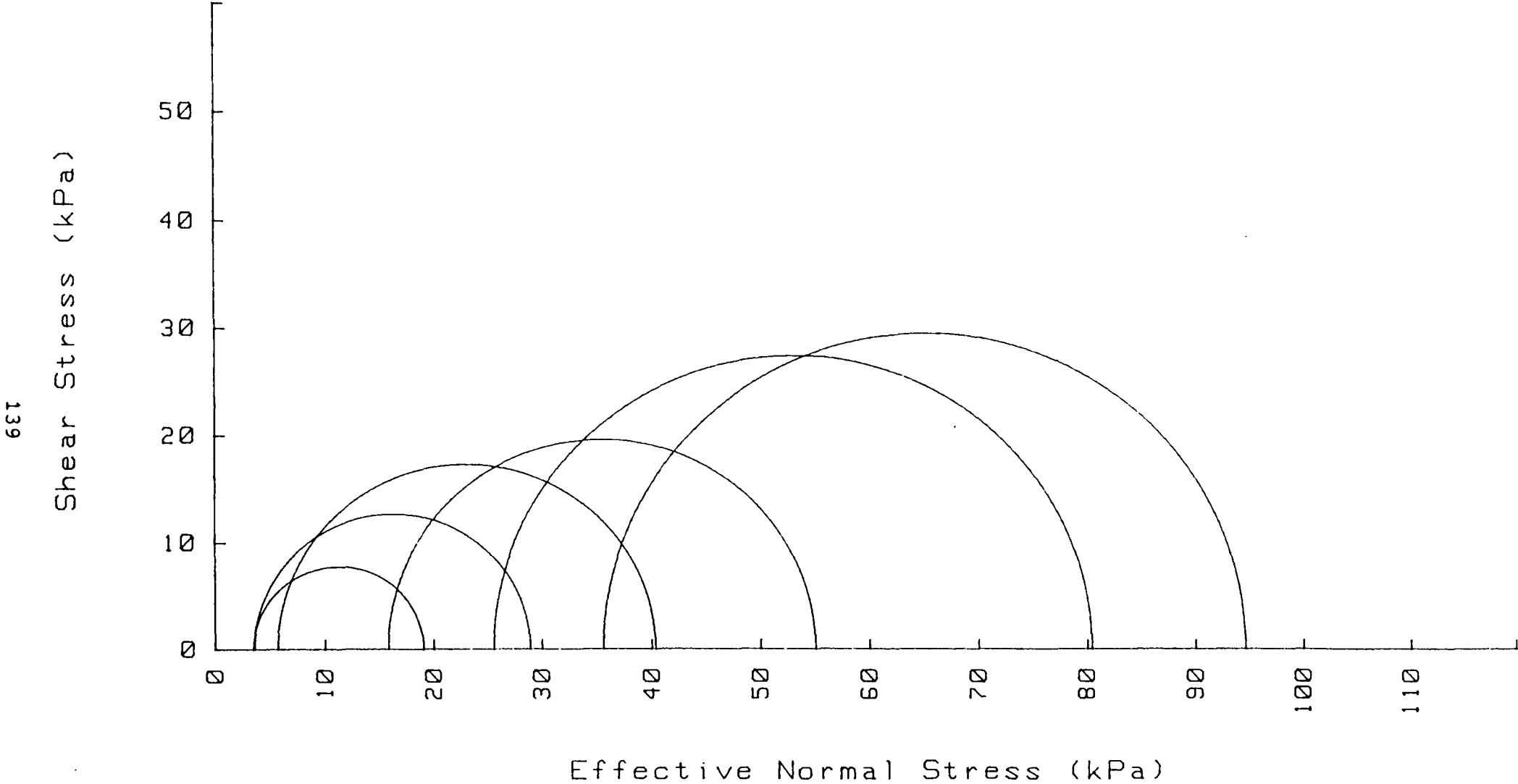


Fig 6/6 Plot of Mohr circles at low effective stresses - Reading Beds clay

WEALD CLAY

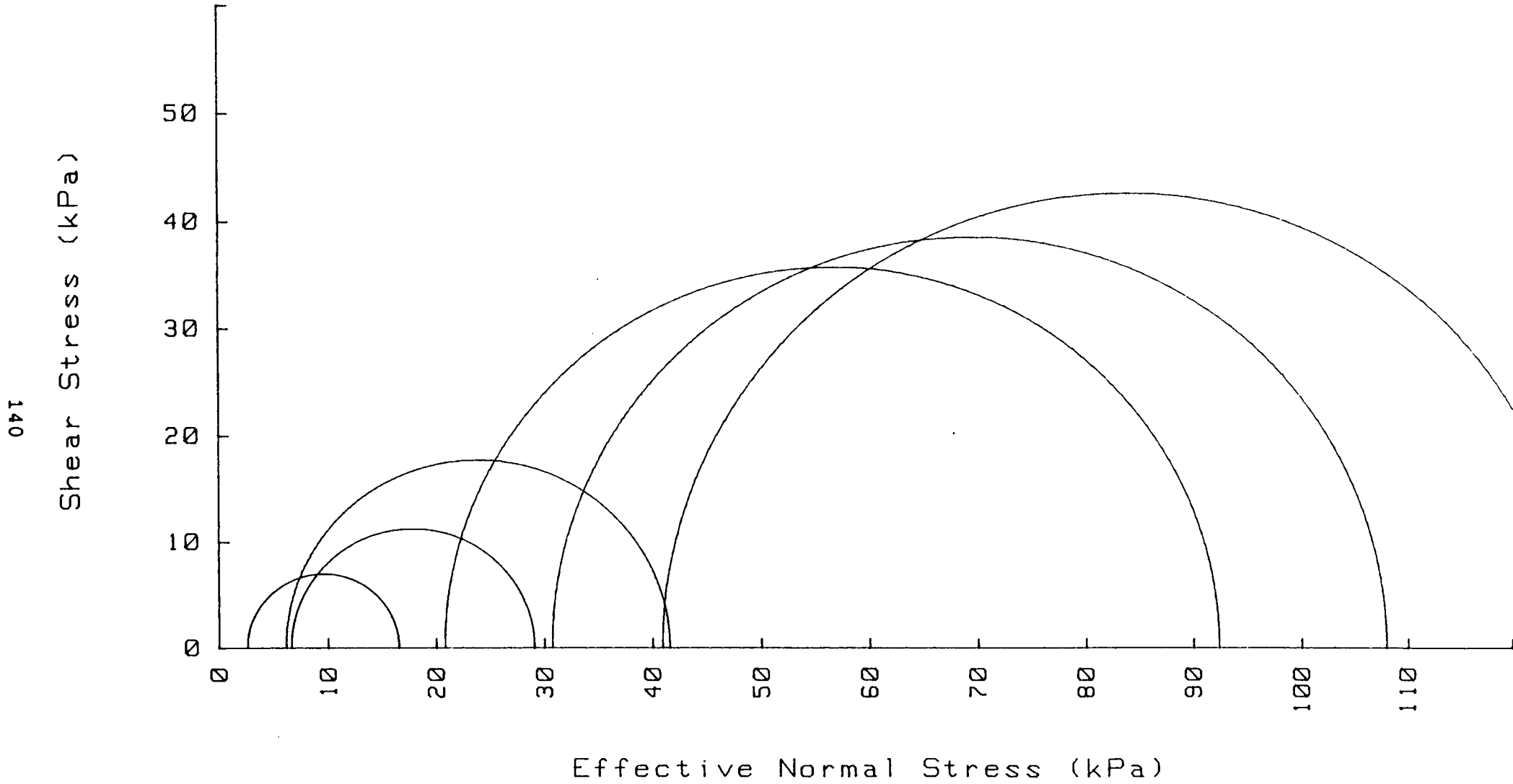


Fig 6/7 Plot of Mohr circles at low effective stresses -
Weald Clay

○ = peak strength • = 'ultimate' strength

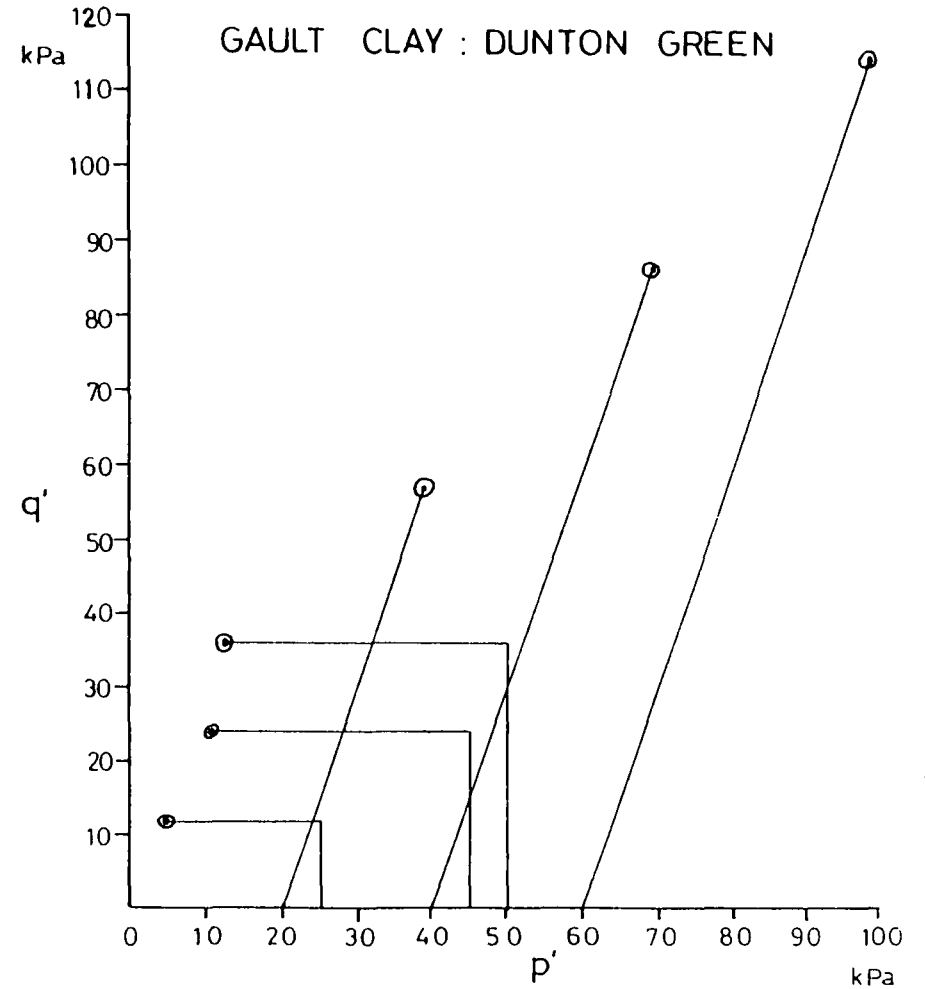
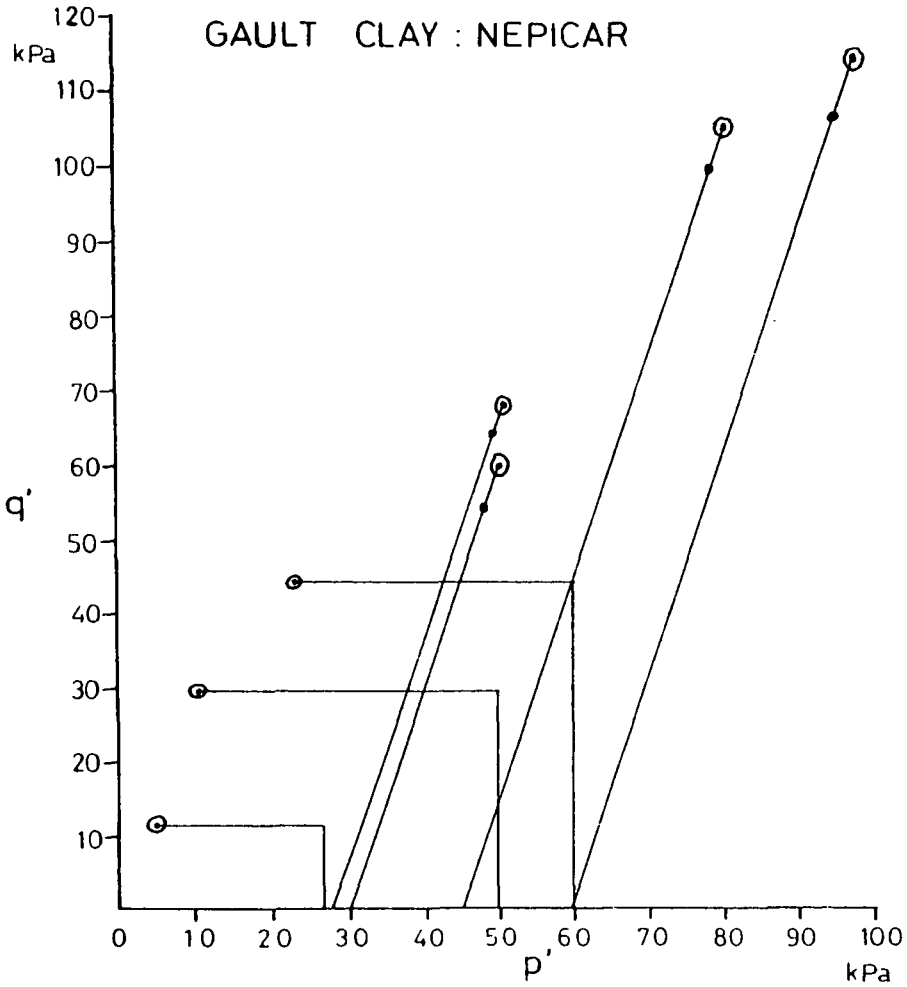


Fig 6/8 Plot of effective deviator stress, q' , against mean normal effective stress, p' , showing stress paths to the peak strength and 'ultimate' strength - Gault Clay

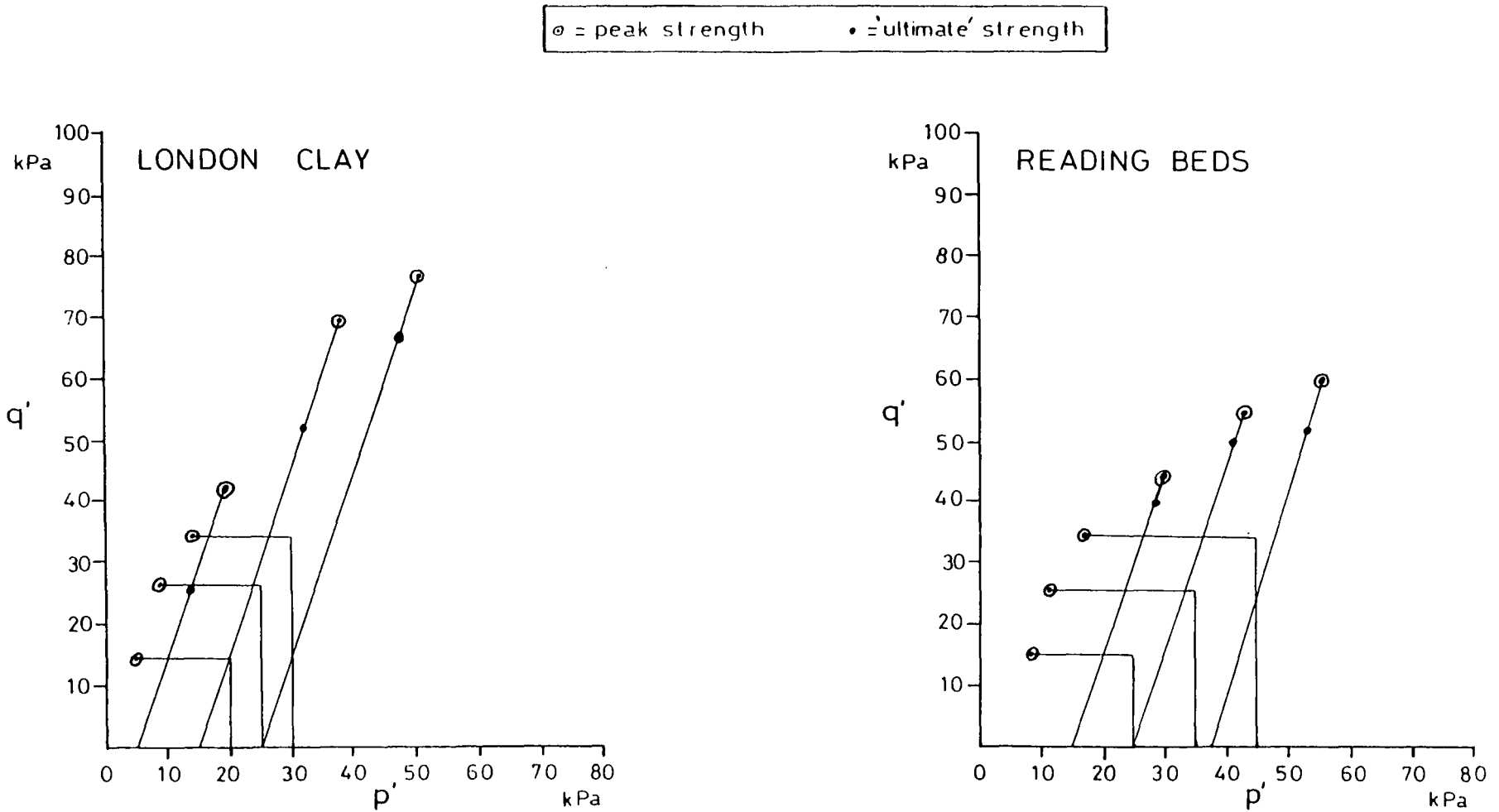


Fig 6/9 Plot of effective deviator stress, q' , against mean normal effective stress, p' , showing stress paths to the peak strength and 'ultimate' strength - London Clay and Reading Beds clay

⊙ = peak strength • = 'ultimate' strength

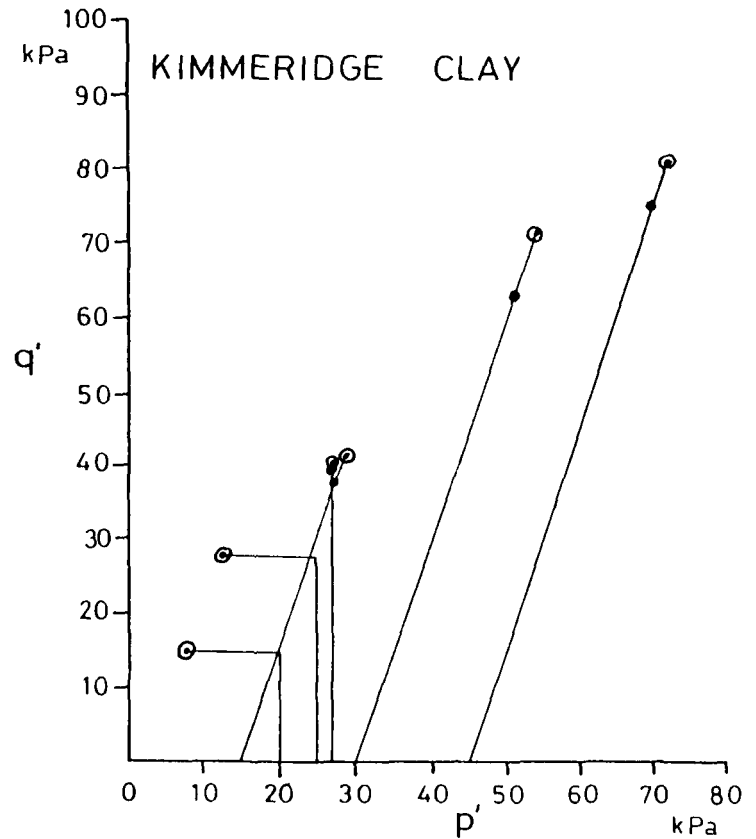
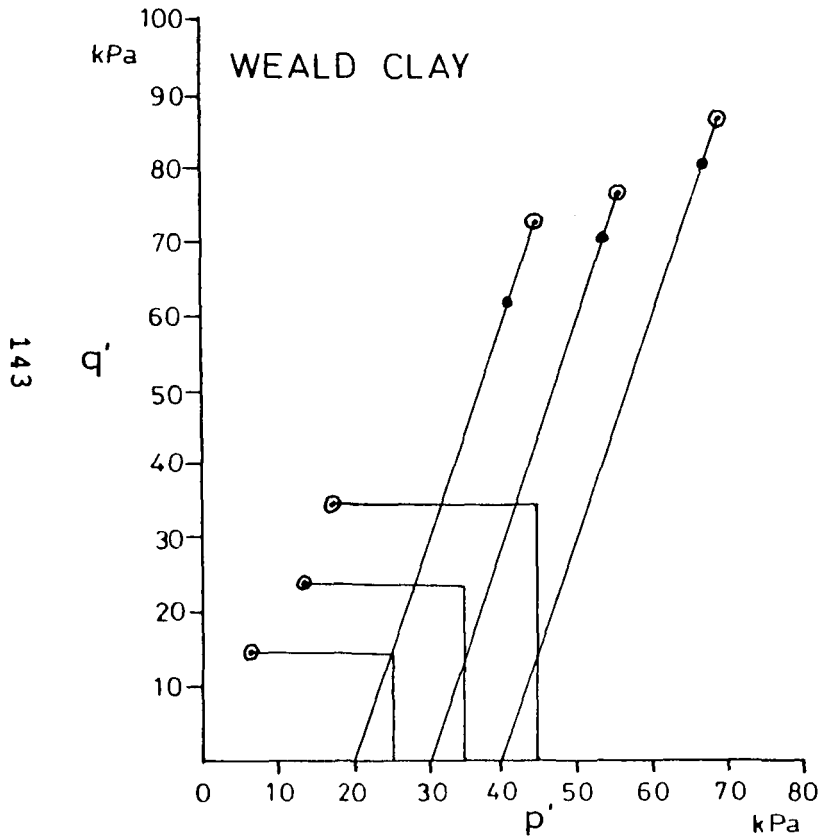


Fig 6/10 Plot of effective deviator stress, q' , against mean normal effective stress, p' , showing stress paths to the peak strength and 'ultimate' strength - Weald Clay and Kimmeridge Clay

○ = peak strength • = 'ultimate' strength

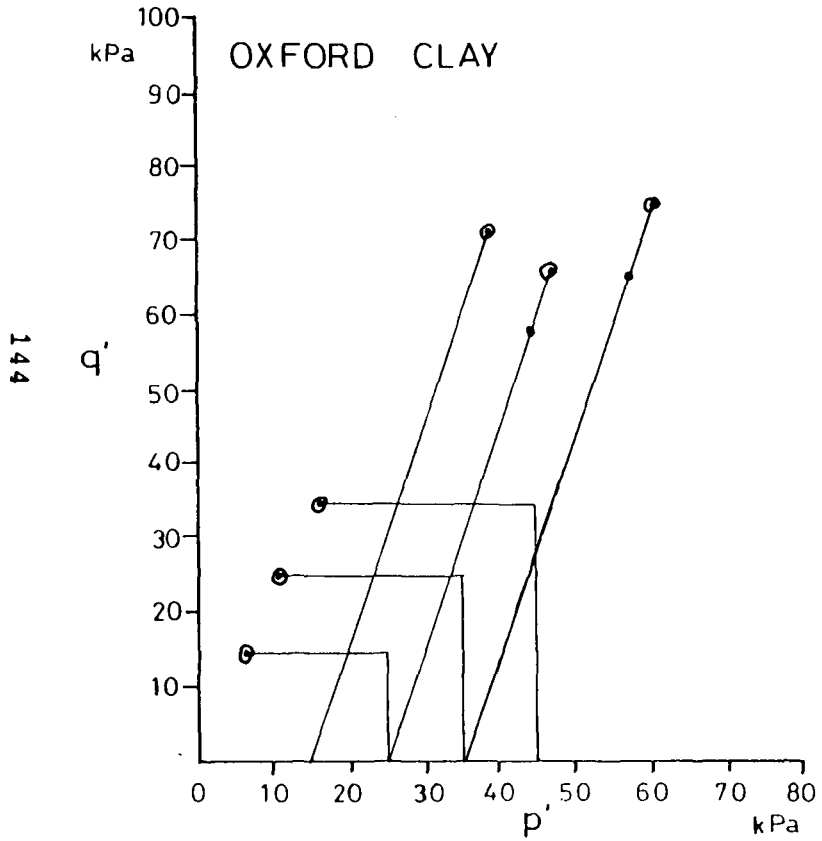


Fig 6/11 Plot of effective deviator stress, q' , against mean normal effective stress, p' , showing stress paths to the peak strength and 'ultimate' strength - Oxford Clay

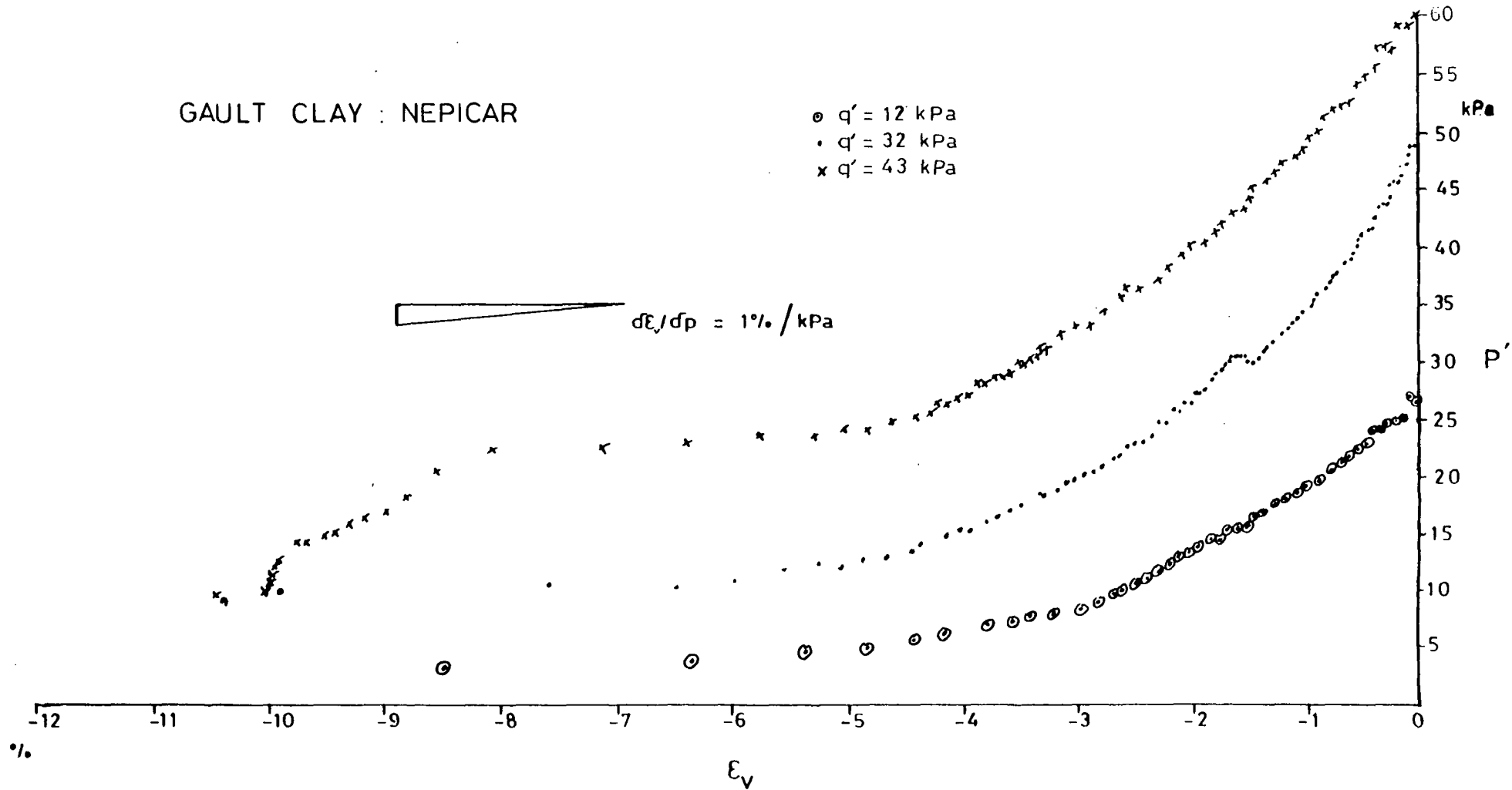


Fig 6/12 Plot of normal effective stress, p' , against volumetric strain, ϵ_v , for increasing pore water pressure tests on undisturbed samples - Gault Clay - Nepicar

GAULT CLAY : DUNTON GREEN

- $q' = 14$ kPa
- $q' = 22$ kPa
- x $q' = 36$ kPa

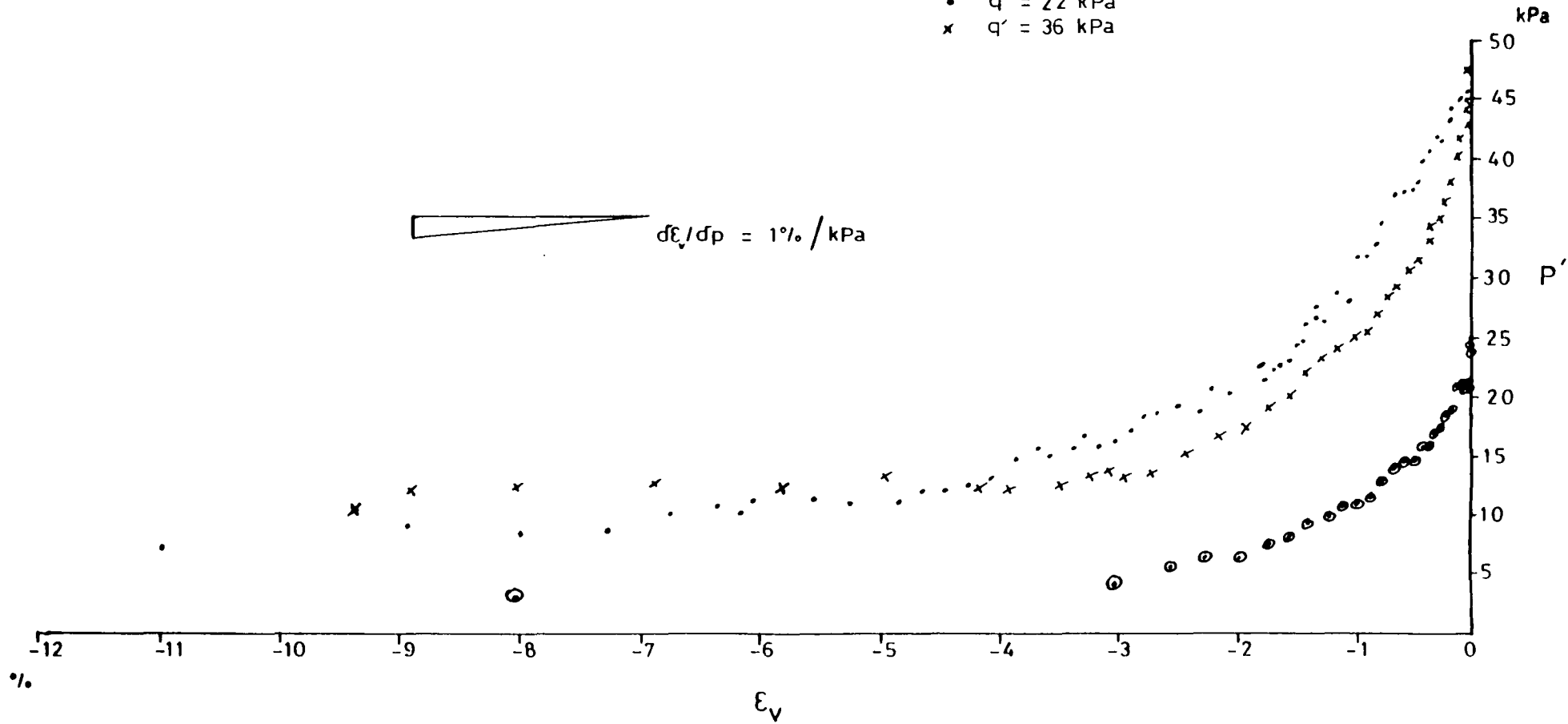


Fig 6/13 Plot of normal effective stress, p' , against volumetric strain, ϵ_v , for increasing pore water pressure tests on undisturbed samples - Gault Clay - Dunton Green

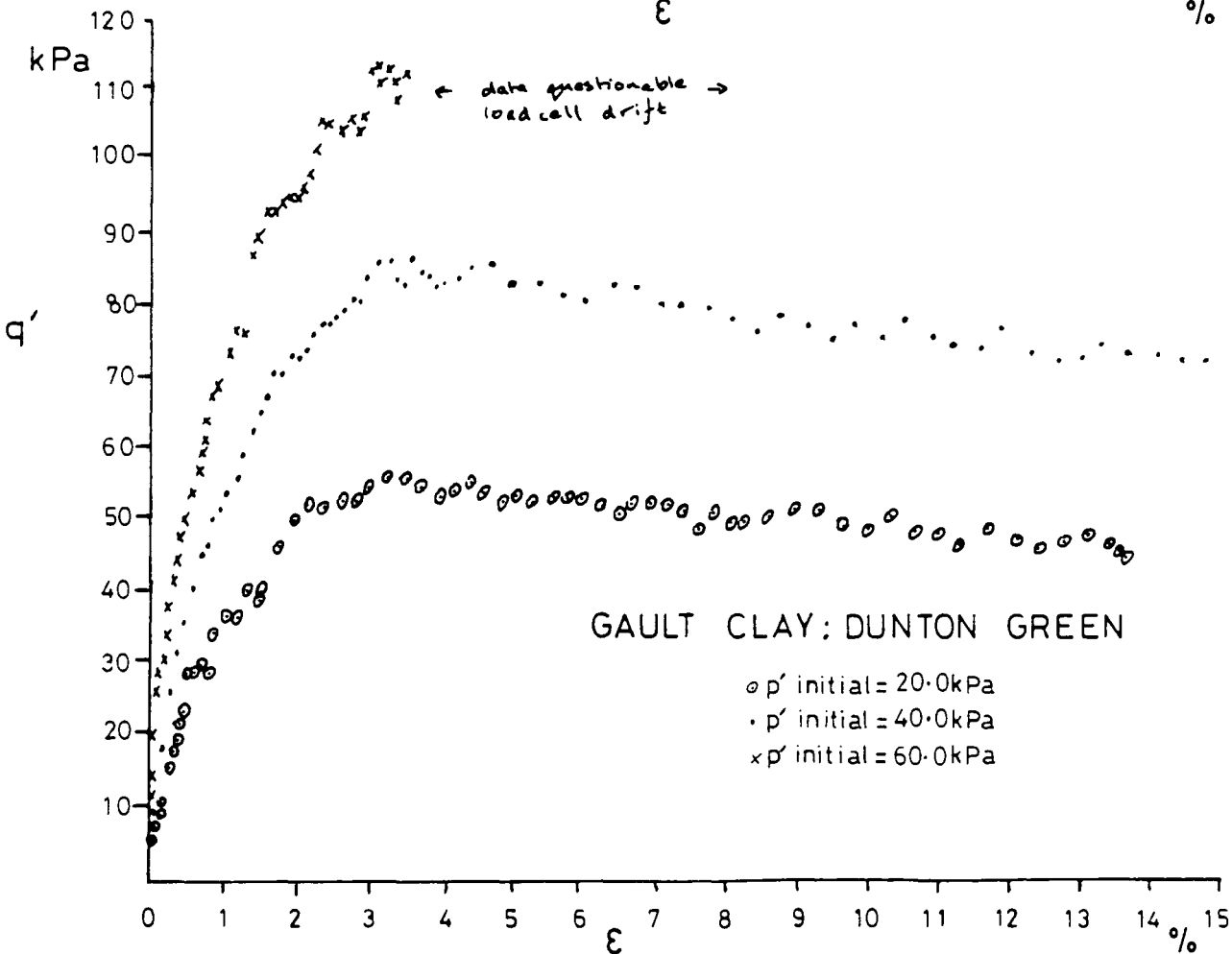
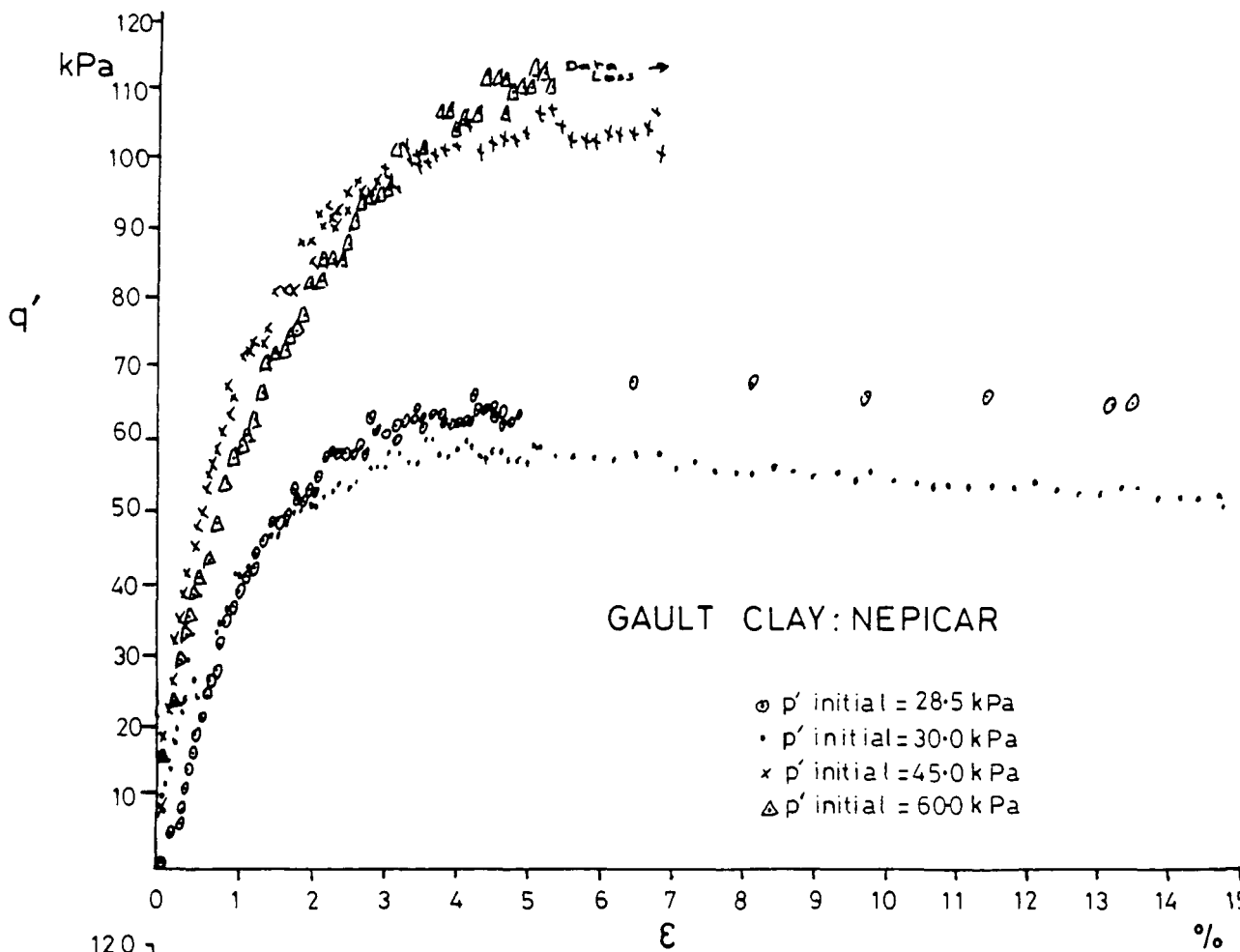


Fig 6/14 Plot of effective deviator stress, q' , against strain, ϵ , for drained tests on undisturbed samples
- Gault Clay

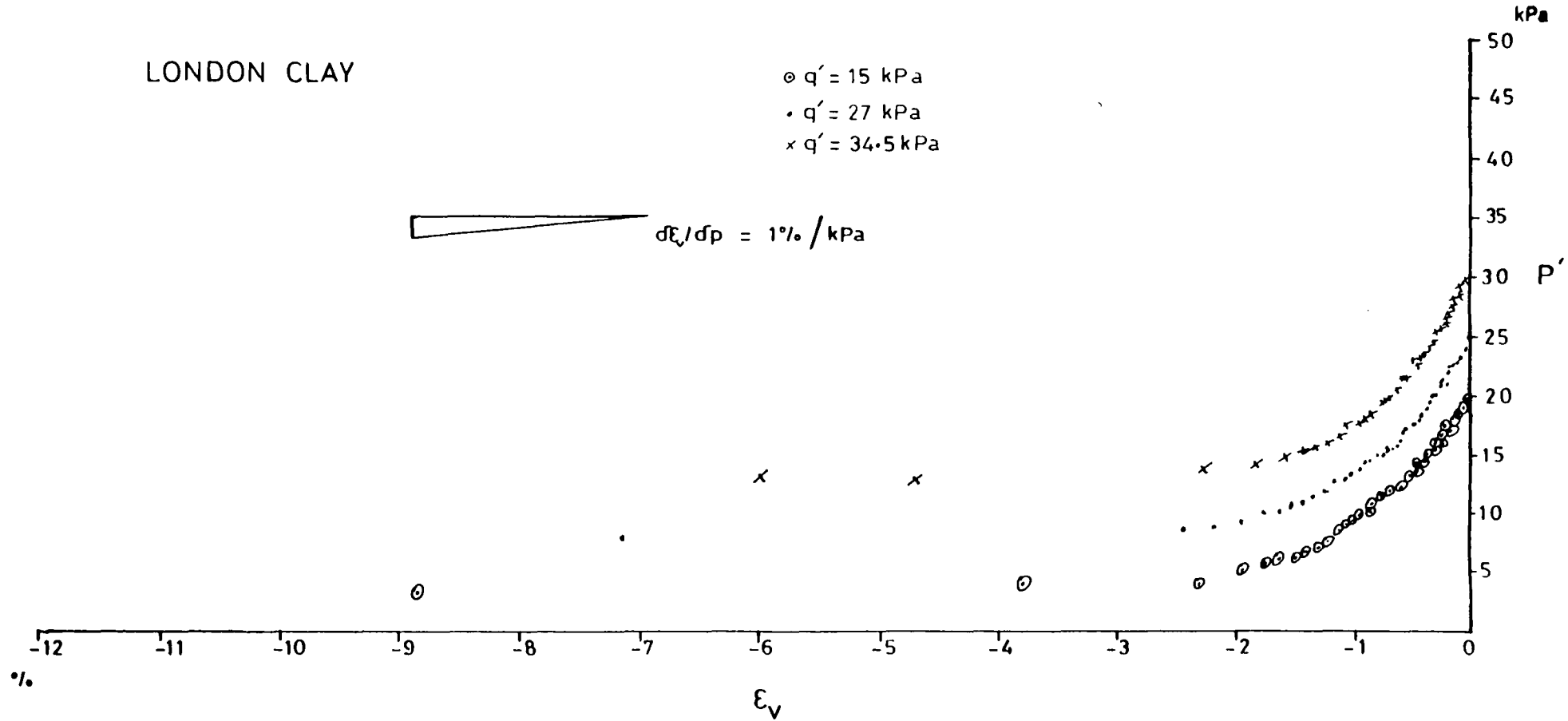
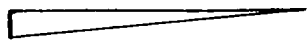
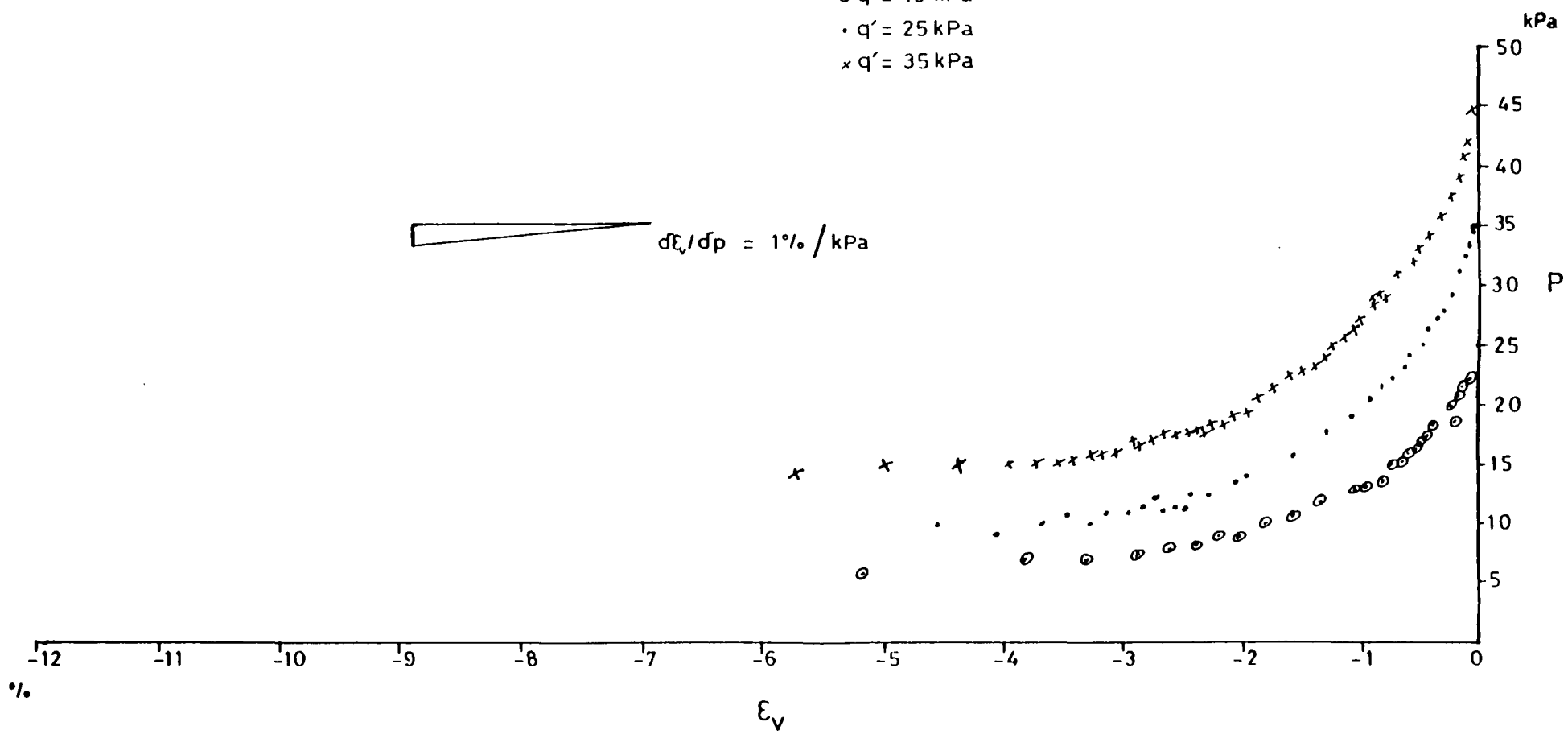


Fig 6/15 Plot of normal effective stress, p' , against volumetric strain, ε_v , for increasing pore water pressure tests on undisturbed samples - London Clay

READING BEDS

- $q' = 15 \text{ kPa}$
- $q' = 25 \text{ kPa}$
- × $q' = 35 \text{ kPa}$

 $d\epsilon_v/dp = 1\% / \text{kPa}$



149

Fig 6/16 Plot of normal effective stress, p' , against volumetric strain, ϵ_v , for increasing pore water pressure tests on undisturbed samples - Reading Beds clay

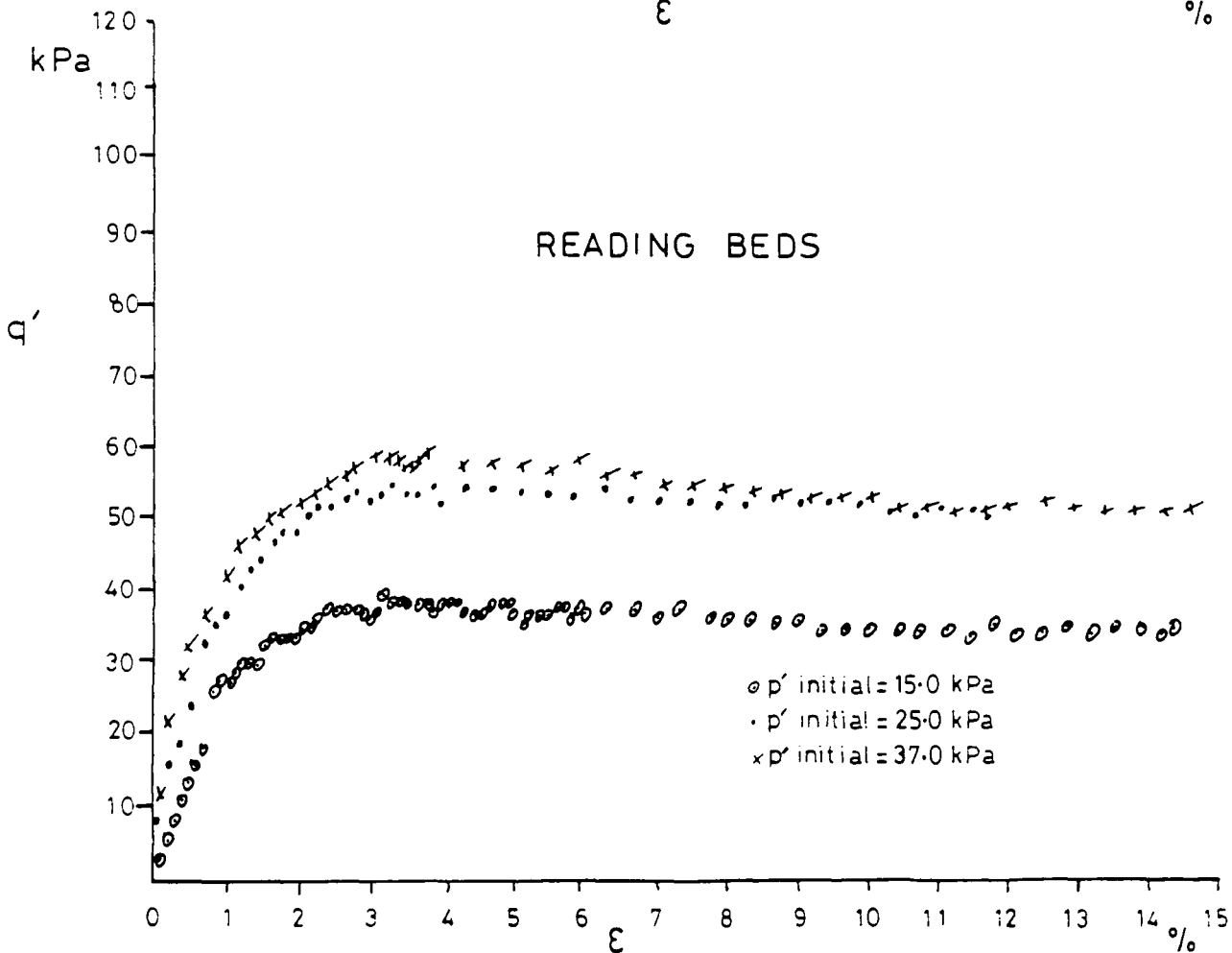
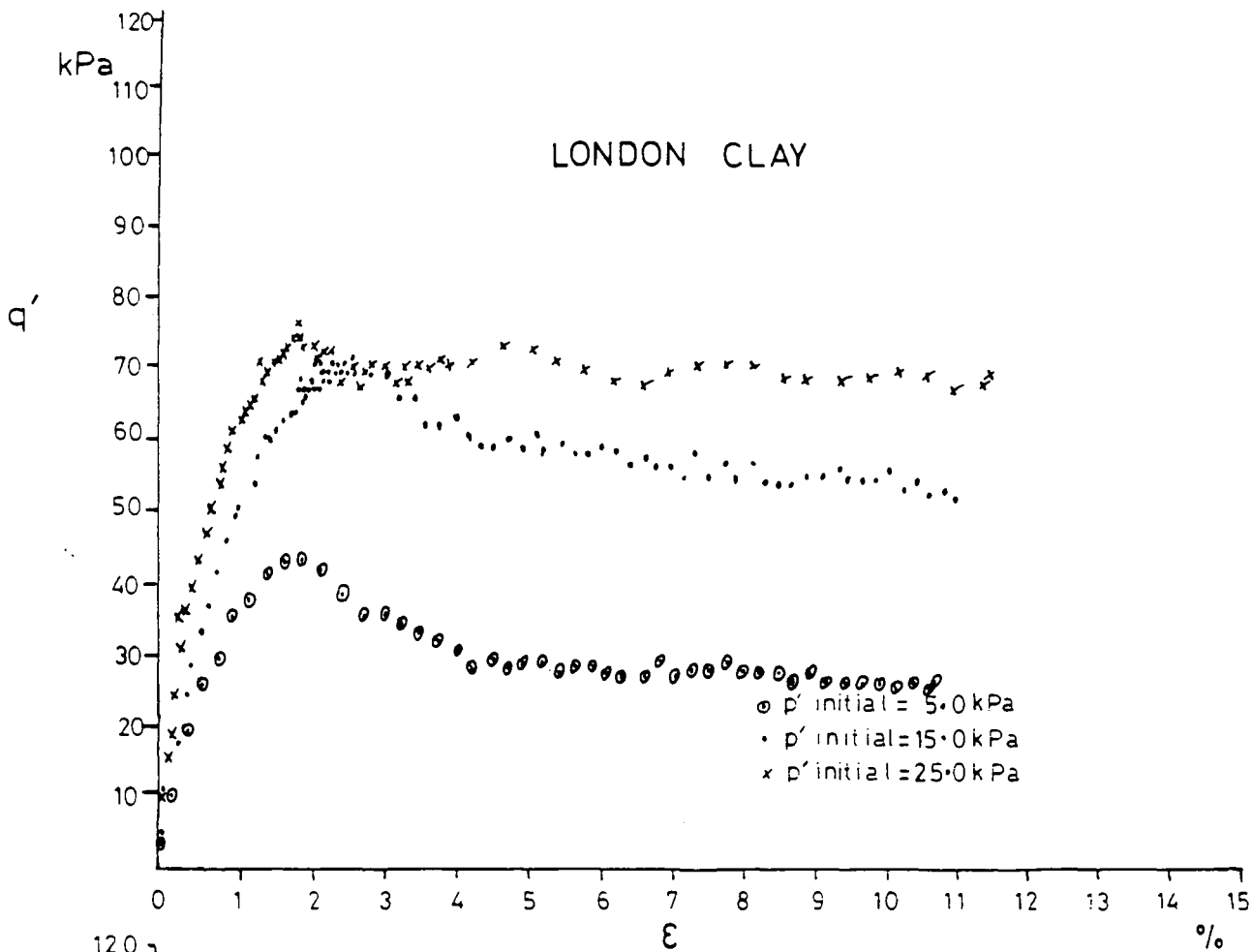
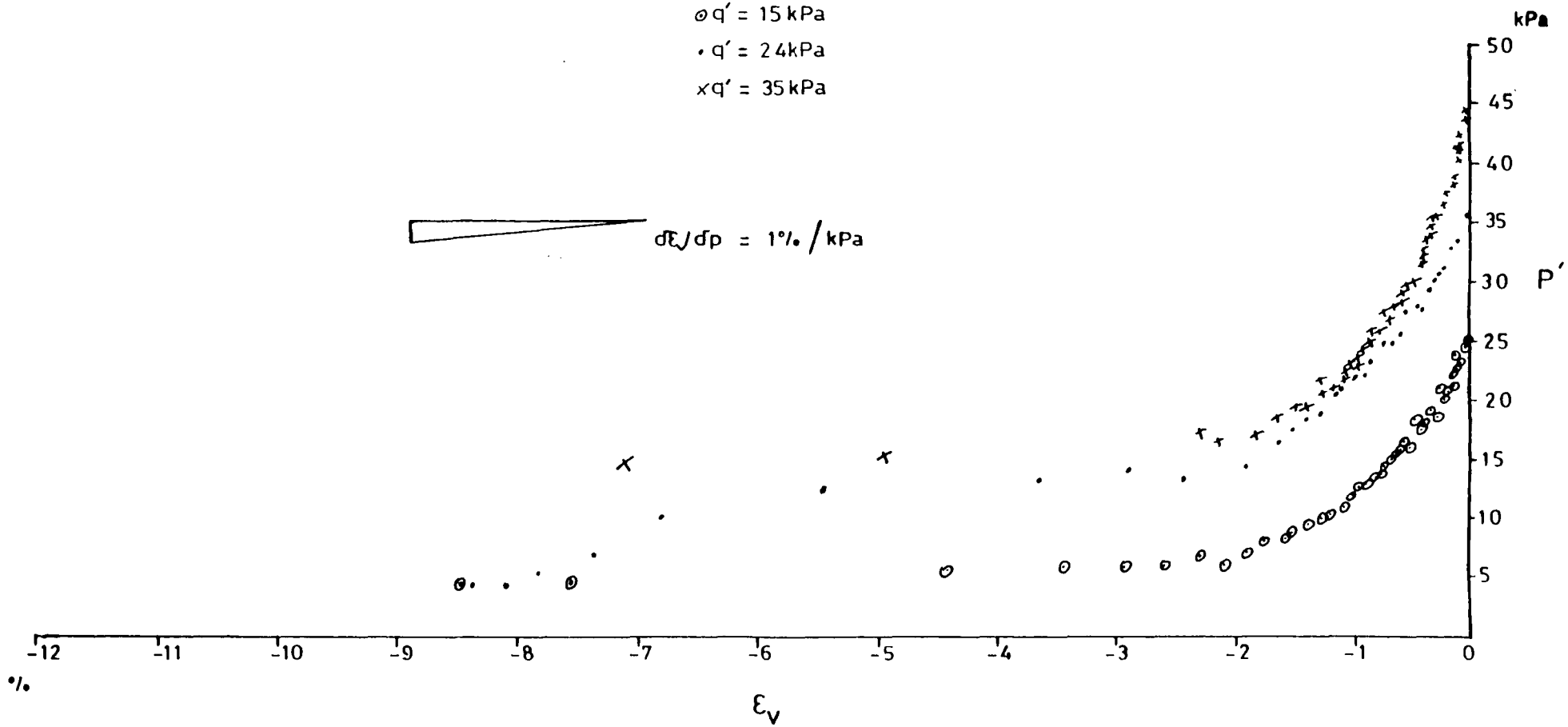


Fig 6/17 Plot of effective deviator stress, q' , against strain, ϵ , for drained tests on undisturbed samples - London Clay and Reading Beds clay

WEALD CLAY



151

Fig 6/18 Plot of normal effective stress, p' , against volumetric strain, ϵ_v , for increasing pore water pressure tests on undisturbed samples - Weald Clay

KIMMERIDGE CLAY

$\sigma q' = 14.5 \text{ kPa}$
 $\cdot q' = 27.5 \text{ kPa}$

$d\epsilon_v/dp = 1\% / \text{kPa}$

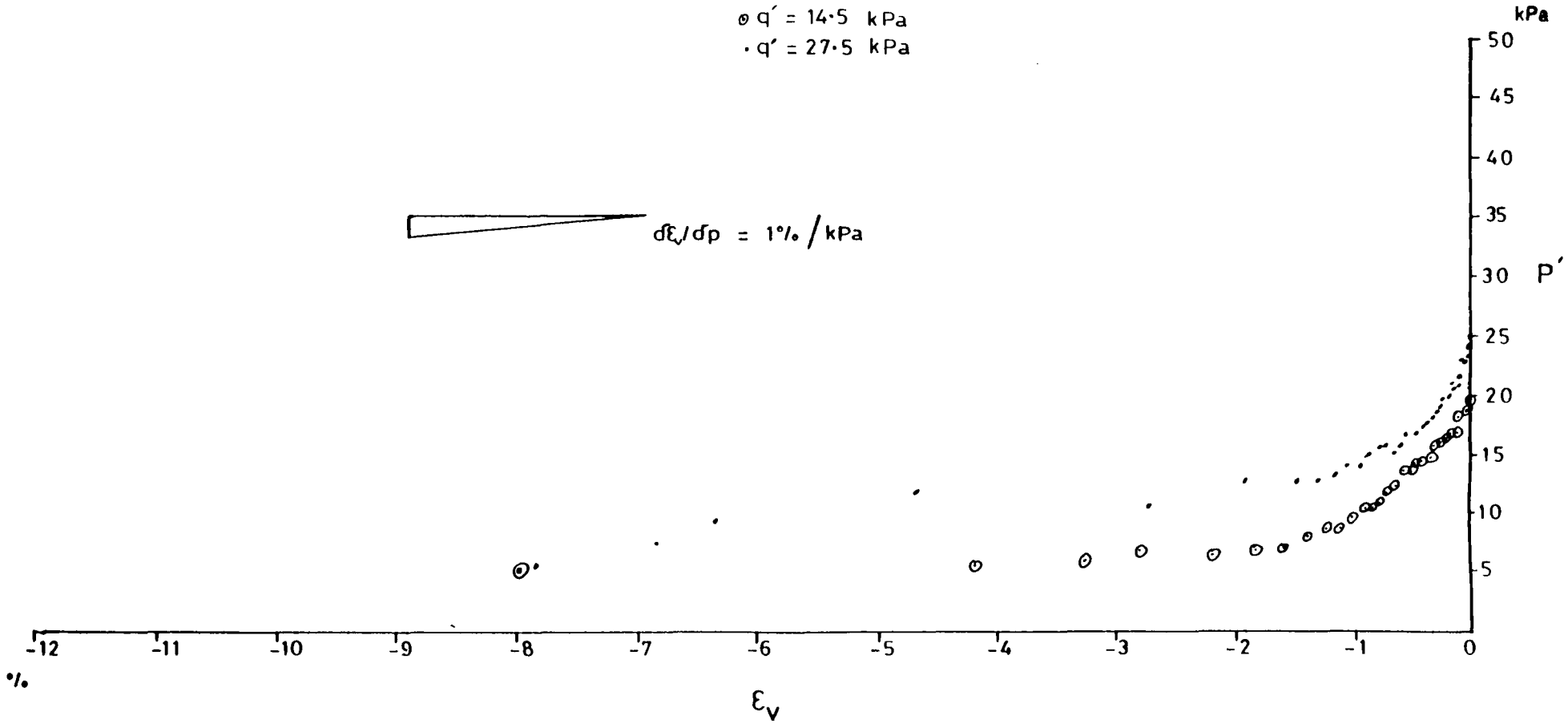


Fig 6/19 Plot of normal effective stress, p' , against volumetric strain, ϵ_v , for increasing pore water pressure tests on undisturbed samples - Kimmeridge Clay

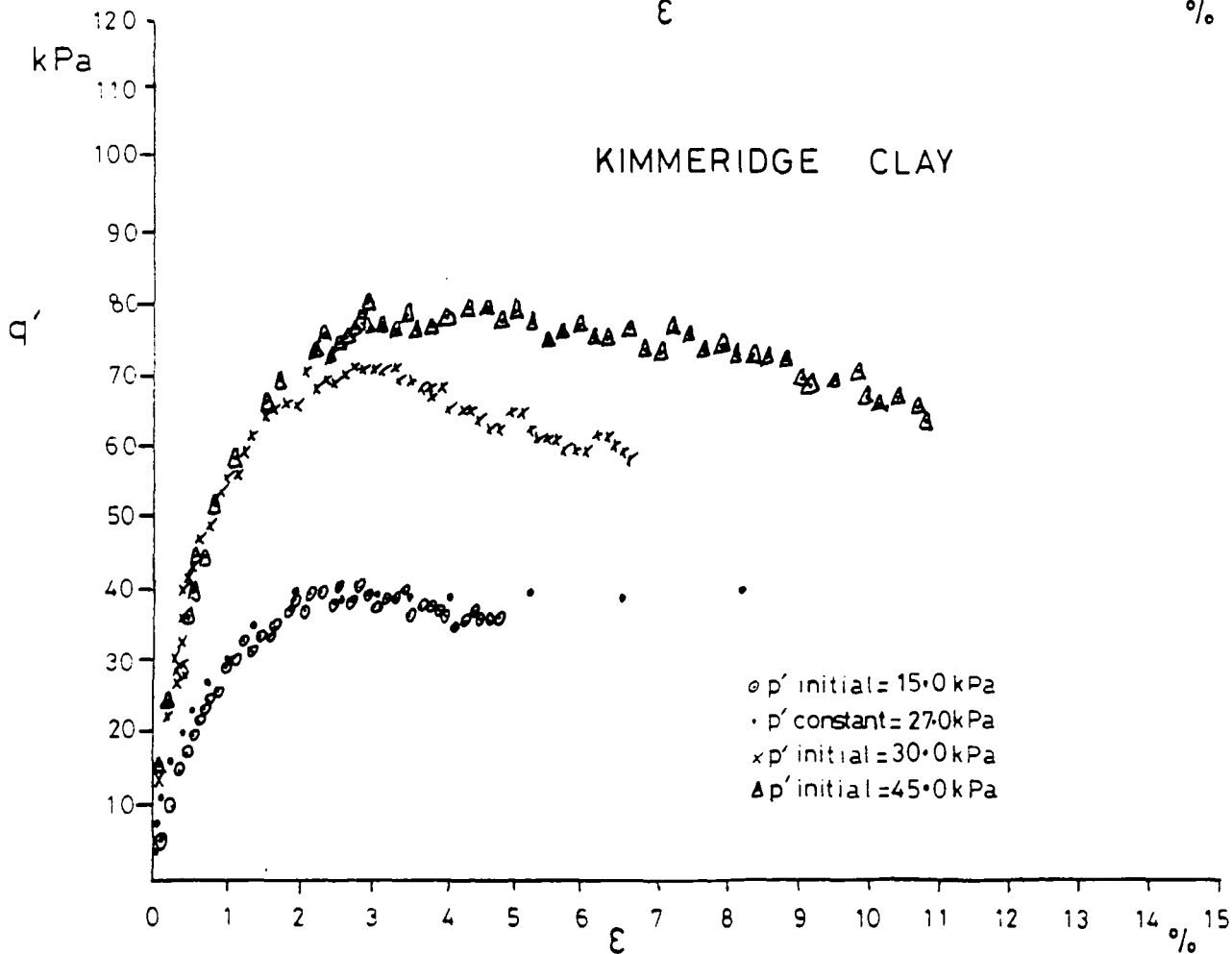
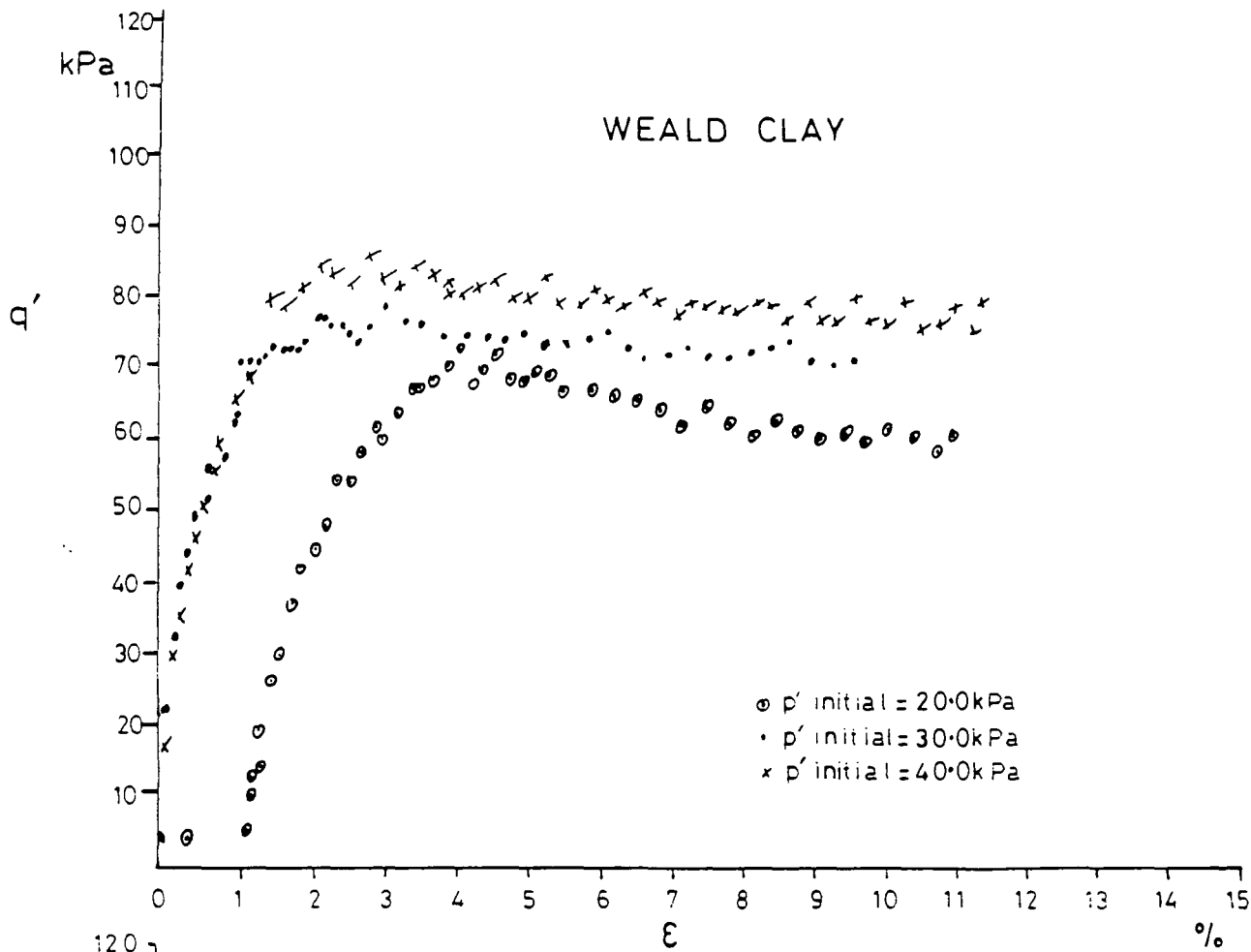
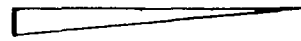


Fig 6/20 Plot of effective deviator stress, q' , against strain, ϵ , for drained tests on undisturbed samples - Weald Clay and Kimmeridge Clay

OXFORD CLAY

- o $q' = 15.5 \text{ kPa}$
- $q' = 25.5 \text{ kPa}$
- x $q' = 35.5 \text{ kPa}$

 $d\epsilon_v/dp = 1\% / \text{kPa}$

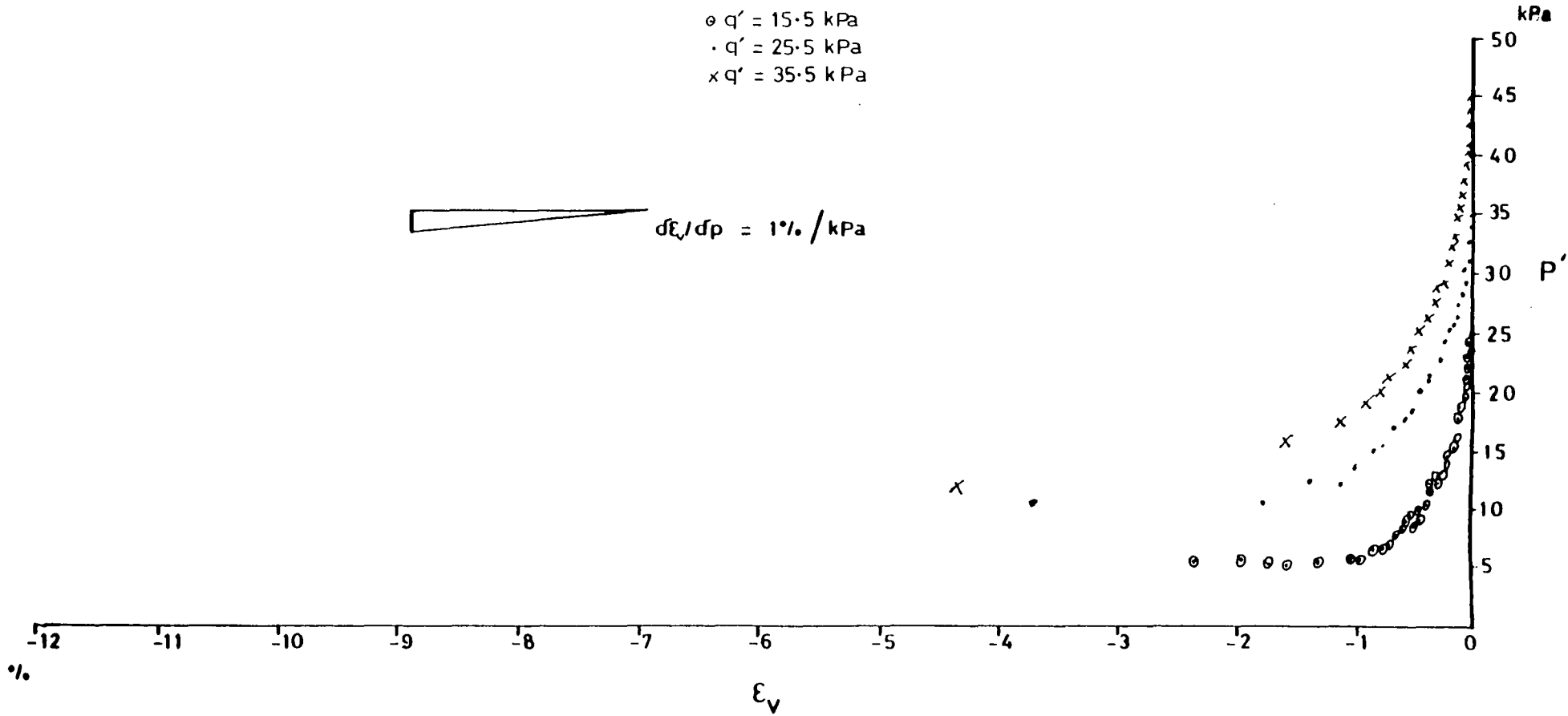


Fig 6/21 Plot of normal effective stress, p' , against volumetric strain, ϵ_v , for increasing pore water pressure tests on undisturbed samples - Oxford Clay

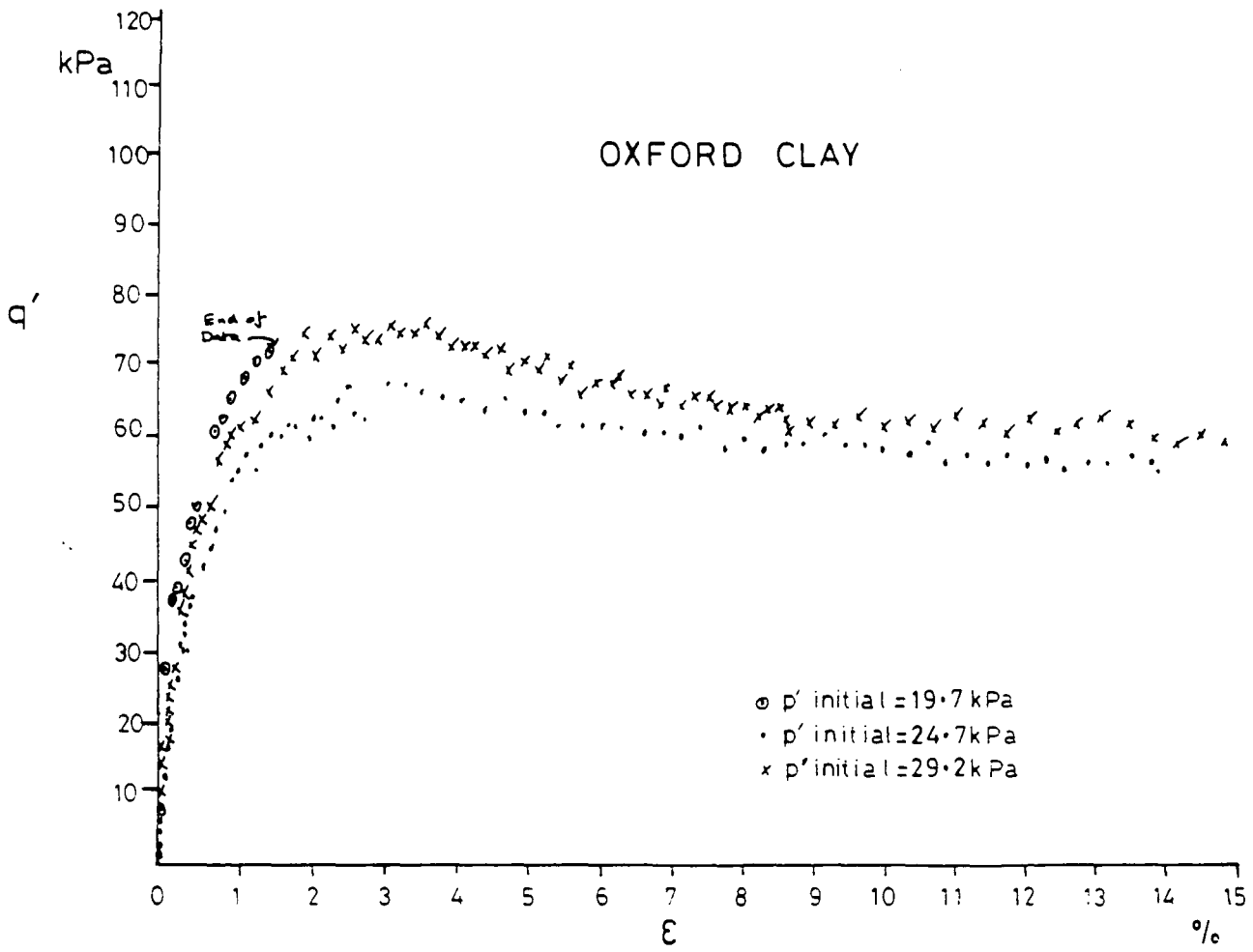
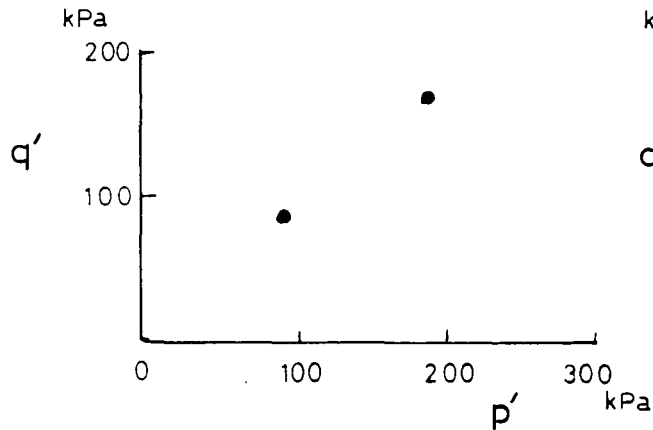
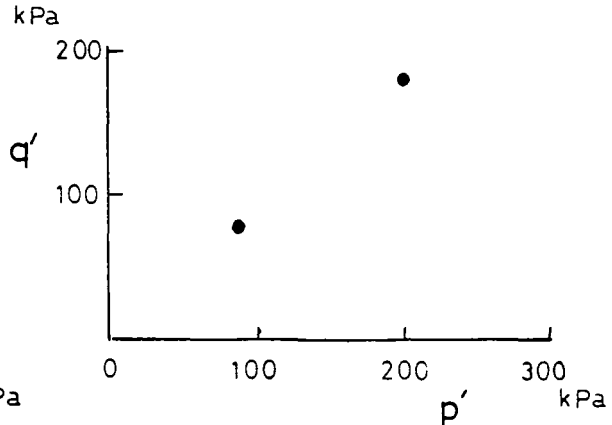


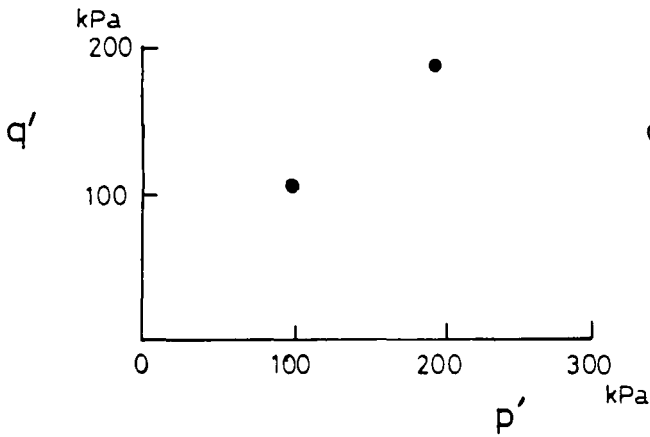
Fig 6/22 Plot of effective deviator stress, q' , against strain, ϵ , for drained tests on undisturbed samples .
 - Oxford Clay



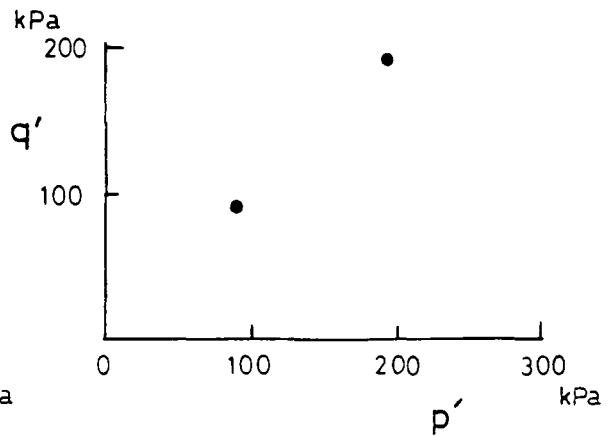
GAULT CLAY: NEPICAR



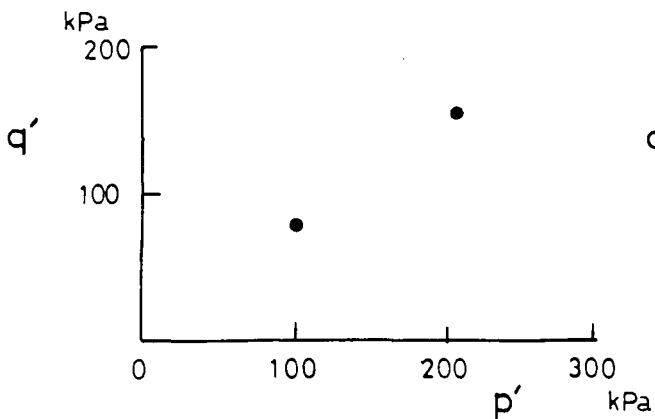
KIMMERIDGE CLAY



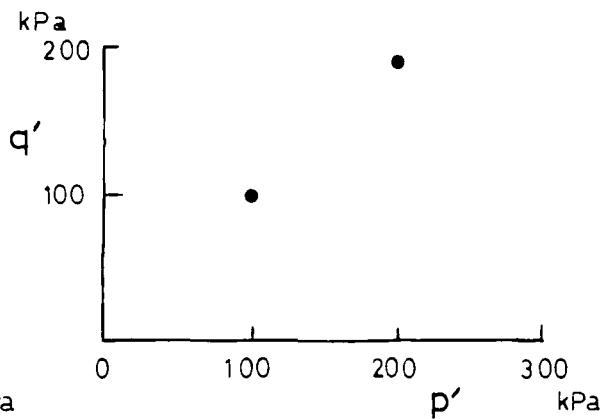
LONDON CLAY



OXFORD CLAY



READING BEDS



WEALD CLAY

Fig 6/23 Plot of effective deviator stress, q' , against mean normal effective stress, p' , at the critical state condition for reconstituted samples

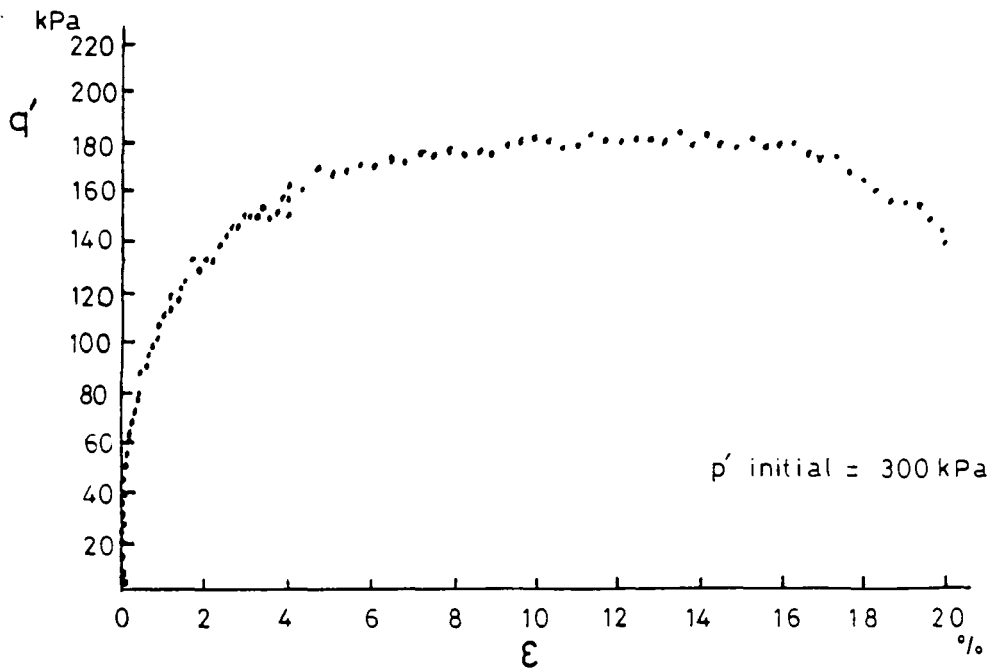
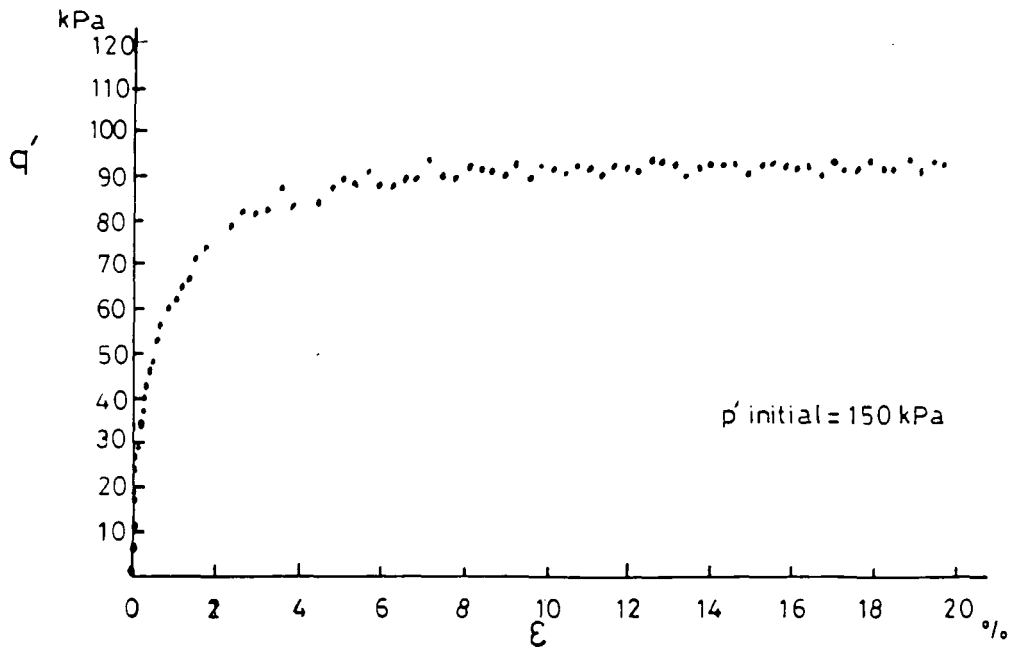


Fig 6/24 Plot of effective deviator stress, q' , against strain, ϵ , for undrained tests on reconstituted samples - Gault Clay - Nepicar

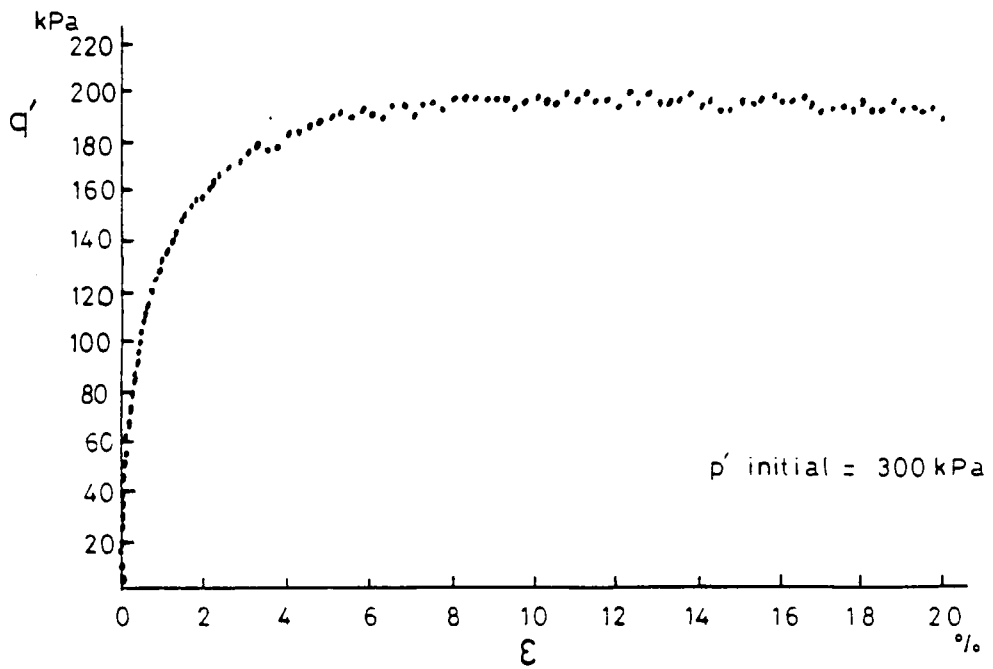
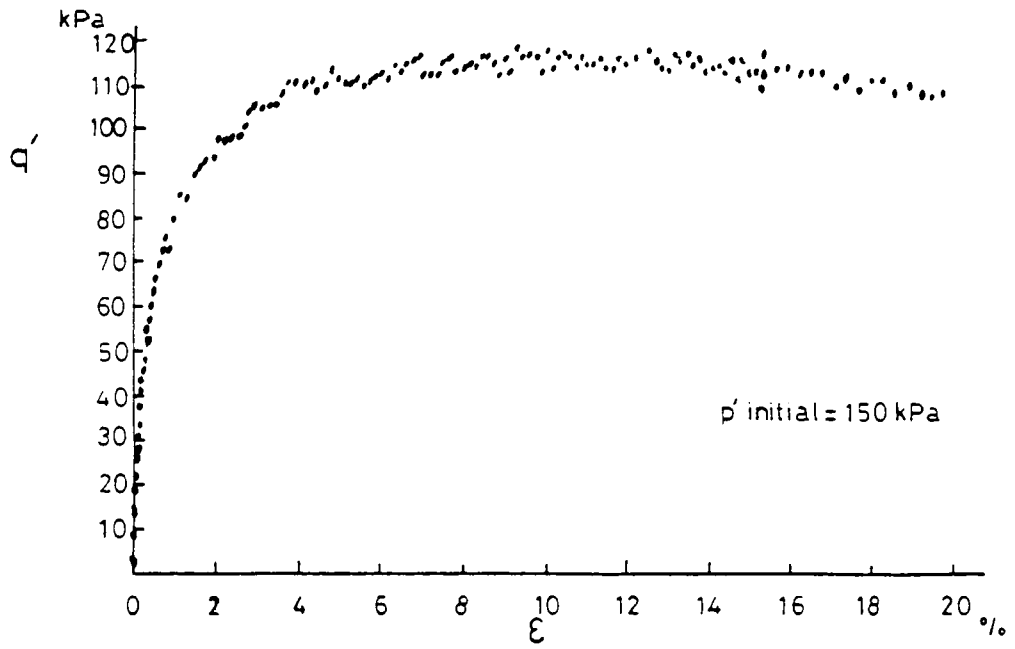


Fig 6/25 Plot of effective deviator stress, q' , against strain, ϵ , for undrained tests on reconstituted samples - London Clay

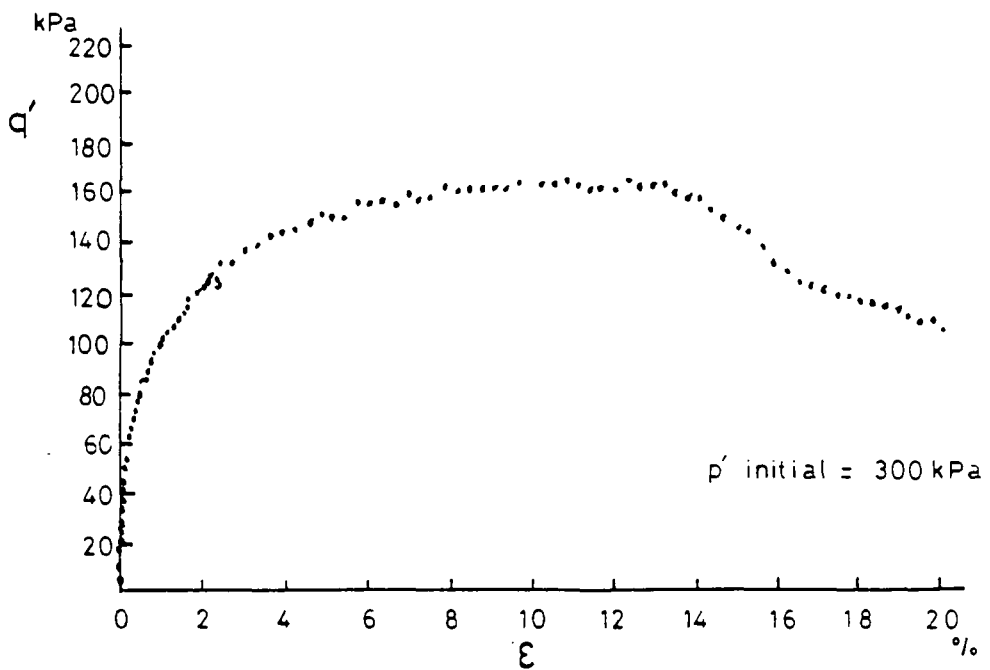
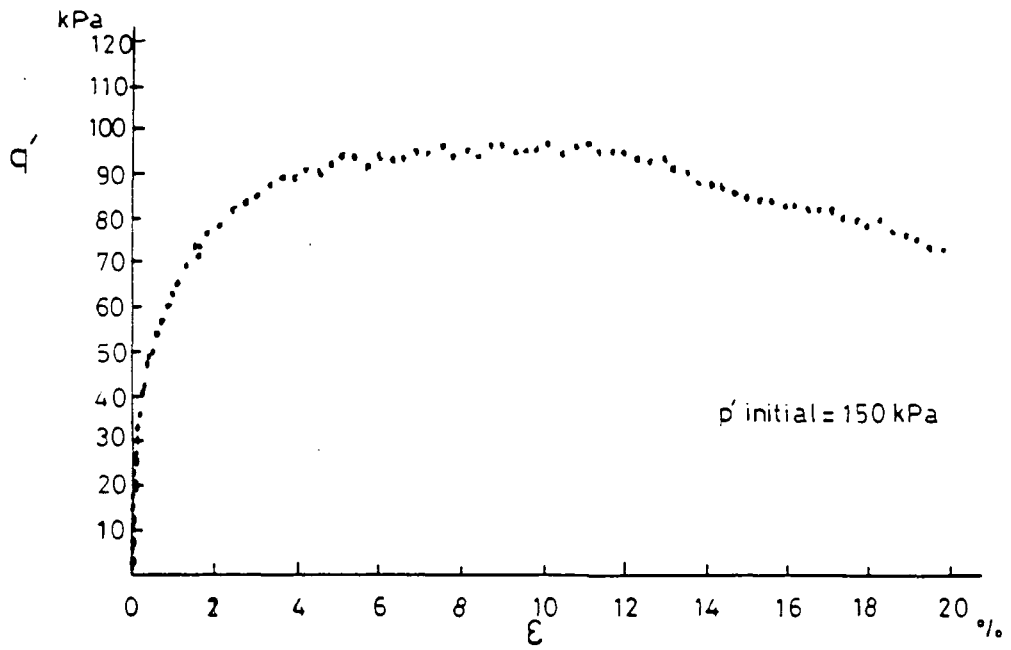


Fig 6/26 Plot of effective deviator stress, q' , against strain, ϵ , for undrained tests on reconstituted samples - Reading Beds clay

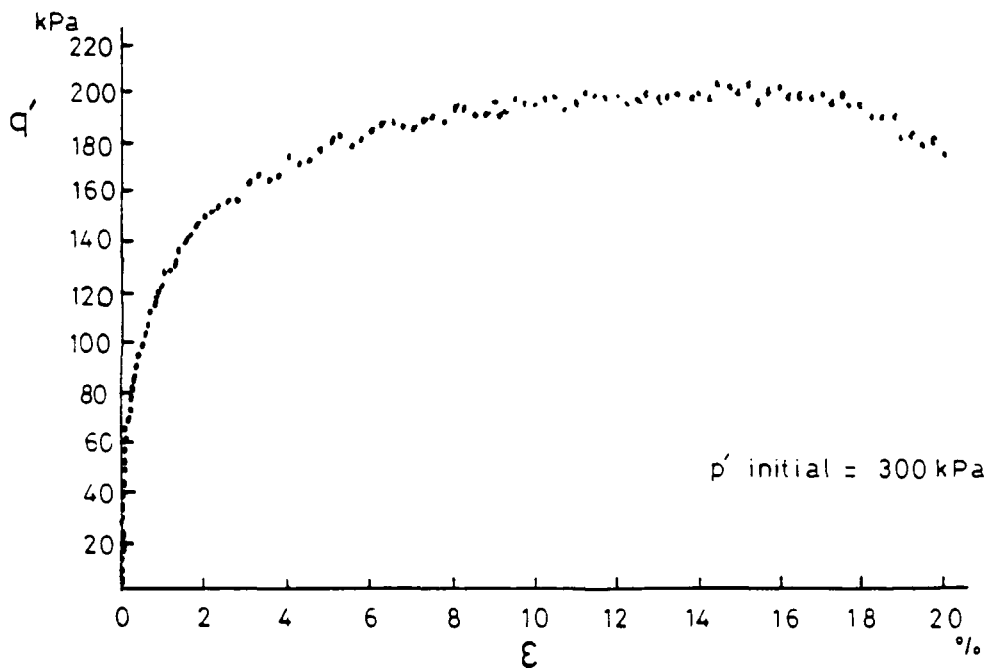
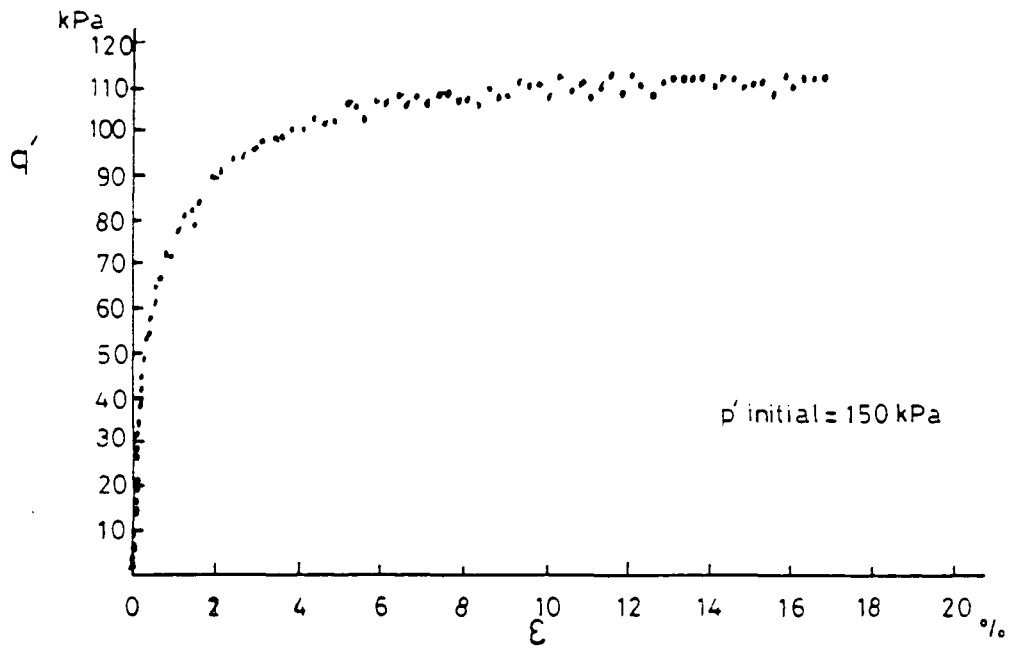


Fig 6/27 Plot of effective deviator stress, q' , against strain, ϵ , for undrained tests on reconstituted samples - Weald Clay

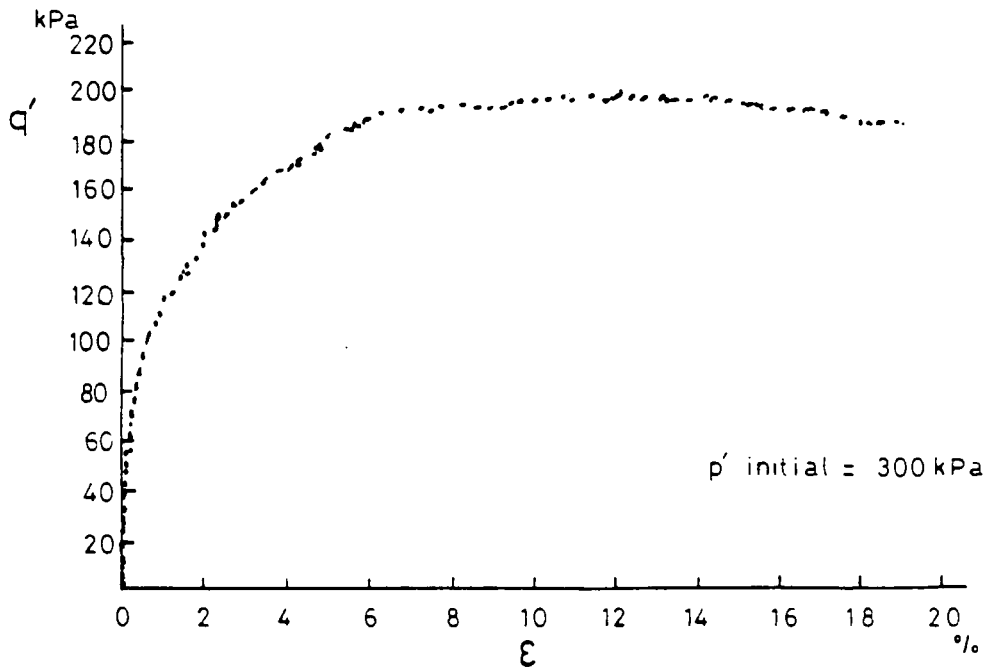
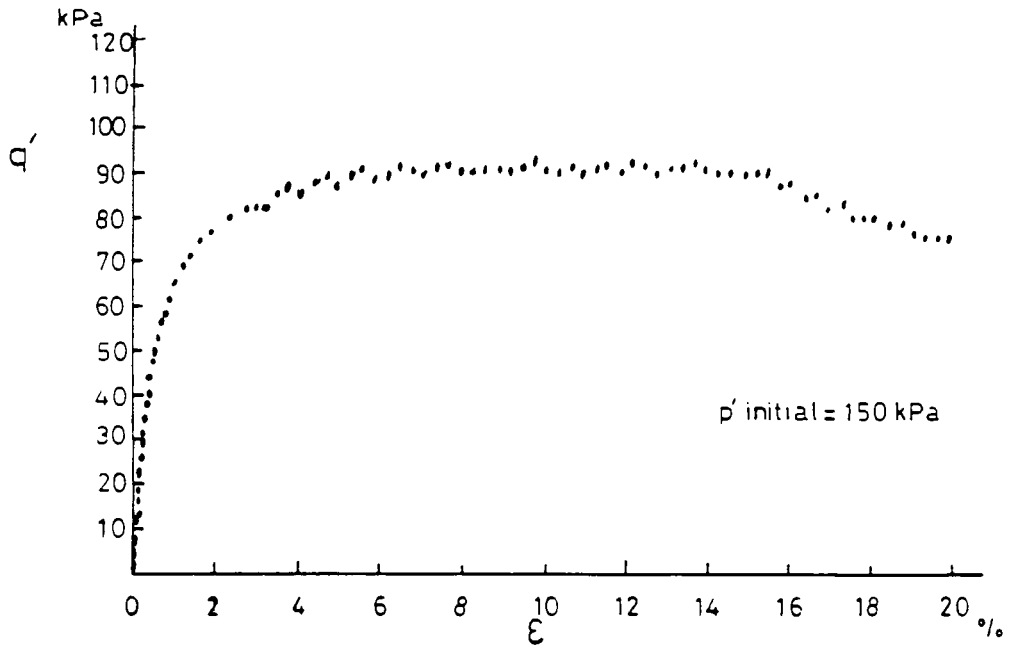


Fig 6/28 Plot of effective deviator stress, q' , against strain, ϵ , for undrained tests on reconstituted samples - Kimmeridge Clay

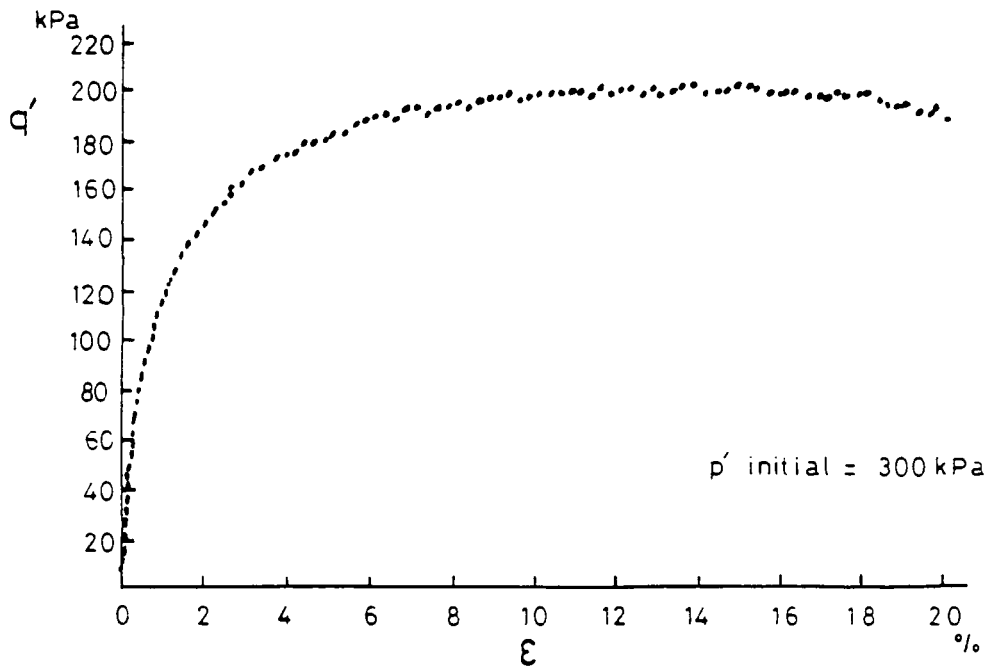
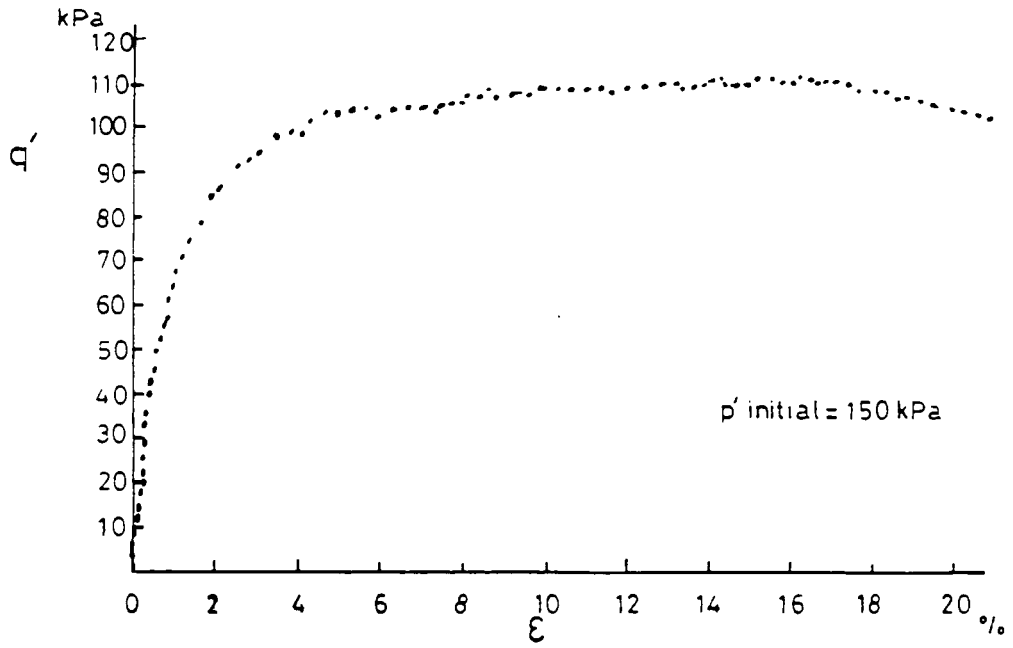


Fig 6/29 Plot of effective deviator stress, q' , against strain, ϵ , for undrained tests on reconstituted samples - Oxford Clay

Linear failure envelopes at low effective stresses

7.1 Introduction

In the previous Chapter, the Mohr circle diagrams for the soils under test indicated that a non-linear failure envelope may be a more accurate indication of peak shear strength than a linear failure envelope. To consider this point, this Chapter investigates the linear failure envelope and Chapter 8 considers the curved failure envelope. The present knowledge of linear envelopes is discussed and taken further to consider a curved envelope and how it may be fitted to experimental data. Analyses of the test results is conducted using the methods developed for fitting curved and linear failure envelopes and an assessment made of the accuracy of these methods. Emphasis will be placed on a power curve relation between shear and normal stress as it is shown that this is more accurate than a straight line relation.

7.2 The Mohr circle diagram and Mohr-Coulomb failure criteria

To understand the concept of the linear shear strength envelope it is first necessary to consider the effects of stress on an element of soil subject to plane deformation ie. the thickness of element is not altered by any change in the stress state (Figure 7/1). σ_1 is the major principal stress and σ_3 is the minor principal stress.

Resolving forces in horizontal and vertical directions gives respectively

$$\sigma_3 \cdot \delta_s \cdot \sin\psi + \tau \cdot \delta_s \cdot \cos\psi - \sigma \cdot \delta_s \cdot \sin\psi = 0 \quad (1)$$

$$\sigma_1 \cdot \delta_s \cdot \cos\psi - \tau \cdot \delta_s \cdot \sin\psi - \sigma \cdot \delta_s \cdot \cos\psi = 0 \quad (2)$$

Combining equations 2 and 1 to eliminate τ , gives

$$\sigma_3 + (\sigma_1 - \sigma_3) \cdot \cos^2\psi = \sigma$$

now from trigonometry identities

$$\cos 2\psi = 2\cos^2\psi - 1$$

so
$$\sigma_3 + \frac{(\cos 2\psi + 1)(\sigma_1 - \sigma_3)}{2} = \sigma$$

$$\frac{(\sigma_1 - \sigma_3)}{2} \cdot \cos 2\psi + \frac{(\sigma_1 + \sigma_3)}{2} = \sigma \quad (3)$$

Substituting equation 3 for σ in equation 2 and applying suitable trigonometry identities gives

$$\frac{(\sigma_1 - \sigma_3)}{2} \cdot \sin 2\psi = \tau \quad (4)$$

Putting values ψ , σ_1 and σ_3 in equations 3 and 4 allows the normal and shear stresses to be calculated theoretically. However a more convenient method is the graphical method used by Mohr in his work on ideal plastic materials.

Consider equations 3 and 4. If these equations are written as follows

$$\frac{(\sigma_1 - \sigma_3)}{2} \cdot \cos 2\psi = \sigma - \frac{(\sigma_1 + \sigma_3)}{2}$$

$$\frac{(\sigma_1 - \sigma_3)}{2} \cdot \sin 2\psi = \tau$$

and then squared and added together

$$\left[\frac{(\sigma_1 - \sigma_3)}{2} \sin 2\psi \right]^2 + \left[\frac{(\sigma_1 - \sigma_3)}{2} \cos 2\psi \right]^2 = \left[\sigma - \frac{(\sigma_1 + \sigma_3)}{2} \right]^2 + \tau^2$$

$$\left[\frac{(\sigma_1 - \sigma_3)}{2} \right]^2 = \left[\sigma - \frac{(\sigma_1 + \sigma_3)}{2} \right]^2 + \tau^2$$

This is the equation of a circle of the form

$$r^2 = (\sigma - a)^2 + (\tau - b)^2$$

where a and b = co-ordinates of centre of circle

and r = radius of circle

The radius of the circle is $\frac{(\sigma_1 - \sigma_3)}{2}$ and the centre has

co-ordinates $\left(\frac{(\sigma_1 + \sigma_3)}{2}, 0 \right)$. The circle represents

all possible states of normal and shear stress. Figure 7/2 illustrates how the Mohr circle diagram presents the stresses on a plane.

The co-ordinates of point Q, which are the normal and shear stresses on a plane at an angle of ψ to the minor principal stress direction, are given by equations 3 and 4. The locus of the stress conditions for all planes through a point in shear and normal stress space is a circle called a stress or Mohr circle. It should be noted that in the case of triaxial testing, which is the basis of the above diagram, the principal planes are on the x-axis because in the triaxial test the imposed stresses are the principal stresses. As a number of circles are drawn from tests where samples have failed, it becomes clear that there is a line which is tangential to all these circles. This line corresponds to the equation developed by Coulomb and its significance is now discussed.

The Mohr-Coulomb yield criteria is one of the major suppositions used in soil mechanics. It assumes that the difference between the major and minor principal stresses is a

function of their sum and that the intermediate stress can be ignored. It has long been the practice to approximate the tangential line to a series of Mohr circles at failure, over a finite stress range, by a single straight line which is known as the failure envelope. The gradient of the envelope is considered to be a measure of the intergranular friction within the soil and is referred to as $\tan\phi$ where ϕ is the angle of internal friction. The intercept on the shear stress axis is taken as a measure of the soils inherent strength at zero stress and is called the cohesion of the soil. Collectively, the intergranular friction and the cohesion of a soil are known as the shear strength. It should be stressed, however, that more emphasis should be placed on c and ϕ as parameters rather than trying to explain them in physical terms. They are not fundamental properties of the material and they vary with the type of soil test, sample size, soil's initial state, rate of stress application and permeability.

The failure envelope is therefore defined by the Coulomb relation in effective stress terms as

$$\tau = \sigma' \cdot \tan\phi' + c'$$

where τ = shear stress at failure

ie. shear strength

σ' = effective normal stress at failure ie. $\sigma - u$, where

u = pore water pressure

σ = total normal stress

ϕ' = angle of friction with

respect to effective stresses
 c' = cohesion with respect to
effective stresses

Figure 7/3 shows the relation graphically. Any deviation of the Mohr circles from the envelope is attributed to experimental error and the inconsistencies between samples. By definition a soil cannot attain a state of stress outside the envelope. Furthermore the line must be a tangent since it represents a stress boundary for the largest possible circle.

7.3 Techniques for fitting the Mohr-Coulomb failure envelope to experimental data

When a number of tests have been conducted, each causing a sample to fail, the Mohr circles are plotted and it is then necessary to construct the failure envelope at a tangent to the circles and is taken to be a straight line obeying the Coulomb relation. There are a number of ways of constructing the failure envelope. One simple method is to draw a tangential straight line by eye but this results in imprecise values of c' and ϕ' . The most common method though is to use the 'Top Point Construction' (Vickers, 1983 for example). This involves taking the 'top point' of each stress circle which is the maximum shear stress and the normal stress for those particular principal stresses (see Figure 7/4).

It is worth pointing out that although the top point is where

the maximum shear stress occurs it is not the failure point and failure occurs at a lower shear stress where the circle just touches the failure envelope at maximum obliquity. Since the straight line failure envelope is rarely an exact tangent to all the circles and consequently precise failure stresses cannot be found, using the top points, which can be found accurately, allows the most representative envelope to be found. A least squares fit regression line is drawn using standard statistical procedures to minimize the vertical distances between the line and top points. The shear stress errors are minimized in this way although errors occur in both shear and normal stresses. The top points may not sit exactly on a straight line because,

(a) assuming the top points lie on a straight line assumes Coulomb's relation is also a straight line. However, the failure envelope for peak stresses is in fact curved (discussed in Chapter 8) and is most marked at low effective stresses (up to 100kPa). At higher stresses the curvature is small over the same stress range and in most cases an approximation to a straight line is appropriate. For shallow failures the effective stresses are extremely low and curvature of the failure envelope will be quite marked.

(b) soil is a very heterogeneous material with variations in mineral types, mineral orientation, cementation, degree of fissuring, degree of consolidation and moisture content. Consequently a collection of samples can have different values of c' and ϕ' when compared to another set of samples from the same location.

(c) experimental errors will occur, the magnitude of which will depend on the accuracy of the apparatus and the method of testing.

When a least square fit line has been drawn through the top points, it can be related to the failure envelope using the similar triangles in Figure 7/5. (c'_{TP} and ϕ'_{TP} are the cohesion intercept and angle of friction of the failure envelope calculated in the top point construction.)

$$x = c'_{TP} \cdot \cot\phi'_{TP}$$

$$\text{and } x = a \cdot \cot\alpha$$

$$\sin\phi'_{TP} = \frac{\frac{\sigma'_1 - \sigma'_3}{2}}{c'_{TP} \cdot \cot\phi'_{TP} + \frac{\sigma'_1 + \sigma'_3}{2}}$$

$$\tan\alpha = \frac{\frac{\sigma'_1 - \sigma'_3}{2}}{c'_{TP} \cdot \cot\phi'_{TP} + \frac{\sigma'_1 + \sigma'_3}{2}}$$

$$\text{resulting in } \sin\phi'_{TP} = \tan\alpha$$

$$\text{Also } \tan\phi'_{TP} = \frac{c'_{TP}}{x} \quad \text{and} \quad \tan\alpha = \frac{a}{x}$$

$$\text{therefore } \frac{\tan\phi'_{TP}}{\tan\alpha} = \frac{\sin\phi'_{TP}}{\cos\phi'_{TP} \cdot \sin\phi'_{TP}} = \frac{1}{\cos\phi'_{TP}}$$

$$\text{resulting in } c'_{TP} \cdot \cos\phi'_{TP} = a$$

An alternative method has been proposed by Lisle and Strom (1982) which minimizes the perpendicular distance between the failure envelope and the Mohr circles. This method is worth considering in some detail as it initially appears to be more accurate.

The most accurate straight line failure envelope is the one produced by a least-squares fit and entails minimizing the sum of the radial distances from the Mohr circles perpendicular to the required failure envelope, $S = \sum \delta_i^2$ (Figure 7/6). If i equals the number of each circle 1,2,3,4..n, then the centre of each circle and the radius of the i th Mohr circle are respectively

$$s'_i = \frac{\sigma'_{1i} + \sigma'_{3i}}{2} \qquad t_i = \frac{\sigma'_{1i} - \sigma'_{3i}}{2}$$

(Note that s'_i and t_i are the mean effective normal stress and maximum shear stress respectively for two dimensions and are defined differently to those used in Chapter 6 which relate to testing only.)

The distance requiring minimizing is given by

$$\delta_i = XY - t_i$$

Also $XY = \tau \cdot \cos \phi'_{Ls}$ where τ is the shear stress at point Z. The Coulomb relation for the straight line at this point on the failure envelope is $\tau = c'_{Ls} + s'_i \cdot \tan \phi'_{Ls}$ and the trigonometry identity used is

$$\cos \phi'_{Ls} = \frac{1}{\sqrt{(\tan^2 \phi'_{Ls} + 1)}}$$

$$\text{so} \qquad \delta_i = \frac{c'_{Ls} + s'_i \cdot \tan \phi'_{Ls}}{\sqrt{(\tan^2 \phi'_{Ls} + 1)}} - t_i$$

$$\text{now} \quad S = \sum (\delta_i)^2 = \sum_{i=1}^n \left[\frac{c'_{Ls} + s'_i \cdot \tan \phi'_{Ls}}{\sqrt{(\tan^2 \phi'_{Ls} + 1)}} - t_i \right]^2$$

The parameters c'_{Ls} and $\tan \phi'_{Ls}$ are as yet unknown so

minimizing S with respect to them ie. $\frac{\delta S}{\delta c'_{Ls}} = 0$

and $\frac{\delta S}{\delta \tan \phi'_{L_s}} = 0$ gives

$$\frac{\delta S}{\delta c'_{L_s}} = 2 \cdot \sum_{i=1}^n \left[\frac{c'_{L_s} + s'_i \cdot \tan \phi'_{L_s} - t_i}{\sqrt{(\tan^2 \phi'_{L_s} + 1)}} \right] \cdot \frac{1}{\sqrt{(\tan^2 \phi'_{L_s} + 1)}} = 0$$

$$0 = \sum_{i=1}^n \left[\frac{c'_{L_s} + s'_i \cdot \tan \phi'_{L_s} - t_i}{\sqrt{(\tan^2 \phi'_{L_s} + 1)}} \right] \quad (5)$$

$$\text{and } \frac{\delta S}{\delta \tan \phi'_{L_s}} = \sum_{i=1}^n 2 \cdot \left[\frac{c'_{L_s} + s'_i \cdot \tan \phi'_{L_s} - t_i}{\sqrt{(\tan^2 \phi'_{L_s} + 1)}} \right]$$

$$\frac{(c'_{L_s} + s'_i \cdot \tan \phi'_{L_s}) \left(\frac{-2 \cdot \tan \phi'_{L_s}}{\sqrt{(\tan^2 \phi'_{L_s} + 1)}} \right) + \frac{s'_i}{\sqrt{(\tan^2 \phi'_{L_s} + 1)}}}{2(\tan^2 \phi'_{L_s} + 1) \cdot \sqrt{(\tan^2 \phi'_{L_s} + 1)}} = 0$$

$$0 = \frac{1}{(\tan^2 \phi'_{L_s} + 1) \sqrt{(\tan^2 \phi'_{L_s} + 1)}} \sum_{i=1}^n \left[\frac{c'_{L_s} + s'_i \cdot \tan \phi'_{L_s} - t_i}{\sqrt{(\tan^2 \phi'_{L_s} + 1)}} \right] \cdot [(-c'_{L_s} - s'_i \cdot \tan \phi'_{L_s}) \tan \phi'_{L_s} + s'_i (\tan^2 \phi'_{L_s} + 1)]$$

$$0 = \sum_{i=1}^n \left[\frac{c'_{L_s} + s'_i \cdot \tan \phi'_{L_s} - t_i}{\sqrt{(\tan^2 \phi'_{L_s} + 1)}} \right] \cdot (-c'_{L_s} \tan \phi'_{L_s} - s'_i \tan^2 \phi'_{L_s} + s'_i \tan^2 \phi'_{L_s} + s'_i)$$

$$0 = \sum_{i=1}^n \left[\frac{c'_{L_s} + s'_i \cdot \tan \phi'_{L_s} - t_i}{\sqrt{(\tan^2 \phi'_{L_s} + 1)}} \right] \cdot (-c'_{L_s} \tan \phi'_{L_s} + s'_i)$$

$$0 = \sum_{i=1}^n \left[\frac{c'_{L_s} + s'_i \cdot \tan \phi'_{L_s} - t_i}{\sqrt{(\tan^2 \phi'_{L_s} + 1)}} \right] \cdot s'_i - \sum_{i=1}^n \left[\frac{c'_{L_s} + s'_i \cdot \tan \phi'_{L_s} - t_i}{\sqrt{(\tan^2 \phi'_{L_s} + 1)}} \right] c'_{L_s} \tan \phi'_{L_s}$$

from equation 5

$$0 = \sum_{i=1}^n \left[\frac{c'_{L_s} + s'_i \cdot \tan \phi'_{L_s} - t_i}{\sqrt{(\tan^2 \phi'_{L_s} + 1)}} \right] \text{ and } c'_{L_s} \tan \phi'_{L_s} \text{ is a constant}$$

$$\text{so } 0 = \sum_{i=1}^n \left[\frac{c'_{L_s} + s'_i \cdot \tan \phi'_{L_s} - t_i}{\sqrt{(\tan^2 \phi'_{L_s} + 1)}} \right] \cdot s'_i \quad (6)$$

Letting $P = \sum_i s'_i$, $Q = \sum_i t_i$, $T = \sum_i s'^2_i$, $R = \sum_i s'_i t_i$

and $N = \sum n$ gives for equations 5 and 6

$$Nc'_{L_s} + P \cdot \tan \phi'_{L_s} - Q \sqrt{(\tan^2 \phi'_{L_s} + 1)} = 0 \quad (7)$$

$$Pc'_{L_s} + T \cdot \tan \phi'_{L_s} - R \sqrt{(\tan^2 \phi'_{L_s} + 1)} = 0 \quad (8)$$

rearranging equation 7

$$c'_{L_s} = \frac{Q \sqrt{(\tan^2 \phi'_{L_s} + 1)} - P \cdot \tan \phi'_{L_s}}{N}$$

and substituting in equation 8

$$\frac{PQ \sqrt{(\tan^2 \phi'_{L_s} + 1)} - P^2 \cdot \tan \phi'_{L_s} + T \cdot \tan \phi'_{L_s} - R \sqrt{(\tan^2 \phi'_{L_s} + 1)}}{N} = 0$$

$$(NT - P^2) \tan \phi'_{Ls} = (NR - PQ) \sqrt{(\tan^2 \phi'_{Ls} + 1)}$$

$$\sqrt{\frac{\tan^2 \phi'_{Ls}}{\tan^2 \phi'_{Ls} + 1}} = \frac{NR - PQ}{NT - P^2}$$

$$1 + \frac{1}{\tan^2 \phi'_{Ls}} = \frac{(NT - P^2)^2}{(NR - PQ)^2}$$

$$\tan \phi'_{Ls} = \frac{NR - PQ}{\sqrt{[(NT - P^2)^2 - (NR - PQ)^2]}} \quad (9)$$

replacing equation 9 in 7

$$Nc'_{Ls} + \frac{P(NR - PQ)}{\sqrt{[(NT - P^2)^2 - (NR - PQ)^2]}} - Q \sqrt{1 + \frac{(NR - PQ)^2}{[(NT - P^2)^2 - (NR - PQ)^2]}} = 0$$

$$Nc'_{Ls} = \frac{Q(NT - P^2) - P(NR - PQ)}{\sqrt{[(NT - P^2)^2 - (NR - PQ)^2]}}$$

$$c'_{Ls} = \frac{QT - PR}{\sqrt{[(NT - P^2)^2 - (NR - PQ)^2]}} \quad (10)$$

Since ϕ'_{Ls} can be found from equation 9, the point nearest to the failure envelope and on the Mohr circle (ie. the nominal failure stress; point W in Figure 7/6) is given by

$$\tau_i = t_i \cdot \cos \phi'_{Ls}$$

$$\text{and } \sigma'_i = s'_i - t_i \cdot \sin \phi'_{Ls}$$

In order to place confidence intervals on the slope $\tan \phi'_{Ls}$ and the intercept c'_{Ls} , it is necessary to consider the statistical procedure known as the major axis theorem (Pearson, 1901).

This procedure fits the line with the least error to a scatter of points using the perpendicular distance between the points and the line. Applying the major axis theorem to the failure stresses produces the same line as applying Lisle and Strom's method to Mohr circles. The two methods are therefore comparable but opposite in approach. One uses the best fit line to calculate the failure stresses while the other uses the failure stresses to calculate the best fit straight line. For both methods all points are given equal weight, which is the

case for the tests undertaken here; if different points are known to be more accurate than others they can be weighted by using a method originated by York (1966). These types of analyses are not invariant under a change of scale; this will not, however, be a problem in shear and normal stress space as the scales are the same in order to allow the stress circles to be constructed.

Confidence interval limits are useful in the design of slopes in new construction in order to obtain an estimate of the variability of the soil properties upon which the design is made (Bland, 1981). The amount of confidence in the deduced soil parameters will, amongst other factors, determine the factors of safety used in the final design. When back-analysing a slope failure, however, the determination of the most likely soil parameters are being investigated and so the mean values of shear strength parameters are usually taken as being representative and a good guide to the likely soil behaviour (Chandler, 1977; Leroueil and Tavenas, 1981; Skempton, 1977). Confidence intervals are given in this Thesis for linear and non-linear failure envelopes so that sufficient information is available for design purposes. The failure mechanism found by back-analysis can, of course, be used in the design of slopes in new construction and for designing preventative measures in existing slopes.

Calculating the failure stresses using Lisle and Strom's method allows the confidence limits to be determined for the gradient,

$\tan\phi'$, and the intercept, c' , using the same calculations as applied to the major axis line. For a straight line of the form $\tau = \tan\phi' \cdot \sigma' + c'$ the parameters of the regression, $\tan\phi'$ and c' , and their standard errors (Kermack and Haldane, 1950) are given by

$$\tan\phi' = \frac{\sum_i V_i^2 - \sum_i U_i^2 + \sqrt{(\sum_i V_i^2 - \sum_i U_i^2)^2 + 4(\sum_i U_i V_i)^2}}{2\sum_i U_i V_i}$$

$$c' = \bar{\tau} - \tan\phi' \cdot \bar{\sigma}'$$

$$e_{\tan\phi'} = \frac{\tan\phi'}{r} \sqrt{\frac{1-r^2}{n}} \quad (11)$$

$$e_{c'} = \sqrt{\frac{(e_{\tau} - e_{\sigma'} \cdot \tan\phi')^2}{n} + (1-r)\tan\phi' \left[2e_{\sigma'} e_{\tau} + \frac{\bar{\sigma}' \tan\phi' (1+r)}{r^2} \right]} \quad (12)$$

where the product moment correlation coefficient

$$r = \frac{\sum_i U_i V_i}{\sqrt{(\sum_i U_i^2 \sum_i V_i^2)}}$$

$$\text{and } U_i = \sigma'_i - \bar{\sigma}'$$

$$V_i = \tau_i - \bar{\tau}$$

e = standard error

The above calculation of coefficients $\tan\phi'$ and c' is of no use for failure envelope determination because the precise failure stresses (τ_i, σ'_i) are not known until the envelope has already been fitted. The standard errors can, however, be determined from equations 11 and 12, using the failure stresses deduced from Lisle and Strom's method, and when multiplied by the t-value for the required probability and degrees of freedom, the limits can be found. The t-value is obtained from the statistical t-distribution for small samples. This method is used in Section 7.4.

At first, therefore, the method of Lisle and Strom appears theoretically to be appropriate. Bland (1980) also comes to the same conclusion but his method is described as requiring the use of an iteration and is not as convenient as that of Lisle and Strom. Bland's method produces equations exactly the same as Lisle and Strom (Bland 1983) and his method is explained below. Bland (1981) carries the procedure further to find confidence limits on the best fit line and non-linear failure envelopes.

The centre and radius of the circle in Figure 7/7 are as before

$$s'_i = \frac{\sigma'_{1i} + \sigma'_{3i}}{2} \qquad t_i = \frac{\sigma'_{1i} - \sigma'_{3i}}{2}$$

The point, W, on the circle with the shortest perpendicular distance from the envelope has normal stress σ'_i and shear stress τ_i and the point on the failure envelope with normal stress σ'_i is the shear stress τ_{Bi} .

From the Figure

$$\delta_i = (\tau_{Bi} - \tau_i) \cdot \cos\phi'_B$$

or
$$\delta_i = (\sigma'_i \cdot \tan\phi'_B + c'_B - t_i \cdot \cos\phi'_B) \cdot \cos\phi'_B$$

now $\sigma'_i = s'_i - t_i \cdot \sin\phi'_B$ and so

$$\delta_i = (s'_i \cdot \tan\phi'_B - t_i \cdot \sin\phi'_B \cdot \tan\phi'_B + c'_B - t_i \cdot \cos\phi'_B) \cdot \cos\phi'_B$$

the trigonometry identities
$$\cos\phi'_B = \frac{1}{\sqrt{(\tan^2\phi'_B + 1)}}$$

and
$$\sin\phi'_B = \frac{\tan\phi'_B}{\sqrt{(\tan^2\phi'_B + 1)}}$$

are used to give

$$\delta_i = \left[s'_i \tan\phi'_B - t_i \frac{\tan^2\phi'_B}{\sqrt{(\tan^2\phi'_B + 1)}} + c'_B - \frac{t_i}{\sqrt{(\tan^2\phi'_B + 1)}} \right] \cdot \frac{1}{\sqrt{(\tan^2\phi'_B + 1)}}$$

$$\delta_i = \left[s'_i \cdot \tan\phi'_B - t_i \cdot \sqrt{(\tan^2\phi'_B + 1)} + c'_B \right] \cdot \frac{1}{\sqrt{(\tan^2\phi'_B + 1)}}$$

$$\delta_i = \frac{s'_i \cdot \tan\phi'_B + c'_B - t_i}{\sqrt{(\tan^2\phi'_B + 1)}}$$

Similarly to Lisle and Strom, considering n Mohr circles,

$$S = \sum_{i=1}^n (\delta_i)^2 = \sum_{i=1}^n \left[\frac{c'_B + s'_i \cdot \tan\phi'_B - t_i}{\sqrt{(\tan^2\phi'_B + 1)}} \right]^2$$

and a minimum occurs when $\frac{\delta S}{\delta \tan\phi'_B} = \frac{\delta S}{\delta c'_B} = 0$

Rather than differentiate with respect to c'_B and include the summation result in the summation of S when it is differentiated with respect to $\tan\phi'_B$ as Lisle and Strom had done, Bland (1983) considers that the two equations are only solvable by iteration.

Differentiating with respect to $\tan\phi'_B$,

$$0 = \sum_{i=1}^n \left[\frac{c'_B + s'_i \cdot \tan\phi'_B - t_i}{\sqrt{(\tan^2\phi'_B + 1)}} - t_i \right] \cdot (-c'_B \cdot \tan\phi'_B + s'_i)$$

$$0 = \sum_{i=1}^n c'_B s'_i + s'_i{}^2 \tan\phi'_B - t_i s'_i \sqrt{(\tan^2\phi'_B + 1)} - c'_B{}^2 \tan\phi'_B - c'_B \cdot s'_i \cdot \tan^2\phi'_B + t_i \cdot c'_B \cdot \tan\phi'_B \cdot \sqrt{(\tan^2\phi'_B + 1)}$$

$$0 = T \tan\phi'_B - R \sqrt{(\tan^2\phi'_B + 1)} - N c'_B{}^2 \tan\phi'_B -$$

$$P c'_B (\tan^2\phi'_B - 1) + Q c'_B \tan\phi'_B \cdot \sqrt{(\tan^2\phi'_B + 1)} \quad (13)$$

in similar notation to Lisle and Strom.

Differentiating with respect to c'_B ,

$$0 = 2 \sum_{i=1}^n \left[\frac{c'_B + s'_i \cdot \tan\phi'_B - t_i}{\sqrt{(\tan^2\phi'_B + 1)}} \right] \cdot \frac{1}{\sqrt{(\tan^2\phi'_B + 1)}}$$

$$0 = N c'_B + P \tan\phi'_B - Q \cdot \sqrt{(\tan^2\phi'_B + 1)} \quad (14)$$

replacing $Q \cdot \sqrt{(\tan^2\phi'_B + 1)}$ in equations 13 from 14

$$\begin{aligned}
0 &= T \cdot \tan\phi'_B - R \cdot \sqrt{(\tan^2\phi'_B + 1) - Nc'_B{}^2 \cdot \tan\phi'_B -} \\
&\quad Pc'_B(\tan^2\phi'_B - 1) + Nc'_B{}^2 \cdot \tan\phi'_B + Pc'_B \cdot \tan^2\phi'_B \\
0 &= T \cdot \tan\phi'_B - R \cdot \sqrt{(\tan^2\phi'_B + 1) + Pc'_B} \quad (15)
\end{aligned}$$

Equations 14 and 15 are identical to equations 7 and 8

where $\phi'_B = \phi'_{Ls}$ and $c'_B = c'_{Ls}$

These equations are then considered to require an iterative process to solve for $\tan\phi'_B$ and then c'_B in equations 14 and 15. Iterations are, in fact, not necessary as shown above in equations 9 and 10. The process developed by Lisle and Strom is, therefore, considerably simpler.

To consider the level of confidence in the failure envelope Bland (1981) applies a normal distribution to the shear stress τ given by the failure envelope for a particular value of effective normal stress σ' . The standard error of τ is given by

$$e_\tau = \sqrt{\left[\frac{\sum_{i=1}^n (\tau_{Bi} - \tau_i)^2}{n - 2} \right] \cdot \left[\frac{1}{n} + \frac{(\sigma' - \bar{\sigma}')^2}{\sum_{i=1}^n (\sigma'_i - \bar{\sigma}')^2} + 1 \right]} \quad (16)$$

based on Bajpai (1977). $\bar{\sigma}'$ is the mean value of σ'_i .

This is useful because for a particular value of σ' from a series of tests the shear stress lower limit can be given by multiplying the standard error by the required t-value. It can then be said with the necessary confidence (at n-2 degrees of freedom) that the shear stress at failure is not less than this lower limit of τ .

In order to find the limits on c'_B , σ' is made equal to 0,

$$e_{c'} = \sqrt{\left[\frac{\sum_{i=1}^n (\tau_{Bi} - \tau_i)^2}{n - 2} \right] \cdot \left[\frac{1}{n} + \frac{\bar{\sigma}'^2}{\sum_{i=1}^n (\sigma'_i - \bar{\sigma}')^2} + 1 \right]} \quad (17)$$

The standard error for $\tan\phi'$ is given by

$$e_{\tan\phi'} = \sqrt{\frac{\sum_{i=1}^n (\tau_{Bi} - \tau_i)^2}{(n - 2) \cdot \sum_{i=1}^n (\sigma'_i - \bar{\sigma}')^2}} \quad (18)$$

The standard errors are, however, using the vertical error in their computations when the perpendicular error is more appropriate since this was used to calculate the best fit line. As a consequence the method used with the major axis is preferred.

Unfortunately Lisle and Strom's, and Bland's, method for determining the best fit line using the least sum of the squares of error, and the determination of the line by top point construction, although derived differently, produce exactly the same line as will now be shown.

When calculating the best fit line with the top point construction, the first step is to calculate the least square fit to the points of maximum stress.

From Figure 7/8

$$\begin{aligned} \delta_i &= XZ - t_i \\ &= \tau_{Ai} - t_i \\ &= a + s'_i \tan\alpha - t_i \end{aligned}$$

where a = intercept of top point line

$\tan\alpha$ = gradient of top point line

The best fit line is given by minimizing $S = \sum \delta_i^2$ ie. minimizing the vertical distances between line and top point of circle.

$$\frac{\delta S}{\delta a} = \frac{\delta S}{\delta \tan \alpha} = 0$$

$$\frac{\delta S}{\delta a} = \sum_{i=1}^n 2(a + s'_i \cdot \tan \alpha - t_i)$$

$$0 = Na + P \cdot \tan \alpha - Q \quad (19)$$

and

$$\frac{\delta S}{\delta \tan \alpha} = \sum_{i=1}^n 2(a + s'_i \cdot \tan \alpha - t_i) s'_i$$

$$0 = Pa + T \cdot \tan \alpha - R \quad (20)$$

rearranging equation 19

$$a = \frac{Q - P \cdot \tan \alpha}{N}$$

substituting in equation 20

$$0 = \frac{P}{N} (Q - P \cdot \tan \alpha) + T \cdot \tan \alpha - R$$

$$0 = PQ - P^2 \cdot \tan \alpha + NT \cdot \tan \alpha - NR$$

$$\tan \alpha = \frac{NR - PQ}{NT - P^2} \quad (21)$$

replacing in 20

$$0 = Pa + \frac{T(RN - PQ)}{NT - P^2} - R$$

$$0 = PNTa - P^3a + TRN - TPQ - TRN + P^2R$$

$$a = \frac{OT - PR}{NT - P^2} \quad (22)$$

comparing equations 9 and 21

$$\tan \phi'_{L_s} = \frac{NR - PQ}{\sqrt{[(NT - P^2)^2 - (NR - PQ)^2]}} \quad \tan \alpha = \frac{NR - PQ}{NT - P^2}$$

$$\tan\phi'_{LS} = \frac{\tan\alpha(NR - PQ)}{\sqrt{[(NR - PQ)^2 - \tan^2\alpha(NR - PQ)^2]}}$$

$$\tan\phi'_{LS} = \frac{\tan\alpha}{\sqrt{(1 - \tan^2\alpha)}}$$

$$\tan\alpha = \sin\phi'_{LS} \quad (23)$$

and is the relation between the angle of the best fit line to the top points and the angle of friction using the Lisle and Strom method. Comparing equations 10 and 22

$$c'_{LS} = \frac{OT - PR}{\sqrt{[(NT - P^2)^2 - (NR - PQ)^2]}} \quad a = \frac{OT - PR}{NT - P^2}$$

$$c'_{LS} = \frac{a(NT - P^2)}{\sqrt{[(NT - P^2)^2 - \tan^2\alpha(NT - P^2)^2]}}$$

$$c'_{LS} = \frac{a}{\sqrt{(1 - \tan^2\alpha)}}$$

since $\tan\alpha = \sin\phi'_{LS}$ and from trigonometry $1 = \sin^2\phi'_{LS} + \cos^2\phi'_{LS}$

$$a = c'_{LS} \cdot \cos\phi'_{LS} \quad (24)$$

From equation 23, $\tan\alpha = \sin\phi'_{LS}$ but $\tan\alpha = \sin\phi'_{TP}$ where ϕ'_{TP} is the angle of friction found using the top point construction. Therefore

$$\sin\phi'_{LS} = \sin\phi'_{TP}$$

$$\phi'_{LS} = \phi'_{TP}$$

From equation 24, $a = c'_{LS} \cdot \cos\phi'_{LS}$ but $a = c'_{TP} \cdot \cos\phi'_{TP}$ where $\phi'_{TP} = \phi'_{LS}$ from above and c'_{TP} is the cohesion intercept found from using top point construction. Therefore

$$c'_{LS} \cdot \cos\phi'_{LS} = c'_{TP} \cdot \cos\phi'_{TP}$$

$$c'_{LS} = c'_{TP}$$

So the angle of friction and cohesion of Lisle and Strom, and Bland, is identical to the conventional top point construction currently in popular use. The major axis theorem also produces identical values of c' and ϕ' using a similar approach. As confirmation, these methods were applied to the tests that were conducted at low effective stresses and all produced the same

values of c' and ϕ' .

There is, therefore, nothing to be gained by using a more complex method than the top point construction for general linear failure envelope determination. However, where the Lisle and Strom method does prove worthwhile is if confidence limits are required as actual failure stresses can be determined. (In the top point construction the failure envelope variance cannot be determined because it does not rely on actual failure stresses.) The failure stresses found can then be used to calculate confidence intervals for c' and $\tan\phi'$ using the same method as described for Pearson's major axis theorem.

7.4 Results from test data using techniques for fitting linear failure envelopes

In order to study the shape of the failure envelope at low effective stresses, a straight line has been fitted to the peak stress data given in Chapter 6. Table 7/1 presents the data; the values of c' and ϕ' are the same using either Top Point Construction, Lisle and Strom's method, Bland's method or Pearson's Major Axis Theorem. The 90 per cent confidence intervals have been calculated using the method for the major axis theorem with the t-value for $n-2$ degrees of freedom and failure stresses deduced from Lisle and Strom's method. In Table 7/1, the ranges of c' and ϕ' are not linked; for example the minimum value of c' does not correspond to the maximum

value of ϕ' . The mean sum of the least squares of error, $S/n = \sum \delta_i^2/n$, is given and will be used as a measure of the accuracy of the shape of the failure envelope. The number in the sample, n , is in this case the number of Mohr circles obtained from tests on each soil type. There are six Mohr circles for each soil type except Gault Clay - Nepicar which has seven. Linear envelopes for these data show a large range within the confidence interval. Also, for this particular stress range, the error at the lower stresses is the highest as this error is compensated for by more frequent smaller errors at higher stresses. This could lead to large errors in the intercept and gradient if this low stress level is appropriate to a particular shallow failure.

Also, in Table 7/2, the results are given for reconstituted samples at higher effective stresses using a linear failure envelope to model the Critical State Condition and for use in the conventional slope stability analysis carried out in Chapter 10. Since the critical state failure envelope must pass through the origin, zero axial and radial stresses have been included with the two other stresses at failure. This assumes the model to be correct and that when the tangent to the two Mohr circles from the tests does not quite pass through the origin it is only because of experimental error and sample inconsistencies. The figures in brackets are the intercepts of the best fit line but for critical state strength analysis it can be assumed that the intercept is zero. The friction angle deduced is the critical state (or constant volume or fully

softened) friction angle.

The values in Table 7/3 are the 'ultimate' strength parameters and are given so that comparison can be made with the critical state strength parameters in Table 7/2. It can be seen that the intercept of the envelope c'_u , which includes the origin as a value for stress, is similar to those bracketed values in Table 7/2. However, the friction angles are much higher. This provides confirmation of the observation in Chapter 6, which was that only the ultimate condition of testing was achieved and that there was an insufficient drop in strength to indicate that the critical state strength had been reached.

TABLE 7/1

Linear strength parameters at the peak strength
for undisturbed samples

Geology	ϕ' (deg)	c' (kPa)	90% confidence intervals		S/n ([kPa] ²)
			ϕ' (deg)	c' (kPa)	
Gault- Dunton	26.5	6	24.0 to 28.5	2 to 11	2.72
Gault- Nepicar	26.5	6	23.0 to 29.5	-1 to 13	6.30
Kimmeridge Clay	26.0	5	22.5 to 29.0	0 to 10	2.22
London Clay	32.5	6	28.0 to 37.0	1 to 11	2.32
Oxford Clay	29.0	6	22.0 to 35.0	-1 to 14	7.66
Reading Beds-clay	22.5	7	18.0 to 27.0	1 to 12	2.70
Weald Clay	30.0	4	25.0 to 34.5	-3 to 12	5.11

TABLE 7/2

Critical state strength parameters

Geology	ϕ'_c (deg)	c' _c (kPa)
Gault- Nepicar	23.0	0 (0)
Kimmeridge Clay	23.5	0 (-1)
London Clay	25.0	0 (2)
Oxford Clay	25.0	0 (0)
Reading Beds-clay	19.5	0 (1)
Weald Clay	24.5	0 (1)

TABLE 7/3

'Ultimate' strength parameters

Geology	ϕ'_{ult} (deg)	c'_{ult} (kPa)
Gault- Nepicar	28.0	0
Kimmeridge Clay	25.0	2
London Clay	35.0	2
Oxford Clay	28.0	0
Reading Beds-clay	25.0	2
Weald Clay	30.0	2

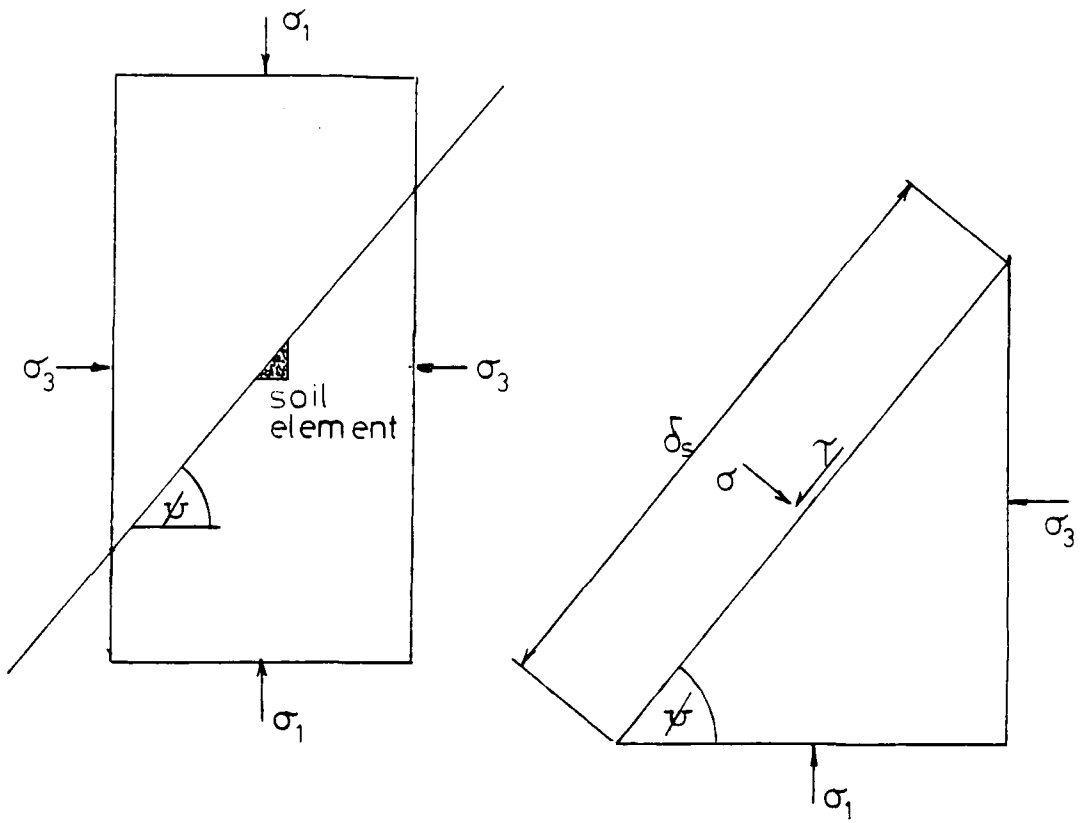


Fig.7/1 Stress conditions in a soil during compression

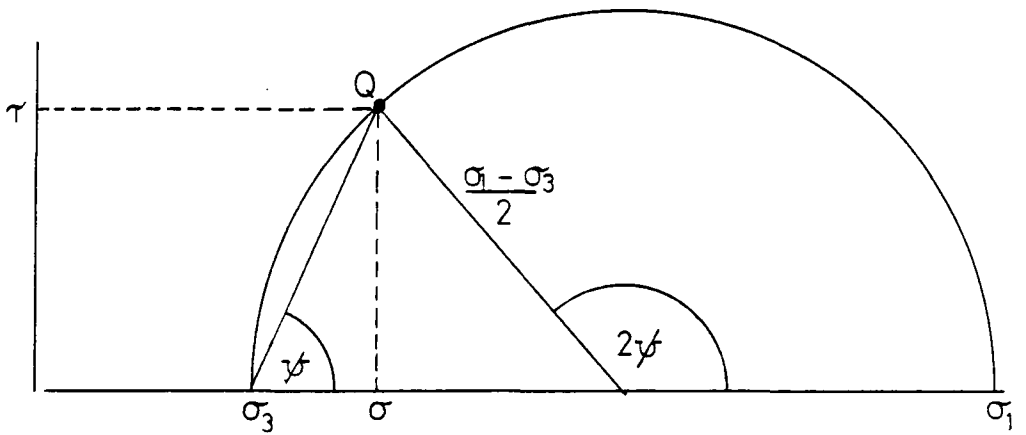


Fig.7/2 The Mohr circle diagram

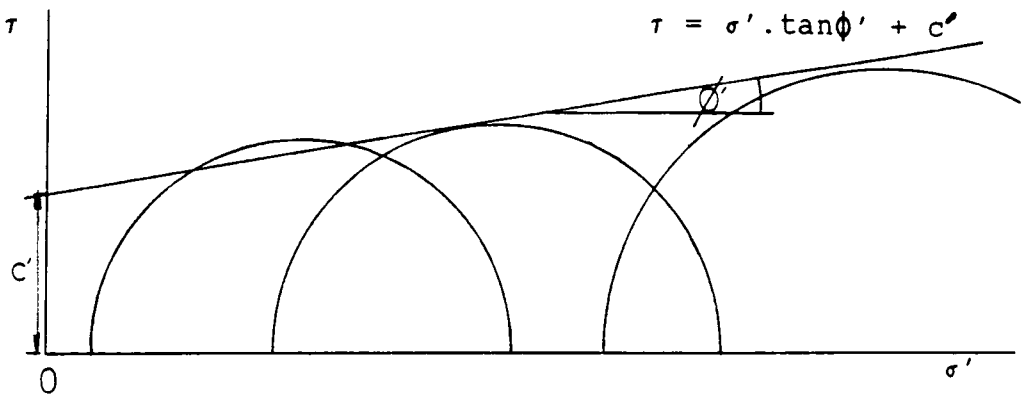


Fig.7/3 The modified Mohr-Coulomb relation

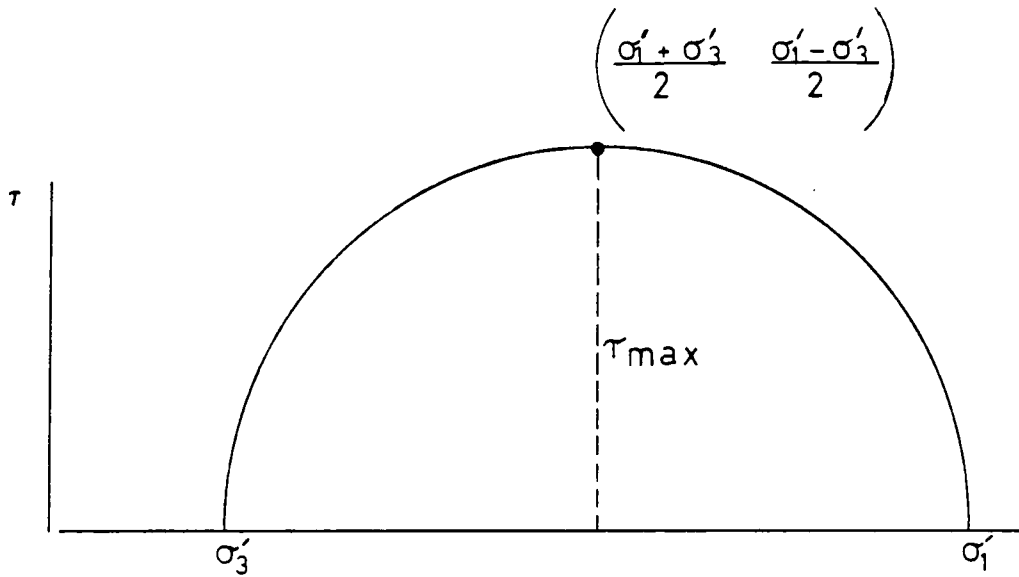


Fig.7/4 Top point of a Mohr circle

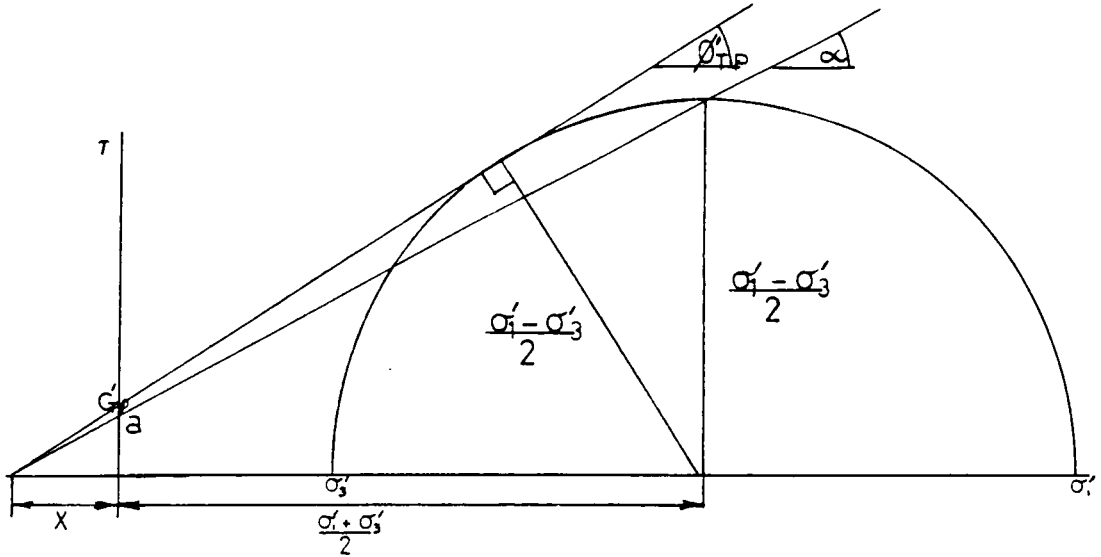


Fig.7/5 The relation between the least square fit line through the maximum shear stresses and the failure envelope

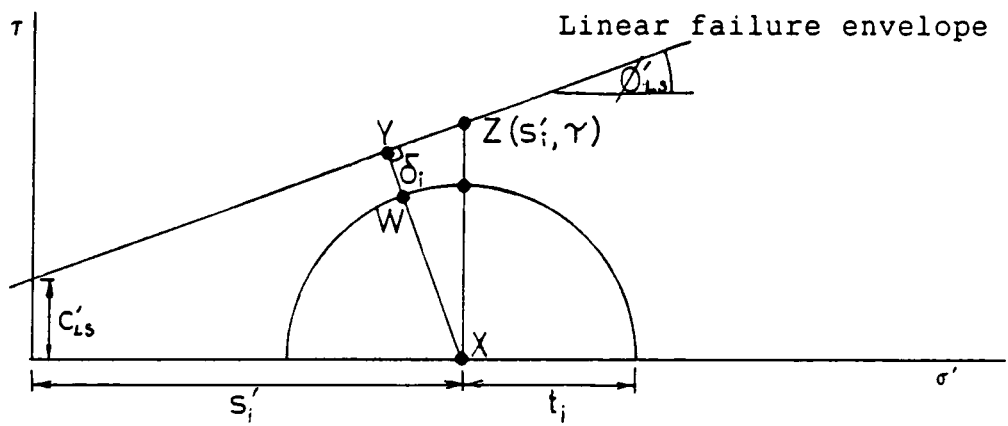


Fig.7/6 Minimizing the distances between Mohr circles and the failure envelope using the method of Lisle and Strom

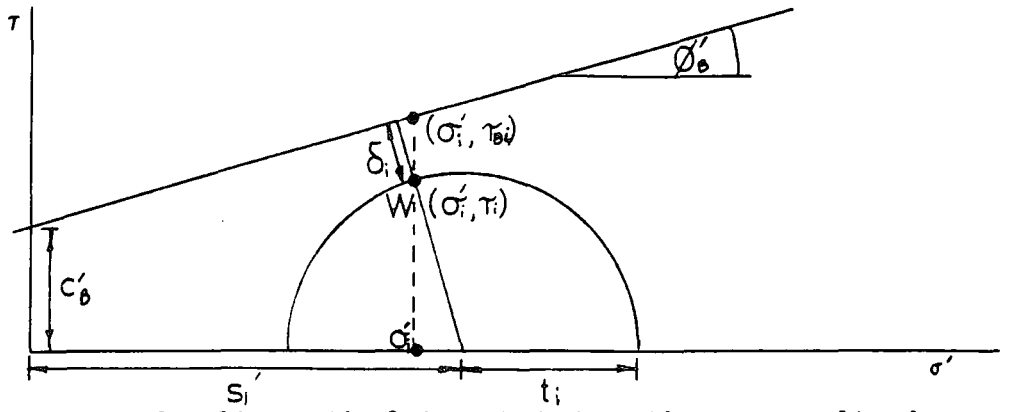


Fig.7/7 Using Bland's method to minimize the perpendicular distance between Mohr circles and the failure envelope

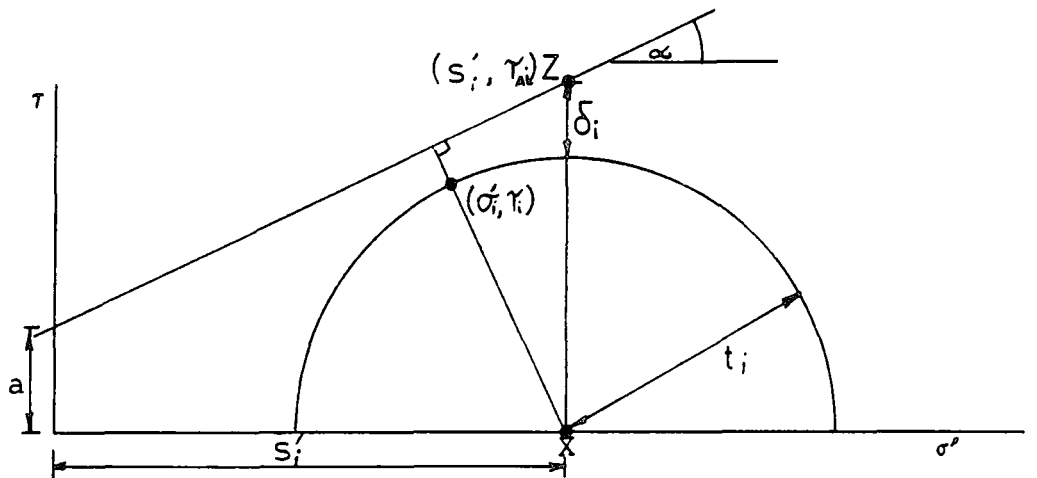


Fig.7/8 Minimizing the error for a top point construction

Non-linear shear strength envelopes at low effective stresses

8.1 Types of non-linear shear strength envelope

Several shapes of non-linear failure envelope have been suggested (Balmer, 1952; Szymanski, 1958; Nowatzki and Karafiath, 1974; De Mello, 1977; Hoek and Brown, 1980; Hoek and Bray, 1981; Charles and Soares, 1984a and 1984b; Taylor, 1984; Atkinson and Farrar, 1985; Hawkins and Privett, 1985; Collins, Gunn and Pender, 1986; West, 1987; Zhang and Chen, 1987; Collins, Gunn, Pender and Yan, 1988). The most common shape used for soil, rockfill and jointed rock is the power curve since it best represents the data measured. The power curve has the function

$$\tau = A\sigma'^b$$

where τ = shear stress

σ' = effective normal stress

A and b = parameters of the function

The parameter b is independent of the units used for stress and the parameter A has dimensions $(\sigma')^{1-b}$.

It is a simple function and only requires the calculation of two parameters. This is an extremely useful property when trying to fit a power curve to Mohr circles as the iterative procedures involved are complex. It will be shown that the power curve rather than the straight line is a more accurate

model of the failure envelope over a range of stresses.

Using the power curve approximation more accurately reflects the shape of the complete failure envelope at low effective stresses and provides parameters, for use in stability analysis, that remain constant at varying effective stresses. By considering a number of Mohr circles the effect of the experimental and sampling errors of a particular circle on the failure envelope is reduced.

The nature of the power curve is given in Figure 8/1 and the following observations can be made:

- (a) as A and b increase so does the gradient of the curve,
- (b) intersection of the curves occur,
- (c) the change of gradient is greatest nearer the origin and the curve is approximately linear at high values of x,
- (d) the curve always passes through the origin,
- (e) the parameter b determines the amount of curvature.

The third property makes this type of function extremely useful for approximating a shear strength envelope at low effective stresses. One of the criticisms that can be made of this model is that a zero intercept is endemic, consequently no 'cohesion' exists at zero stress. Many of the authors referenced at the beginning of this Chapter considered this point and concluded that for soil, rockfill and jointed rocks a zero cohesion intercept is a very good approximation even if it may not be physically appropriate. It certainly provided a more accurate simulation than a linear approximation.

8.2 Techniques for fitting a power curve to Mohr circles

One of the problems with using a power curve as a function for shear strength is that fitting the curve to a series of Mohr circles requires a more complicated procedure than is used for linear envelopes. All the authors who considered triaxial testing, have deduced the curved strength envelope by sketching the best fit curve and, by eye, taking the nearest points on the Mohr circles as the failure stresses. Up until this Thesis, there has not been an accurate method available for fitting the best fit curve. In this Section, six methods are considered comprising the free-hand method and five new procedures. One method in particular is recommended as being the most accurate and is used to determine the strength envelopes for the soils tested for use in subsequent slope stability back-analysis.

A description and assessment of each method is given in the following Sections. Later in this Chapter the relative accuracies of these methods are discussed with respect to the Mohr diagrams in Chapter 6. Each method, in different ways, tries to overcome the main problem of determining the stresses at failure.

8.2.1 Free-hand method for fitting a power curve to Mohr circles (Method 1)

This method involves sketching a curve which is judged by eye to be the best fit. The judgement is based on keeping the sum of the perpendicular distances between the curve and the Mohr circles to a minimum (Figure 8/2). The point on the Mohr circle nearest, if the circle is below the curve, and furthest, if the circle intersects the curve, are taken as the failure stresses. These points can then be assumed to lie approximately on a power curve. Taking logarithms of the failure stresses and plotting them, results in a straight line of the form $\ln r = \ln A + b \ln \sigma'$. The best fit straight line through these points is found using the standard statistics method of least square fitting. The parameter A can then be calculated from the intercept of the line on the vertical axis and the parameter b can be calculated directly from the gradient of the line.

This method is prone to considerable errors especially near the origin where the radius of the curve is similar to the radius of the circle. Interpretation by different workers is, of course, likely to be the main source of error.

8.2.2 Top point construction (Method 2)

Since the top point construction is used so widely in the engineering profession for linear failure envelopes, it seems

only logical to see if the method can be adapted to curved failure envelopes. First the top points are plotted as logarithms, $\ln t_i = \ln C + d \ln s'_i$, in order to determine the best fit line through these points using a statistical regression. C and d are the parameters describing the power curve through the top points. From the resulting power curve, $t_i = C s'_i{}^d$, a range of values of t_i and s'_i are chosen, which lie on this curve, and Mohr circles plotted. This procedure provides a more uniform pattern of Mohr circles so that a power curve can be drawn by hand. The points of intersection of the curve and the circles are taken as the failure stresses. By taking logarithms of the failure stresses the parameters A and b can be found as explained in the previous Section.

There are several procedures involved in this method all of which can be subject to error. The sketching of the curve by hand is subject to the same errors as given in the previous Section. Smoothing out any irregularities in the Mohr circles may not produce a failure envelope which is representative.

8.2.3 Method requiring an approximation of the failure stresses using a tangent through the origin (Method 3)

In order to determine the failure stresses, a tangent can be drawn which passes through the origin of the Mohr diagram (Figure 8/3). The point of intersection of the tangent and the circle is an approximation of the stresses at failure, τ_i and

σ'_i , and can be calculated for each circle using the angle the tangent makes with the effective normal stress axis:

$$\tau_i = t_i \cdot \cos\theta \text{ and } \sigma'_i = s'_i - t_i \cdot \sin\theta$$

Using $\sin\theta = t_i/s'_i$:

$$\tau_i = \frac{t_i}{s'_i} (s'^2_i - t_i^2)^{1/2} \text{ and } \sigma'_i = \frac{1}{s'_i} (s'^2_i - t_i^2)$$

When the failure stresses have been calculated using this method, the power curve can be deduced, as before, by taking logarithms, fitting the best fit straight line and finding the parameters A and b.

The method of calculating the failure stresses is clearly an approximation, an approximation whose error increases at the higher stresses where the gradient of the line is much greater than that of the power curve. The approximation is therefore not a good one.

8.2.4 Method using a power curve or straight line between two Mohr circles to determine the failure stresses (Method 4)

The first consideration here is to fit a power curve which touches two circles and passes through the origin (Figure 8/4).

For a circle, the general equation is

$$t_i^2 = (s'_i - \sigma'_i)^2 + (z - \tau_i)^2$$

for a Mohr diagram $z = 0$

$$\begin{aligned}\tau_i^2 &= t_i^2 - (s'_i - \sigma'_i)^2 \\ \tau_i^2 &= t_i^2 - s_i'^2 + 2s'_i\sigma'_i - \sigma_i'^2\end{aligned}\quad (1)$$

For a power curve the equation is

$$\tau = A\sigma'^b \quad (2)$$

If the failure envelope meets at one point with a circle, it is a tangent for small increment of curve and will have the same gradient. Hence from equation 1

$$\begin{aligned}2\tau_i \cdot d\tau_i/d\sigma'_i &= 2s'_i - 2\sigma'_i \\ d\tau_i/d\sigma'_i &= (s'_i - \sigma'_i)/\tau_i\end{aligned}\quad (3)$$

From equation 2

$$d\tau/d\sigma' = A \cdot b \cdot \sigma'^{b-1} \quad (4)$$

At the point of intersection $d\tau_i/d\sigma'_i = d\tau/d\sigma'$

and so
$$\tau_i = (s'_i - \sigma'_i)/(A \cdot b \cdot \sigma_i'^{b-1}) \quad (5)$$

Three equations now exist for one circle, equations 1, 2, and 5. If two consecutive circles are studied, six equations will exist, equations 1, 2 and 5 for each circle. Both will have the same values of A and b since a power curve is taken as joining them both.

Combining equations 2 and 1,

$$A^2 \cdot \sigma_i'^{2b} = t_i^2 - s_i'^2 + 2s'_i\sigma'_i - \sigma_i'^2 \quad (6)$$

and equations 2 and 5.

$$\begin{aligned}A \cdot \sigma_i'^b &= (s'_i - \sigma'_i)/A \cdot b \cdot \sigma_i'^{b-1} \\ A^2 \cdot b \cdot \sigma_i'^{2b} &= s'_i \cdot \sigma'_i - \sigma'_i\end{aligned}\quad (7)$$

Four equations have been deduced, equations 6 and 7 for two

circles, a solution is possible as there are four unknowns, A, b, σ'_i and σ'_{i+1} . This would, however, be difficult to achieve without a computer iterative procedure. Since the values of A and b would have to be averaged over the complete number of pairs of circles the method is not strictly accurate or mathematically rigorous. Also, in practice, Mohr circles do not always occur consecutively and circles can occur within larger circles rendering them impossible to be included in this procedure.

Using a straight line between consecutive circles may be a simple method for determining the failure stresses, from which a power curve can be fitted using the method described in Section 8.2.1. Consider Figure 8/5.

By geometry

$$\sigma'_i = s'_i - t_i \cdot \sin\theta \quad (8)$$

$$\sigma'_{i+1} = s'_{i+1} - t_{i+1} \cdot \sin\theta \quad (9)$$

$$\tau_i = t_i \cdot \cos\theta \quad (10)$$

$$\tau_{i+1} = t_{i+1} \cdot \cos\theta \quad (11)$$

$$\sin\theta = (t_{i+1} - t_i) / (s'_{i+1} - s'_i) \quad (12)$$

$$\text{and } \tan\theta = (\tau_{i+1} - \tau_i) / (\sigma'_{i+1} - \sigma'_i) \quad (13)$$

Combining equations 8 and 12, and 9 and 12 gives

$$\sigma'_i = [s'_i(s'_{i+1} - s'_i) - t_i(t_{i+1} - t_i)] / (s'_{i+1} - s'_i) \quad (14)$$

$$\sigma'_{i+1} = [s'_{i+1}(s'_{i+1} - s'_i) - t_{i+1}(t_{i+1} - t_i)] / (s'_{i+1} - s'_i) \quad (15)$$

From equations 12 and 13

$$(t_{i+1} - t_i)/(s'_{i+1} - s'_i) =$$

$$(\tau_{i+1} - \tau_i) \cdot \cos\theta / (\sigma'_{i+1} - \sigma'_i) \quad (16)$$

Subtracting equation 14 from 15 and substituting for $(\sigma'_{i+1} - \sigma'_i)$ in equation 16,

$$\cos\theta = \frac{(t_{i+1} - t_i) \cdot (s'_{i+1} - s'_i)^2 - (t_{i+1} - t_i)^3}{(\tau_{i+1} - \tau_i) \cdot (s'_{i+1} - s'_i)}$$

Substituting for $\cos\theta$ in equations 10 and 11 provides two equations from which τ_i and τ_{i+1} can be calculated independently

$$\tau_i = \frac{t_i \cdot [(s'_{i+1} - s'_i)^2 - (t_{i+1} - t_i)^2]^{1/2}}{(s'_{i+1} - s'_i)} \quad (17)$$

$$\tau_{i+1} = \frac{t_{i+1} \cdot [(s'_{i+1} - s'_i)^2 - (t_{i+1} - t_i)^2]^{1/2}}{(s'_{i+1} - s'_i)} \quad (18)$$

Equations 14 and 17, and 15 and 18 can be used to calculate the failure stresses for two consecutive circles. Two failure stresses will be produced for each circle (except the first and last) and so a mean will need to be taken. When failure stresses have been calculated for all the circles, a power curve can be fitted.

In a similar way to using the power curve between consecutive circles, this method cannot cope with cases where one circle is within another and also approximations have to be made for the failure stresses.

8.2.5 Using Mohr circles in logarithmic space (Method 5)

Since a power curve will become a straight line in log space, that is when the axes are the logarithms of the variables, it

is conceivable that if the Mohr circles are plotted as log. 'circles' the best fit common tangent to all of them will be the strength envelope. An example is given in Figure 8/6. It can be seen that this method does not remove the erratic nature of some Mohr circles and the problem of determining the stresses at failure still remains.

8.2.6 Method for determining the 'best fit' of a power curve to a series of Mohr circles (Method 6 - Least sum of squares method)

This method is considered to be the most accurate, as will be proved later, and to be the most rigorous. It follows statistical practice for the best fit curve and considers only the shortest (perpendicular) distance between circles and curve. Consider Figure 8/7 which shows one of a series of Mohr circles. In order to find the best fit curve, the total error of the curve must be a minimum. In other words the best fitting curve will have the minimum total square of the perpendicular distances of the power curve to the circles.

The coordinates of the point X are $(s'_i - R \sin\theta, R \cos\theta)$ and so the power curve can be expressed as

$$R \cos\theta = A(s'_i - R \sin\theta)^b \quad (19)$$

To minimize δ_i , the error of the curve for a particular value of θ , R is differentiated with respect to θ : $\delta_i = R - t_i$ and so

$$d\delta_i/d\theta = dR/d\theta.$$

$$dR/d\theta \cdot \cos\theta - R \cdot \sin\theta = A \cdot b (s'_i - R \cdot \sin\theta)^{b-1} \cdot (-dR/d\theta \cdot \sin\theta - R \cdot \cos\theta)$$

$dR/d\theta = 0$ at the minimum, and so

$$R \cdot \sin\theta = A \cdot b \cdot R \cdot \cos\theta (s'_i - R \cdot \sin\theta)^{b-1}$$

or
$$R \cdot \sin\theta = s'_i - [\tan\theta / (A \cdot b)]^{1/b-1} \quad (20)$$

Replacing equation 20 in 19 to eliminate R gives

$$\tan\theta = Ab[s'_i - A^{1/(1-b)} b^{b/(1-b)} (\tan\theta)^{(2b-1)/(b-1)}]^{b-1} \quad (21)$$

Values of A and b are chosen and using equation 21, θ is calculated by iteration for minimum value of R. R, itself, is calculated using this value of θ in equation 20. The error can then be calculated by $\delta_i = R - t_i$. Hence for a particular circle and values of A and b, the error has been calculated. A series of δ_i values are then found for all Mohr circles considered and the sum of the square of the errors, $\sum \delta_i^2 = S$, calculated. The values of A and b chosen must then be varied in order to determine the curve with the minimum value of S. This is done using the matrix method described in Draper and Smith (1981) with the partial differentials of the power relation with respect to A and b being evaluated at the point

X. This method, however, only applies to iterations in the y-axis direction. Therefore the δ_i value from each circle is corrected in a vertical direction such that the error in the y direction equals $\delta_i \cdot \cos\theta$. The criteria that $\sum(\delta_i \cdot \cos\theta)^2$ should be a minimum is only used to find which curve has the least error in the matrix procedure although the curve's actual error remains as S. S only is used in any analysis. If necessary, the coordinates of the failures stresses can be found using the derived values of A and b, θ from equation 20 and R from equation 21.

This method provides a more rigorous approach than any of the other methods and is statistically sound. It can be applied to any arrangement of Mohr circles and provides a statistical parameter to describe the accuracy of the curve fitted. The variance of the residuals is weighted in favour of the lowest values (Taylor, 1984) which is an advantage as it makes the fitting of the curve sensitive to the lower values which are the most critical.

In order to make the computations easier and quicker the procedure explained above has been written as a computer program which is given in Appendix D. The program was written for a Hewlett-Packard 9816 desk-top computer in Basic 3.0 language. This computer has a facility for handling matrices which made iterations of this type easier. The program is intended to be user-friendly and includes plotting facilities for the screen or on paper. The program also includes the

option of fitting a straight line to Mohr circles for higher stress levels. When fitting a power curve to data it is essential that reasonable initial values of A and b are chosen in order for the iteration process to converge to the curve with minimum error. It is possible for an iteration process of this type to converge on incorrect values if the initial values are too far from the correct answer (Draper and Smith, 1981). Values of 3.0 and 0.7 are recommended as starting values for A and b respectively as they are near to those values found for the soils studied here. The calculation of parameters A and b which produces the curve with the least error is very quick and the resulting curve can be plotted on the Mohr diagram. The value of S is also given so that the accuracy of the curve can be seen.

Since this method is considered to be a statistically rigorous method, the accuracies of the other methods can be determined. The program calculates S for the values of A and b found by the other methods; no iterations for A and b are conducted and S is calculated using equations 20 and 21. It could be argued that when a method is used to test another method then the first method is bound to appear more accurate. However since Method 6 is an extension of existing sound and widely accepted statistical techniques, then accurate results must be assured and other methods should be gauged against it.

8.3 Results and accuracies of methods developed

The parameters A and b for the power curves representing the failure envelopes at the peak strength of the soils under study, found by each of the methods described in Section 8.2, are given in Table 8/1. Note that values are not given for Methods 4 and 5. As described in Sections 8.2.4 and 8.2.5, Method 4 cannot be used in some cases and values could not be calculated using Method 5. The accuracies of all the methods can be determined using the computer program developed for Method 6. The most accurate method, both linear and curved is determined by considering the mean sum of the squares of the errors S/n , where n is the number of Mohr circles.

For all the materials studied, Method 6 produced the least error of all the methods considered for fitting a power curve. Also, Method 6 was more accurate than a straight line approximation for all materials except Gault Clay-Nepicar (compare the errors in Table 8/1 with the errors in Table 7/1). Gault Clay - Nepicar showed an error of 6.30 for a linear relation, and an error of 6.58 for a power relation.

The shear strength envelopes using the least sum of squares program have been plotted with their Mohr circles in Figures 8/8 to 8/14.

The confidence intervals for the parameters A and b can be calculated using the 'Jackknife' statistical procedure (Efron

and Gong, 1983). This procedure requires estimates of A and b to be made for a set of data with one observation removed. In this case an estimate of A and b is made using the computer program with one Mohr circle removed. The procedure is repeated with the Mohr circle replaced and a different Mohr circle removed. This continues until all the Mohr circles have been removed once. The number of estimates of $A_{(i)}$, and $b_{(i)}$, $i=1\dots n$, should therefore equal the number of Mohr circles, n, for that material. The means of these values, $A_{(.)} = (1/n) \cdot \sum A_{(i)}$, and $b_{(.)} = (1/n) \cdot \sum b_{(i)}$, are then calculated. The Jackknife estimates of the standard errors for A and b are given by

$$e_A = \left[\frac{n-1}{n} \sum_{i=1}^n (A_{(i)} - A_{(.)})^2 \right]^{1/2}$$

and

$$e_b = \left[\frac{n-1}{n} \sum_{i=1}^n (b_{(i)} - b_{(.)})^2 \right]^{1/2}$$

Multiplying these standard errors by the t-value for n-2 degrees of freedom, as mentioned in Section 7.3, gives the range of values of A and b with the required confidence. Table 8/2 gives the values of A and b and their range for a 90% confidence interval considering only Method 6. The confidence interval is large but is probably not unusual and is of the same order as the range for the linear strength parameters given in Table 7/1. It is suggested, therefore, that confidence limits be used as a guide to the Designer as to variability of the test results rather than as a strict limit. In general, Engineers use only a single value which they consider representative and adjust their design for any

variability of testing (and material of course). The ranges of A and b are not linked and so, for example, the minimum value of A does not correspond the maximum value of b.

Table 8/3 shows the results of fitting a power curve to the 'ultimate' strength data for undisturbed samples. These values of shear strength parameters are based on the two, three or, in one case four, Mohr circles given in Chapter 6. They also represent the higher section of the stress range used for the values in Table 8/2. As discussed in Section 8.2.6 the power curve parameters are very sensitive to low values. Since these have been removed it is likely that any subsequent analysis is going to be influenced considerably and it is unlikely that any relevant comparison can be made between results using these parameters and the parameters found at the peak strength.

TABLE 8/1

Power curve parameters, A and b, for curved failure envelopes
at the peak strength of undisturbed samples,
using methods developed

Geology	Parameter	Method			
		1	2	3	6
Gault- Dunton	A	2.6	3.0	2.5	2.3
	b	0.65	0.61	0.66	0.69
	S/n	2.96	7.38	3.89	2.31
Gault- Nepicar	A	2.4	2.5	2.4	1.9
	b	0.67	0.66	0.66	0.73
	S/n	7.39	9.06	9.09	6.58
Kimmeridge Clay	A	1.7	2.0	1.7	1.8
	b	0.72	0.68	0.72	0.71
	S/n	1.46	2.38	1.43	1.34
London Clay	A	2.9	5.8	3.0	3.7
	b	0.66	0.41	0.63	0.58
	S/n	1.21	--	0.89	0.41
Oxford Clay	A	2.3	2.8	2.2	3.4
	b	0.69	0.63	0.70	0.58
	S/n	5.16	4.48	5.33	4.08
Reading Beds-clay	A	2.1	2.6	2.2	2.8
	b	0.66	0.60	0.64	0.58
	S/n	1.95	1.42	1.79	1.36
Weald Clay	A	1.3	1.5	1.5	2.2
	b	0.84	0.79	0.79	0.70
	S/n	4.58	3.56	3.57	2.73

TABLE 8/2

Non-linear strength parameters at peak
strength of undisturbed samples

Geology	A	b	90% confidence intervals	
			A	b
Gault-Dunton	2.3	0.69	0.6 to 3.9	0.51 to 0.87
Gault-Nepicar	1.9	0.73	0.4 to 3.4	0.55 to 0.91
Kimmeridge Clay	1.8	0.71	0.9 to 2.8	0.57 to 0.85
London Clay	3.7	0.58	2.9 to 4.5	0.51 to 0.65
Oxford Clay	3.4	0.58	1.3 to 5.6	0.41 to 0.76
Reading Beds-clay	2.8	0.58	1.3 to 4.4	0.43 to 0.72
Weald Clay	2.2	0.70	0.4 to 4.0	0.50 to 0.90

TABLE 8/3

Non-linear strength parameters at test's ultimate
condition for undisturbed samples

Geology	A	b
Gault-Nepicar	0.8	0.92
Kimmeridge Clay	2.5	0.60
London Clay	2.1	0.71
Oxford Clay	6.4	0.37
Reading Beds-clay	5.8	0.37
Weald Clay	4.1	0.52

Comparison of
power function relations

$$y = Ax^b$$

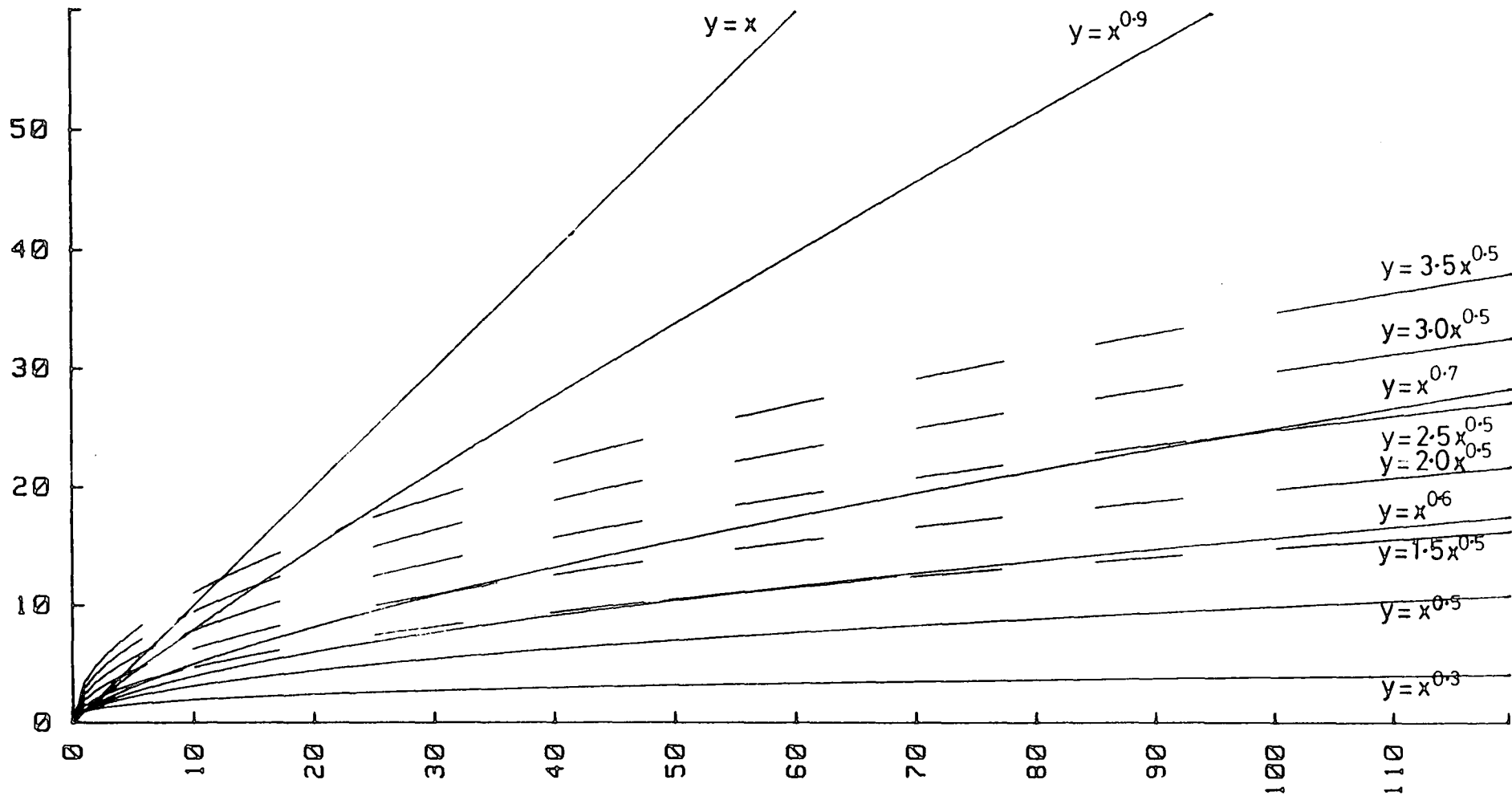


Fig 8/1 Nature of power functions

KIMMERIDGE CLAY

209

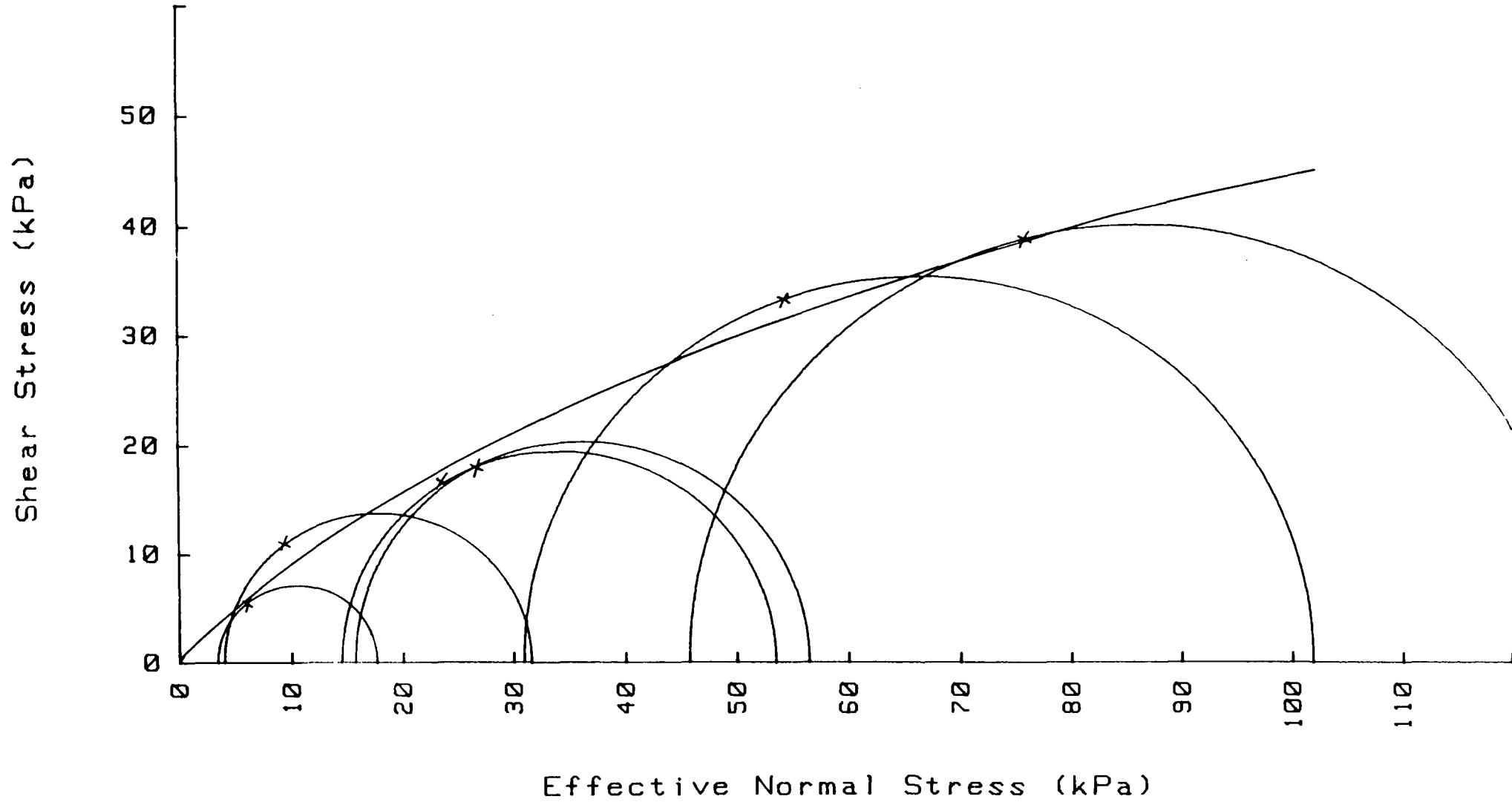


Fig 8/2 Curve fitting using Method 1

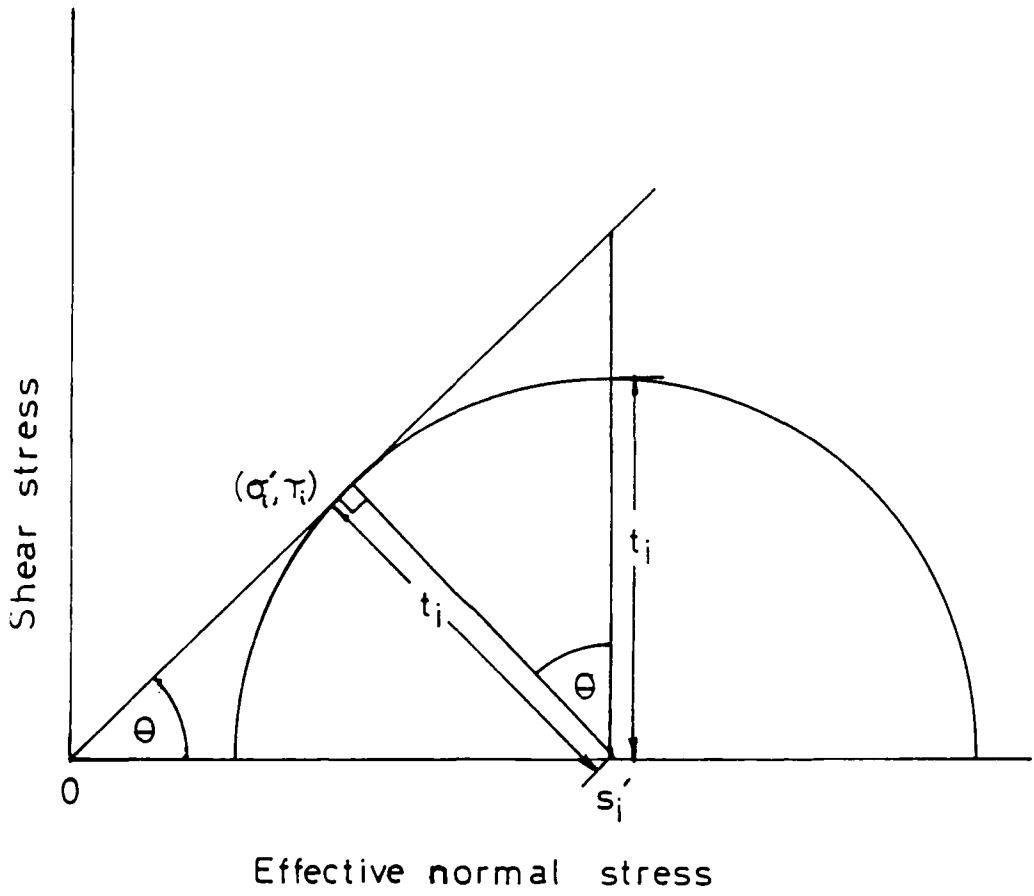


Fig 8/3 Determination of failure stresses using Method 3

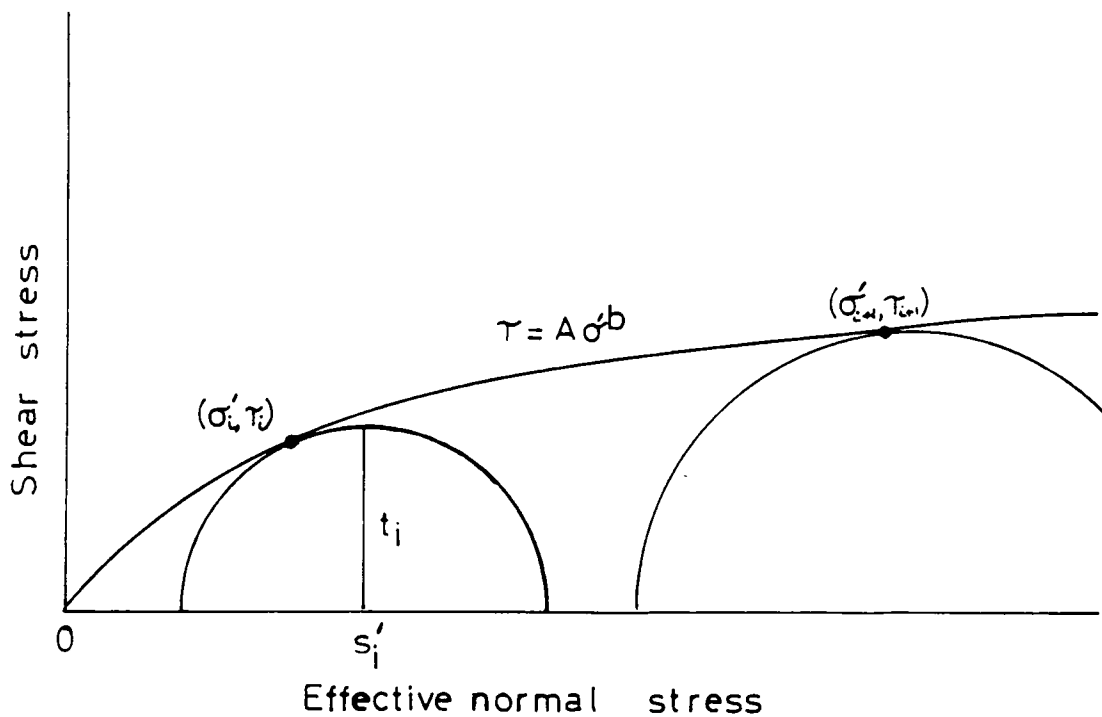


Fig 8/4 Curve fitting using Method 4 assuming a power curve between Mohr circles

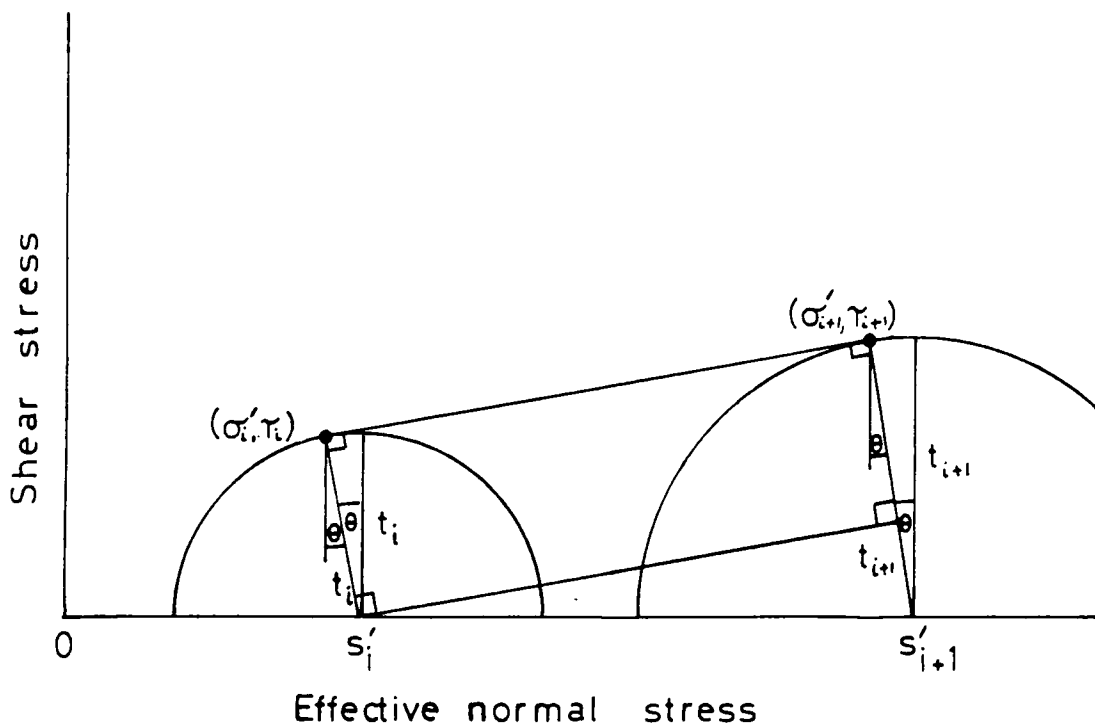


Fig 8/5 Curve fitting using Method 4 assuming a straight line between Mohr circles

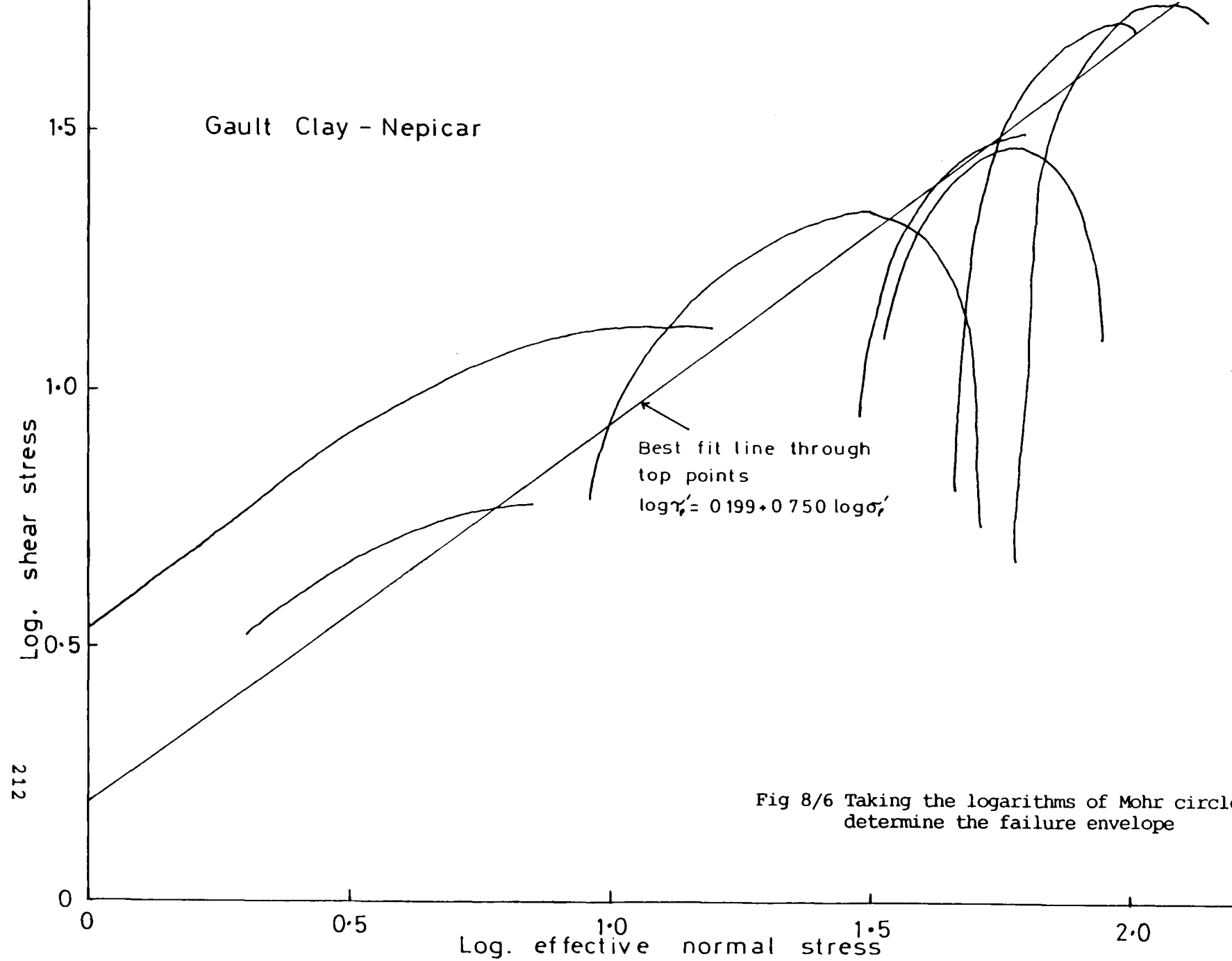


Fig 8/6 Taking the logarithms of Mohr circles in order to determine the failure envelope

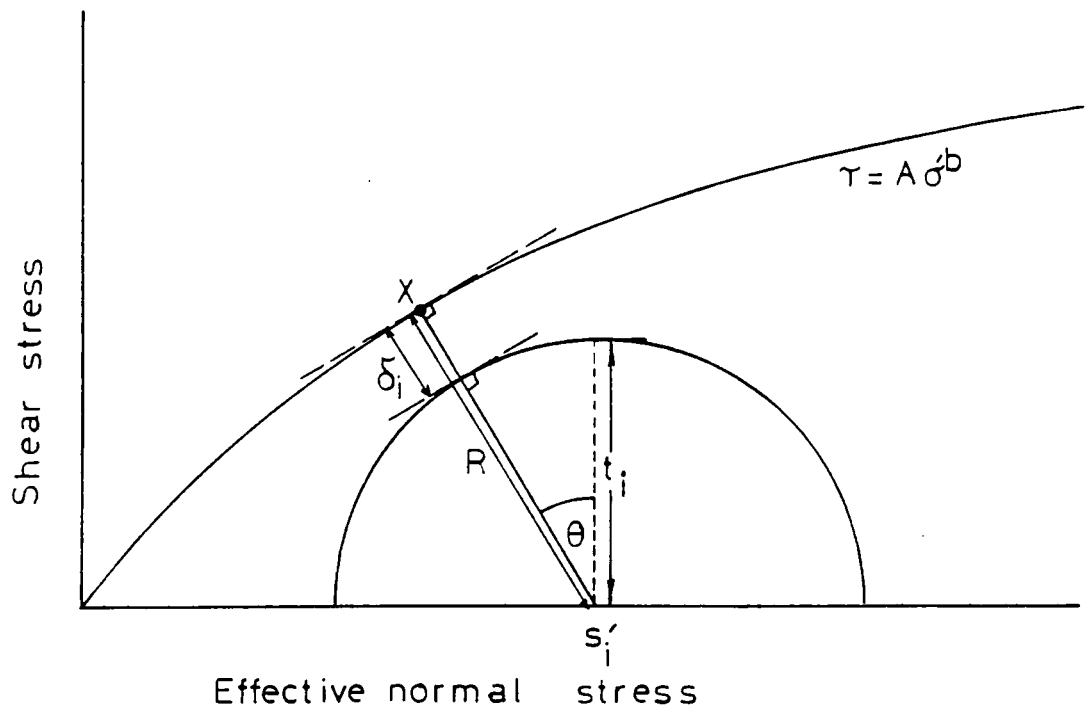


Fig 8/7 Least square of the error of a curved failure envelope

DUNTON GAULT

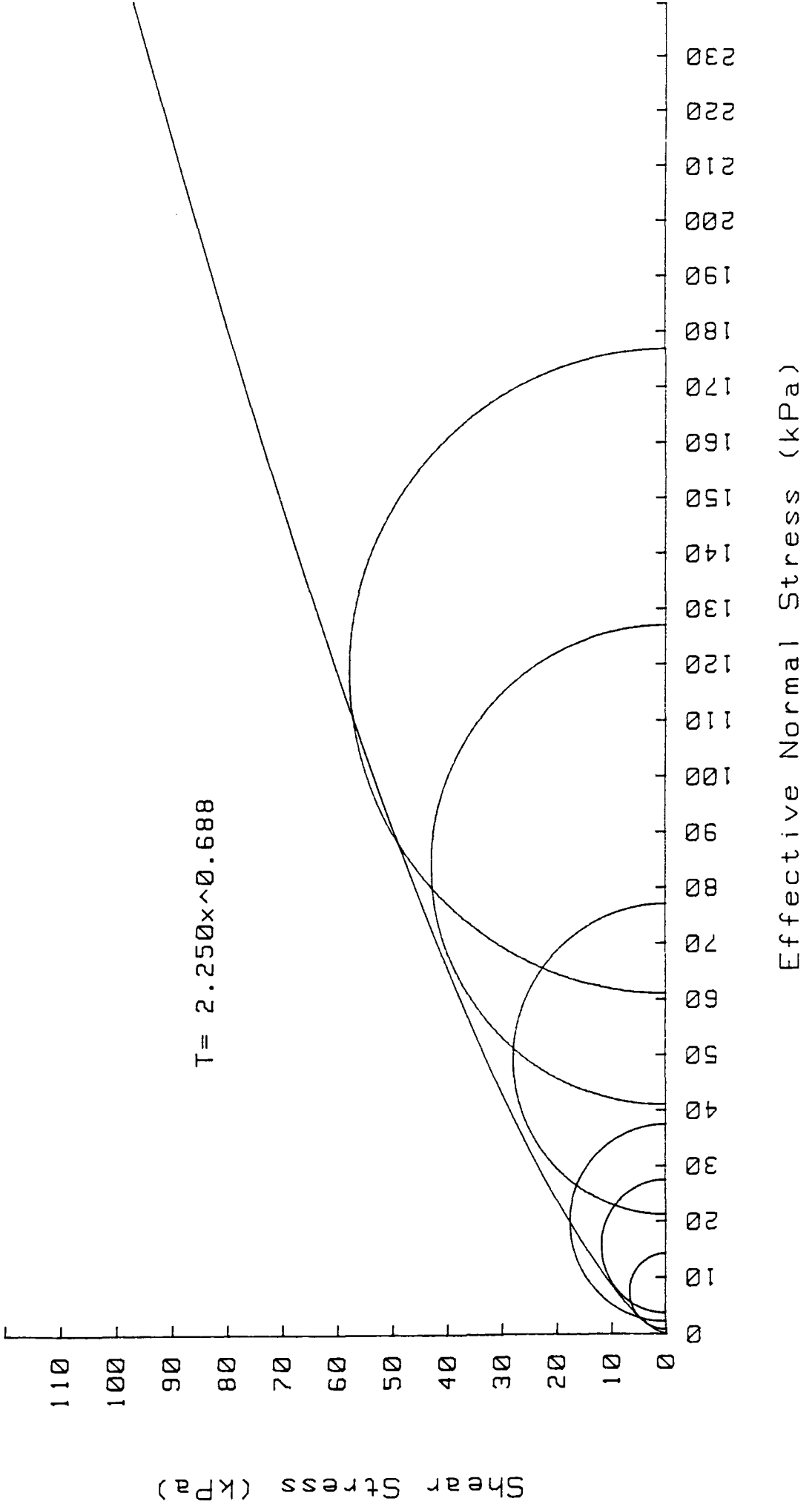


Fig 8/8 Best fit power curve to peak strengths - Dunton Gault

NEPICAR GAULT

215

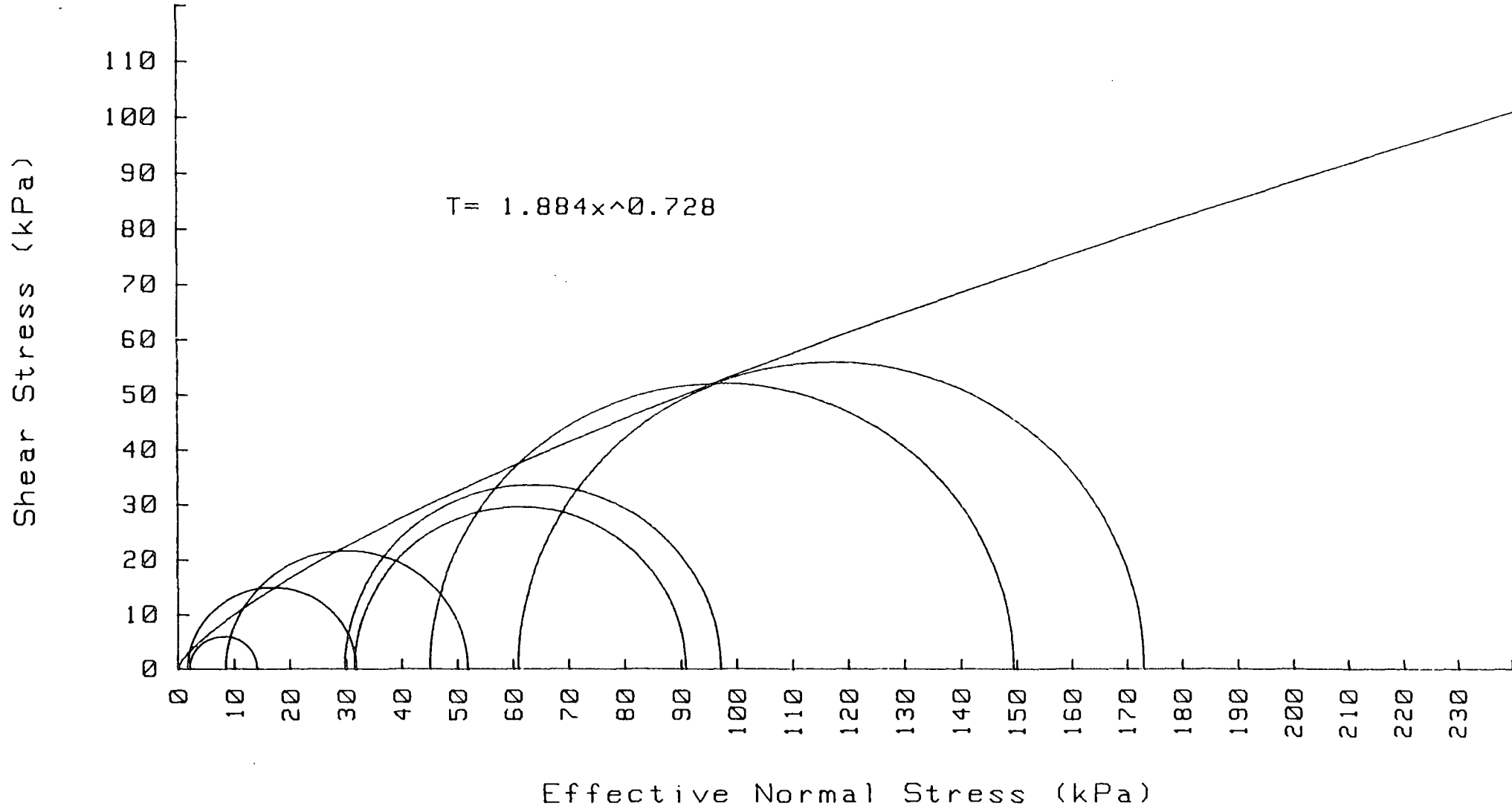


Fig 8/9 Best fit power curve to peak strengths - Nepicar Gault

KIMMERIDGE CLAY

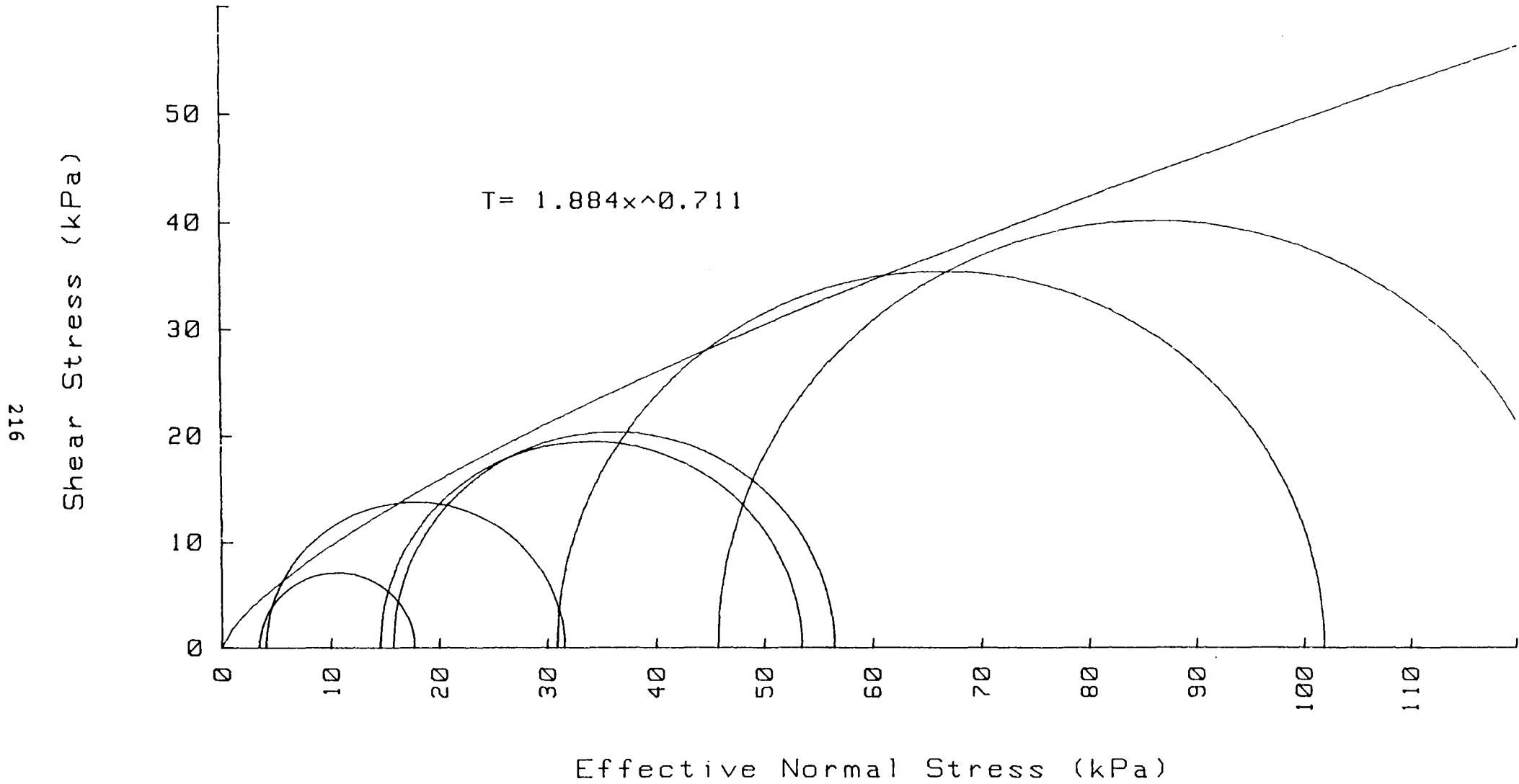


Fig 8/10 Best fit power curve to peak strengths - Kimmeridge Clay

LONDON CLAY

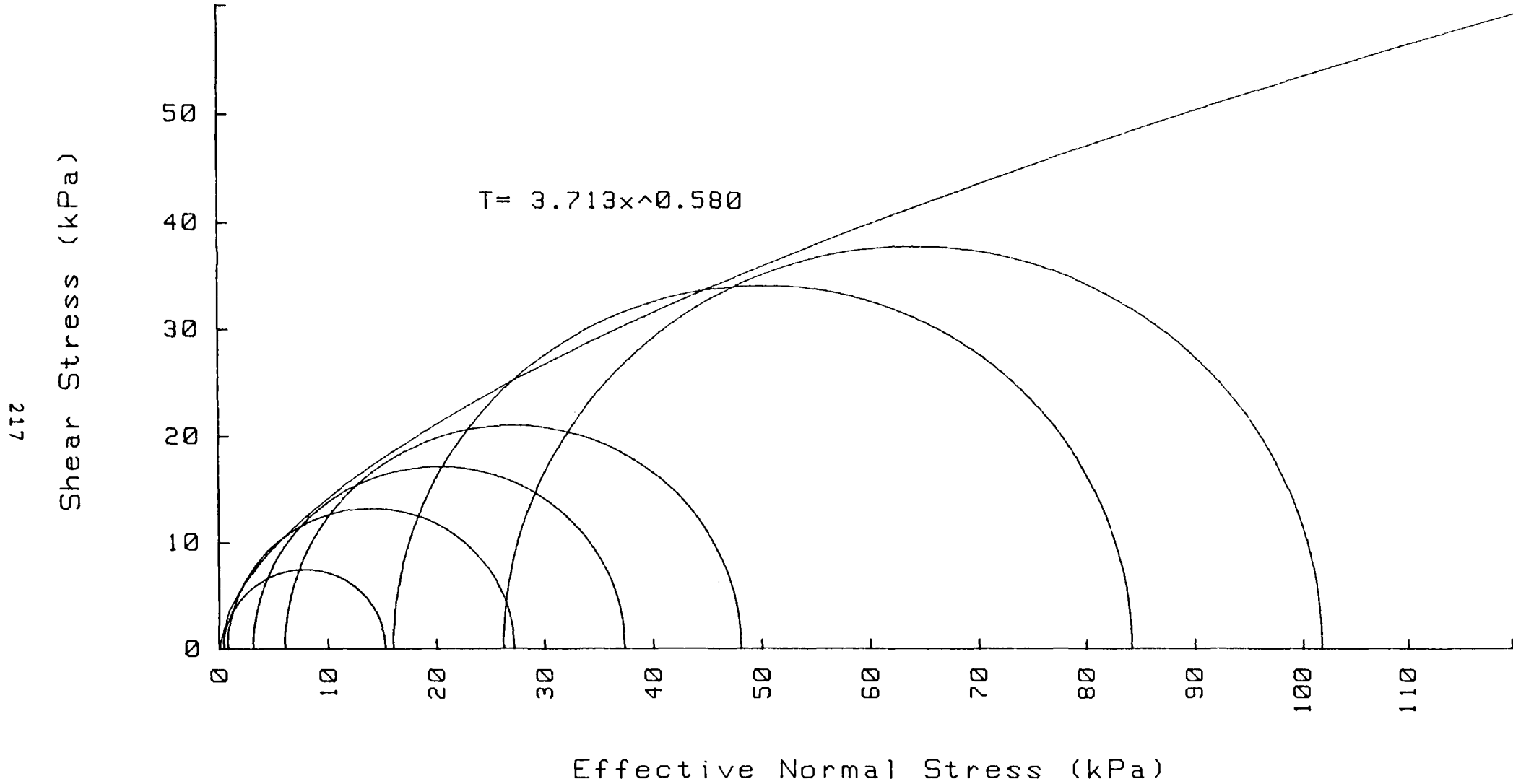


Fig 8/11 Best fit power curve to peak strengths - London Clay

OXFORD CLAY

218

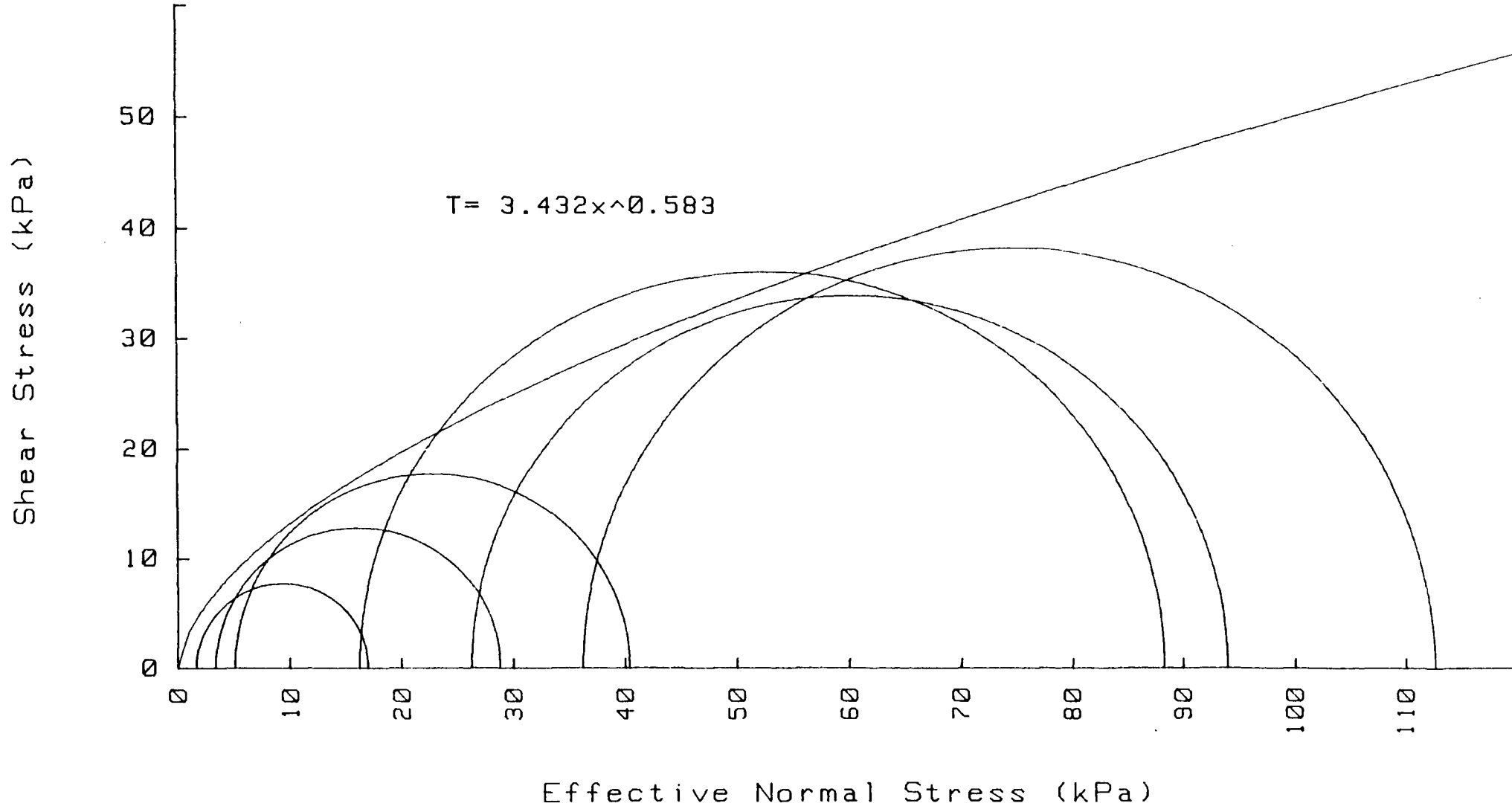


Fig 8/12 Best fit power curve to peak strengths - Oxford Clay

READING BEDS CLAY

219

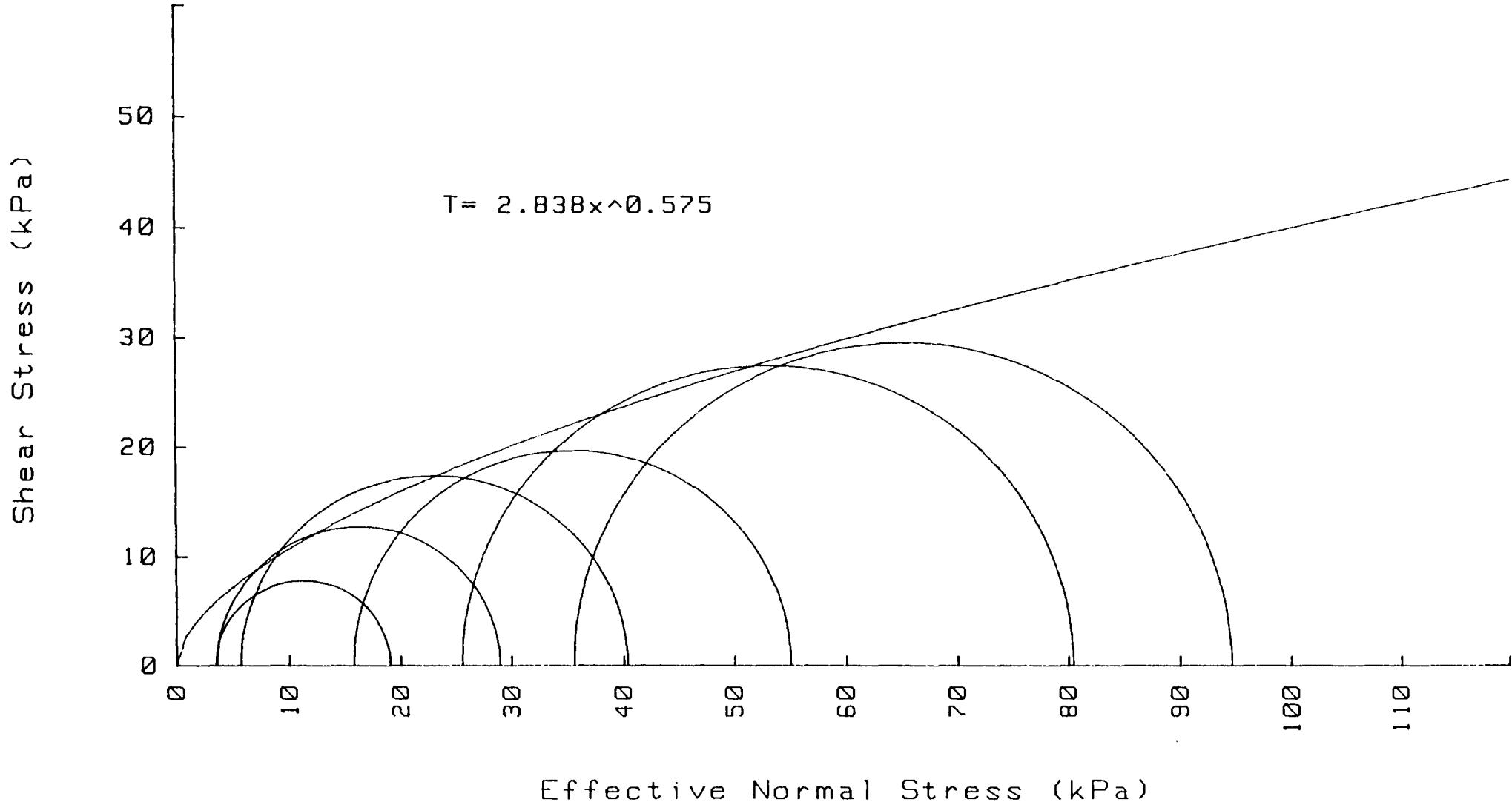


Fig 8/13 Best fit power curve to peak strengths - Reading Beds clay

WEALD CLAY

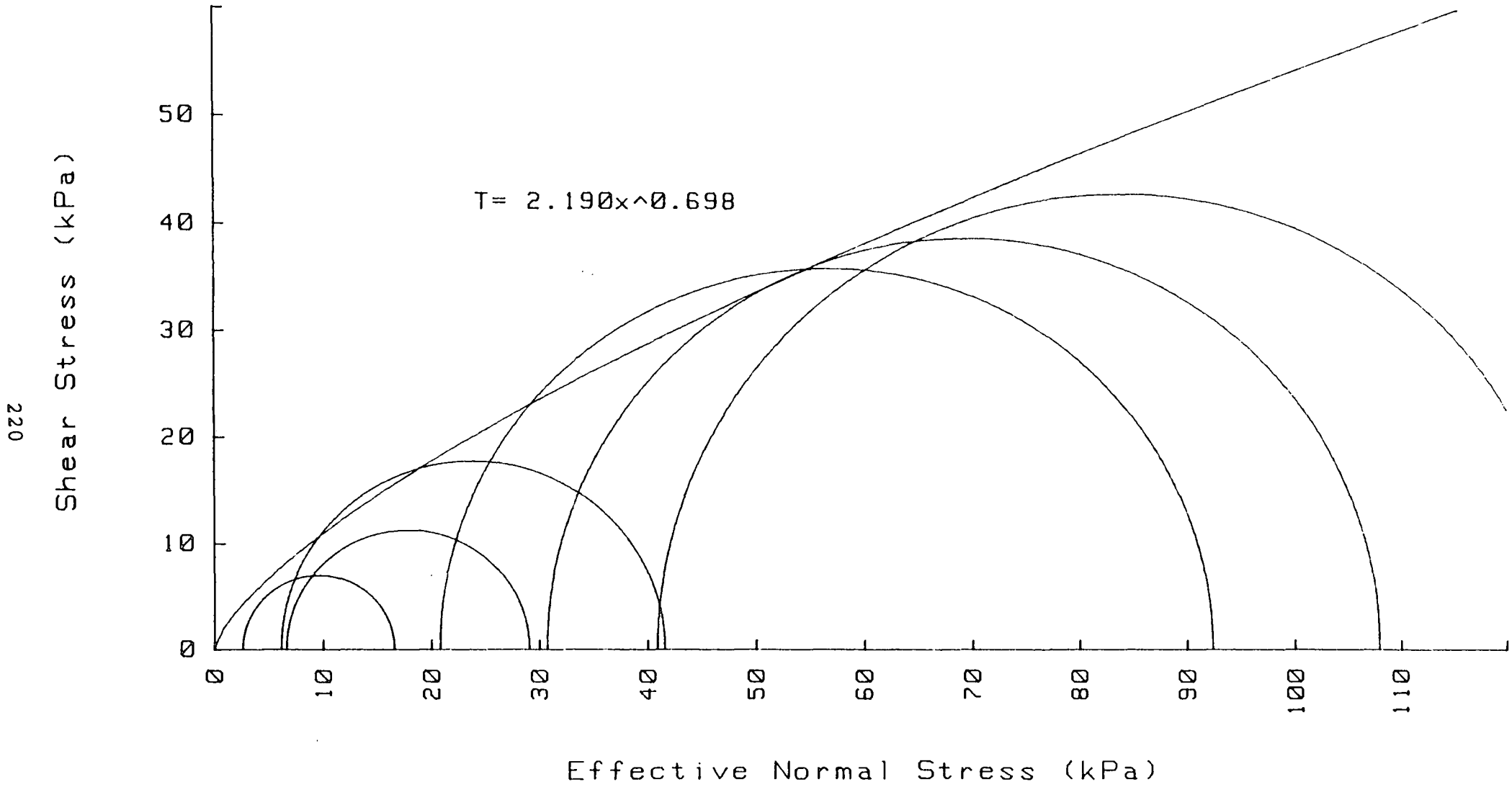


Fig 8/14 Best fit power curve to peak strengths - Weald Clay

Chapter 9

A slope stability method of analysis for soils with a non-linear strength envelope

9.1 Introduction

Since new strength parameters are introduced, new methods of analysis are required. In slope stability, a method is therefore required for back-analysing existing failures for which a curved failure envelope is more accurate than a linear one. This problem is taken in hand in this Chapter which develops a slope stability method of analysis using these strength parameters.

9.2 A suitable existing method for conversion

The obvious procedure for developing a method for slope stability analysis based on a non-linear failure criterion is to consider what existing methods are available, see how applicable they are for these types of shallow failure and use the most appropriate method as a basis for the new method. There are numerous existing methods available using a linear failure criterion. They have been developed for particular types of failure, for various degrees of accuracy and for various soil types and profiles. As the area of slope stability analysis has developed, the degree of sophistication has increased with many methods trying to cover as many of the factors as possible which contribute to instability. The

increasing development of computers has made this easier, taking a lot of the tedium out of calculations and allowing methods to be devised which would otherwise have not been feasible at all. Most modern analyses are therefore extremely involved. The following is a list of the limit equilibrium methods, currently known to the author, and a broad description of their application.

(a) Method of slices - Rigorous methods where the difference in inter-slice stresses is not taken as zero.

(i) Failure surfaces of arbitrary shape

1. Janbu's generalised procedure of slices
(1954a, 1957, 1973)
2. Nonveiller's method (1965)
3. The Morgenstern and Price method (1965)
4. Spencer's method (1967, 1973)
5. Sarma's method (1973)
6. Bell's method (1968)

(ii) Circular failure surfaces

1. Bishop's method (1952)
2. The $\phi_u=0$ method-circular arc analysis
(Fellenius, 1918)

(b) Method of slices - Simplified methods which accept a value for the factor of safety that satisfies moment equilibrium if the difference in inter-slice stresses is zero.

1. Bishop's simplified method (1955)
2. The ordinary, conventional, USBR (United States Bureau of Reclamation), or Swedish method
(Fellenius, 1927 and 1936)

3. Janbu's simplified generalised procedure of slices
(Janbu et al, 1956)
 4. Kenney's method (1956)
 5. Greenwood's method (1983)
 6. Nonveiller's simplified method (1965)
- (c) Planar failure surfaces
1. The wedge method
 2. The infinite slope analysis (Haefeli, 1948)
 3. The $\phi_u=0$ analysis for a vertical cut
- (d) Non-dimensional methods of analysis
1. The Fellenius-Taylor stability numbers
(Taylor, 1937 and 1948)
 2. The Gibson and Morgenstern stability numbers (1962)
 3. The Hunter and Schuster stability numbers (1968)
 4. Bishop and Morgenstern's stability coefficients
(1960)
 5. Spencer's stability charts (1967)
 6. Morgenstern's stability charts for rapid draw down
(1963)
 7. Janbu's dimensionless parameters
(Janbu, 1954b)
- (e) 3-D methods
1. Hungr (1987)
 2. Zhang (1988)
 3. Michalowski (1989)
- (f) Probabilistic methods
1. Chowdhury and A-Grivas (1982)
 2. McGuffey, Grivas, Iori and Kyfor (1982)

3. Rosenbaum and Jarvis (1985)
4. Chowdhury, Tang and Sid (1987)
5. Li and Lumb (1987)

(g) Methods using a non-linear failure envelope

1. Charles and Soares (1984a, 1985b)
2. Hill (1950)
3. Kingston and Spencer (1970)
4. Collins, Gunn and Pender (1986)

(h) Differential equation approach

1. Kotter (1903)
2. Sokolovskiis (1965)

Before choosing a method it is necessary to consider a number of points. Firstly, what method is best suited to the types of failure under analysis? The types of failure being considered here are,

(a) shallow failures with failure surfaces rarely exceeding 1.5m depth below the surface of the slope,

(b) the failure surface is usually planar, parallel to the ground surface and not of infinite length,

(c) the failures are occurring after a considerable period of time, when an effective stress approach is the most appropriate.

Secondly, what method is appropriate for simple conversion to a shear strength which is non-linear?

And thirdly, a rigorous method should give more accurate

results which is important for a new method of analysis based on a fundamentally different set of strength parameters to those usually used.

From the list of available analysis methods, the first point excludes all the methods in (a) (ii), (c) and (g), the second criteria excludes all the methods in (d), (e), (f) and (h), at least at an initial stage, and the third point excludes all the methods in (b). Only the methods in paragraph (a)(i) therefore remain. The method of Charles and Soares is considered later in Section 9.9 as a non-linear failure criteria is used in analysing circular failures. The accuracies of the methods in (a)(i), for the relatively simple slopes considered here, are very similar, plus or minus 5%, according to Fredlund and Krahn (1977), Duncan and Wright (1980) and Anderson and Richards (1987). The method chosen is therefore not too critical. The rigorous methods require the use of a computer and it is always desirable to use a method, with the appropriate program, with which the operator is familiar and experienced. It is risky to switch to a new program, in search of greater accuracy, as serious errors can arise unless a full understanding of its capabilities has been grasped. Of these remaining methods the author is familiar with Janbu's general procedure of slices which is sufficiently straightforward to be used as a basis for conversion to a stability analysis with a non-linear failure criteria. It also has the advantage of being simple enough to be used with a hand calculator if desired. Janbu's method is used throughout the civil engineering profession and is

generally accepted as being sufficiently accurate for the analysis of simple slopes.

9.3 The Janbu generalised procedure of slices

Janbu first published an outline of his method in 1954, extending the formulations to cover the analysis of bearing capacity and earth pressures in 1957. In 1973 he published a full account of his method and included comprehensive worked examples. The method can be applied to both circular and non-circular slip surfaces. It was the first method of slices in which overall force equilibrium and overall moment equilibrium were satisfied. A detailed derivation of the method will not be given here as a similar procedure will be followed in the next Section to find a method with a non-linear failure criteria rather than a linear one.

9.4 A limit equilibrium slope analysis method for soils exhibiting a non-linear shear strength

Considering the slice of the potential slope failure given in Figure 9/1, for force equilibrium,

resolving vertically

$$P \cdot \cos\psi + S \cdot \sin\psi = W - (X_{n+1} - X_n)$$

$$\text{Now } (\sigma' + u) \cdot l = P \quad \text{and}$$

$$\tau \cdot l = S$$

where σ' = effective normal stress
at the base of the slice

τ = shear stress at the base
of the slice

u = pore water pressure at
the base of the slice

so

$$(\sigma' + u).l.\cos\psi + \tau.l.\sin\psi = W - (X_{n+1} - X_n) \quad (1)$$

The non-linear shear strength criterion is given by $\tau = A(\sigma')^b$
and if a factor of safety is applied, $\tau = \frac{A(\sigma')^b}{F}$. Replacing τ
in (1) and rearranging

$$\sigma' = \frac{W}{l.\cos\psi} - u - \frac{A(\sigma')^b}{F}.\tan\psi - \frac{(X_{n+1} - X_n)}{l.\cos\psi} \quad (2)$$

Resolving parallel to base of slice

$$S = [W - (X_{n+1} - X_n)].\sin\psi - (E_{n+1} - E_n).\cos\psi$$

$$\tau.l = [W - (X_{n+1} - X_n)].\sin\psi - (E_{n+1} - E_n).\cos\psi$$

Replacing τ with the non-linear shear strength criteria and
rearranging gives

$$E_{n+1} - E_n = [W - (X_{n+1} - X_n)].\tan\psi - l.\frac{A(\sigma')^b}{F}.\sec\psi \quad (3)$$

Summing all the slices in the slope

$$\sum E_{n+1} - E_n = \sum [W - (X_{n+1} - X_n)].\tan\psi - l.\frac{A(\sigma')^b}{F}.\sec\psi \quad (4)$$

In the absence of any surface loading

$$\begin{aligned} \sum E_{n+1} - E_n &= 0 \\ \sum X_{n+1} - X_n &= 0 \end{aligned}$$

so

$$F = \frac{\sum l.A(\sigma')^b.\sec\psi}{\sum [W - (X_{n+1} - X_n)].\tan\psi} \quad (5)$$

Taking moments about the centre of the base of the slice, ie
where the resultant normal stress occurs and where the total
vertical stress acts, and assuming that α is the same for the
whole width of the slice,

$$(X_n + X_{n+1}).\frac{t}{2} - E_n(h - \frac{t}{2}.\tan\psi + t.\tan\alpha) + E_{n+1}(h - \frac{t}{2}.\tan\psi) = 0 \quad (6)$$

where h = height of thrust line above the failure

surface on the lower side of the slice.

α = angle thrust line makes with the horizontal when acting on the lower side of the slice and is assumed to be straight across the width of the slice.

Now let $X_{n+1} - X_n = \Delta X$ or $X_n = X_{n+1} - \Delta X$ and

$E_{n+1} - E_n = \Delta E$ or $E_n = E_{n+1} - \Delta E$ and

Replacing in (6)

$$(2.X_{n+1} - \Delta X) \cdot \frac{t}{2} - (E_{n+1} - \Delta E) \left(h - \frac{t}{2} \cdot \tan\psi + t \cdot \tan\alpha \right) + E_{n+1} \left(h - \frac{t}{2} \cdot \tan\psi \right) = 0$$

If t is very small then $\Delta X \cdot t \rightarrow 0$

and $\Delta E \cdot t \rightarrow 0$.

$$t \cdot X_{n+1} + \Delta E \cdot h - E_{n+1} \cdot t \cdot \tan\alpha = 0$$

$$X_{n+1} + \frac{h}{t} \cdot (E_{n+1} - E_n) - E_{n+1} \cdot \tan\alpha = 0 \quad (7)$$

Equations (2), (3), (5) and (7) are the working equations that will be used in the stability analysis and are reproduced below.

$$\sigma' = \frac{W}{1 \cdot \cos\psi} - u - \frac{A(\sigma')^b \cdot \tan\psi}{F} - \frac{(X_{n+1} - X_n)}{1 \cdot \cos\psi} \quad (2)$$

$$E_{n+1} - E_n = [W - (X_{n+1} - X_n)] \cdot \tan\psi - \frac{1 \cdot A(\sigma')^b \cdot \sec\psi}{F} \quad (3)$$

$$F = \frac{\sum 1 \cdot A \cdot \sec\psi}{\sum [W - (X_{n+1} - X_n)] \cdot \tan\psi} \cdot \left[\frac{W}{1 \cdot \cos\psi} - u - \frac{A(\sigma')^b \cdot \tan\psi}{F} - \frac{(X_{n+1} - X_n)}{1 \cdot \cos\psi} \right]^b \quad (5)$$

$$X_{n+1} = E_{n+1} \cdot \tan\alpha - \frac{h}{t} \cdot (E_{n+1} - E_n) \quad (7)$$

9.5 A computer program using a rigorous solution and non-linear failure envelope

A computer program has been written using the above analysis

and is included in Appendix E. It is intended for use in the fairly simple situations described in the survey where the slopes are usually fairly homogeneous and not multi-layered. The convention of a slope decreasing in height to the right has been adopted and should be used when entering geometrical data. The coordinates should be in metres.

The following data are required to input into the program:

- (a) the number of slices to be analysed, N ;
- (b) the X coordinate of the top of the slope, $X(0)$;
- (c) the bottom and top Y coordinates of the higher side of the first slice on the left, Y_b and Y_t ;
- (d) the Y coordinate of the phreatic surface at the top of the slope, $Y_w(0)$.

And for each slice

- (e) failure envelope parameters A and b, $A(I)$ and $B(I)$
- (f) unit weight in kN/m^3 , $G_a(I)$
- (g) the X coordinate of the right side of the slice, $X(I)$
- (h) the Y coordinate of the bottom of the right side of the slice, $Y_b(I)$
- (i) the Y coordinate of the top of the right side of the slice, $Y_t(I)$
- (j) the Y coordinate of the phreatic surface on the right side of the slice, $Y_w(I)$
- (k) the angle of the line of thrust at the right side of the slice in degrees, $\text{Alph}(I)$

(1) the Y coordinate of the height of the line of thrust above the bottom of the right side of the slice, $Ht(I)$

Several iterations are required to examine a failure and the following routine is used in the computer program (see the flow diagrams in Figures 9/2).

In the first phase, the simplified solution, the Fellenius assumption is made that the inter-slice forces can be ignored. A value of $\sigma' = \gamma \cdot h \cdot \cos^2 \psi - u$ can therefore be used for each slice, I, and the factor of safety calculated by iteration from equation 5 using the total number of slices, N. (The factor of safety of the previous cycle, F_L , and the new factor of safety, F , are compared until the difference between the two is extremely small.) The factor of safety is then used in equation 2 and the values of σ' found by iteration for each slice; the value of the effective normal stress from the previous cycle, σ'_L , is compared with the new value, σ' . The values of σ' and the factor of safety from the previous cycle, F_a , which included iterations of the factor of safety and effective normal stress, are then used in equation 5 to find a new value of F. The new value of F allows new values of σ' to be calculated and so on until successive values of σ' and F are within a very small percentage of each other. At this point the interslice forces have been ignored. Now that the values of F and σ' are known for the simplified case, the interslice forces can be included and the rigorous solution calculated. Using the value of F and values of σ' for each slice, ΔE can

be calculated for each slice using equation 3. The individual horizontal forces can now be found and used in equation 7 to obtain the first approximation to the interslice shear forces for each slice. The values of the shear force are inserted in equation 2 to find the values of σ' for each slice and a similar procedure followed as before in the simplified solution phase. This results in new iterated values for σ' and F for the first approximation to the interslice forces. The whole procedure is then repeated with these new values, first being used to find ΔE (using the previous iterations values for X) and then E; the new values calculated for X can then be used in the iterations for σ' and F. The values of X lapse one iteration behind the other values. This procedure continues until the difference between the values of the effective normal stresses and factors of safety, σ'_a and F_b (from the previous cycle which included iterations of factor of safety, effective normal stress and calculations of interslice forces) and the new values of effective normal stress and factor of safety, σ' and F, is so small, ≤ 0.001 and ≤ 0.0001 respectively, so as to be ignored. A very rapid iteration convergence is achieved, usually less than ten iterations for F, using the program.

An example of the type of calculations that are carried out is given in Table 9/1 and Figures 9/3 and 9/4.

9.6 Effect of varying the position of the line of thrust

In order to see how sensitive the factor of safety is to the

position of the line of thrust, an analysis has been conducted using the shallow failure and the deep failure given in Figures 9/3 and 9/4; the results are given in Table 9/2. The calculations of the factor of safety for the cases where the line of thrust is in extreme positions vary from the factor of safety of the most likely position of the line of thrust by less than 1% in all cases. It is clear that the position of the line of thrust has very little effect on the factor of safety. Janbu (1973) made the same observation for his method.

9.7 Effect of soil parameters on the factor of safety

To investigate the effect of soil parameters on the factor of safety F , an analysis has been conducted on the Gault Clay at Nepicar. Figure 9/5 shows the effect on the factor of safety F when varying A , b , the depth of slip, slope height, phreatic surface and the slope angle.

There is an approximately linear increase in F with A over the range considered and F becomes increasingly sensitive to higher values of b .

An increase of F occurs at shallower depths of failure, a result that is not surprising given the shape of the failure surface taken and the increasing instability caused by increasing the size and weight of the slice as a result of a deeper failure plane. Since the shape of the slip surface is correct, as this is the shape observed, this result would seem

to indicate that other factors such as much weaker embankment edges on a stronger core are having an effect and restricting the position of the failure plane. In Greenwood et al (1985), a minimum F is calculated for a particular shallow depth of failure plane which could be a direct result of the shape of failure plane used. Significant toe restraint is included for deeper failures, as the slip becomes shallower this restraint becomes proportionally smaller when compared to the weight of block it is supporting and so F reduces. At very shallow slips the weight of block is much less and the restraint is probably more efficient and hence F increases again. Since the shape of failure surface observed by Greenwood et al (1985) was not observed for the failures studied in this Thesis it is unlikely that such a solution will be applicable.

In Figure 9/5, F reduces as the height of slope increases which is exactly what was seen on the slopes during the survey.

Since the factors of safety were so high, the effect of the phreatic surface is not so representative but it can be seen that small movements of the phreatic surface near the slope surface cause the greatest change in F .

Reducing the slope angle results in an increase in the rate of change in F , given that no other mechanisms are at work such as rates of water infiltration at different slope angles.

These results indicate that the method of analysis developed

appears to be behaving as expected from observations in the field.

9.8 Applications of the computer program

The program and the analysis developed here, will be used to analyse shallow failures on clay slopes, but the methods could easily be used for other materials where a non-linear failure envelope is appropriate, such as rock fills and jointed rock masses. The results of back-analyses are invariably used in the design of slopes in new construction as a way of preventing or quantifying further failures. The determination of soil parameters and stability for the design of new slopes can be assessed using the program and analysis presented in this Thesis.

9.9 The method of Charles and Soares

Charles and Soares published two papers in 1984, one on the stability of compacted rock fills, and the other on the stability of soil slopes, both used a non-linear failure envelope. In both situations a power curve is used with a circular arc stability analysis. The method is only appropriate to circular failures and employs an analysis based on the semi-rigorous analysis of Bishop (1955). This involves the assumption that the resultants of the interslice forces act horizontally. The derivation of the equations used in the analysis is straightforward using a similar approach to that

used by Bishop. The working equations require iterations of the factor of safety and effective normal stress in the same way as described in Section 9.5. A computer program was written by Charles and Soares and, from the results, stability charts were compiled using stability numbers. However, for slopes which fail with arbitrary shaped failure surfaces stability charts are not readily appropriate as there is no consistent failure surface geometry on which to base them. Also, varying slope geometry, surcharge loading, pore water pressures and shear strength can easily be accommodated by a computer program.

The equations derived by Charles and Soares are similar, but not the same, as equations 2 and 5.

$$\sigma' = \frac{W}{l \cdot \cos\psi} - u - \frac{A(\sigma')^b \cdot \tan\psi}{F}$$

$$F = \frac{\sum l \cdot A}{\sum [W - \sin\psi]} \cdot \left[\frac{W}{l \cdot \cos\psi} - u - \frac{A(\sigma')^b \cdot \tan\psi}{F} \right]$$

This method could be used for shallow slips on simple slopes with a circular failure surface as occasionally occurs.

Charles and Soares mention that iteration problems occurred with their method when the soil parameter b was greater than 0.75. No such problems were encountered with the analysis given in this Thesis for any value up to $b=1.0$. Problems were encountered, however, for steep slopes in the same way as the Charles and Soares method. For slope angles greater than those given in Figure 9/5, problems were encountered with the

iterative process which calculates the effective normal stress at the base of the slice. This has no effect on the analysis of most soils but may have some effect on steep slopes in rock. This restraint was not a problem for any of the back-analyses carried out in Chapter 10.

9.10 Methods used for rock fill and closely jointed rock.

Highly weathered rock slopes or rock fills behave more like soils than fresh insitu rock slopes which are governed by pre-existing features such as faults, bedding planes and joints. Consequently, methods applicable to rocks of this type can be used with soils and vice versa. As with soils, the failure surface in degraded rock and rock fills are free to adopt the shape of 'least resistance'. There is ample empirical evidence to show that the relation between shear and normal stress is non-linear at all stress levels (Hoek and Bray, 1981). As mentioned above, Charles and Soares (1984b) used a non-linear failure envelope, a slip circle, and the method of slices to obtain stability factors for a certain class of non-linear failure envelope. Hoek (1983) used two block collapse mechanisms to study particular cases of closely jointed rock. Collins, Gunn and Pender (1986) considered a non-linear failure envelope for wedge, block and log spiral failure using a partial differential stress distribution.

TABLE 9/1

An example of the computations involved in the determination of a factor of safety using the rigorous method of slices with a non-linear failure envelope.

- P(I) = angle of the shear plane with the horizontal, ψ .
= $\arctan[Y_b(I) - Y_b(I-1)] / [X(I-1) - X(I)]$
- L(I) = the length of the slice's shear surface, l.
= $\sqrt{[Y_b(I) - Y_b(I-1)]^2 + [X(I) - X(I-1)]^2}$
- U(I) = average pore water pressure, u.
= $9.81/2. \{ [Y_b(I-1) + Y_b(I)] - [Y_w(I) + Y_w(I-1)] \}$
- W(I) = weight of slice, W.
= $\gamma/2. [X(I) - X(I-1)]. [Y_t(I) + Y_t(I-1) - Y_b(I) - Y_b(I-1)]$
- TH(I) = thickness of slice, t.
= $X(I) - X(I-1)$

SLICE NOS.	1	2	3	4	5
P(I)	24.23	23.63	24.63	23.63	0
L(I)	4.39	4.37	4.39	4.37	4.00
U(I)	9.81	9.81	9.81	9.81	4.91
W(I)	78.80	78.80	78.80	78.80	39.40
TH(I)	4	4	4	4	4

Initial value of factor of safety, F = 1.000

S(I)	6.57	6.73	6.57	6.72	4.95
------	------	------	------	------	------

Iterated value of F = 1.1983

S(I) (iterated)	7.10	7.16	7.10	7.16	4.95
-----------------	------	------	------	------	------

Iterated value of F = 1.1805

.....continues until.....

S(I) (iteration complete)	7.07	7.13	7.07	7.13	4.95
---------------------------	------	------	------	------	------

Iterated value for the simplified solution, F = 1.1816.

Rigorous solution including inter-slice forces.....

$\Delta X(I)$	0	0	0	0	0	
$\Delta E(I)$ (NB $\Sigma \Delta E=0$)	5.304	4.414	5.304	4.414	-19.436	
E(between slices)	0	5.304	9.718	15.022	19.436	0
K(between slices)	0	2.129	3.963	6.251	5.874	0
$\Delta X(I)$ (NB $\Sigma \Delta X=0$)	2.129	1.834	2.288	-0.377	-5.874	

S(I) (iterated)	6.65	6.77	6.63	7.21	6.41
-----------------	------	------	------	------	------

Iterated value of F = 1.216

.....when S(I) and F are within the required tolerances, new inter-slice forces are calculated and the procedure repeated. The computation finishes when no further improvement in the factor of safety and the effective normal stress can be achieved.

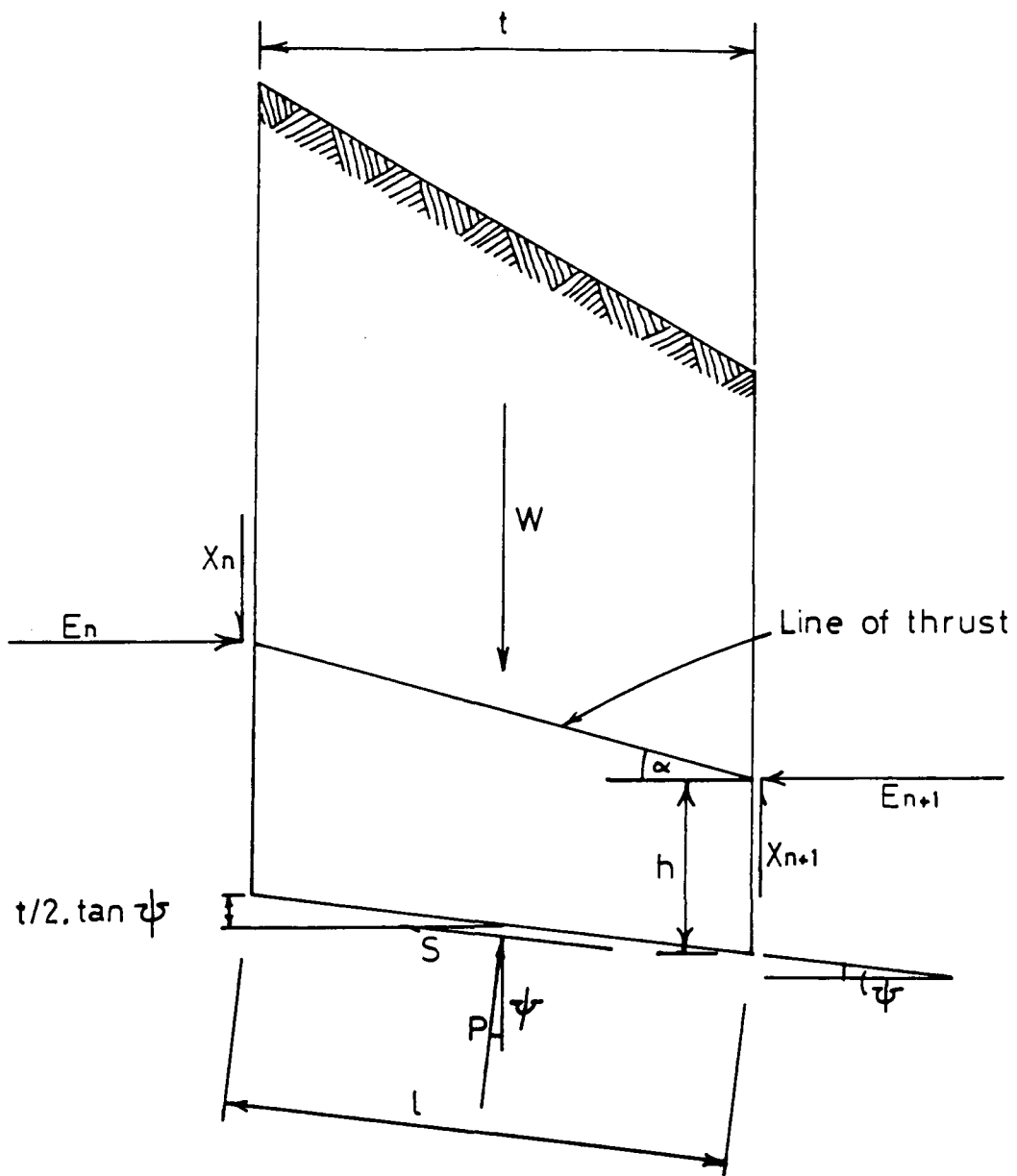
$\Delta X(I)$	2.564	2.270	2.782	-0.524	-7.092
S(I) (iteration complete)	6.64	6.75	6.60	7.30	6.72

Factor of safety = 1.220

TABLE 9/2

Effect of the position of the line of thrust on the factor of safety

	Angle of thrust for each slice, ALPH (Deg)	Height above base for each slice, HT (m)	Factor of safety	Difference in factor of safety
SHALLOW FAILURE				
Likely position of line of thrust	25	0.26	1.22	
	24	0.33		
	24	0.37		
	18	0.40		
Extreme variations	26	0.22	1.21	0.6%
	24	0.25		
	24	0.25		
	15	0.33		
	24	0.40	1.23	0.4%
	24	0.45		
	24	0.45		
	20	0.50		
DEEP FAILURE				
Likely position of line of thrust	42	5.00	0.92	
	26	7.30		
	18	7.50		
	6	6.00		
Extreme variations	44	2.50	0.93	0.6%
	27	3.60		
	18	3.80		
	5	3.00		
	40	6.00	0.92	0.0%
	26	9.50		
	20	10.00		
	7	7.30		



- E = horizontal interslice force } n and $n+1$ designate the
 X = vertical interslice force } higher and lower sides
 W = total weight of slice } respectively
 t = width of slice
 P = total normal force on the base of the slice over
a length l
 S = shear force mobilized on the base of the slice
 α = angle of line of thrust
 h = height of line of thrust
 ψ = angle of base of slice

Fig 9/1 Forces acting on a slice

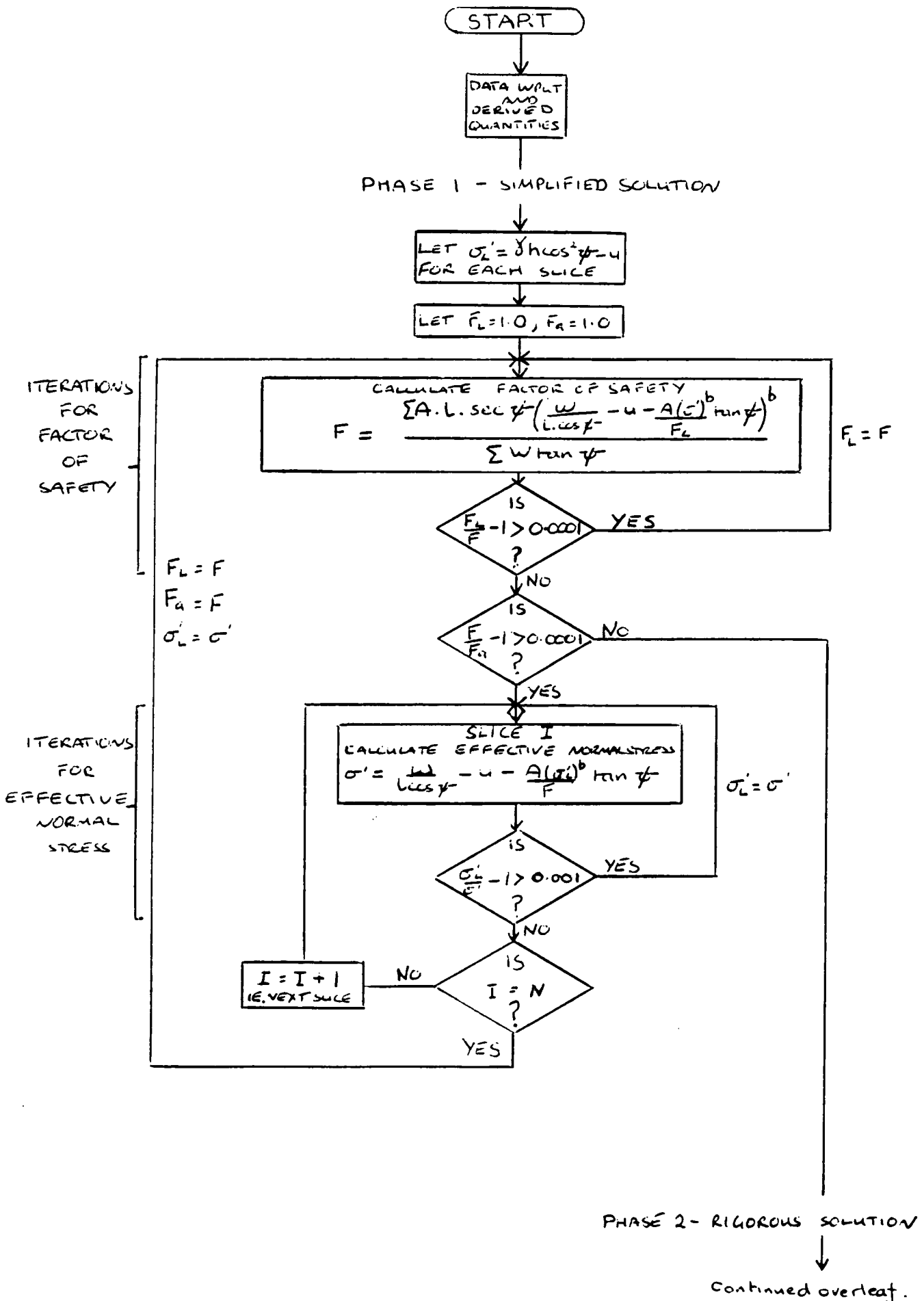


Fig 9/2 Flow diagram describing a computer program using a non-linear failure envelope for arbitrary shaped failure surfaces

PHASE 2 RIGOROUS SOLUTION

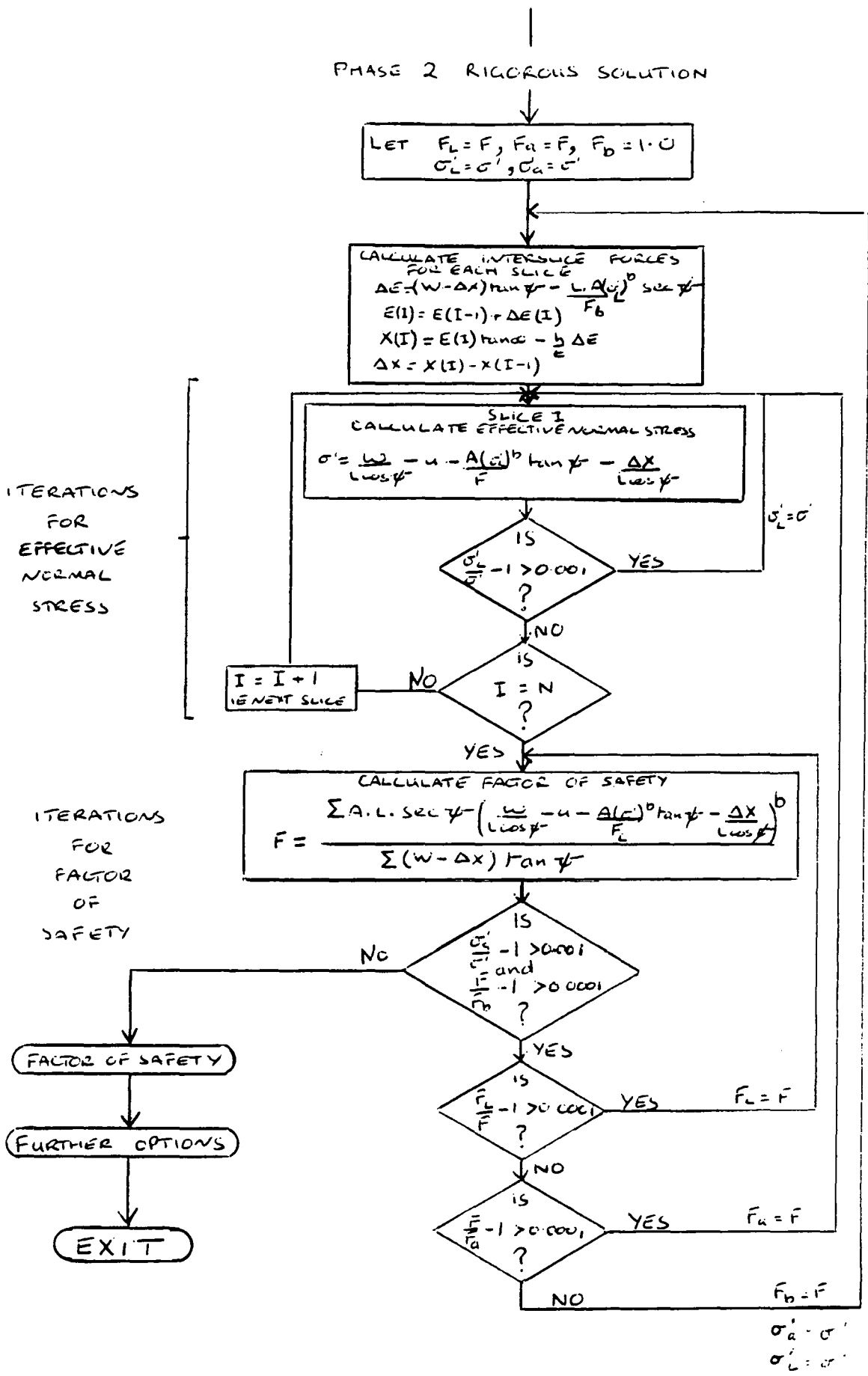


Fig 9/2 continued

Number of slices 5
 X co-ordinate of top of slope (m) 2
 Bottom and top Y co-ordinate, left side of top slice (m) (7.1, 8.1)
 Water table level (m) 8.1

	A	b	Gamma kN/m ³	X (m)	YB (m)	YT (m)	YW (m)	ALPH (deg)	HT (m)
SLICE 1	1.844	0.711	19.7	6	5.30	6.30	6.30	25	0.26
SLICE 2	1.844	0.711	19.7	10	3.55	4.55	4.55	24	0.33
SLICE 3	1.844	0.711	19.7	14	1.75	2.75	2.75	24	0.33
SLICE 4	1.844	0.711	19.7	18	0	1.0	1.0	18	0.40
SLICE 5	1.844	0.711	19.7	22	0	0	0	0	0

Y (m)

FACTOR OF SAFETY = 1.22

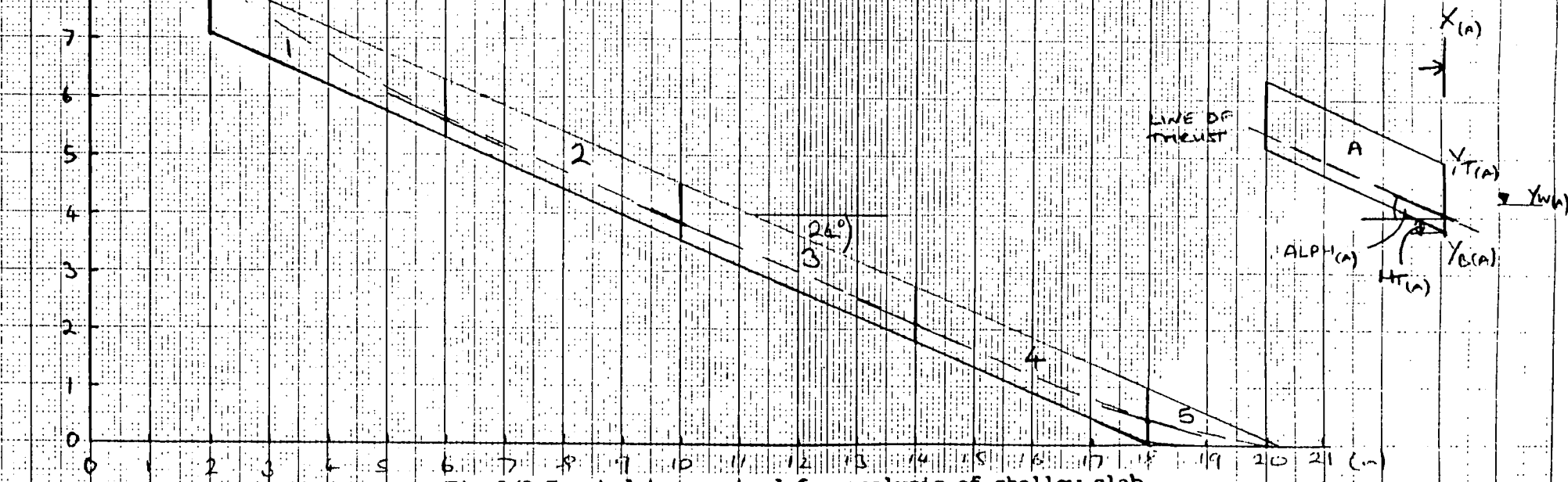


Fig 9/3 Input data required for analysis of shallow slab failures

Number of slices 5
 X co-ordinate of top of slope (m) 4
 Bottom and top Y co-ordinate,
 left side of top slice (m) (53, 53)
 Water table level (m) 0

A	b	Gamma kN/m ³	X (m)	YB (m)	YT (m)	YW (m)	ALPH (deg)	HT (m)
SLICE 1								
2	0.7	21.6	20	27.2	45	0	42	5.0
SLICE 2								
2	0.7	21.6	40	12.0	35	0	26	7.3
SLICE 3								
2	0.7	21.6	60	3.5	25	0	18	7.5
SLICE 4								
2	0.7	21.6	80	0.5	15	0	6	6.0
SLICE 5								
2	0.7	21.6	105	2.8	2.8	0	0	0

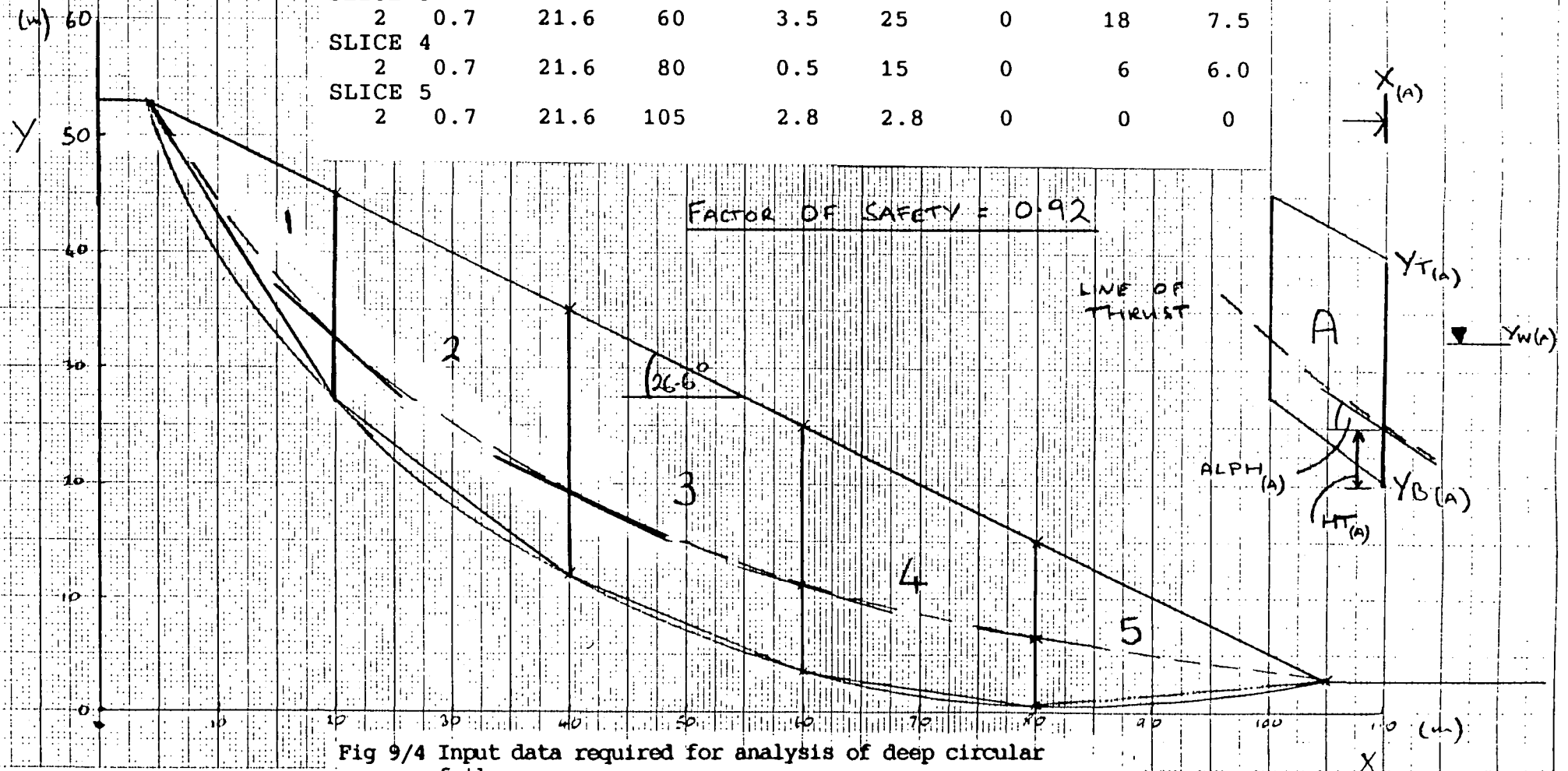


Fig 9/4 Input data required for analysis of deep circular failures

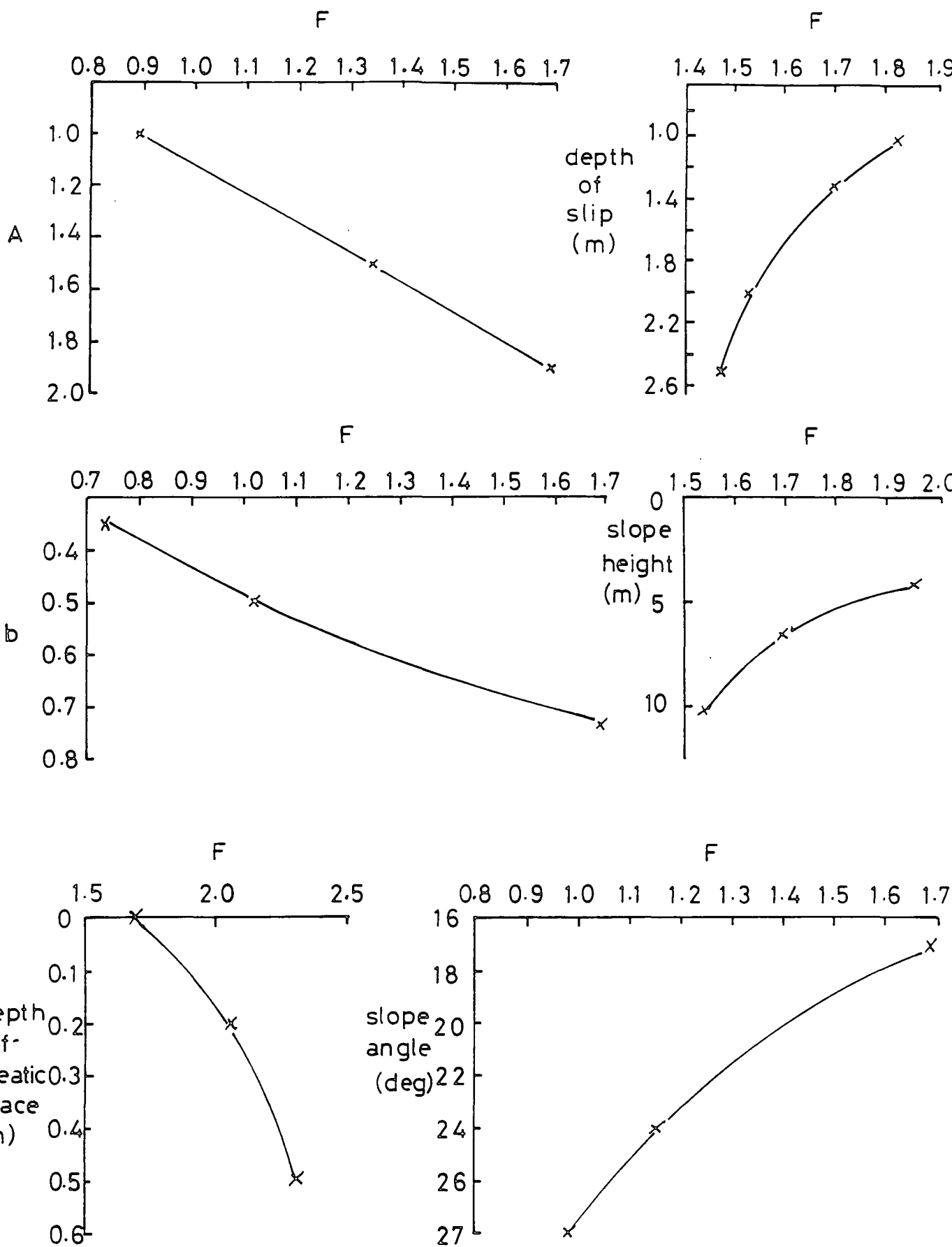


Fig95 The variation of factor of safety with different parameters

Back-analyses of shallow failures

10.1 General

In order to conduct any reasonable back-analysis of slope failures the details of the slope itself must be accurately observed, sampling should be as representative as possible, testing should be carried out at the stress levels encountered in the field and be as accurate as current technology allows, and pore water pressures should be assessed to a high degree of confidence. Based on the philosophy of Leroueil and Tavenas (1981) and Chandler (1977) the following criteria have been met:

(a) every aspect of slope behaviour has been considered as accurately as possible without losing sight of observations in the field, that is the survey.

(b) a good understanding of the problem has been gained from the literature as well as the results of the survey.

(c) theories, such as a non-linear failure envelope, have been led by observation, not observation led by theories.

10.2 Characteristics of slopes and soil properties

Back-analyses are conducted on the six embankment failures given in Table 6/1. Emphasis has been placed on embankments as they were highlighted in the survey as being more of a problem than cuttings. Also embankments have not received the same

level of attention as cuttings and so more work is needed to investigate their behaviour.

Table 10/1 summarizes the characteristics of the slopes. The profile of the slope, the profile of the failure surface (Figure 10/1) and the soil properties are entered into the stability program as described in Section 9.5 and Figure 9/3. The failure surface profile is considered to be a plane parallel to the slope surface. This profile is based on observations of these particular failures, failures observed during the survey and a report for TRRL describing the shape of a failure surface as observed in a trench cut through a shallow failure on a Gault Clay embankment on the A45 in Cambridgeshire (Figure 10/2). In Figure 10/1, the depth of slip increases as the slope angle decreases for the geologies studied, a phenomena discussed in Chapter 11.

Back-analyses are conducted using a non-linear failure envelope for the peak strength parameters (Table 8/1), representing the maximum strength of the soils in a natural state, and the 'ultimate' strength parameters (Table 8/2). The stability analysis method developed in Chapter 9 is used for these parameters. Further analysis is conducted using the critical state strength parameters (Table 7/2) which represents homogeneous strain conditions at the point when initial failure of the soil mass occurs. Residual strength requires larger strains and the formation of a pre-existing shear plane before failure which were not observed at the site locations. These

strengths are illustrated in Figure 10/3. Note that the residual strength failure envelope is generally curved at low effective stresses (Lupini, Skinner and Vaughan, 1981) in a similar manner to the peak strength envelope.

10.3 Pore water pressures

Pore water pressures were not measured at the exact location of all the slips. However there is sufficient evidence from the Nepicar site (Crabb, West and O'Reilly, 1987) and from other similar highway earthworks for a realistic assessment to be made. Observations in the field at the sites of the failures indicated that the soil was saturated mainly in the lower half of the embankment to the full depth of the slip. This is evidenced by standing water, shrinkage cracking on the failure plane, mud flow structure, water loving plants and inspection with the simple probe used during the survey for any signs of wetness. The work of Crabb and West (1985), Crabb et al (1987) and Anderson and Kneale (1980a and 1980b) on measuring pore water pressures in embankments of Gault Clay, and Oxford or Kimmeridge Clay indicates that pore water pressures in the outer 1.5m of the embankment, the part most effected by failure, periodically become positive, or more positive, in winter especially in the lower part of the slope. During periods when measurements were taken the phreatic surface was at or near the lower slope surface. Shrinkage cracking can allow relatively rapid changes in pore water pressures to occur within the outer layer, an effect recorded both by Anderson,

Hubbard and Kneale (1982) and Crabb et al (1987). Failure of the slope occurred while Anderson and Kneale (1980a and 1980b) were taking readings and the positive pore pressures measured indicated a phreatic surface at the surface of the lower part of the slope. The readings of Crabb et al (1987) indicate lower positive pore water pressures. The pore water pressures higher up the slope were zero. Towards the core of the embankment, negative pore water pressures were measured some of which were very high. This pore water regime is similar to that described for cuttings (Chandler and Skempton, 1974).

10.4 Results of back-analyses

Considering the evidence in Section 10.3, it would seem that taking a phreatic surface at the surface of the slope and peak strength parameters would be a good initial assumption on which to conduct an analysis. This initial approach is recommended by Bromhead (1986). The 'ultimate' strength, that is the ultimate condition for testing as explained in Chapter 6, is analysed in the same way. Progression can then be made to consider critical state strengths for slopes with zero pore water pressures to the full depth of the slip, and slopes with zero pore water pressures at the high levels of the slip and positive pore water pressures at the toe of the embankment. The latter regime represents the situation measured by Anderson and Kneale (1980a and 1980b), and Crabb et al (1985 and 1987) and is considered to apply to all the soils being analysed. Slight variations in the regime were necessary to achieve

failure and reflect different rates of consolidation or swelling of each material.

Using the slope characteristics observed, the peak shear strength parameters measured and a phreatic surface at the surface of the slope in the slope stability analysis method for the curved failure envelope results in the factors of safety given in Table 10/2. Since a factor of safety of unity has in no way been achieved, these results indicate that since the accuracies of the parameters entered into the analysis are known to be reasonable then an incorrect assumption has been made. The most likely assumption to be at fault is that peak strength conditions prevailed. This would cause the shear strength to be too high and that lower shear strengths are actually occurring. This effect was noted by Crabb et al (1987), and by Coxon (1986) in connection with the Carsington Dam failure in 1984. Furthermore if a three dimensional analysis could be devised for curved failure envelopes the factor of safety would have been even higher.

The factors of safety calculated for the 'ultimate' condition from undisturbed samples with a phreatic surface at the slope surface samples are given in Table 10/3. These are not consistently lower than the factors of safety for the peak strength as would be expected. The results illustrate how much the stresses near the origin influence the fitting of a power curve and hence the calculated shear strength values as mentioned in Section 8.3.

Since the peak strengths and 'ultimate' strengths have produced factors of safety which are too high, and since residual strengths did not occur in the field, the application of the critical state strength, in the context of progressive failure, may be more appropriate.

Progressive failure (for example Bishop, 1952 and 1967) results from a non-uniform mobilization of shear strength along a potential failure surface. This is particularly appropriate to the over-consolidated fissured clays studied here, where large strains can develop irregularly along a potential failure surface due to stress concentrations at fissures, shrinkage cracks or other discontinuities. This results in the peak strength being reached, followed by a gradual decrease in strength at these areas of large strain. It also facilitates load shedding to neighbouring clay elements which in turn may become over-stressed. Load shedding is one of the implications of brittle materials with strain softening characteristics such as those studied here (Figures 6/14, 6/17 and 6/22). The average mobilized strength along a potential failure surface will then be somewhat less than the peak strength and can approach the critical state strength (Schofield and Wroth, 1968) or fully softened condition (Skempton, 1970). The critical state strength represents the average strength at failure for a slip surface; that is not to say that critical state strength is the actual mobilized condition but it seems to give a comparable strength to that developed due to

progressive failure. The critical state strength represents a useful lower bound strength for first-time slides, and this has been confirmed by back-analysis of failures in cuttings (Skempton, 1977). In cuttings, large strains can develop at fissures and for embankments this may still be the case but to a lesser extent as the material has been disrupted during the construction process. Shrinkage cracks may play a more important part (Anderson, Hubbard and Kneale, 1982), as well as the large strains developed during excavation, removal, deposition and during the compaction process (Whyte and Vakalis, 1987; Coxon, 1986).

The factors of safety using conventional linear failure envelopes, the Janbu rigorous method and a phreatic surface at the slope surface are shown in Table 10/4 for the critical state strength of reconstituted samples. As can be seen, the factors of safety are extremely low. Assuming zero pore water pressures and critical state strengths increases the factor of safety to above unity in most cases (Table 10/5). Using the most likely pore water regime, a phreatic surface at the toe of the embankment and zero pore water pressures elsewhere (Figure 10/1), and a critical state strength results in factors of safety of unity in most cases. This model is therefore the most likely failure mechanism for most of the soils studied. Table 10/6 and Figure 10/1 show, for each geology studied, the proportion of slope surface required to be effected by a phreatic surface in order to achieve a factor of safety of unity in the analyses. The proportions for Kimmeridge Clay,

Oxford Clay, Reading Beds clay and Weald Clay slopes are what can be expected in the field based on past research. Gault Clay, however, required a greater proportion of the slope to be effected than might be expected and London Clay fails whatever the position of the phreatic surface.

TABLE 10/1

Slope characteristics and soil bulk density

Geology	Angle of slope (deg)	Height of slope (m)	Depth of slip (m)	Bulk Density (kN/m ³)
Gault Clay- Nepicar	17	6.7	1.3	18.8
Kimmeridge Clay	24	8.1	1.0	19.7
London Clay	29	6.5	0.5	19.5
Oxford Clay	25	7.3	1.5	19.7
Reading Beds-clay	19	7.5	2.0	19.9
Weald Clay	24	6.7	1.5	20.5

TABLE 10/2

Factors of safety from back-analysis using a non-linear failure envelope and peak strength for undisturbed samples (phreatic surface at surface of slope)

Geology	Gault Clay- Nepicar	Kimmeridge Clay	London Clay	Oxford Clay	Reading Beds- Clay	Weald Clay
Factor of safety	1.69	1.11	1.70	1.42	1.46	1.29

TABLE 10/3

Factors of safety from back-analysis using a non-linear failure envelope and 'ultimate' strength for undisturbed samples (phreatic surface at surface of slope)

Geology	Gault Clay- Nepicar	Kimmeridge Clay	London Clay	Oxford Clay	Reading Beds- Clay	Weald Clay
Factor of safety	1.04	1.21	1.10	1.62	1.69	1.58

TABLE 10/4

Factors of safety from back-analysis using a conventional linear failure envelope and critical state strength from reconstituted samples (phreatic surface at surface of slope)

Geology	Gault Clay- Nepicar	Kimmeridge Clay	London Clay	Oxford Clay	Reading Beds- Clay	Weald Clay
Factor of safety	0.70	0.45	0.33	0.51	0.57	0.55

TABLE 10/5

Factors of safety from back-analysis using a conventional linear failure envelope and critical state strength from reconstituted samples (zero pore water pressures)

Geology	Gault Clay- Nepicar	Kimmeridge Clay	London Clay	Oxford Clay	Reading Beds- Clay	Weald Clay
Factor of safety	1.58	1.06	0.88	1.18	1.22	1.19

TABLE 10/6

Proportion of slope surface requiring a phreatic surface to achieve a factor of safety of unity

Geology	Gault Clay- Nepicar	Kimmeridge Clay	London Clay	Oxford Clay	Reading Beds- Clay	Weald Clay
Proportion of slope	0.6	0.1	----	0.2	0.4	0.3

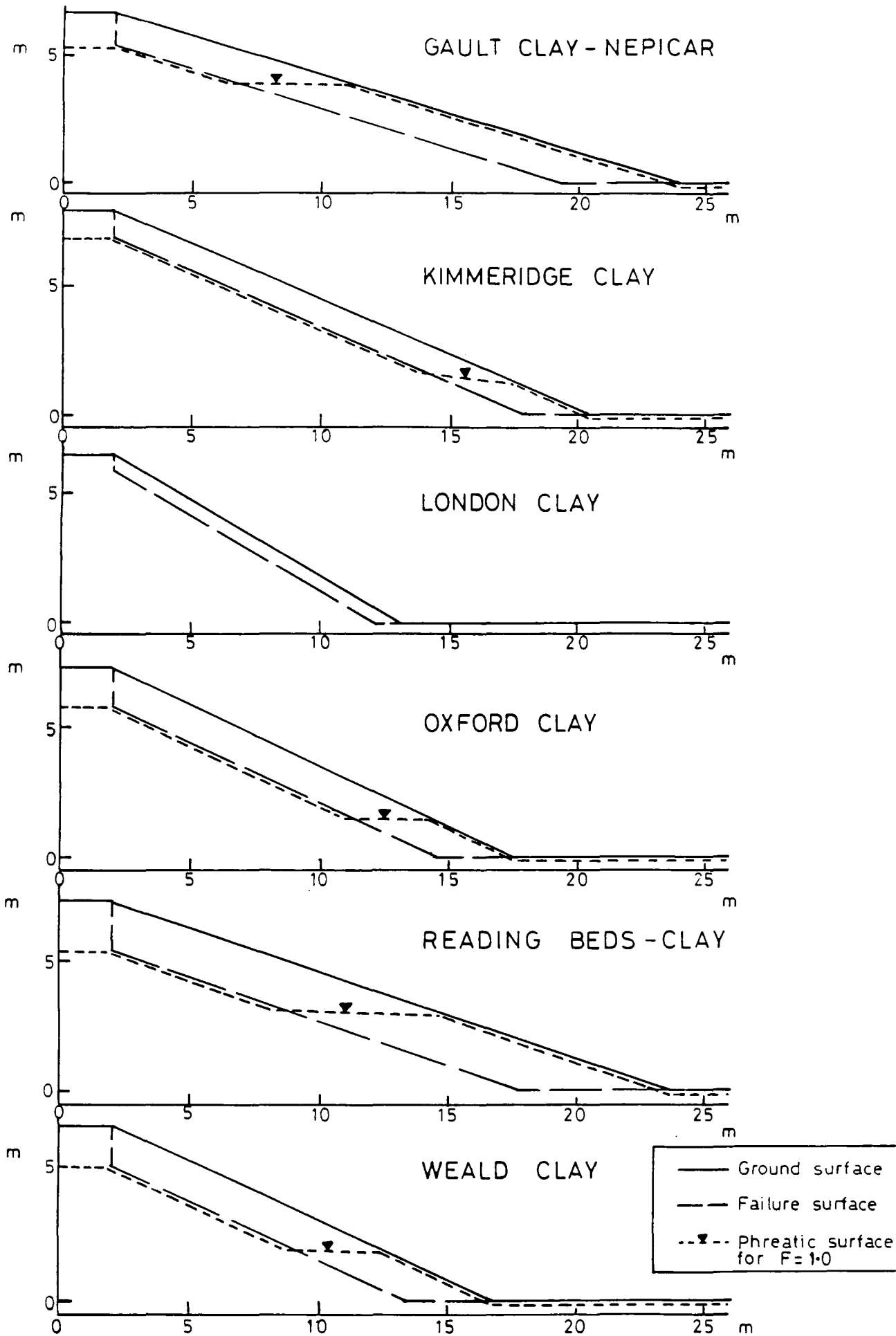
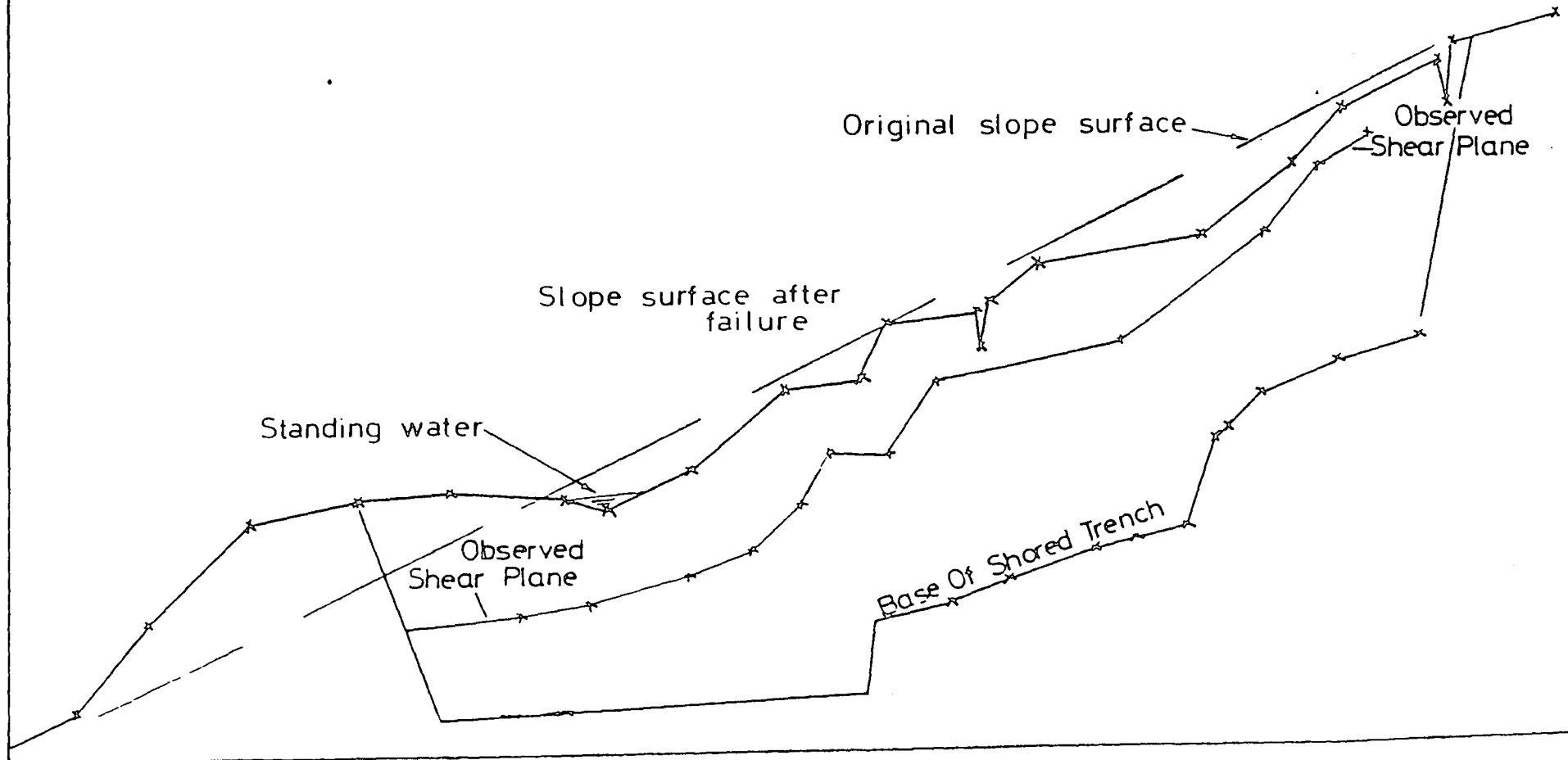


Fig 10/1 The slope and failure surface profiles used in the back-analyses, with the likely positions of the phreatic surface at failure.

Fig10/2 A-45 CAMBRIDGE BY-PASS SLOPE FAILURE INVESTIGATION



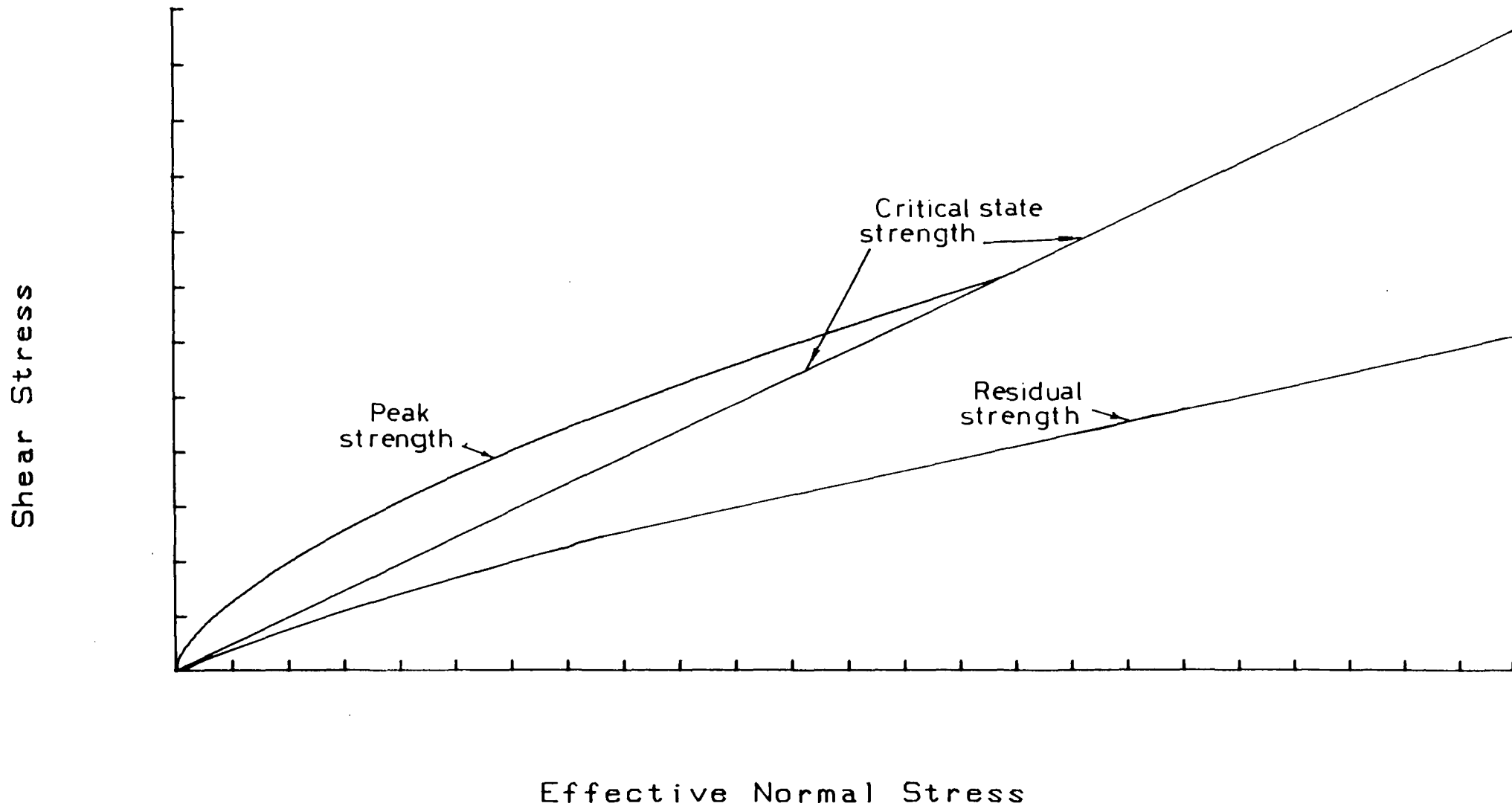


Fig 10/3 The relation between peak strength, critical state strength and residual strength

Chapter 11

Discussion

The survey described in this Thesis covered 1500km of motorway slope, which were selected in order to include a large number of geologies and a variety of geometries, motorway ages and types of drainage. This it has done very successfully, with the exception of some cases of motorway age, and in so doing has generated the largest computer database of its kind in Britain and probably the world. Since the failure of cutting and embankment slopes is a continuing process, the database can be used in the future to study the long-term performance of the motorway earthworks surveyed.

Table 11/1 shows the top six single geologies, in embankments and cuttings, whose slopes have the highest percentages of failure.

For embankments, the Table includes most of the well known over-consolidated clays, illustrating their susceptibility to failure. Most of the failures in Lower Keuper Sandstone are of the topsoil and not of the fill itself as was the case with the other geologies listed. In cuttings well known over-consolidated clays are again included as well as the Enville Beds, which were found on the M5 in Hereford and Worcester. London Clay, a well documented material because of its unstable behaviour, is not one of the six geologies in cuttings with the highest percentages of failure. The percentage of failure in

this material was only 0.3 per cent with a predominant slope angle of 1:3, much less than that for embankments which may reflect the cautious approach adopted for cuttings in this material.

Considering embankment slopes with a combination of two geologies, Glacial Gravel with Middle Lias (Silts and Clays) has the highest percentage of failure of 11.0 per cent. In cuttings, Middle Lias (Silts and Clays) with Lower Lias has the highest percentage of failure of 13.1 per cent. However, none of these geologies individually has a percentage of failure greater than 0.6 per cent. In some cases, therefore, a combination of geologies can have a higher percentage of failure than the individual geologies.

In relation to age, higher percentages of failure were recorded in the more recently constructed embankment slopes of London Clay, Oxford Clay and London Clay with Reading Beds. To explain this, additional detailed studies would be required into the soil properties, specifications, design standards and construction practices for each individual motorway.

The study of the effect of geometry on slope stability has unexpectedly revealed that the steepest slope angle on over-consolidated clay soils is not necessarily associated with the highest percentage of failure. The phenomenon is not yet well understood and long-term studies of embankments on Gault Clay are being undertaken to find an explanation (Crabb and West,

1985 and 1987). Cutting and embankment slopes in over-consolidated clay soils have a high initial strength due to negative pore water pressures (Skempton, 1977; Crabb et al, 1987). The rate at which these pressures change (Vaughan and Walbancke, 1973; Chandler and Skempton, 1974; Chandler, 1984) is, amongst other things, related to slope angle, with the most rapid reductions occurring on flatter slopes which do not shed water as readily as steeper slopes.

On the other hand disturbing forces are greatest on the steepest slopes and failures result from an interaction between this and the reducing shear strength with depth due to pore pressure equilibration. A possible implication is that in the longer term the slopes with steeper angles will reach at least the same percentages of failure as those flatter slope angles currently exhibiting the highest percentages of failure.

Interestingly the CHASE study of the more homogeneous rocks in Hong Kong (Denness, 1982) showed that the number of failures increased with decreasing slope angles, the same behaviour as observed in this survey. In Hong Kong, steeper slopes were more stable for heights greater than 10m; slopes between 50 degrees and 75 degrees became more stable as slope height increased, a phenomenon not observed in the motorway survey. These observations indicate that slope processes are extremely complex, that designing a less steep slope does not necessarily make it more stable, and empirical design has a very useful role to play especially for the more homogeneous slopes of

embankments and cuttings in clays.

Further evidence that infiltration may be causing less steep slopes to fail over greater lengths than steeper slopes, may reasonably be deduced from a study of the depth of failure surface and slope angle. Table 11/2 presents the results of a limited study which includes three of the major problematical geologies used in the construction of earthworks. The depths of failure surface given are weighted means for the particular geometries given. Although not conclusive, there appears to be some evidence that deeper failures tend to occur on less steep slopes. A more extensive study was restricted as many slips had been reinstated and so measurements of depth of failure surface could not be made for a particular combination of geology, age and geometry.

Other factors which may affect stability are the presence of shear surfaces induced by compaction plant (Whyte and Vakalis, 1987; Coxon, 1986) which could have a detrimental effect on stability, and the roots of trees, shrubs and grasses (Barker, 1986) which may have a beneficial effect on stability. The normal variations in soil properties (for example Cripps and Taylor, 1986 and 1987) could possibly account for differences in the behaviour of some geologies. Access of water into slopes can be assisted by the presence of shrinkage cracks initiated in hot, dry spells, the lack of compaction near the outer edges of embankments, if not overfilled and trimmed to a slope, and the opening up of fissures, near the slope surface

of cuttings, due to stress relief. Also, disturbance of the slope by tree planting can assist water infiltration.

When comparing embankments and cuttings with each other, the types of failures (for example slab type failures), the depths of the failure surfaces beneath the slopes and the areas of slopes affected by individual slips, were all found to be similar. So, whatever the different causes of failure may be in each of the earthwork types, the geometry of the resulting slips are very much alike.

The effect on the percentage of failure of the three major types of drainage has been studied at the bottom of embankment slopes and the top of cutting slopes. Drift deposits, or mixtures including Drift deposits, have a lower percentage of failure on slopes with open ditches when compared to slopes with no drainage, but slopes of Solid deposits show the opposite behaviour. These results are difficult to explain but are likely to be related to the different permeabilities of these materials. Drift deposits, which generally have a high permeability, may be effectively drained by open ditches and, consequently, slopes in this material have fewer failures than when no drainage is provided. Solid deposits are usually of low permeability and so open ditches would be as ineffective as no drainage at all. The factors which cause open ditches to have a detrimental effect on stability in Solid deposits could be associated with the lack of restraint at the bottom of embankments or the flow of groundwater on to the slopes of

cuttings where open ditches are located. In Drift deposits, these factors seem to be more than outweighed by the beneficial effects of the drainage.

There is no consistent pattern of behaviour between the percentage of failure of slopes and orientation except for Reading Beds (cohesive) which in both embankments and cuttings had significantly greater percentages of failure on north facing slopes. There are many opposing factors to be taken into consideration when determining the effect of climate on embankment and cutting slopes. For example, the north side of a slope may remain wetter for longer periods but since the south side receives more sunshine the soil can dry out; shrinkage cracks may then develop allowing water to enter deeper into the earthwork when precipitation occurs. This may explain the irregular pattern of failures seen for nearly all the geologies when correlated with orientation; a pattern observed in Hong Kong for slopes included in the CHASE project described earlier. In the case of Reading Beds (cohesive), the north facing slopes appear to be more consistently affected by the wetter micro-climate associated with that orientation.

Figure 11/1 shows the maximum recommended slope angle for the least stable geology, or one of the least stable geologies, in each of the deposits studied. This Figure uses the information on single geologies given in the tables of maximum slope angle for new earthwork construction. The slope angles given restrict the percentage of failure to less than 1 per cent for

all earthworks over 5.0m high. It is clear that the younger Jurassic, Cretaceous and Eocene deposits contain geologies with a high percentage of failure at flatter slope angles. In slope design, slope geometries derived by empirical means, such as presented in this Thesis, are extremely useful as they provide the Designer with a 'bottom line' for stability. If he designs steeper slopes than those found by empirical design and the slope characteristics appear to be the same, then failures should be expected. The cost of repairing such failures might well be minimal compared to the amount of land required to sustain a slope angle of 1:5 for example. However, if he designs an over-consolidated clay slope at 1:2 in areas where land is relatively inexpensive, it is extremely likely that the cost of repairing the large number of failures which are inevitably going to occur will be more than the extra landtake for a slope angle of 1:3. Each design must be considered individually. Consideration should also be given to preventative and reinforcement methods if steeper slopes are required. In heterogeneous materials, such as jointed and weathered rock, empirical design is unlikely to include all the variations in properties that are likely to occur and consequently a large enough sample could never be taken to be representative.

Similar recommended angles to those given in this Thesis are given by Newman (1890) and Gardner (1921) who based their designs on the experience gained during the construction of most of Britain's railway system. It is likely that these

recommendations are based on a number of observations of slope failures. Failures of the sort seen on modern highways might well therefore have occurred in the past on railway earthworks. Although specific geologies are not mentioned by name, embankment slope angles of 1 in 6 and 1 in 3 are quoted by Newman for 'brown laminated clay' and 'damp clay soil' respectively. Gardner recommends slope angles between 1:3 and 1:5 for wet clay slopes.

From casual observation, it appears that railway earthworks are stable at steeper slope angles than are found on highways. If clays or clayey materials were used in embankments with steep angles, it could be that the method of construction only allowed stronger materials to be used. In a similar way to earth embankment dams, lack of compaction and smaller negative pore water pressures as a result of considerable remoulding during construction of embankments may have resulted in only those clays or clayey materials of sufficient strength remaining stable after construction. Because of the smaller negative pore water pressures, failures in the long-term may not have occurred to the same extent as in highways.

Conversely, clays retaining high negative pore water pressures which are initially stable in highway embankments but fail much later could not have been used in railway embankments of similar slope geometry and would form a basis for Newman's and Gardner's recommendations.

In cuttings, the behaviour of slopes on highways and railways

should be similar as the method of construction should have no effect on the slope. It is, therefore, difficult, without conducting a detailed survey, to explain why railway slopes in the same clays as highway slopes appear to be more stable at steeper slope angles.

The general steepness of railway earthwork slopes may be explained by the greater choice of railway alignment when compared to highways. Where there has been a choice between construction in sound material and construction through problematical materials the railways, which were constructed before most major highways, have, naturally, taken the easier option leaving the highway to be constructed in poorer materials at less steep slope angles. The M26 motorway is a good example of this; it had to be constructed through the Gault Clay because the railway and other traffic routes had taken the line through the better materials (Garrett and Wale, 1985). Also most conurbations were constructed on the better materials because of the better foundation conditions and the proximity of the main transport routes.

Other factors which can effect railway earthwork stability include the large amounts of granular ash that have accumulated on slopes during the age of the steam engine and areas of replaced track ballast that have also accumulated on slopes as a result of maintenance procedures. The loading and draining effect of these materials at the toe of cutting slopes could have a long-term stabilizing effect on those materials beneath

which are susceptible to pore water pressure increases. Where placed down the whole slope of embankments, the granular ash provides a drainage medium but if irregularly placed with more material at the crest, the slope may become overloaded and result in failure.

Rea (1956) recommends slope angles of 1:3.5 for 'wet clay' cutting slopes while Harger and Bonney (1927) recommend a much steeper slope angle of 1:2 for highway cutting slopes. However, Harger and Bonney suggest a slope angle of 1:4 would be more suitable for highway embankments.

Horner (1981) suggests angles up to 1 in 6 for cuttings in clay and 1 in 2.5 for clay embankments based on his experience of earthworks. The survey suggests that embankment slopes should be less steep than those given by Horner.

Having observed the problems in the survey, studies were conducted into the failure mechanism, not only to explain how failures were occurring but also to provide a tool for designing slopes in unusual situations not encountered in the survey and for designing preventative and reinforcing methods.

From the testing of undisturbed samples at low effective stresses it is observed that the peak strength failure envelope is markedly curved. This curvature is usually not critical at higher and limited ranges of effective stress but becomes important not only for shallow failures but for conditions

covering a large stress range (Bishop, Webb and Lewis, 1965).

There is a good case for using the least sum of squares method for fitting a curved failure envelope to a set of test data, from a statistical and from an accuracy point of view, and there is little doubt it is the most appropriate. This method is not only suitable for low effective stress soil mechanics but can be used for fitting a power curve to triaxial results from samples of rockfill and jointed rocks. Areas requiring care with the method encompass the correct choice of starting values for A and b in the iteration procedures of the computer program so that the correct values are converged on.

Additional Mohr circles will be required than are usually in practice in order to cover a wider range of stresses, as the best fit line is influenced by values from zero to the stress level being considered. For these reasons the method is recommended for studies of soils at low effective stresses, and for rocks where a curved failure envelope is appropriate and tests have been conducted over a wide range of stresses.

Rather than use the parameters A and b from a power curve relation at low effective stresses, a straight line may be drawn at the particular stress level being considered which is tangential to this curve. This has the advantage of allowing c' and ϕ' to be found and conventional analysis to be conducted. It does, however, have the disadvantage that any changes in pore water pressure can not be easily accommodated as new values of c' and ϕ' have to be calculated.

An alternative method which allows c' and ϕ' to be calculated is to draw a tangent to two Mohr circles at the stress level being considered without calculating the non-linear relation. In addition to the disadvantage above, this method is strongly influenced by any experimental errors; the power curve includes all the Mohr circles and hence is more representative of the material properties.

It is clear from the results of the back-analysis that peak shear strengths are not representative of the conditions that were prevailing at the time of failure of these shallow failures. The likely mechanism for failure for most of the slopes studied involves an average shear strength equivalent to the critical state strength at the failure surface, mobilized as a result of significant strains within the slope but not as high as those required for the residual strength condition (Atkinson and Bransby, 1978), with positive pore water pressures only at the lower part of the slope. For design purposes, therefore, it is necessary to deduce the critical state friction angle of a material. Rather than reconstitute the sample, high stress testing can be carried out and the friction angle of the peak strengths taken as the critical state friction angle (Skempton, 1970; Coxon, 1986). Table 11/3 compares critical state friction angles calculated from the tests by City University on reconstituted samples, with friction angles from tests, conducted by a commercial testing laboratory for TRRL, on the same material type and from the

same location as the reconstituted samples but using conventional high stress triaxial testing on undisturbed samples. The maximum difference is four degrees, well within the experimental errors of the two types of test and inconsistencies between samples.

In the back-analysis of embankment failures, the Gault Clay embankment required the most slope surface to be effected by a phreatic surface. The critical state strength is not particularly high compared to the other geologies, but the slope angle is the flattest of all six geologies. The extent of high pore water pressures may well be appropriate for flatter slopes as water infiltration could be higher as evidenced by the studies of the effect of geometry on instability in the survey.

The London Clay slope is too weak at the critical state strength even with zero pore water pressures and has the highest factor of safety for peak strength and a phreatic surface at the surface of the whole slope. It would appear therefore that London Clay exhibits an average shear strength between peak and critical, probably reflecting progressive failure within the slope.

TABLE 11/1

Geologies with a high percentage of failure

	Geology	Percentage of failure	Predominant slope angle
Embankments	Gault Clay	8.2	1:2.5
	Reading Beds	7.6	1:2
	Kimmeridge Clay	6.1	1:2
	Oxford Clay	5.7	1:2
	Lower Keuper		
	Sandstone	4.9	1:1.5
	London Clay	4.4	1:2
Cuttings	Gault Clay	9.6	1:2.5
	Enville Beds	5.8	1:2.5
	Oxford Clay	3.2	1:2
	Reading Beds	2.9	1:3
	Bunter Pebble Beds	2.3	1:2
	Lower Old Red Sandstone-		
	St Maughan's Group	1.7	1:2

TABLE 11/2
Comparison of depth of failure surface in embankments of different
ages and geometries

Geology	Age (years)	Height (m)	Slope angle (v:h)	Depth of failure (m)
		2.5-5.0	1:2.5	1.7
			1:2	1.0
			1:1.75	0.5
Reading Beds	10	5.0-7.5	1:2.5	2.5
			1:2	1.7
			1:1.75	0.5
		7.5-10.0	1:2	0.8
			1:1.75	0.3
Kimmeridge Clay	10	2.5-5.0	1:2.5	1.0
			1:2	1.1
			1:1.75	1.3
		5.0-7.5	1:2	0.7
			1:1.75	1.3
		0-2.5	1:2	0.5
			1:1.75	0.4
	10	2.5-5.0	1:2	0.6
			1:1.75	0.6
		5.0-7.5	1:2.5	1.0
			1:2	0.7
			1:1.75	0.5
Oxford Clay		0-2.5	1:2.5	1.5
			1:2	0.6
			1:1.75	0.3
	22	2.5-5.0	1:2.5	1.5
			1:2	1.1
			1:1.75	1.0
		5.0-7.5	1:2.5	1.4
			1:2	1.0
			1:1.75	1.2

TABLE 11/3

Comparison of critical state strength friction angles and friction angles from triaxial tests at high stress levels on undisturbed samples

	Gault Clay-Nepicar	Kimmeridge Clay	London Clay	Oxford Clay	Reading Beds-Clay	Weald Clay
ϕ'_c	23	23	25	25	19	24
ϕ'	25	19	21	23	19	21

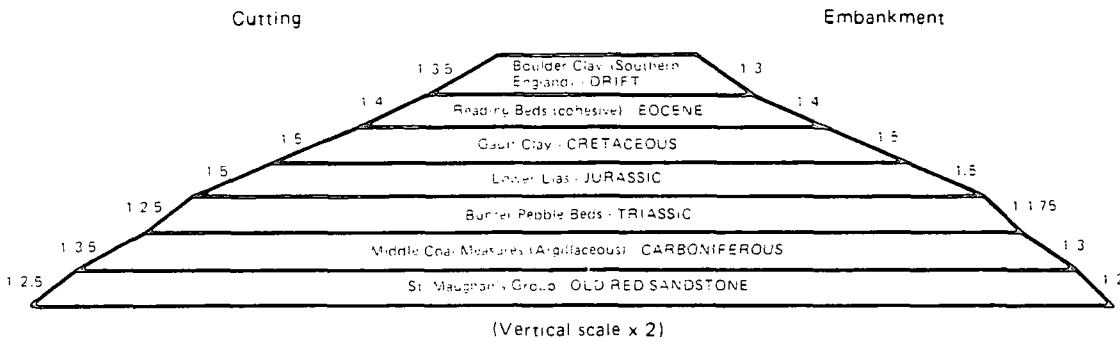


Fig.11/1 Maximum recommended slope angles for less than 1 per cent failure on slopes greater than 5.0m high

Chapter 12

Conclusion

Shallow slope failures are a significant problem on motorway earthworks. Of the 570km of motorway surveyed, over 17km of embankment slope and over 5.5km of cutting slope have failed with the failure surface rarely exceeding 1.5m in depth. The types of failures, depths to the failure surfaces and areas of slopes affected by individual slips, were similar in both embankments and cuttings. The method of repair of shallow slips involved replacement of the failed soil with a free draining material.

A study of the survey data confirmed that the principal factors having an influence on the extent of failures were geology, age of earthworks and geometry of slope.

The greatest incidence of failure occurred in high plasticity over-consolidated clays. In some of these materials the percentage of failure unexpectedly decreased with increasing slope angle. The majority of geologies, however, show an increase in the percentage of failure with increasing slope angle. Also, for most of the geologies studied, the percentage of failure increases as the height of slope increases.

For some geologies in embankments, higher percentages of failure were recorded in the more recently constructed slopes. Cutting slope failures occurred at a number of ages but

generally the older earthworks showed higher percentages of failure.

Fifty per cent or more of embankment slopes have failed for a number of geologies with particular combinations of slope angle, height and age. In cuttings there are a much smaller number of geologies that have percentages of failure greater than 25 per cent for particular geometries and age.

In Solid deposits, embankments with an open ditch at the bottom of the slope usually have a higher percentage of failure than similar slopes with no drainage at all. The same effect can be seen with these types of drainage at the top of cutting slopes. In Drift deposits, however, the opposite occurs for slopes under similar conditions. Slope drains increased the stability of slopes in materials susceptible to shallow failures. The survey shows that the orientation of the slopes studied was not a cause of failure for most geologies.

General guidance on the design of new earthwork side slopes can be gained from the results of the survey and the identification of areas at risk of failure in the longer term will be aided by reference to the maximum recommended slope angles given in this Report.

A conservative estimate of failures in the future suggests that three times as many slopes are likely to fail than have failed so far if no preventative measures are taken.

The construction, specifications and design methods used on the motorways studied have been successful at reducing shallow slope failures for many of the older deposits and for some of the more recent deposits.

There is no point in using sophisticated statistical methods to fit linear failure envelopes to Mohr circle data, unless a degree of confidence is required in the data, as conventional 'Top Point Construction' gives the same answer.

The peak strength failure envelope is markedly curved at low effective stresses and a useful method has been developed for fitting a power curve shaped failure envelope to laboratory triaxial data.

The shear strength parameters for a curved failure envelope can be used in a specially developed slope stability analysis for failure surfaces of arbitrary shape. This analytical method overcomes the need to approximate or restrict the study of slope failures to linear shear strength parameters, allowing the design and back-analysis of soil slopes at low effective stresses. As well as considerable potential in soil mechanics, the method could also be applied to jointed rock, weathered rock and rock fill.

For most of the slopes studied, the mechanism involved in the formation of shallow failures entails a reduction in average

shear strength from peak to critical state, at which time progressive failure occurs in association with the development of positive pore water pressures only in the lower part of the slope.

Theoretically, Gault Clay requires a high proportion of the slope surface to be effected by a phreatic surface before progressive failure occurs at the critical state strength. This may be occurring, as flatter slopes may be subject to higher pore water pressures. London Clay exhibits an overall average shear strength between peak and critical state.

This Thesis presents the early stages of a continuing process.

Areas for further study include the following:

(a) the computer database is a very useful source of information for the future. If the surveyed motorway lengths are studied again in say ten years time, either on the ground or from the air, an accurate assessment can be made of the increase in failures and the rate at which this is occurring. Together with the historical survey using aerial photographs by Andrews (1990), there is an extensive and exhaustive amount of information which should be an investment for the future.

(b) further research is needed into pore water pressure variations in slopes of the same material but of different slope angles. This would help to explain the variations in failures with slope steepness.

(c) since high negative pore water pressures have been

recorded in highway embankments (Crabb et al, 1987) there is the possibility that deep-seated failures as well as shallow failures may occur in the future based on the evidence of old cuttings (Skempton, 1977). Consequently, pore water pressures should continue to be monitored to study the rate at which these pressures increase or, perhaps equilibrate, in the core of embankments.

(d) vegetation may or may not have a stabilizing effect on shallow failures (Coppin and Richards, 1990); trials need to be conducted with various likely stabilizing arrangements of vegetation of varying species. Account must be taken not only of the slope's stability but of the maintenance costs, accessibility and resources required to keep the plants healthy.

(e) a survey, of the type described in this Thesis, of railway cuttings would provide valuable information on the extent of future failures on the slopes of highway cuttings.

(f) the computer program developed in this Thesis is shown to be useful in analysing the stability of earthwork slopes. It could, however, be made more sophisticated by incorporating existing data handling and graphics programs.

REFERENCES

- ANDERSON M G, HUBBARD M G and KNEALE P E (1982). The influence of shrinkage cracks on pore-water pressures within a clay embankment. Quart. Journal Eng. Geol., 15 pp 9-14.
- ANDERSON M G and KNEALE P E (1980a). Pore water pressure and stability conditions on a motorway embankment. Earth surface processes, 5 pp 37-46.
- ANDERSON M G and KNEALE P E (1980b). Pore water pressure changes in a road embankment. The Highway Engineer, May 1980 pp 11-17
- ANDERSON M G and RICHARDS K S (1987). Slope Stability. Wiley and Sons.
- ANDREWS R D (1990). Determining the age of failure of motorway earthworks from aerial survey photographs. Department of Transport, TRRL Report RR257. Transport and Road Research Laboratory, Crowthorne.
- ATKINSON J H and BRANSBY P L (1978). The mechanics of soils: an introduction to critical state soil mechanics. University Series in Civil Engineering. McGraw-Hill, London.
- ATKINSON J H, EVANS J S and SCOTT C R (1985). Developments in stress path testing equipment for measurement of soil parameters. Ground Engineering, 18 pp 15-22.
- ATKINSON J H and FARRAR D M (1985). Stress path tests to measure soil strength parameters for shallow landslips. Proceedings of the eleventh international conference on soil mechanics and foundation engineering, San Francisco, Vol 2 pp 983-986.
- AYRES D J (1985). Stabilization of slips in cohesive soil by grouting. Proceedings of the international symposium on failures in earthworks, London, Thomas Telford. pp 424-427.
- BALMER G (1952). A general analytical solution for Mohr's envelope. Journal of the American Society for Testing and Materials, 52 pp 1260-1271.
- BAJPAI A C (1977). Advanced engineering mathematics. Wiley.
- BARKER D H (1986). Enhancement of slope stability by vegetation. Ground Engineering, April 1986 pp 11-15.
- BELL J M (1968). General slope stability analysis. Journal of Soil Mechanics and Foundations Division, ASCE, 94 pp 1253-1270.
- BISHOP A W (1952). The stability of earth dams. PhD Thesis, University of London.

- BISHOP A W (1955). The use of the slip circle in the stability analysis of slopes. Geotechnique, 5 (1) pp 7-17.
- BISHOP A W (1967). Progressive failure - with special reference to the mechanism causing it. Panel discussion. Proceedings of the geotechnical conference, Oslo, Vol 2 pp 142-150.
- BISHOP A W and MORGENSTERN N R (1960). Stability coefficients of earth slopes. Geotechnique, 10 pp 129-150.
- BISHOP A W, WEBB D L and LEWIN P I (1965). Undisturbed samples of London Clay from the Ashford Common shaft: strength-effective stress relationships. Geotechnique, 15 pp 1-30
- BISHOP A W and WESLEY L D (1975). A hydraulic triaxial apparatus for controlled stress path testing. Geotechnique, 25 pp 657-670.
- BLACKLOCK J R and WRIGHT P J (1986). Injection stabilization of failed highway embankments. Transportation Research Record 1104, Transportation Research Board, National Research Council, pp 7-18.
- BLAND J A (1980). Numerical determination of the Mohr envelope and confidence analysis. Proc. Inst. Civ. Engrs., 69 (2) pp 1029-1033
- BLAND J A (1981). Confidence in the failure envelope. Proc. Inst. Civ. Engrs., 71 (2) pp 537-541
- BLAND J A (1983). Discussion on 'Least-squares fitting of the linear Mohr envelope' by Strom and Lisle. Quart. Journal Eng. Geol., 16 pp 85
- BRADBEER B F J (1953). Discussion on : Soil stability problems in road engineering. Proc. Inst. Civ. Engrs., (2) pp 254-256.
- BRAND E W and HUDSON R (1982). CHASE-An empirical approach to the design of cut slopes in Hong Kong soils. Proceedings of the seventh Southeast Asia geotechnical conference, Hong Kong, Vol 1 pp 1-16.
- BROMHEAD E N (1986). The stability of slopes. Surrey University Press. Chapman and Hall, New York.
- CHANDLER R J (1977). Back analysis techniques for slope stabilization works: a case history. Geotechnique, 27 (4) pp 479-495.

CHANDLER R J (1984). Recent European experience of landslides in over-consolidated clays and soft rocks. Proceedings of the fourth international symposium on landslides, Toronto, Vol 1 pp 61-81.

CHANDLER R J and SKEMPTON A W (1974). The design of permanent cutting slopes in stiff fissured clays. Geotechnique, 24 (4) pp 457-466.

CHARLES J A and BODEN J B (1985). The failure of embankment dams in the United Kingdom. Proceedings of the international symposium on failures in earthworks, London, Thomas Telford. pp 181-202.

CHARLES J A and SOARES M (1984a). The stability of slopes in soils with nonlinear failure envelopes. Canadian Geotechnical Journal, 21 pp 397-406.

CHARLES J A and SOARES M (1984b). Stability of compacted rockfill slopes. Geotechnique, 34 (1) pp 61-70.

CHOWDHURY R N and GRIVAS D (1982). Probabilistic model of progressive failure of slopes. Journal Geotech. Eng. Div., 108 (GT6) pp 803-819.

CHOWDHURY R N, TANG W H and SID I (1987). Reliability model of progressive slope failure. Geotechnique, 37 (4) pp 467-481.

COLLINS I F, GUNN C I M and PENDER M J (1986). Slope stability analyses for materials with a nonlinear failure envelope. Report No 404, Department of Theoretical and Applied Mechanics, University of Auckland.

COLLINS I F, GUNN C I M, PENDER M J and WANG YAN (1988). Slope stability analyses for materials with a nonlinear failure envelope. Int. Journal for Numerical and Analytical Methods in Geomechanics, 12 pp 533-550.

COPPIN N J and RICHARDS I G (1990). Use of vegetation in civil engineering. CIRIA. Butterworths.

COXON R E (1986). Failure of Carsington embankment. Department of Environment, HMSO.

CRABB G I and WEST G (1985). Monitoring pore water pressures in an embankment slope. Proceedings of the international symposium on failures in earthworks, London, Thomas Telford. pp 406-410.

CRABB G I, WEST G and O'REILLY M P (1987). Groundwater conditions in three highway embankment slopes. Proceedings of the ninth European conference on soil mechanics and foundation engineering, Dublin. Rotterdam/Brookfield: A Balkema. pp 401-406.

CRIPPS J C and TAYLOR R K (1986). Engineering characteristics of British over-consolidated clays and mudrocks. I. Tertiary deposits. Engineering Geology, 22 pp 349-376.

CRIPPS J C and TAYLOR R K (1987). Engineering characteristics of British over-consolidated clays and mudrocks, II. Mesozoic deposits. Engineering Geology, 23 pp 213-253.

DAY R W and AXTEN G W (1989). Surficial stability of compacted clay slopes. Journal of Geotechnical Engineering, ASCE, 115 (4) pp 577-580.

DE MELLO V F B (1977). Reflections on design decisions of practical significance to embankment dams. Geotechnique, 27 (3) pp 279-355.

DENNESS B (1982). Discussion on: CHASE-An empirical approach to the design of cut slopes in Hong Kong soils. Proceedings of the seventh Southeast Asia geotechnical conference, Hong Kong, Vol 1 pp 69-70.

DEPARTMENT OF TRANSPORT (1981). Road layout and geometry: highway link design. Department Standard TD 9/81. Department of Transport, London.

DEPARTMENT OF TRANSPORT (1988). Transport statistics, Great Britain, 1977-1987. London: HMSO.

DRAPER N and SMITH H (1981). Applied regression analysis. Second Edition, Wiley & Sons, New York.

DUNCAN J M and WRIGHT S G (1980). The accuracy of equilibrium methods of slope stability analysis. Proceedings of the third international symposium on landslides, New Delhi.

EFRON B and GONG G (1983). A leisurely look at the bootstrap, the jackknife, and cross-validation. The American Statistician, 37 (1) pp 36-42

FELLENIOUS W (1918). Kaj-och jordrasen i Goteborg. Teknisk Tidsskrift V U, 48 pp 17-19.

FELLENIOUS W (1927). Erdstatische Berechnungen mit Reibung and Kohesion, Ernst, Berlin.

FELLENIOUS W (1936). Calculation of stability of earth dams, Transactions of the second congress on large dams, Vol 4 pp 445.

FRANCIS S C (1987). Slope development through the threshold slope concept. In: Slope Stability. Ed. M G Anderson and K S Richards, Wiley and Sons, New York. pp 601-624.

FREDLUND D G and KRAHN J (1977). Comparison of slope stability methods of analysis. Canadian Geotechnical Journal, 14 pp 429-439.

GARDNER J W F (1921). Earthwork in railway engineering. Glasgow Text Books, London.

GARRETT C and WALE J H (1985). Performance of embankments and cuttings in Gault Clay in Kent. Proceedings of the international symposium on failures in earthworks, London, Thomas Telford. pp 93-111.

GIBSON R E and MORGENSTERN N R (1962). A note on the stability of cuttings in normally consolidated clays. Geotechnique, 12 (3) pp 212-216.

GLOSSOP R and WILSON G C (1953). Soil stability problems in road engineering. Proc. Inst. Civ. Engrs. (2) pp 219-253.

GREENWOOD J R (1983). A simple approach to slope stability. Ground Engineering, 16 (4) pp 45-48.

GREENWOOD J R, HOLT D A and HERRICK G W (1985). Shallow slips in highway embankments constructed of overconsolidated clay. Proceedings of the international symposium on failures in earthworks, London, Thomas Telford. pp 79-92.

HAEFELI R (1948). The stability of slopes acted upon by parallel seepage. Proceedings of the second international conference on soil mechanics and foundation engineering, Rotterdam, Vol 1 pp 57-62.

HARGER W G and BONNEY E A (1927). Highway engineers handbook. Fourth edition. McGraw-Hill, New York.

HAWKINS A B and PRIVETT K D (1985). Measurement and use of residual shear strength of cohesive soils. Ground Engineering, 18 (8) pp 22-29.

HILL R (1950). The mathematical theory of plasticity. Clarendon Press, Oxford.

HOEK E (1983). Strength of jointed rock masses. Geotechnique, 33 pp 187-223.

HOEK E and BRAY J W (1981). Rock slope engineering. 3rd Edition. Institution of Mining and Metallurgy.

HOEK E and BROWN E T (1980). Empirical strength criterion for rock masses. Journal Geotech. Eng. Div., ASCE, 106 (GT9) pp 1013-1035.

HORNER P C (1981). Earthworks. ICE Works Construction Guides. Thomas Telford Ltd, London.

- HORNER P C (1985). Discussion in: Proceedings of the international symposium on failures in earthworks, London, Thomas Telford. pp 123-124.
- HUNGR O (1987). An extension of Bishop's simplified method of slope analysis to three dimensions. Geotechnique, 37 (1) pp 113-117.
- HUNTER J H and SCHUSTER R L (1968). Stability of simple cuttings in normally consolidated clays. Geotechnique, 18 pp 372-378.
- JANBU N (1954a). Application of composite slip surfaces for stability analysis. European conference on stability of earth slopes, Stockholm, Discussion, Vol 3 pp 43-49.
- JANBU N (1954b). Stability analysis of slopes with dimensionless parameters. Harvard Soil Mechanics Series, No 46 pp 811.
- JANBU N (1957). Earth pressure and bearing capacity calculations by generalized procedure of slices. Proceedings of the fourth international conference on soil mechanics and foundation engineering, London, Vol 2 pp 207-212.
- JANBU N (1973). Soil stability computations. Embankment dam engineering, Casagrande volume. Ed. by R C Hirshfeld and S J Poulos, Wiley, New York. pp 47-87.
- JANBU N, BJERRUM L and KJAERNSLI B (1956). Veiledning ved Iosning av fundamenterings oppgaver (in Norwegian with English summary: Soil mechanics applied to some engineering problems). Norwegian Geotechnical Institute. Publ. No 16.
- JOHNSON P E (1985). Maintenance and repair of highway embankments: studies of seven methods of treatment. Department of Transport, TRRL Report RR30. Transport and Road Research Laboratory, Crowthorne.
- KENNEY T C (1956). An examination of the methods of calculating the stability of slopes. MSc Thesis, Imperial College.
- KERMACK K A and HALDENE J B S (1950). Organic correlation and allometry. Biometrika, 37, pp 30-41.
- KINGSTON M R and SPENCER A J M (1970). General yield conditions in plane deformations of granular media. Journal of the Mechanical Physics of Solids, 18 pp 233-243.
- KOBASHI S (1971). Erosion and surface stratum failure of steep slopes and their prevention methods. Proceedings of the fourth Asian regional conference on soil mechanics and foundation engineering, Bangkok, Vol 1.

- KOTTER F (1903). Die Bestimmung des Druckes an gekrummter Gleitflächen eine Aufgabe aus der Lehre vom Erddruck. Ber. Akad. Wiss., Berlin, pp 229-233.
- KRAHN J, FREDLUND D G and KLASSEN M J (1989). Effect of soil suction on slope stability at Notch Hill. Canadian Geotechnical Journal, 26 pp 269-278.
- LAGUROS J G, KUMAR S and MEDHANI R (1982). Failure of slopes in weathered overconsolidated clay. Transportation Research Record 873, Transportation Research Board, National Research Council, pp 12-14.
- LEONARDS G A (1979). Stability of slopes in soft clays. Proceedings of the sixth pan-American conference on soil mechanics and foundation engineering, Lima, Vol 1 pp 225-274.
- LEROUEIL S and TAVENAS F (1981). Pitfalls of back-analysis. Proceedings of the tenth international conference on soil mechanics and foundation engineering, Stockholm, Vol 1 pp 185-190.
- LI K S and LUMB P (1987). Probabilistic design of slopes. Canadian Geotechnical Journal, 24 pp 520-535.
- LISLE R J and STROM C S (1982). Least-squares fitting of the linear Mohr envelope. Quart. Journal Eng. Geol., 15 pp 55-56
- LUPINI J F, SKINNER A E and VAUGHAN P R (1981). The drained residual strength of soils. Geotechnique, 31 (2) pp 181-213.
- MCGUFFEY V, GRIVAS D, IORI J and KYFOR Z (1982). Conventional and probabilistic embankment design. Journal Geotech. Eng. Div., ASCE, 108 (GT10) pp 1246-1254.
- MICHALOWSKI R L (1989). Three-dimensional analysis of locally loaded slopes. Geotechnique, 39 (1) pp 27-38.
- MISSOURI HIGHWAY AND TRANSPORTATION DEPARTMENT (1984). Evaluation of the effectiveness of various vegetation covers in controlling slope distress. Missouri cooperative highway research program, Study no. 81-1, Final report.
- MORGENSTERN N R (1963). Stability charts for earth slopes during rapid drawdown. Geotechnique, 13 (2) pp 121-131.
- MORGENSTERN N R and PRICE V E (1965). The analysis of the stability of general slip surfaces. Geotechnique, 15 (1) pp 79-93.
- MURRAY R T, WRIGHTMAN J and BURT A (1982). Use of fabric reinforcement for reinstating unstable slopes. Department of Transport, TRRL Report SR751. Transport and Road Research Laboratory, Crowthorne.

NEWMAN J (1890). Earthwork slips and subsidences upon public works. E & F N Spon, New York.

NONVEILLER E (1965). The stability analysis of slopes with a slip surface of general shape. Proceedings of the sixth international conference on soil mechanics and foundation engineering, Montreal, Vol 2 pp 522-525.

NOWATZKI E A and KARAFIATH L (1974). General yield conditions in a plasticity analysis of soil-wheel interaction. Journal of Terramechanics, 11 (1) pp 29-44.

PARSONS A W and BROAD B A (1970). A study of the feasibility of using belt conveyors for earthmoving in road construction. Ministry of Transport, TRRL Report LR336. Transport and Road Research Laboratory, Crowthorne.

PARSONS A W and PERRY J (1985). Slope stability problems in ageing highway earthworks. Proceedings of the international symposium on failures in earthworks, London, Thomas Telford. pp 63-78.

PEARSON K (1901). On lines and planes of closest fit to systems of points in space. Philosophical Magazine, 2 (6) pp 559-572.

PERRY J (1985). Incidence of highway slope stability problems in Lower Lias and Weald Clay. Proceedings of the international symposium on failures in earthworks, London, Thomas Telford. pp 439-441.

PERRY J (1989). A survey of slope condition on motorway earthworks in England and Wales. Department of Transport, TRRL Report RR199. Transport and Road Research Laboratory, Crowthorne.

REA J T (1956). How to estimate. Twelfth edition. B T Batsford, London.

ROSENBAUM M S and JARVIS J (1985). Probabilistic slope stability analysis using a microcomputer. Quart. Journal Eng. Geol., 18 pp 353-356.

SARMA S K (1973). Stability analysis of embankments and slopes. Geotechnique, 23 (2) pp 423-433.

SCHOFIELD A N and WROTH C P (1968). Critical state soil mechanics. McGraw-Hill, London.

SKEMPTON A W (1953). Discussion on: Soil stability problems in road engineering. Proc. Inst. Civ. Engrs., (2) pp 265-268.

SKEMPTON A W (1964). Long term stability of clay slopes. Geotechnique, 14 pp 77-101.

- SKEMPTON A W (1970). First-time slides in overconsolidated clay. Geotechnique, 20 pp 320-324.
- SKEMPTON A W (1977). Slope stability of cuttings in brown London Clay. Proceedings of the ninth international conference on soil mechanics and foundation engineering, Tokyo, Vol 3 pp 261-270.
- SKEMPTON A W and HUTCHINSON J N (1969). Stability of natural slopes and embankment foundations. Proceedings of the seventh international conference on soil mechanics and foundation engineering, Mexico City, State of the Art Volume, pp 291-340.
- SOKOLOVSKIIS V (1965). Statics of granular media. Pergamon Press, Oxford.
- SOTIR R B and GRAY D H (1989). Fill slope repair using soil bioengineering systems. Proceedings of the twentieth international conference on erosion control, Vancouver, pp 415-425.
- SPENCER E (1967). A method of analysis for stability of embankments using parallel inter-slice forces. Geotechnique, 17 (1) pp 11-26.
- SPENCER E (1973). The thrust line criterion in embankment stability analysis. Geotechnique, 23 (1) pp 85-101.
- STAUFFER P A and WRIGHT S G (1984). An examination of earth slope failures in Texas. Center for transportation research, Project 3-8-83-353, Research Report 353-3F, University of Texas.
- SUZUKI H and MATSUO M (1988). Procedure of slope failure prediction during rainfall based on the back analysis of actual case records. Soils and Foundations, 28 (3) pp 51-63.
- SYMONS I F (1970). The magnitude and cost of minor instability in the side slopes of earthworks on major roads. Department of Transport, TRRL Report LR331. Transport and Road Research Laboratory, Crowthorne.
- SZYMANSKI C (1958). Some plane problems of the theory of limiting equilibrium of loose and cohesive, non-homogeneous isotropic media in the case of a non-linear limit curve. In: Non-homogeneity in elasticity and plasticity. Ed. by W Olszak, Pergamon Press, London. pp 241-250.
- TAVENAS F and LEROUEIL S (1981). Creep and delayed failure of slopes in clays. Canadian Geotechnical Journal, 18 pp 106-120.
- TAYLOR D W (1937). Stability of earth slopes. Journal of the Boston Society of Civil Engineers, 24 pp 197-246.

- TAYLOR D W (1948). Fundamentals of Soil Mechanics, Wiley, New York.
- TAYLOR R K (1984). Composition and engineering properties of British colliery discards, National Coal Board, London.
- TEMPLETON A E, SILLS G L and COOLEY L A (1984). Long term failure in compacted clay slopes. Proceedings of the international conference on case histories in geotechnical engineering, pp 749-754.
- VAUGHAN P R and WALBANCKE H J (1973). Pore Pressure changes and the delayed failure of cutting slopes in over-consolidated clay. Geotechnique, 23 (4) pp 531-539.
- VICKERS B (1983). Laboratory work in soil mechanics. Second Edition. Granada, London.
- WEST G (1987). Shape of the failure envelope for a jointed rock specimen. Quart. Journal Eng. Geol., 20 pp 183-185.
- WHYTE I L and VAKALIS I G (1987). Shear surfaces induced in clay fills by compaction plant. Proceedings of the conference on compaction technology, London, Thomas Telford. pp 125-137.
- WIDGER R A and FREDLUND D G (1979). Stability of swelling clay embankments. Canadian Geotechnical Journal, 16 pp 140-151.
- YORK D (1966). Least-squares fitting of a straight line. Canadian Journal of Physics, 44 pp 1079-1086.
- ZHANG X J (1988). Three-dimensional stability analysis of concave slopes in plan view. Journal of Geotechnical Engineering, 114 (6) pp 658-671.
- ZHANG X J and CHEN W F (1987). Stability analysis of slopes with general nonlinear failure criterion. Int. Journal for Numerical and Analytical Methods in Geomechanics, 11 pp 33-50.

Appendix A

Glossary of terms

Slope angle is the angle of a slope expressed either as the gradient of the slope, in terms of the vertical to horizontal distance (eg 1:3), or in degrees to the horizontal.

The percentage of failure is the length of failed slope (parallel to the centre line of the road) expressed as a percentage of the total length of slope involved; only repaired and unrepaired slips were considered as failures.

Age is the time between a motorway being opened to traffic and the survey.

Drift and Solid deposits are here defined as they would appear on a geological survey map, ie Drift is all superficial deposits including glacial, fluvio-glacial and alluvial, and Solid is all non-superficial deposits.

Features are lengths of slope where there is no change of any of its characteristics. Where a change occurs a new feature begins and so the motorway is divided into sections for storage as a computer database and subsequent analysis.

Earthworks are embankments and cuttings used in the construction of roads, railways, waterways etc..

Appendix B
Details of motorways surveyed

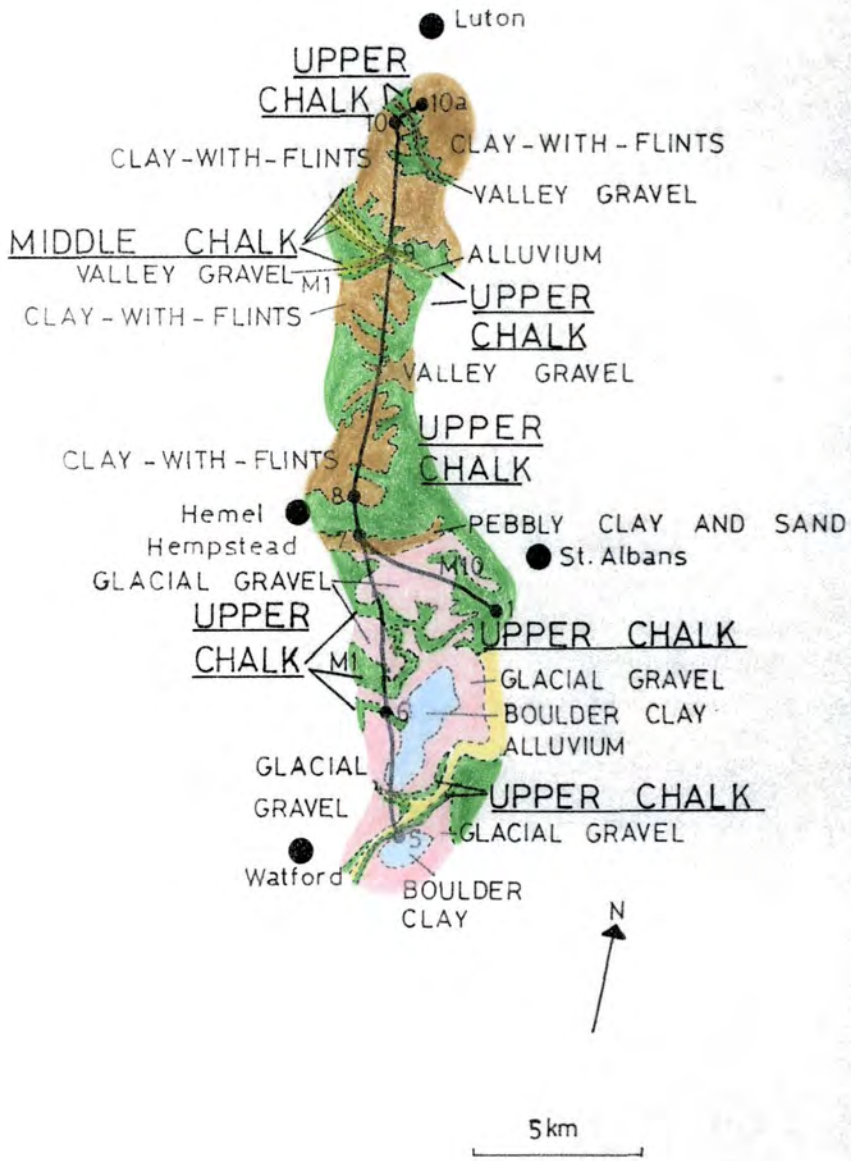
TABLE B1
Motorways surveyed

Motorway	County	Section	Chainage	Length (km)	Date of opening	Age when surveyed (years)	
M1	Hertfordshire	J5 (Berrygrove)	27.7		66/67	14.0	
		J5-J7 - St Albans By-Pass	27.7-36.5	8.8	Jan 60	22.0	
		2-section being widened during 84/86					
		J7 and M10 to J10 and Luton Spur - St Albans By-Pass 1	36.5-49.6	13.1	Nov 59	22.0	
				21.9			
M1	Bedfordshire	J10-J13 (Luton to Ridgmont)	49.6-73.2	23.6	Nov'59	22.0	
				23.6			
M1	Buckinghamshire	J13-ch.94.0 (Ridgmont to maintenance limit)	73.2-94.0	20.8	Nov'59	22.0	
				20.8			
M1	South Yorkshire	J30-J32 (Barlborough to Morthen)	239.2-250.5	11.3	Dec'67	15.0	
		J32-J34 (Morthen to Tinsley)	250.5-260.0	10.0	Dec'67	15.0	
		J34-J38 (Tinsley to Haigh)	260.0-284.2	24.2	Oct'68	14.0	
				45.5			
M1/M45	Northamptonshire	J16-J17 (M1) (A45 to M45)	109.5-123.7	14.2	Nov'59	25.0	
		J17-A45 U/B (M45) (Northants C C)	0.0-9.8	9.8	Nov'59	25.0	
		A45 U/B to end M5 (Warwicks C C)	9.8-12.6	2.8	Nov'59	25.0	
				26.8			
M4	Wiltshire	J18-J15 (Tormarton to Liddington)	169.5-123.5	46.0	Dec'71	10.0	
				46.0			
M4	Berkshire	J15-J8/9 (Liddington to Holyport)	123.5-44.5	79.0	Dec'71	10.0	
		Maidenhead and Slough by-pass widening	44.5-31.0	13.5	Dec'71	10.0	
				92.5			
		Maidenhead by-pass (side roads for M4)			1962	19.0	
		Slough by-pass (side roads for M4)			Apr'63	18.0	
		A329(M) A4 to Lodden Bridge			74/75	6.0	
		A329(M) A321 Twyford Road to A329			75/76	5.0	
M4	Mid-Glamorgan	J34-J35 (Miskin to Pencoed)	253.3-264.5	11.2	Dec'77	9.5	
		J35-E of J37 (Bridgend Northern By-Pass)	264.5-278.8	14.3	Sept'81	4.5	
		J37 Additional work			Sept'81	4.5	
				25.5			
		Advanced works at Hoel Las Embankment			Sept'81	4.5	
M4	South Glamorgan	J29-J32 (Castleton to Coryton)	232.8-244.9	12.1	Dec'77	9.5	
		J32-J34 (Coryton to Miskin)	244.9-253.3	7.0	Jul'80	6.5	
		J33 Culverhouse Link	249.8-251.2	1.4	Mar'85	2.0	
				20.5			
M4	Gwent	J23-J24 (Magor to Coldra)	211.2-218.2	7.0	Mar'67	20.0	
		J24-J28 (Newport By-Pass)	218.2-228.4	10.2	Apr'67	20.0	
		J28-J29A and A48(M) (Tredegar Park to St Mellons)	228.4-236.1	7.7	Oct'77	9.5	
				24.9			
		J24-J25 Widening (Coldra to Caerlon)	218.2-222.1		Apr'82	5.0	
		J26-J28 Widening (Malpas to Tredegar Park)	224.8-227.4		Apr'80	7.0	

Motorway	County	Section	Chainage	Length (km)	Date of opening	Age when surveyed (years)
M5	Gloucestershire	J12—ch.94.2 (Moreton Valence section)	97.3—94.2	3.1	Apr'71	13.0
		ch.94.2—ch.74.1 (Cheltenham and Gloucester section)	94.2—74.1	20.1	Apr'71	13.0
		ch.74.1—J9 (Tewkesbury section)	74.1—70.2	3.9	Apr'71	13.0
				<u>27.1</u>		
M5	Worcester and Hereford	Canal U/B to J4 (Lydiate Ash)	42.9—22.9	20.0	Jul'62	23.0
		J4 (Lydiate Ash to Frankley Service Area (Midlands Link C1.))	22.9—16.5	6.4	Nov'65	19.5
		Addition of crawler lanes on NB carriageway	30.6—28.9 26.8—25.2		1975	10.0
		Widening to 3 lane dual carriageway north of J4 1) Lydiate Ash to Dayhouse Bank (ch.21.4) 2) Dayhouse Bank to J3	one cut affected		1984	1.0
					original slope	
M6	Staffordshire	J13—J14 (Dunston to Stafford)	219.9—230.9	11.0	Sept'62	23.0
		J14—ch.241.3 (Stafford to Tittensor)	230.9—241.3	10.4	Dec'62	23.0
		ch.241.3—J15 (Tittensor to Hanchurch)	241.3—246.4	5.1	Dec'62	23.0
				<u>26.5</u>		
M6	Cumbria	N of J38—Thrimby	433.0—447.8	14.8	Oct'70	16.0
		Thrimby—Hackthorpe	447.8—451.6	3.8	Aug'69	17.0
		Hackthorpe—J40 (Penrith By-Pass)	451.6—459.2	7.6	Nov'68	18.0
				<u>26.2</u>		
M11	Essex	J3—J5 (Redbridge to Loughton)	10.0—18.5	8.5	1976	6.0
		J5—J7 (Loughton to South Harlow)	18.5—31.0	12.5	1976	6.0
		J7—J8 (South Harlow to A120)	31.0—46.5	15.5	June'75	7.0
		J8—J9 (A120 to Stump Cross)	46.5—71.0	24.5	Nov'79	3.0
				<u>61.0</u>		
M23	Surrey	J7—J8 (Hooley to Merstham)	27.0—30.2	3.2	Dec'74	9.0
		M23/M25 Junction 8	30.2—32.9	2.7	Dec'74	9.0
		J8—J11 (Bletchingley to Pease Pottage)	32.9—54.4	21.5	Dec'74	9.0
				<u>27.4</u>		
M62	West Yorkshire	Gatwick Link			Nov'75	8.0
		J22—J23 (Moss Moor to Outlane)	75.5—87.4	11.9	Dec'70	15.0
		J23—J24 (Outlane to Ainley)	87.4—89.7	2.3	Dec'72	13.0
		J24—J26 (Ainley to Chain Bar)	89.7—100.5	10.8	Jul'73	12.5
				<u>25.0</u>		
			Total Surveyed	567.6		

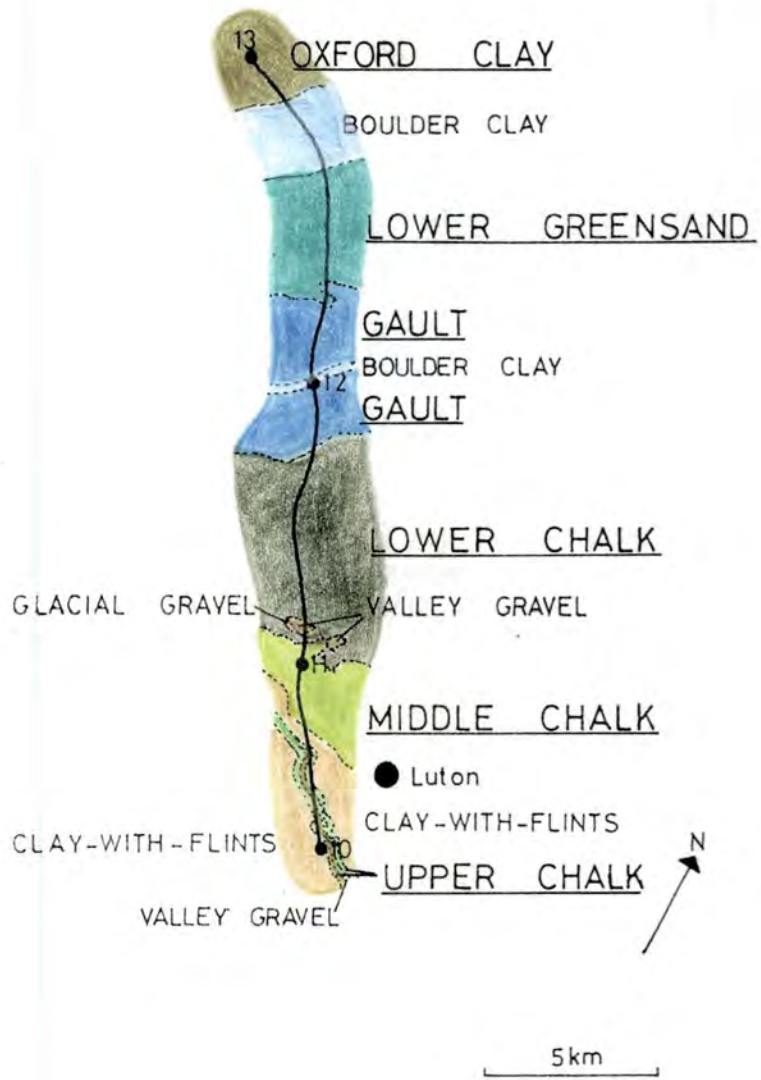


FigB1 Map of motorway sections studied

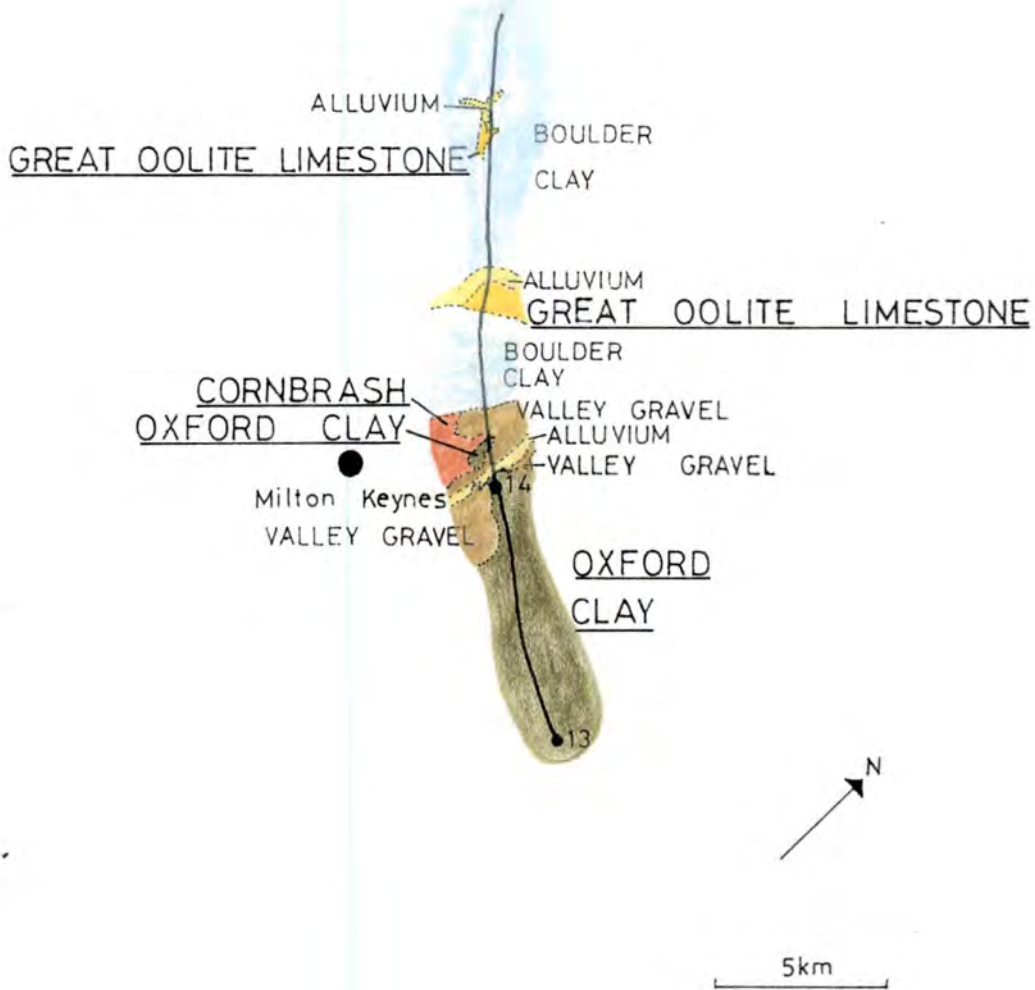


FigB2 The geological strata encountered along the M1 and M10 motorways in Hertfordshire

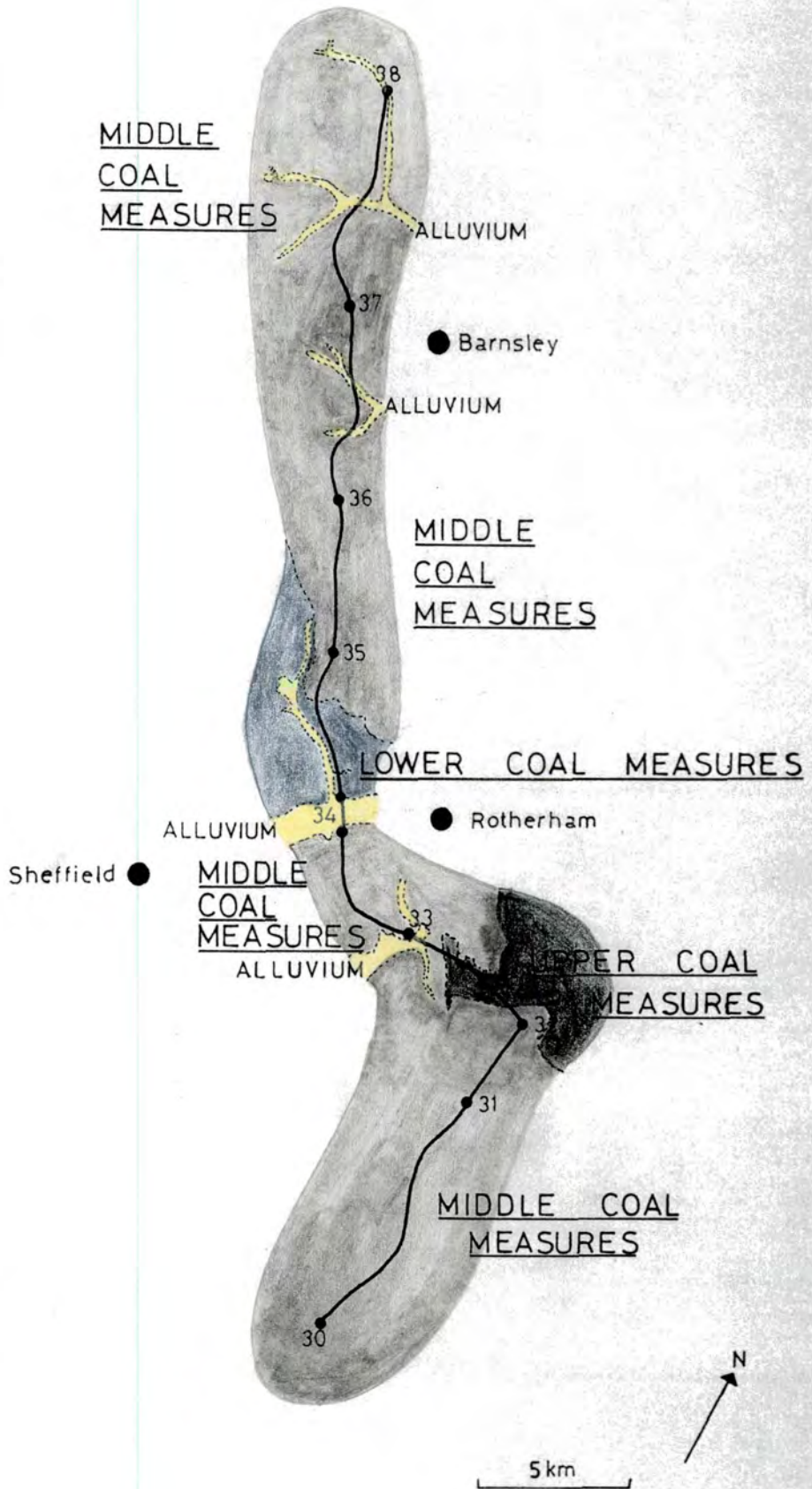
Milton Keynes



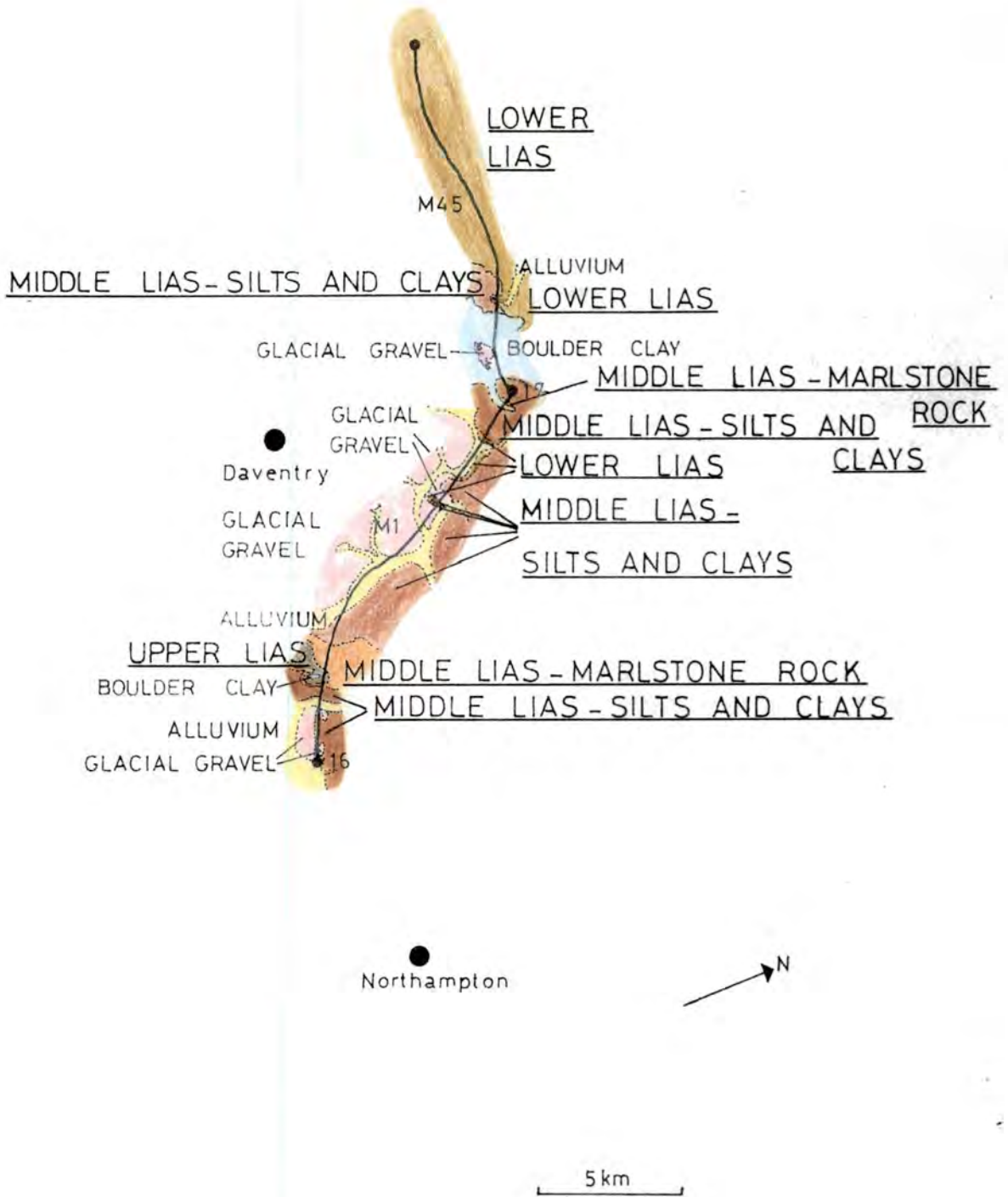
FigB3 The geological strata encountered along the M1 motorway in Bedfordshire



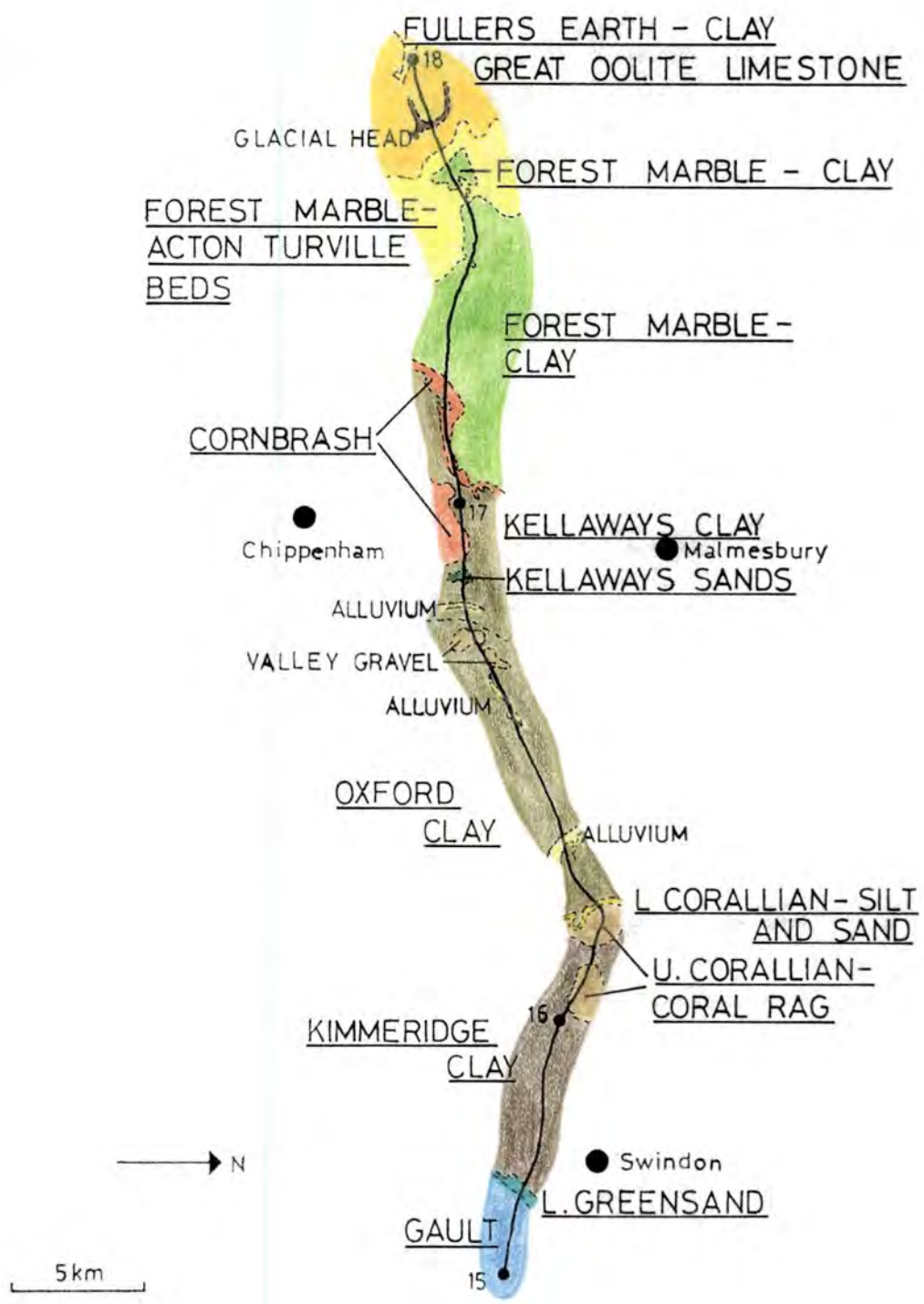
FigB4 The geological strata encountered along the M1 motorway in Buckinghamshire



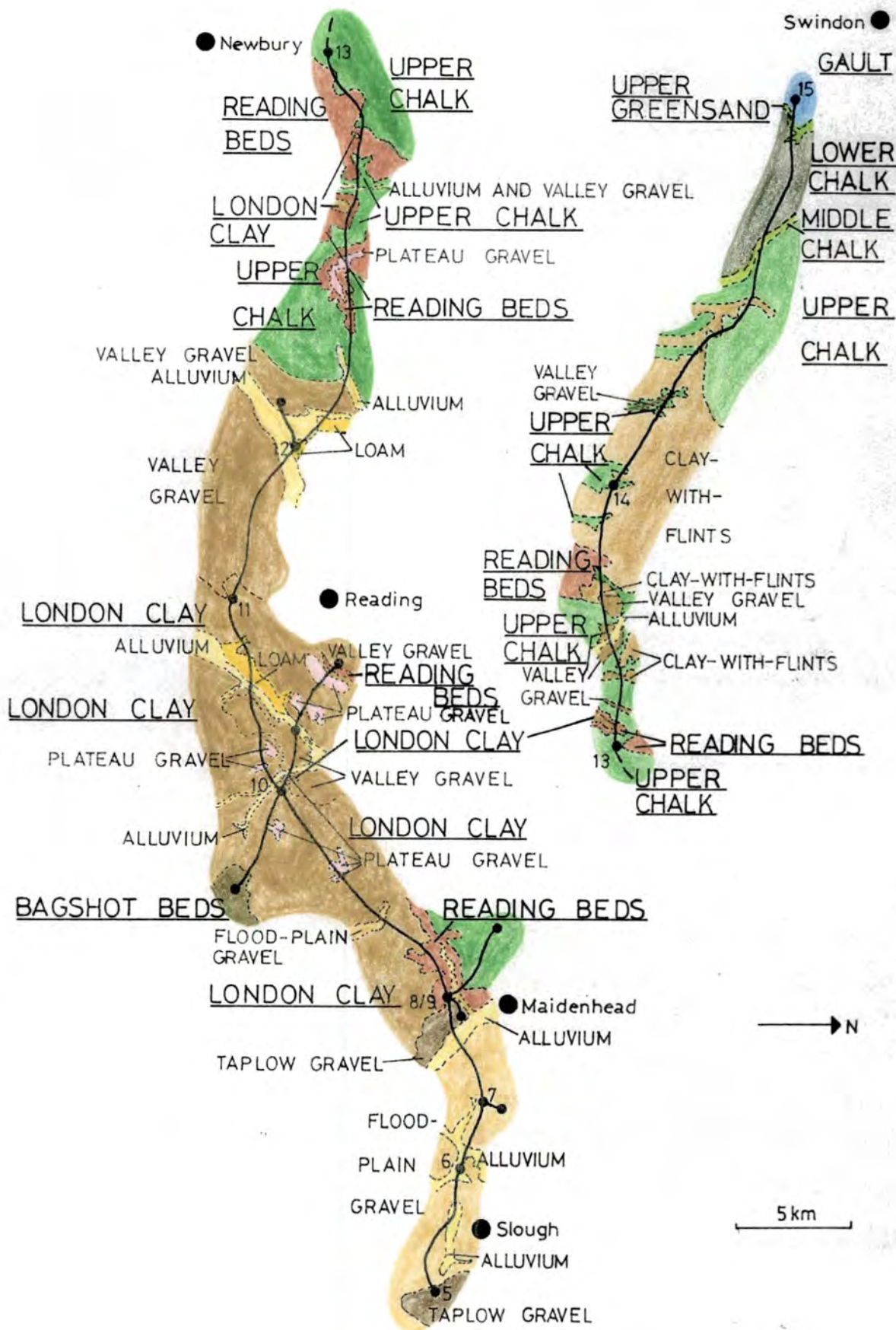
FigB5 The geological strata encountered along the M1 motorway in South Yorkshire



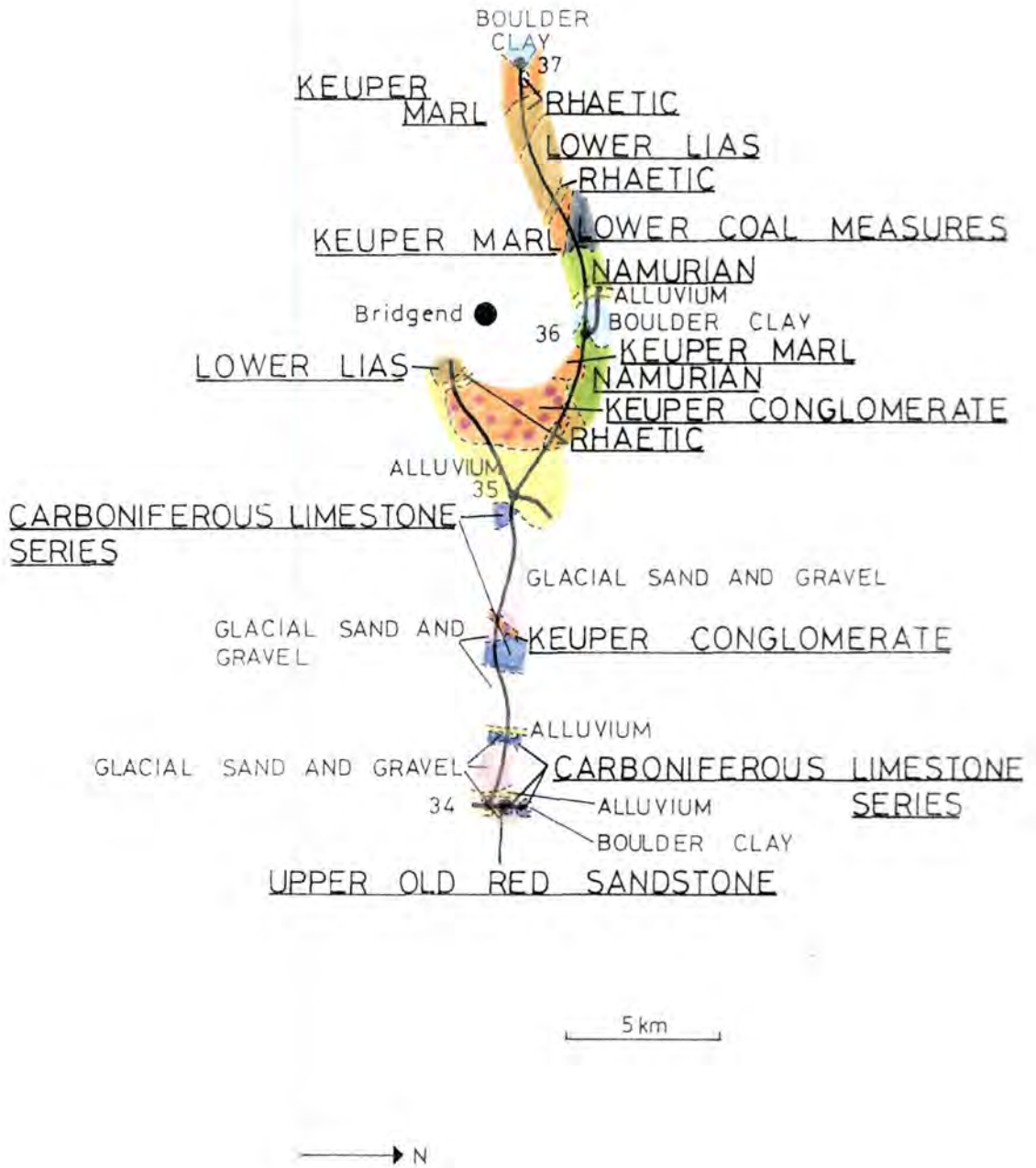
FigB6 The geological strata encountered along the M1 and M45 motorways in Northamptonshire



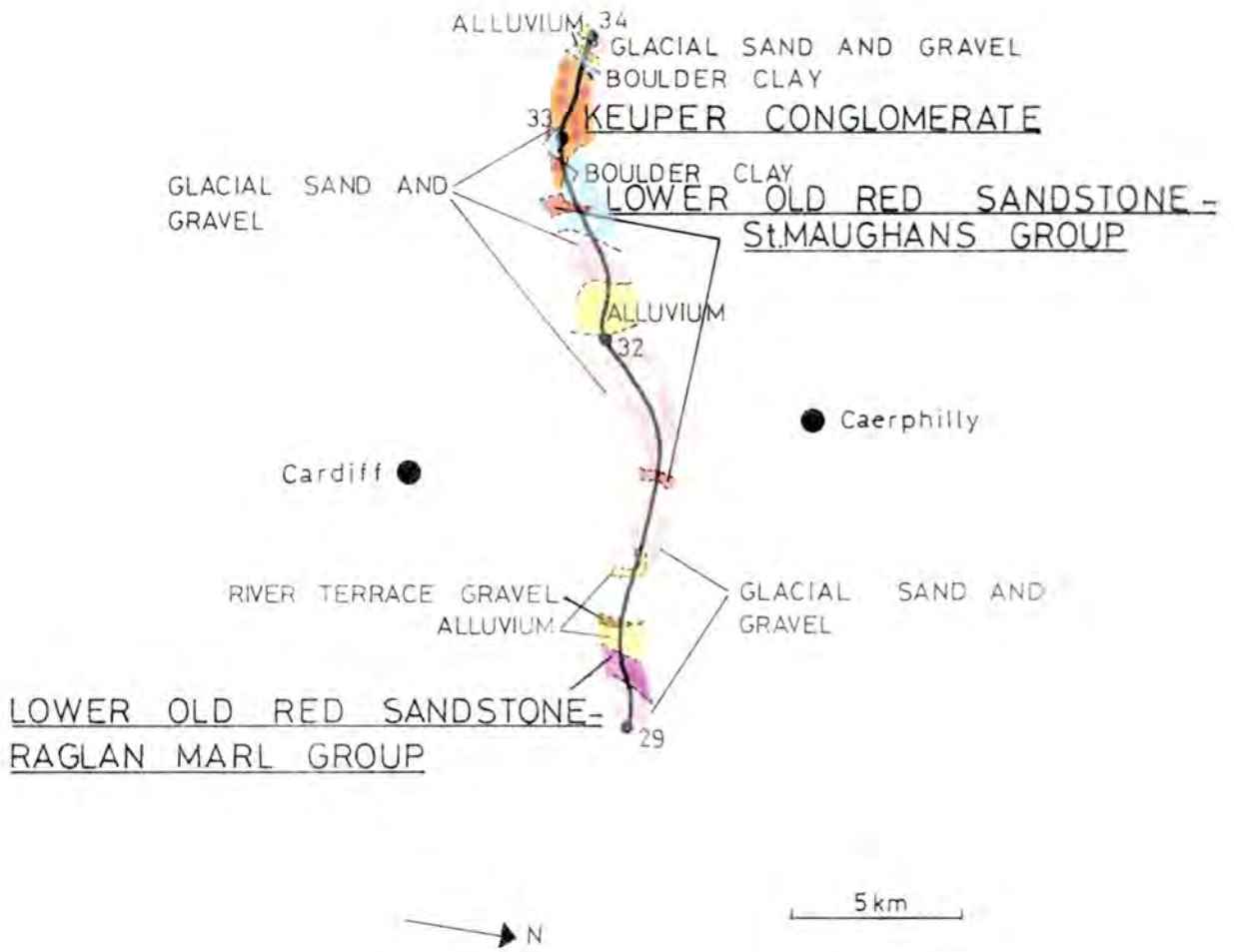
FigB7 The geological strata encountered along the M4 motorway in Wiltshire



FigB8 The geological strata encountered along the M4 motorway in Berkshire

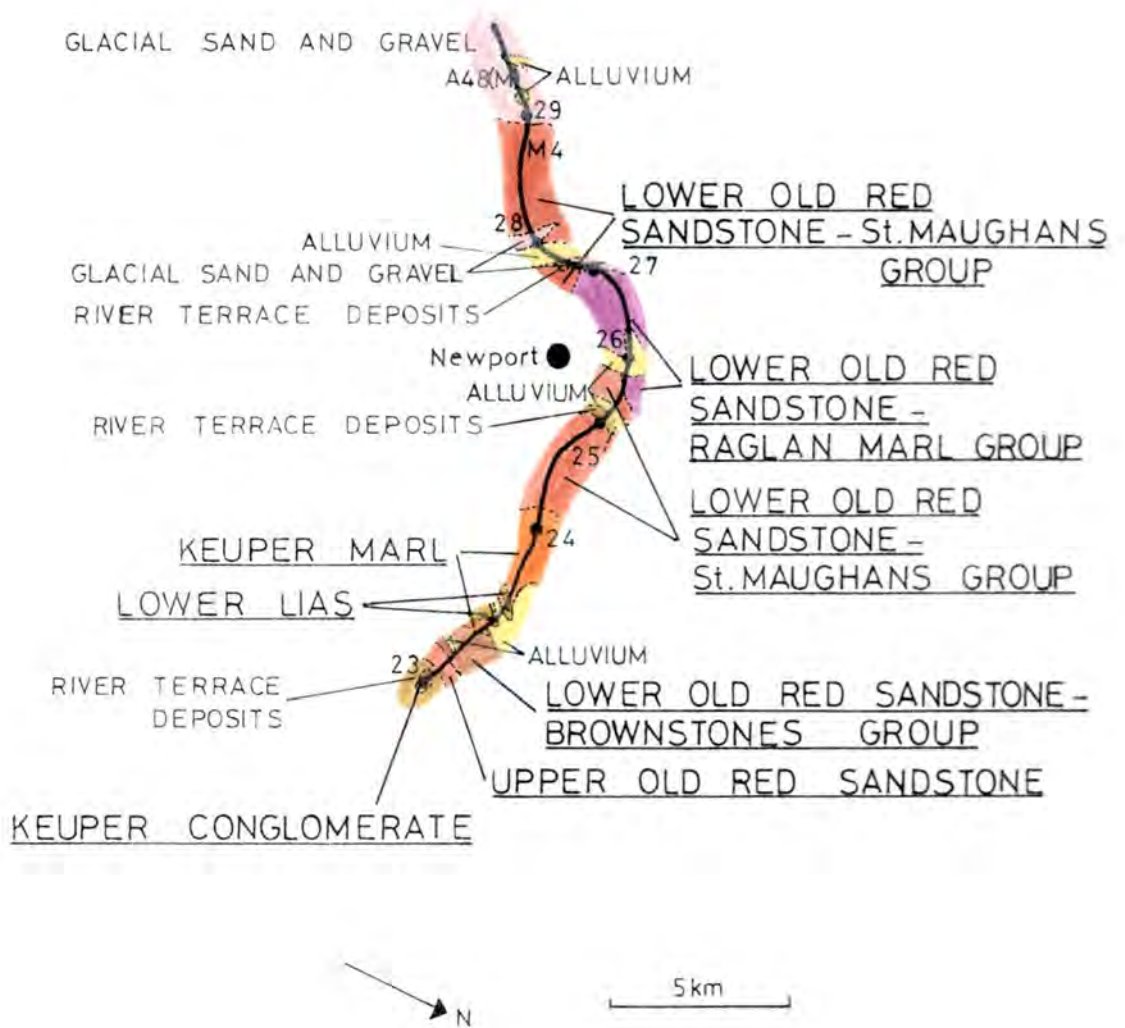


FigB9 The geological strata encountered along the M4 motorway in Mid - Glamorgan

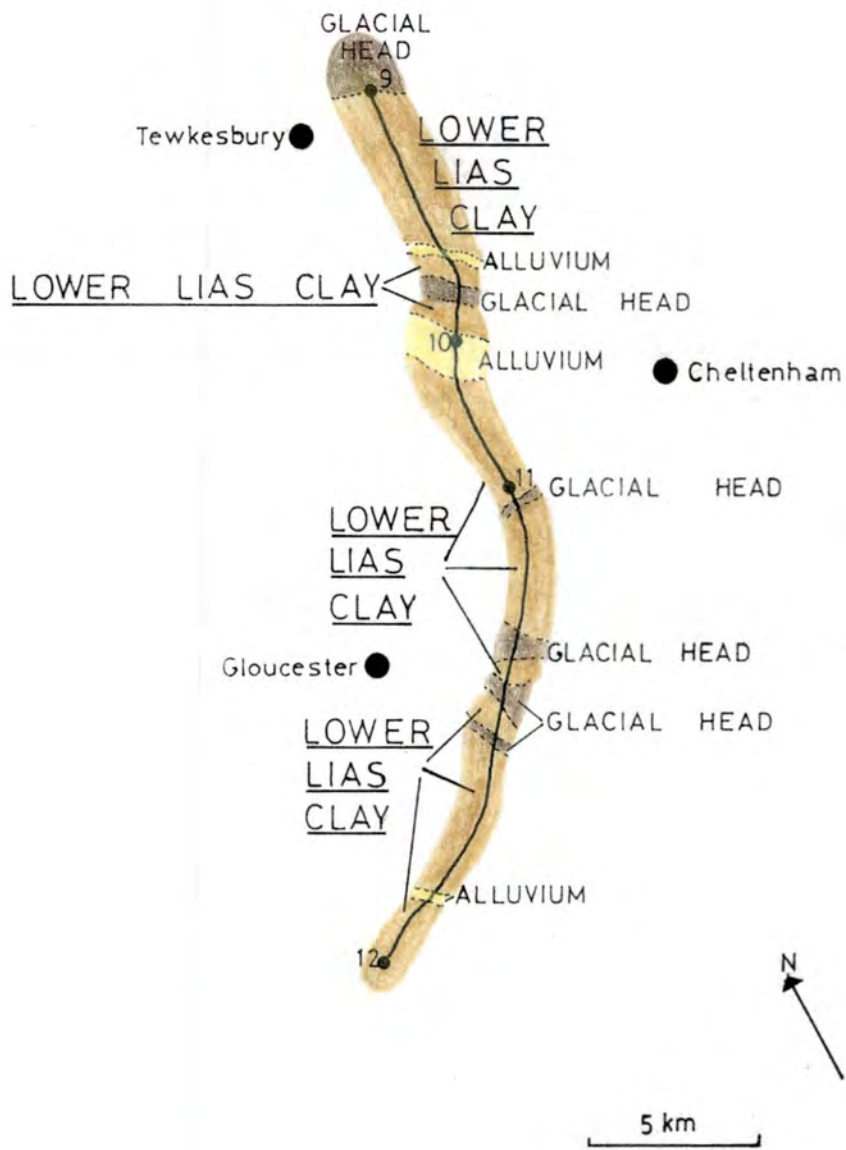


Lower Old Red Sandstone outcrops beneath the Glacial Sand and Gravel at the base of some cuttings

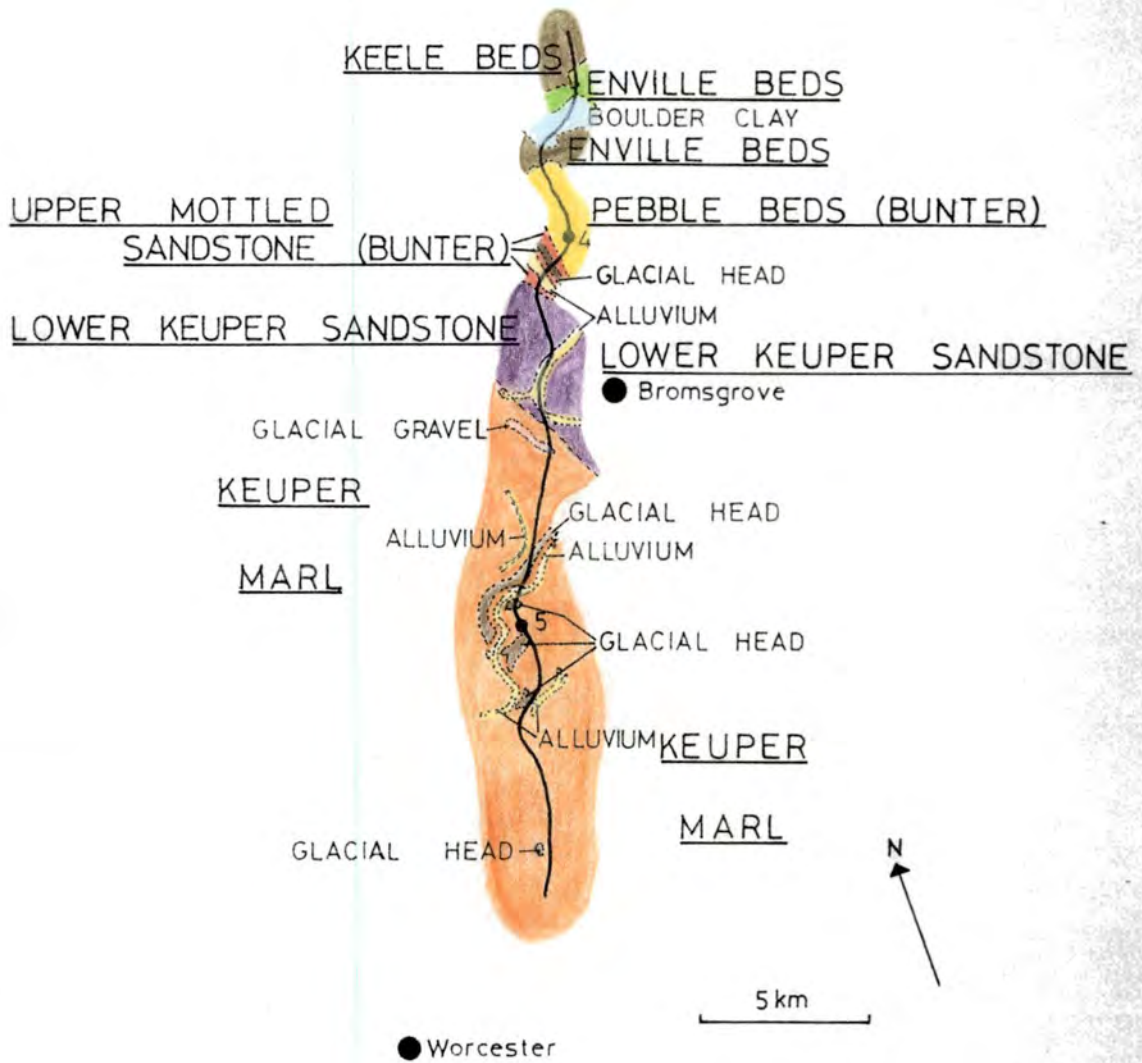
FigB10 The geological strata encountered along the M4 motorway in South Glamorgan



FigB11 The geological strata encountered along the M4 motorway in Gwent



FigB12The geological strata encountered along the M5 motorway in Gloucestershire



FigB13 The geological strata encountered along the M5 motorway in Hereford and Worcester

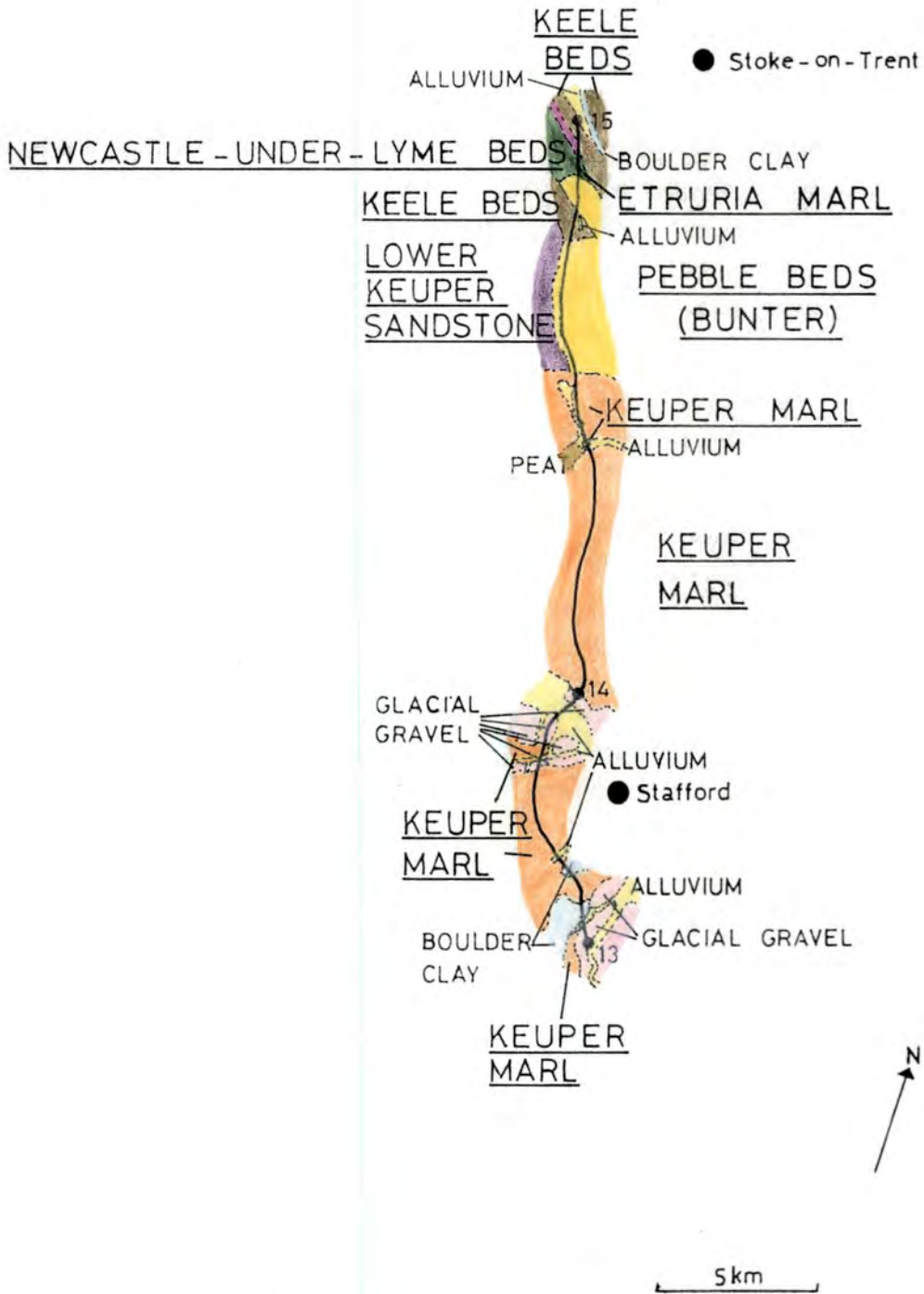
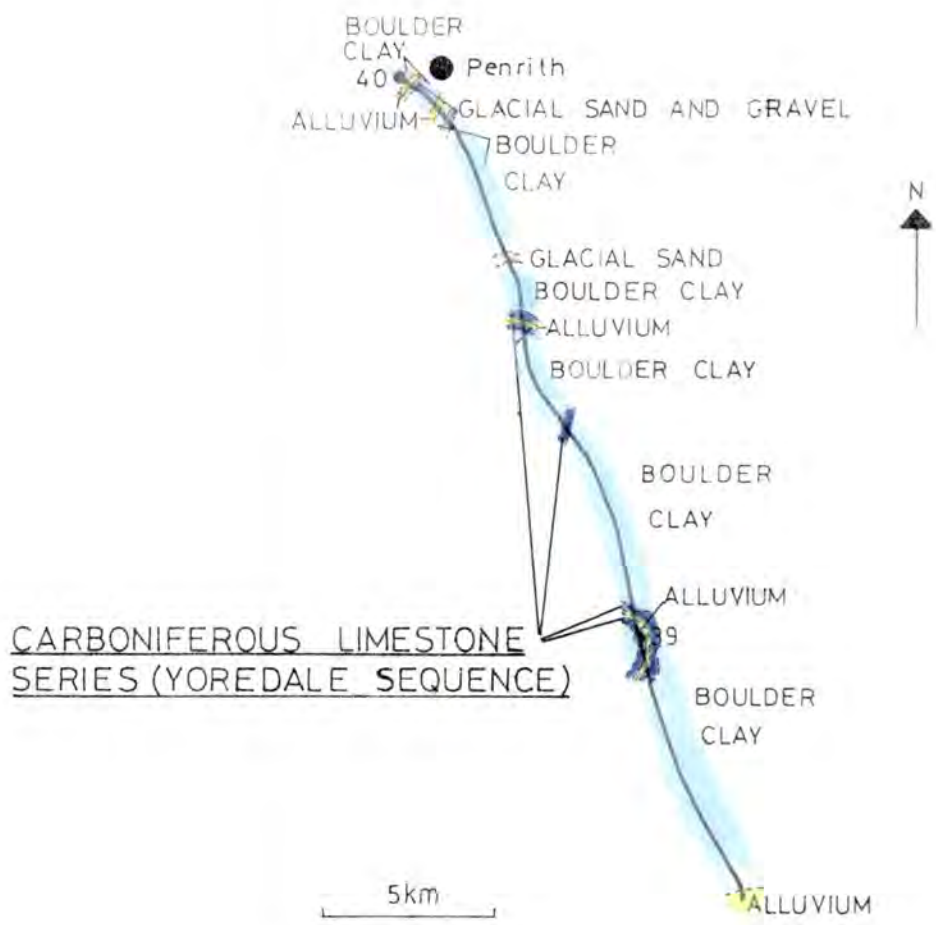


Fig.B14 The geological strata encountered along the M6 motorway in Staffordshire



Carboniferous Limestone Series (Yoredale Sequence) outcrops beneath the Boulder Clay at the base of some cuttings.

FigB15 The geological strata encountered along the M6 motorway in Cumbria

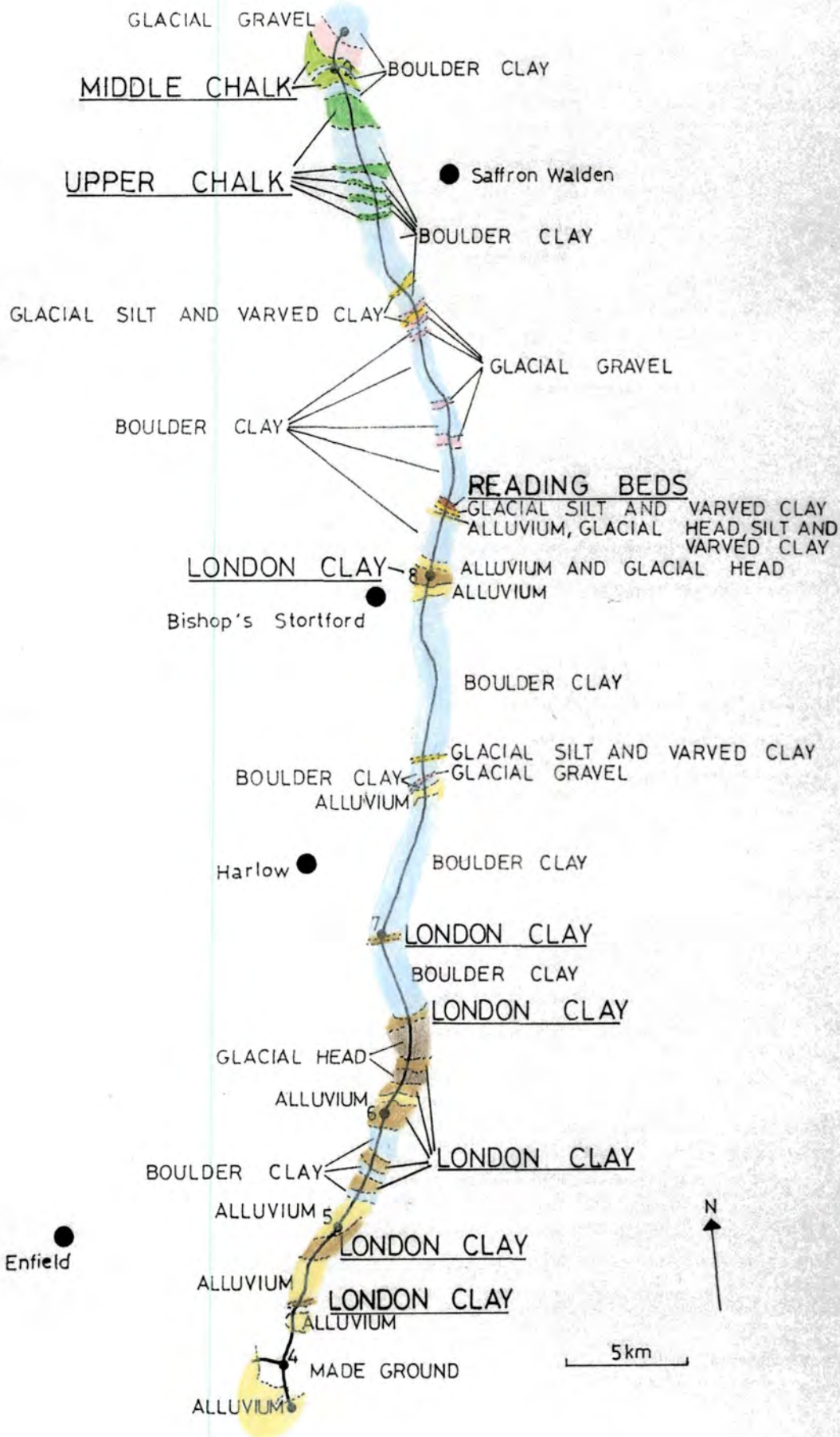


Fig.B16 The geological strata encountered along the M11 motorway in Essex

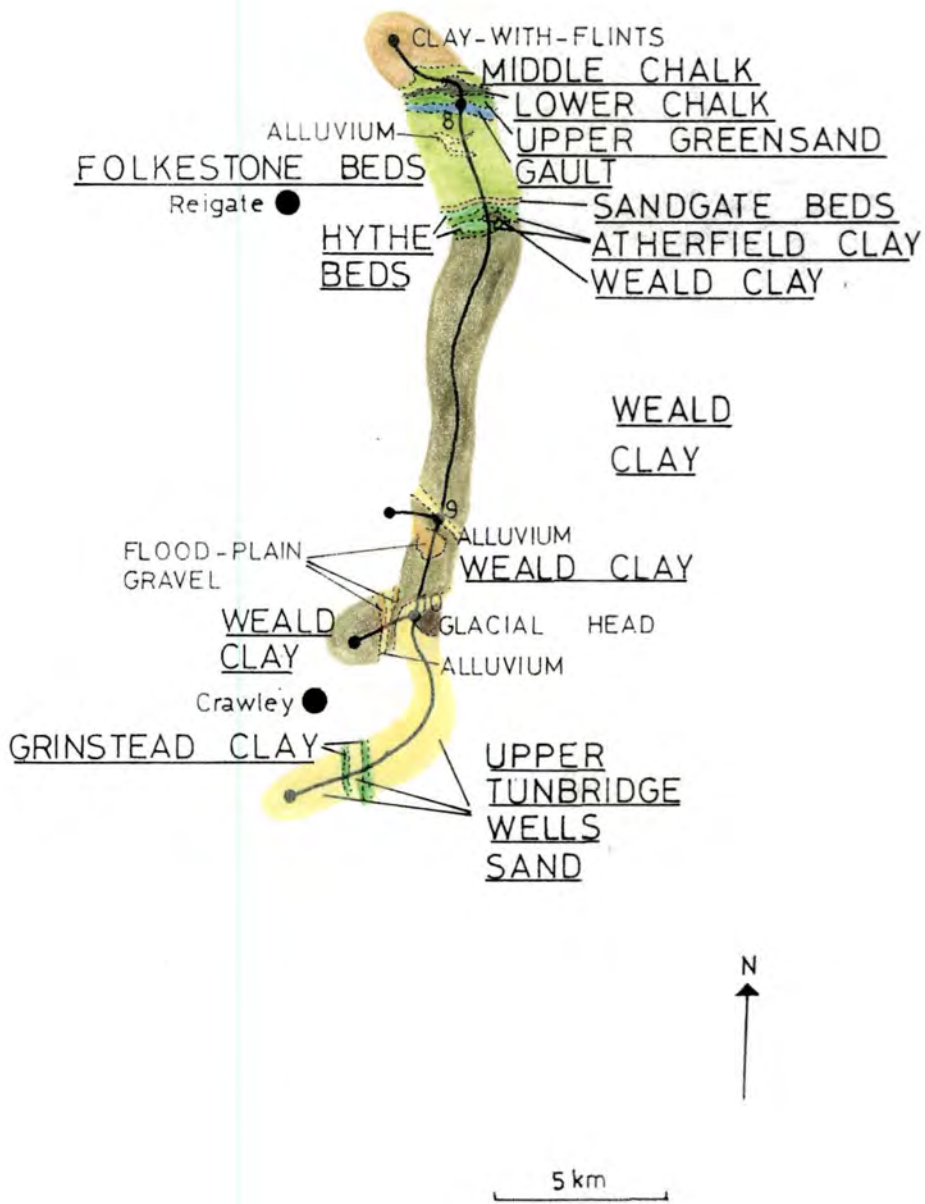


Fig. B17 The geological strata encountered along the M23 motorway in Surrey

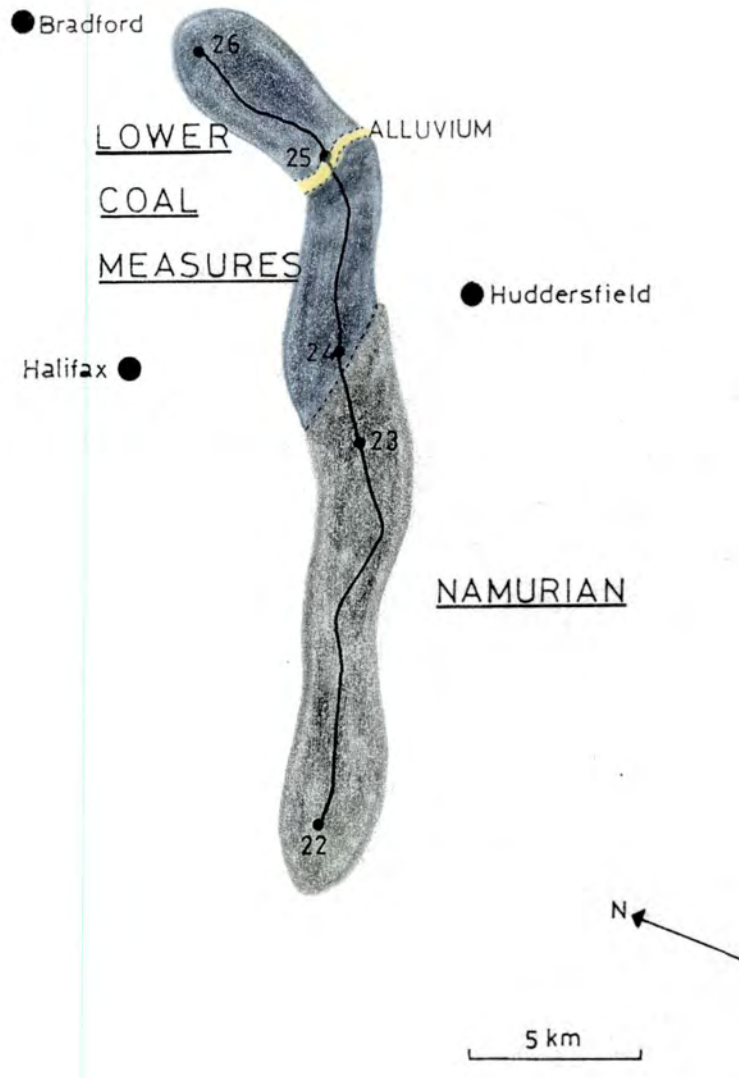


Fig B18 The geological strata encountered along the M62 motorway in West Yorkshire

Appendix C

Membrane correction for triaxial tests at low effective stresses

Assumptions for membrane correction

- (a) sample remains a right cylinder
- (b) no initial axial stretch in fitting membrane
- (c) initial radial stretch occurs, the initial diameter of an unstretched membrane being 36.25mm
- (d) all membranes have a initial thickness of 0.2mm
- (e) no wrinkling occurs

Nomenclature

$A_{m,s}$ = cross sectional area of membrane, soil

$d_{m,s}$ = diameter of membrane, soil

E = Young's Modulus of membrane = 1300 kPa

l_o, l_p = initial and final length of sample

r_o, r_p = initial and current radius of sample

t_o, t_p = initial and current thickness of membrane

V = volume of membrane

ϵ_a = axial strain in soil, membrane

ϵ_r = radial strain in soil, membrane

γ = Poisson's ratio of rubber = 1/2

Δa = axial stress membrane correction

$\Delta \sigma_r$ = radial stress membrane correction

1. To calculate current membrane thickness, t_p

Volume of membrane is constant

Volume of membrane, $V = l_o \cdot 2\pi(ro + t_o/2) \cdot t_o$

$$= 2\pi \cdot ro \cdot l_o \cdot t_o$$

At peak/failure $V = 2\pi \cdot r_p \cdot l_p \cdot t_p$

$$\text{therefore } t_p = t_o \cdot ro \cdot l_o / (r_p \cdot l_p)$$

$$\epsilon_r = (r_p - ro) / ro$$

$$1 + \epsilon_r = (ro + (r_p - ro)) / ro = r_p / ro$$

similarly, $\epsilon_a = (l_p - l_o) / l_o$

$$\text{therefore } 1 + \epsilon_a = l_p / l_o$$

$$\text{and } t_p = t_o / (1 + \epsilon_r)(1 + \epsilon_a) \text{ mm}$$

2. Axial stress correction

$$\Delta\sigma = \frac{-A_m \cdot E(\epsilon_a + \gamma \epsilon_r)}{A_s(1 - \gamma^2)}$$

$$\text{let } \epsilon_A = \epsilon_a + \gamma \epsilon_r$$

$$A_m = 2\pi \cdot r_p \cdot t_p \quad \text{where } r_p = \frac{ds + t_p}{2}$$

$$= 2\pi(ds + t_p) \cdot t_p / 2 = \pi ds \cdot t_p$$

$$A_s = \pi ds^2 / 4 \quad \text{therefore } A_m / A_s = 4t_p / ds$$

$$\text{therefore } \Delta\sigma_a = \frac{-4t_p \cdot E \cdot \epsilon_A}{ds(1 - \gamma^2)} = -6933 \cdot t_p \cdot \epsilon_A / ds \text{ kPa}$$

3. Radial stress corrections

$$\Delta\sigma_r = \frac{-2E \cdot t_p(\epsilon_r + \gamma \epsilon_a)}{dm(1 - \gamma^2)} \quad \text{where } dm = ds + t_p / 2$$

$$\text{let } \epsilon_R = \epsilon_r + \gamma \epsilon_a$$

$$\text{therefore } \Delta\sigma_r = \frac{-2E \cdot t_p \cdot \epsilon_R}{dm(1 - \gamma^2)} = -3467 \cdot t_p \cdot \epsilon_R / dm \text{ kPa}$$

Appendix D

Computer program for 'best fit' power curve

```

10      ! MOHR'S CIRCLE PLOT AND CURVE FITTING
20      COM Sig(1:50,1:2),Setup
30      COM /Plot/ Sigmax,INTEGER Co
40      COM /Env/ Est,Fcu
50      PRINTER IS 1
60      GRAPHICS OFF
70      PLOTTER IS 3,"INTERNAL"
80      Est=0
90      Fcu=0
100     DIM Title$(20)
110     INTEGER No
120     Setup=0
130     PRINT CHR$(12);
140     PRINT "MOHR'S CIRCLE PLOT"
150     LOOP
160         GRAPHICS OFF
170         Sigmax=0
180         Co=0
190         PRINT
200         DISP "SELECT DATA SOURCE"
210         ON KEY 0 LABEL "DISC" GOTO Disc
220         ON KEY 4 LABEL "KEYBOARD" GOTO Keybd
230         GOTO 230
240     Disc:OFF KEY
250         DISP ""
260         CALL Retrieve(Sig(*),No,Title$)
270         CALL List(Sig(*),No,Title$)
280         PAUSE
290         GOTO L1
300         !
310     Keybd:OFF KEY
320         DISP ""
330         INPUT "TITLE?",Title$
340         PRINT Title$
350         INPUT "NUMBER OF CIRCLES",No
360         PRINT
370         PRINT No;" Circles"
380         REDIM Sig(1:No,1:2)
390         PRINT
400         PRINT "Circle","Sigma_a","Sigma_r"
410         FOR N=1 TO No
420             DISP "CIRCLE ";N;
430             INPUT ", ENTER Sigma_a,Sigma_r",Siga,Sigr
440             PRINT N,Siga,Sigr
450             Sig(N,1)=Siga
460             Sig(N,2)=Sigr
470         NEXT N
480         !
490     L1: FOR N=1 TO No
500         Co=1
510         NEXT N
520         Sigmax=MAX(Sig(*))
530         CALL Plot(Sig(*),No,Title$)
540         DISP ""
550         PRINT CHR$(12);
560     END LOOP
570     END
580     !
590     !*****
600     !
610     Plot:SUB Plot(Sig(*),INTEGER No,Title$)
620         COM /Plot/ Sigmax,INTEGER Co
630         COM /Env/ C,0,Limitx,Limity,Line,A,B
640         COM /Set/ Setup
650         INTEGER Addf1
660         Line=0          ! NO ENVELOPE
670         C=0

```

```

680      Limitx=0
690      Limity=0
700      A=0
710      E=0
720      GRAPHICS OFF
730      INTEGER Device,I,P1,P2,P3,P4,X,Y,Pen,Entry,Sc
740      !
750      !
760      !
770 New: OFF KEY
780      DISP ""
790      GRAPHICS OFF
800      PRINT CHR$(12)
810      ALPHA ON
820      !
830      DISP "SCREEN OR PLOTTER"
840      ON KEY 0 LABEL "SCREEN" GOTO Screen
850      ON KEY 5 LABEL "PLOTTER" GOTO Plotter
860      GOTO 860
870 Screen:OFF KEY
880      Device=1
890      PRINT
900      PRINT "PLOT ON SCREEN"
910      GOTO Ques
920 Plotter:OFF KEY
930      Device=0
940      PRINT
950      PRINT "PLOT ON PLOTTER"
960 Ques: !
970      ON KEY 0 LABEL "PROCEED" GOTO Next
980      ON KEY 5 LABEL "RESTART" GOTO New
990      GOTO 990
1000     !*****
1010 Next:DISP ""
1020     IF Device THEN
1030         GINIT
1040         PLOTTER IS 3,"INTERNAL"           !ALSO GCLEARs AFTER GINIT
1050         ALPHA OFF
1060         GRAPHICS ON
1070         VIEWPORT 0,100*RATIO,10,98
1080         GOTO Start_plot
1090     END IF
1100     !
1110     !*****
1120     !-----
1130     ! INITIALIZE PLOTTER TO CONVENIENT GRID POINTS MAINTAINING      |
1140     ! NEAR MAXIMUM PLOTTING AREA BEFORE P1 AND P2 ARE READ BY THE  |
1150     ! 'PLOTTER IS' STATEMENT                                         |
1160     !-----
1170 Copy:OFF KEY
1180     Device=0
1190     ON TIMEOUT 7,5 GOSUB Time
1200     IF NOT Set_plotter THEN
1210         GRAPHICS OFF
1220         ALPHA ON
1230         PRINT CHR$(12)
1240         PRINT "LOAD ONE PEN IN LEFT PEN HOLDER (FOR AXES AND LABELS),"
1250         PRINT
1260         PRINT "AND ANOTHER IN RIGHT (FOR DATA); LOAD PAPER ,THEN CONT"
1270         PAUSE
1280         PRINT CHR$(12)
1290         !
1300         OUTPUT 705;"OS"
1310         ENTER 705;Status
1320         IF NOT BIT(Status,4) THEN
1330             DISP "PAPER NOT LOADED"
1340             GOTO 1240
1350         END IF
1360         !
1370         IF NOT Setup THEN
1380             OUTPUT 705;"IN;IP140,60,10890,7260"
1390             Setup=1

```



```

1400     END IF
1410     OUTPUT 705;"OF"
1420     ENTER 705;P1,P2,P3,P4
1430     OUTPUT 705;"SP1"
1440     OUTPUT 705;"PA";P1;" ";P2;" ";PD;PU"
1450     DISP "IS THE PEN ALIGNED WITH A CENTIMETER INTERSECTION"
1460     ON KEY 0 LABEL "YES" GOTO Yes
1470     ON KEY 5 LABEL "NO" GOTO No
1480     GOTO 1480
1490 No:   OFF KEY
1500     DISP "THERE ARE 40 UNITS/mm, ENTER 'X' AND 'Y' INCREMENTS TO CORRECT
";
1510     INPUT " ",X,Y
1520     P1=P1+X
1530     P2=P2+Y
1540     GOTO 1440
1550 Yes:  OFF KEY
1560     OUTPUT 705;"PA";P3;" ";P4;" ";PD;PU"
1570     DISP "IS THE PEN ALIGNED WITH A CENTIMETER INTERSECTION"
1580     ON KEY 0 LABEL "YES" GOTO Yes2
1590     ON KEY 5 LABEL "NO" GOTO No2
1600     GOTO 1600
1610 No2: OFF KEY
1620     DISP "ENTER 'X' AND 'Y' INCREMENTS TO CORRECT";
1630     INPUT " ",X,Y
1640     P3=P3+X
1650     P4=P4+Y
1660     GOTO 1560
1670 Yes2: OFF KEY.
1680     DISP ""
1690     Set_plotter=1
1700     OUTPUT 705;"IN;IP";P1;" ";P2;" ";P3;" ";P4
1710     END IF
1720     GINIT
1730     PLOTTER IS 705,"HPGL"
1740     ON KEY 4 LABEL "ABORT" GOTO Exit
1750     GOTO Start_plot
1760     !
1770! *****
*
1780 Time: !
1790     BEEP
1800     GRAPHICS OFF
1810     ALPHA ON
1820     DISP "PLOTTER NOT RESPONDING; Check, Power, Paper load, 'View' released"
1830     RETURN
1840! *****
1850!
1860 Start_plot: !
1870     GRAPHICS ON
1880     !
1890     GOSUB Scale0
1900     PEN 1
1910     !                               AXES
1920     IF Sigmax<=480 THEN
1930         AXES 10,10
1940     ELSE
1950         AXES 50,50
1960     END IF
1970     !                               !Y-AXIS LABELS
1980     MOVE 0,0
1990     DEG
2000     LDIR 0
2010     LORG 8
2020     CSIZE 3
2030     CLIP OFF
2040     SELECT Sigmax
2050     CASE <=240
2060         FOR I=Cbot TO Ctop-1 STEP 10
2070             MOVE Cleft,I
2080             LABEL USING "DDDD,X";I
2090         NEXT I

```

```

2100
2110 CASE <=480
2120   FOR I=Cbot TO Ctop-1 STEP 20
2130     MOVE Cleft,I
2140     LABEL USING "DDDD,X";I
2150   NEXT I
2160   !
2170 CASE <=960
2180   FOR I=Cbot TO Ctop-1 STEP 50
2190     MOVE Cleft,I
2200     LABEL USING "DDDD,X";I
2210   NEXT I
2220   !
2230 END SELECT
2240 MOVE 0,0
2250 LDIR 90
2260 LORG 8
2270 SELECT Sigmax
2280 CASE <=240
2290   FOR I=Cleft TO Cright-1 STEP 10
2300     MOVE I,0
2310     LABEL USING "X,DDD,X";I
2320   NEXT I
2330   !
2340 CASE <=480
2350   FOR I=Cleft TO Cright-1 STEP 20
2360     MOVE I,0
2370     LABEL USING "X,DDD,X";I
2380   NEXT I
2390   !
2400 CASE <=960
2410   FOR I=Cleft TO Cright-1 STEP 50
2420     MOVE I,0
2430     LABEL USING "X,DDD,X";I
2440   NEXT I
2450   !
2460 END SELECT
2470 IF Sc=1 THEN MOVE Cleft-15,(Cbot+Ctop)/2
2480 IF Sc=2 THEN MOVE Cleft-30,(Cbot+Ctop)/2
2490 IF Sc=4 THEN MOVE Cleft-60,(Cbot+Ctop)/2
2500 IF Sc=8 THEN MOVE Cleft-120,(Cbot+Ctop)/2
2510 LDIR 90
2520 CSIZE 3.5
2530 LORG 6
2540 LABEL "Shear Stress (kPa)"
2550 IF Sc=1 THEN MOVE (Cleft+Cright)/2,Cbot-10
2560 IF Sc=2 THEN MOVE (Cleft+Cright)/2,Cbot-20
2570 IF Sc=4 THEN MOVE (Cleft+Cright)/2,Cbot-40
2580 IF Sc=8 THEN MOVE (Cleft+Cright)/2,Cbot-80
2590 LDIR 0
2600 LORG 6
2610 LABEL "Effective Normal Stress (kPa)"
2620 MOVE (Cleft+Cright)/2,Top
2630 CSIZE 4
2640 LORG 6
2650 LDIR 0
2660 LABEL Title$
2670 !*****
2680 !
2690 CLIP ON
2700 !
2710 PEN 2
2720 FOR N=1 TO No
2730   Centre=(Sig(N,1)+Sig(N,2))/2
2740   Radius=(Sig(N,1)-Sig(N,2))/2
2750   Start=180
2760   End=0
2770   Step=2
2780   FOR I=Start TO End STEP -Step
2790     PLOT Centre+Radius*COS(I),Radius*SIN(I)
2800   NEXT I
2810 PENUM

```

PLOT DATA

!CHANGE PEN

```

2820     NEXT N
2830     PRINT CHR$(12)
2840     IF Line THEN
2850         IF Line=1 THEN CALL Line(Cright,Ctop,Device)
2860         IF Line=2 THEN CALL Curve(Cright,Ctop,Device)
2870     END IF
2880 K:   ON KEY 0 LABEL "HARD COPY" GOTO Copy
2890     ON KEY 1 LABEL "NEW DATA" GOTO Exit
2900     ON KEY 2 LABEL "LIST DATA" GOTO Li
2910     ON KEY 3 LABEL "STORE DATA" GOTO St
2920     ON KEY 4 LABEL "EDIT DATA" GOTO Ed
2930     ON KEY 5 LABEL "CHANGE SCALE" GOTO Sc
2940     ON KEY 6 LABEL "PRINTER" GOTO Fri
2950     ON KEY 7 LABEL "FIT ENVELOPE" GOTO Fit
2960     ON KEY 8 LABEL "FLOT ENVELOPE" GOTO Env
2970     ON KEY 9 LABEL "ADD ENVELOPE" GOTO Add
2980     GOTO 2980
2990 Fit:OFF KEY
3000     ON KEY 5 LABEL "CURVE" GOTO Fwr
3010     ON KEY 6 LABEL "LINE" GOTO Str
3020     GOTO 3020
3030 Ed:  OFF KEY
3040     CALL Edit(Sig(*),No,Title$)
3050     GOTO K
3060 Sc:  OFF KEY
3070     ON KEY 5 LABEL "UP SCALE" GOTO Sc2
3080     ON KEY 6 LABEL "DOWN SCALE" GOTO Sc1
3090     GOTO 3090
3100 Fri:OFF KEY
3110     ON KEY 5 LABEL "SCREEN" GOTO Scrpt
3120     ON KEY 6 LABEL "PRINTER" GOTO Prprt
3130     GOTO 3130
3140 Scrpt:PRINTER IS CRT
3150     DISP "Printer is screen"
3160     GOTO K
3170 Prprt:PRINTER IS PRT
3180     DISP "Printer is external printer"
3190     GOTO K
3200 Li:  OFF KEY
3210     GRAPHICS OFF
3220     ALPHA ON
3230     CALL List(Sig(*),No,Title$)
3240     GOTO K
3250 Fwr:OFF KEY
3260     CALL Sqfit(Cright,Ctop,No,Device,Title$)
3270     Cur=1
3280     GOTO K
3290 Str:OFF KEY
3300     CALL Ss(Cright,Ctop,No,Device)
3310     GOTO K
3320 St:  OFF KEY
3330     CALL Store(Sig(*),No,Title$)
3340     GOTO K
3350 Sc1:OFF KEY
3360     SELECT Sigmax
3370     CASE 480 TO 960
3380         Sigmax=470
3390         GOTO New
3400     CASE 240 TO 480
3410         Sigmax=230
3420         GOTO New
3430     CASE 130 TO 240
3440         Sigmax=120
3450         GOTO New
3460     CASE ELSE
3470         BEEP
3480         DISP "LARGEST SCALE"
3490         WAIT 2
3500         Sigmax=120
3510         GOTO K
3520     END SELECT
3530 Sc2:OFF KEY

```

```

3540     SELECT Sigmax
3550     CASE <130
3560         Sigmax=140
3570         GOTO New
3580     CASE <240
3590         Sigmax=250
3600         GOTO New
3610     CASE <480
3620         Sigmax=490
3630         GOTO New
3640     CASE ELSE
3650         BEEP
3660         DISP "SMALLEST SCALE"
3670         WAIT 2
3680         Sigmax=490
3690         GOTO K
3700     END SELECT
3710 Add:OFF KEY
3720     Addf1=1
3730     GOTO 3760
3740 Env:OFF KEY
3750     Addf1=0
3760     CALL Envelope(Cright,Ctop,Device,Addf1)
3770     MOVE 0,0
3780     PEN 0
3790     GOTO K
3800 Exit:    !
3810     SUBEXIT
3820     !*****
3830 Scale0:  COMPRESSION TEST
3840     SELECT Sigmax
3850     CASE <=130
3860         Left=-15
3870         Right=120
3880         Bottom=-20
3890         Top=70
3900         Cleft=0
3910         Cright=120
3920         Cbot=0
3930         Ctop=60
3940         Sc=1
3950     CASE <=240
3960         Left=-30
3970         Right=240
3980         Bottom=-40
3990         Top=140
4000         Cleft=0
4010         Cright=240
4020         Cbot=0
4030         Ctop=120
4040         Sc=2
4050     CASE <=480
4060         Left=-60
4070         Right=480
4080         Bottom=-80
4090         Top=280
4100         Cleft=0
4110         Cright=480
4120         Cbot=0
4130         Ctop=240
4140         Sc=4
4150     CASE <=960
4160         Left=-120
4170         Right=960
4180         Bottom=-160
4190         Top=560
4200         Cleft=0
4210         Cright=960
4220         Cbot=0
4230         Ctop=480
4240         Sc=8
4250     CASE ELSE

```

```

4260      BEEP
4270      DISP "FLOT TOO LARGE"
4280      WAIT 2
4290      END SELECT
4300      GOSUB Set
4310      RETURN
4320
4330 Set: IF Device THEN          SCREEN
4340      SHOW Left,Right,Bottom,Top
4350      ELSE
4360      WINDOW Left,Right,Bottom,Top: PLOTTER
4370      END IF
4380      CLIP Cleft,Cright,Cbot,Ctop
4390      RETURN
4400 SUBEND
4410 !
4420 !*****
4430 Envelope: !
4440 SUB Envelope(Cright,Ctop,INTEGER Device,Addf1)
4450 COM /Env/ C,@,Limitx,Limity,Line,A,B
4460 IF Device AND NOT Addf1 THEN      ! ERASE IF SCREEN AND NOT ADDING
4470 GRAPHICS OFF                      ! ENVELOPE
4480 IF Line=1 THEN
4490 MOVE 0,C
4500 PEN 0
4510 DRAW Limitx,Limity
4520 END IF
4530 IF Line=2 THEN
4540 PEN -1
4550 GOSUB Cur
4560 END IF
4570 END IF
4580 DISP "YOU MAY PLOT A STRAIGHT LINE OR A POWER CURVE"
4590 ON KEY 0 LABEL "LINE" GOTO Line
4600 ON KEY 4 LABEL "CURVE" GOTO Curve
4610 GOTO 4610
4620 !
4630 Line:OFF KEY
4640 INPUT "Enter C' in kPa and 0'in degrees",C,@
4650 CALL Line(Cright,Ctop,Device)
4660 SUBEXIT
4670 Curve:OFF KEY
4680 INPUT "Enter 'A' and 'b'(T=a.x^b)",A,B
4690 CALL Curve(Cright,Ctop,Device)
4700 SUBEXIT
4710 !
4720 Cur:MOVE 0,0
4730 FOR X=0 TO Cright
4740 Y=A*(X^B)
4750 DRAW X,Y
4760 NEXT X
4770 RETURN
4780 !
4790 SUBEND
4800 !
4810 !
4820 !*****
4830 !
4840 Store: !
4850 SUB Store(Sig(*),INTEGER No,Title$)
4860 GRAPHICS OFF
4870 DISP "INSERT DATA DISC IN DRIVE 1, CONT. WHEN READY"
4880 PAUSE
4890 PRINT CHR$(12)
4900 CAT ":",700,1"
4910 Inp:INPUT "ENTER FILENAME ON WHICH TO STORE DATA",File$
4920 ON ERROR GOTO Error
4930 Recs=INT((No*8+24+2)/256)+1
4940 Create:CREATE BDAT File$&"":,700,1",Recs
4950 ASSIGN @File TO File$&"":,700,1"
4960 OUTPUT @File;Title$,No,Sig(*)
4970 ASSIGN @File TO *

```

```

4980 SUBEXIT
4990 Error:OFF ERROR
5000 IF ERRN=54 THEN
5010 DISP "FILE EXISTS DO YOU WANT TO OVERWRITE Y/N";
5020 INPUT "",Yesno#
5030 IF Yesno#="Y" THEN
5040 PURGE File#&":,700,1"
5050 GOTO Create
5060 END IF
5070 GOTO Inp
5080 END IF
5090 DISP ERRM#&" CONT. WHEN READY"
5100 PAUSE
5110 SUBEND
5120 !
5130 !*****
5140 Ret: !
5150 SUB Retrieve(Sig(*),INTEGER No,Title#)
5160 DISP "INSERT DATA DISC IN DRIVE 1, CONT. WHEN READY"
5170 PAUSE
5180 PRINT CHR$(12)
5190 CAT ":,700,1"
5200 INPUT "ENTER FILENAME CONTAINING REQUIRED DATA",File#
5210 ASSIGN @File TO File#&":,700,1"
5220 ENTER @File;Title#,No
5230 REDIM Sig(1:No,1:2)
5240 ENTER @File;Sig(*)
5250 ASSIGN @File TO *
5260 SUBEND
5270 !
5280 !*****
5290 List: !
5300 SUB List(Sig(*),INTEGER No,Title#)
5310 INTEGER Entry
5320 PRINT USING "///"
5330 PRINT
5340 PRINT Title#
5350 PRINT
5360 PRINT USING ""CIRCLE",10X,"Sigma a",3X,"Sigma r""
5370 FOR Entry=1 TO No
5380 PRINT USING "DD,14X,S3Z.D,4X,S3Z.D";Entry,Sig(Entry,1),Sig(Entry,2)
5390 NEXT Entry
5400 PRINT USING "///"
5410 SUBEND
5420 !
5430 !
5440 !*****
5450 !
5460 Sqfit: !
5470 SUB Sqfit(Cright,Ctop,INTEGER Num,Device,Title#)
5480 OPTION BASE 1
5490 COM /Env/ C,0,Limitx,Limity,Line,A,B
5500 GRAPHICS OFF
5510 INTEGER I,K
5520 COM Sig(*),Setup
5530 ALLOCATE Sqerr(Num),Theta(Num),Diff(Num)
5540 DEG
5550 PRINT USING "///"
5560 PRINT "POWER CURVE FITTING ROUTINE FOR MOHR'S CIRCLES"
5570 PRINT
5580 PRINT Title#
5590 PRINT
5600 PRINT TAB(3);"A";TAB(18);"b";TAB(25);"Sum of error squares"
5610 Ans#="A"
5620 INPUT "Manual or auto iteration on A,b (M,A, Default A)?",Ans#
5630 Iter=0
5640 IF Ans#="A" THEN Iter=1
5650 Start:INPUT "Enter starting values of A,b",A,B
5660 IF Iter THEN Iter
5670 FOR I=1 TO Num
5680 GOSUB Funct
5690 NEXT I

```

```

5700      GOSUB Print
5710      GOTO Another
5720      !-----
5730      Iter: !
5740      ALLOCATE Fm(2),Fm1(2),Z(Num,2),Der(Num),Zt(2,Num),Zt1(2,2),Zt_inv(2,2),
Z2(2),Z3(2)
5750      Flag=0
5760      Crit=.0001
5770      Fm1(1)=A
5780      Fm1(2)=B
5790      LOOP
5800          Lsum=Sumsq
5810          MAT Fm1= Fm
5820          MAT Z= (0)
5830          MAT Diff= (0)
5840          MAT Der= (0)
5850          MAT Zt= (0)
5860          MAT Zt1= (0)
5870          MAT Zt_inv= (0)
5880          MAT Z2= (0)
5890          MAT Z3= (0)
5900          MAT Theta= (0)
5910          Fm(1)=A
5920          Fm(2)=B
5930          FOR I=1 TO Num                ! FOR EACH CIRCLE
5940              GOSUB Funct
5950              CALL Partial(Fm(*),Sigma-R*SIN(Theta(I)),Der(*))
5960              FOR K=1 TO 2
5970                  Z(I,K)=-Der(K)
5980              NEXT K
5990          NEXT I
6000          IF NOT Flag THEN GOSUB Print
6010          MAT Zt= TRN(Z)
6020          MAT Zt1= Zt*Z
6030          MAT Zt_inv= INV(Zt1)
6040          MAT Z2= Zt*Diff
6050          MAT Z3= Zt_inv*Z2
6060          MAT Pm= Fm+Z3
6070          A=Pm(1)
6080          B=Pm(2)
6090          FOR I=1 TO Num
6100              GOSUB Funct
6110          NEXT I
6120          Flag=1
6130          GOSUB Print
6140          EXIT IF ABS(Sumsq-Lsum)<Crit AND ABS(Pm(1)-Fm1(1))<Crit
6150          END LOOP
6160          DEALLOCATE Pm(*),Fm1(*),Z(*),Der(*),Zt(*),Zt1(*),Zt_inv(*),Z2(*),Z3(*)
6170          !
6180          !
6190          GOTO Another
6200      !-----
6210      !
6220      Funct: !
6230          Sigma=(Sig(I,1)+Sig(I,2))/2
6240          Tau=(Sig(I,1)-Sig(I,2))/2
6250          CALL Iterate(A,B,Theta(I),Sigma)                ! EVALUATE THETA
6260                                                    ! EVALUATE FUNCTION
6270          R=(Sigma-(TAN(Theta(I))/(A*B))^(1/(B-1)))/SIN(Theta(I))
6280          Di=(R-Tau)
6290          Diff(I)=Di*COS(Theta(I))
6300          Sqerr(I)=Di^2
6310          Sumsq=SUM(Sqerr)                ! sum of squares of errors for a set of circles
6320          RETURN
6330      !-----
6340      Print: !
6350          PRINT
6360          PRINT USING "Z.5D,7X,Z.5D,6X,5D.5D";A,B,Sumsq
6370          RETURN
6380      !-----
6390      !
6400      Another: Ans$="Y"

```

```

6410 Line=2 ! FOR CURVE
6420 INPUT "Another A and b (Y/N)?",Ans#
6430 IF NOT (Ans#="N") THEN Start
6440 P1: INPUT "Plot curve (Y/N)?",Ans#
6450 IF Ans#="N" THEN SUBEXIT ! ++++++ EXIT
6460 ! ----- PLOT -----
6470 CALL Curve(Cright,Ctop,Device)
6480 SUBEND
6490 !
6500 !
6510 !*****
6520 !
6530 !
6540 SUB Iterate(A,B,Theta,Sigma)
6550 Crit=.001
6560 IF B>.5 THEN
6570 Theta=89
6580 ELSE
6590 Theta=1
6600 END IF
6610 Th2=Theta
6620 REPEAT
6630 Theta=(Theta+2*Th2)/3
6640 F1=A^(1/(1-B))
6650 F2=(TAN(Theta))^(2*B-1)/(B-1)
6660 F3=B^(B/(1-B))
6670 F4=A*B*(Sigma-(F1*F2*F3))^(B-1)
6680 Th2=ATN(F4)
6690 UNTIL ABS(Th2-Theta)<Crit
6700 SUBEND
6710 !
6720 !
6730 !*****
6740 !
6750 ! FOR Y=A*X^b
6760 SUB Partial(P(*),X,Der(*))
6770 Der(1)=X^P(2)
6780 Der(2)=P(1)*X^P(2)*LOG(X)
6790 SUBEND
6800 !
6810 !
6820 !*****
6830 !
6840 !
6850 SUB Edit(Sig(*),INTEGER No,Title$)
6860 INTEGER N
6870 GRAPHICS OFF
6880 M: DISP "CHANGE existing ADD new data, or EXIT?"
6890 ON KEY 0 LABEL "CHANGE" GOTO Ch
6900 ON KEY 2 LABEL "ADD" GOTO Add
6910 ON KEY 4 LABEL "EXIT" GOTO Exit
6920 Wt: GOTO Wt
6930 Ch: OFF KEY
6940 CALL List(Sig(*),No,Title$)
6950 LOOP
6960 In: INPUT "ENTER NUMBER OF CIRCLE TO CHANGE, ZERO TO EXIT",N
6970 EXIT IF N=0
6980 IF N<1 OR N>No THEN
6990 BEEP
7000 GOTO In
7010 END IF
7020 INPUT "ENTER Sigma_a,Sigma_r",Siga,Sigr
7030 PRINT
7040 PRINT "Sig_a=";Siga;TAB(20);"Sig_r=";Sigr
7050 Sig(N,1)=Siga
7060 Sig(N,2)=Sigr
7070 END LOOP
7080 GOTO M
7090 !
7100 Add: OFF KEY
7110 INPUT "HOW MANY CIRCLES TO ADD?",N
7120 IF N+No>50 THEN

```



```

7130      BEEP
7140      DISP "TOTAL 50 CICLES MAX AT PRESENT"
7150      WAIT 2
7160      GOTO Add
7170      END IF
7180      No=No+N
7190      REDIM Sig(1:No,1:2)
7200      PRINT
7210      PRINT "Circle","Sigma_a","Sigma_r"
7220      FOR N=No-N+1 TO No
7230          DISP "CIRCLE ";N;
7240          INPUT ", ENTER Sigma_a,Sigma_r",Siga,Sigr
7250          PRINT N,Siga,Sigr
7260          Sig(N,1)=Siga
7270          Sig(N,2)=Sigr
7280      NEXT N
7290      !
7300 L1: FOR N=1 TO No
7310          Co=1
7320      NEXT N
7330      Sigmax=MAX(Sig(*))
7340      GOTO M
7350      !
7360      !
7370 Exit: SUBEND
7380      !
7390      !
7400 !*****
7410 !
7420 !
7430 SUB Line(Cright,Ctop,INTEGER Device)
7440     COM /Env/ C,Ø,Limitx,Limity,Line,A,B
7450     Line=1
7460     Limitx=Cright
7470     Limity=C+Cright*TAN(Ø)
7480     ALPHA OFF
7490     GRAPHICS ON
7500     IF Device THEN
7510         PEN 0
7520     ELSE
7530         PEN 1
7540     END IF
7550     MOVE 0,C
7560     DRAW Limitx,Limity
7570     GOSUB Lab
7580     IF Device THEN
7590         ALPHA ON
7600         PRINT TABXY(30,4);
7610         PRINT USING ""C'="",2Z.2D,"" kPa"";C
7620         PRINT TAB(30);
7630         PRINT USING ""Ø'="",2Z.2D,"" '"";Ø
7640     ELSE
7650         MOVE Cright*.2,Ctop*.80
7660         LABEL USING ""C'="",2Z.2D,""kPa"";C
7670         LABEL USING ""Ø'="",2Z.2D,"" '"";Ø
7680     END IF
7690     SUBEXIT
7700 Lab: !
7710     CSIZE 3
7720     LORG 2
7730     PEN 1
7740     LDIR 0
7750     RETURN
7760     !
7770 SUBEND
7780     !
7790     !
7800 !*****
7810 !
7820 !
7830 SUB Curve(Cright,Ctop,INTEGER Device)
7840     COM /Env/ C,Ø,Limitx,Limity,Line,A,B

```

```

7850     PEN 2
7860     ALPHA OFF
7870     GRAPHICS ON
7880     Line=2
7890     GOSUB Cur
7900     GOSUB Lab
7910     IF Device THEN
7920         ALPHA ON
7930         PRINT CHR$(12)
7940         IF Addf1 THEN
7950             PRINT TABXY(20,7);
7960             PRINT USING ""T= "",Z.3D,""x^"",Z.3D,10X";A,B
7970         ELSE
7980             PRINT TABXY(20,6);
7990             PRINT USING ""T= "",Z.3D,""x^"",Z.3D,10X";A,B
8000         END IF
8010     ELSE
8020         IF Addf1 THEN
8030             MOVE Cright*.2,Ctop*.60
8040         ELSE
8050             MOVE Cright*.2,Ctop*.7
8060         END IF
8070         LABEL USING ""T= "",Z.3D,""x^"",Z.3D";A,B
8080     END IF
8090     SUBEXIT
8100 Cur:MOVE 0,0
8110     FOR X=0 TO Cright
8120         Y=A*(X^B)
8130         DRAW X,Y
8140     NEXT X
8150     RETURN
8160 Lab:
8170     CSIZE 3
8180     LORG 2
8190     PEN 1
8200     LDIR 0
8210     RETURN
8220 SUBEND
8230     !
8240     !
8250     !*****
8260     !
8270     !
8280 Ss:
8290 SUB Ss(Cright,Ctop,INTEGER No,Device)
8300 COM /Env/ C,0,Limitx,Limity,Line,A,B
8310 COM Sig(*),Setup
8320 INTEGER I
8330 GRAPHICS OFF
8340 FOR I=1 TO No
8350     Sigt=(Sig(I,1)+Sig(I,2))/2
8360     Taut=(Sig(I,1)-Sig(I,2))/2
8370     P=P+Sigt
8380     Q=Q+Taut
8390     T=T+Sigt*Sigt
8400     R=R+Sigt*Taut
8410 NEXT I
8420     F1=No*R-P*Q
8430     F2=(No*T-P*P)^2
8440     F3=(No*R-P*Q)^2
8450     Mu=F1/SQR(F2-F3)
8460     Ø=ATN(Mu)
8470     F4=Q*T-P*R
8480     C=F4/SQR(F2-F3)
8490 FOR I=1 TO No
8500     Sigt=(Sig(I,1)+Sig(I,2))/2
8510     Taut=(Sig(I,1)-Sig(I,2))/2
8520     Error=((C+Mu*Sigt)/SQR(1+Mu*Mu))-Taut
8530     Sumsq=Sumsq+Error*Error
8540 NEXT I
8550 PRINT TAB(3);"C";TAB(18);"Ø";TAB(25);"Sum of error squares"
8560 PRINT USING "/,ZZ.5D,7X,ZZ.5D,6X,5D.5D";C,Ø,Sumsq

```

```
8570     Ans#="Y"  
8580     INPUT "PLOT LINE (Y/N)?",Ans#  
8590     IF Ans#<>"N" AND Ans#<>"Y" THEN 8580  
8600     IF Ans#="N" THEN SUBEXIT  
8610     PRINT CHR$(12)  
8620     CALL Line(Cright,Ctop,Device)  
8630     SUBEND
```

Appendix E

Computer program for slope stability analyses using
a non-linear failure envelope

```

10 !NON-LINEAR FAILURE ENVELOPE : SLOPE ANALYSIS : RIGOROUS METHOD
20 !
30 DIM A(20),B(20),L(20),P(20),U(20),W(20),Alph(20),Delx(20),Dele(20)
40 DIM X(20),Xb(20),Yt(20),Ga(20),S(20),Ht(20),E(20),Sh(20),Th(20)
50 DEG
60 !
70 !*****
80 !
90 !INPUT THE DATA
100 !
110 INPUT "ENTER NUMBER OF SLICES",N
120 PRINT N
130 INPUT "ENTER X COORDINATE OF TOP OF SLOPE (M):",X(0)
140 PRINT X(0)
150 INPUT "ENTER BOTTOM AND TOP Y COORDS.,LEFT SIDE OF TOP SLICE (M):",Yb(
0),Yt(0)
160 PRINT Yb(0),Yt(0)
170 INPUT "ENTER WATER TABLE LEVEL AT TOP OF SLOPE (M):",Yw(0)
180 PRINT Yw(0)
190 PRINT "ENTER DATA FOR EACH SLICE:"
200 GOSUB 1230
210 FOR I=1 TO N
220 GOSUB 1260
230 NEXT I
240 !
250 !*****
260 !
270 !CALCULATE DERIVED QUANTITIES
280 !
290 FOR I=1 TO N
300 P(I)=ATN((Yb(I)-Yb(I-1))/(X(I-1)-X(I)))
310 L(I)=SQR(((Yb(I)-Yb(I-1))^2)+(X(I)-X(I-1))^2))
320 U(I)=9.81*.5*(Yw(I)+Yw(I-1)-Yb(I)-Yb(I-1))
330 IF U(I)<0 THEN U(I)=0
340 W(I)=Ga(I)*(X(I)-X(I-1))*0.5*(Yt(I)+Yt(I-1)-Yb(I)-Yb(I-1))
350 Th(I)=X(I)-X(I-1)
360 NEXT I
370 !
380 !*****
390 !
400 !CALCULATE FACTOR OF SAFETY,INITIAL GUESS 1.0
410 !
420 Fb=1.0
430 Fa=1.0
440 F=1.0
450 T=0
460 R=0
470 FOR I=1 TO N
480 S(I)=Ga(I)*0.5*(Yt(I)+Yt(I-1)-Yb(I)-Yb(I-1))*((COS(P(I)))^2)-U(I)
490 G=S(I)^B(I)*A(I)*TAN(P(I))/F
500 T=T+((W(I)/(L(I)*COS(P(I)))-U(I)-G)^(B(I))*A(I)*L(I)*(1/COS(P(I))))
510 R=R+W(I)*TAN(P(I))
520 NEXT I
530 F1=F
540 F=T/R
550 IF ABS(F1/F-1)>.0001 THEN 450
560 Delx(I)=0
570 IF Delx(I)=0 THEN 810
580 !
590 !*****
600 !
610 ! CALCULATE INTERSLICE FORCES
620 !
630 Fb=F
640 FOR I=1 TO N
650 Dele(I)=((W(I)-Delx(I))*TAN(P(I)))-((S(I)^B(I))*A(I)*L(I))/(Fb*COS(P
(I)))

```

```

660     NEXT I
670     FOR I=1 TO N
680         E(0)=0
690         E(I)=E(I-1)+Dale(I)
700     NEXT I
710     FOR I=1 TO N
720         Sh(I)=(E(I)*TAN(Alph(I)))-((Ht(I)*Dele(I))/Th(I))
730     NEXT I
740     FOR I=1 TO N
750         Sh(0)=0
760         Delx(I)=Sh(I)-Sh(I-1)
770     NEXT I
780     !
790     !*****
800     !
810     Fa=F
820     FOR I=1 TO N
830         Sa(I)=S(I)
840     NEXT I
850     !
860     FOR I=1 TO N
870         S(I)=Ga(I)*.5*(Yt(I)+Yt(I-1)-Yb(I)-Yb(I-1))*((COS(F(I)))^2)-U(I)
880         G=(S(I)^B(I)*(A(I))*TAN(F(I)))/F
890         H=Delx(I)/(L(I)*COS(F(I)))
900         Sl(I)=S(I)
910         S(I)=(W(I)/(L(I)*COS(F(I))))-U(I)-G-H
920         IF ABS(Sl(I)/S(I)-1)>.001 THEN 880
930     NEXT I
940     GOTO 1330
950     !
960     !*****
970     !
980     PRINT "FACTOR OF SAFETY (JANBU RIGOROUS METHOD) IS",F
990     !
1000    !*****
1010    !
1020    !OPTIONS ON CHANGING DATA
1030    !
1040    PRINT "ENTER -2 TO CHANGE POSITION OF SLIP SURFACE"
1050    PRINT "      -1 TO CALCULATE FACTOR OF SAFETY"
1060    PRINT "      0 TO EXIT"
1070    PRINT "      1..N TO CHANGE DATA FOR A SLICE (GIVE SLICE NUMBER)"
1080    INPUT I
1090    IF I=0 THEN STOP
1100    IF I=-1 THEN 290
1110    IF I=-2 THEN 1150
1120    GOSUB 1230
1130    GOSUB 1260
1140    GOTO 1040
1150    PRINT "ENTER NEW YB COORDINATES ALONG SLIP SURFACE"
1160    FOR I=0 TO N
1170        INPUT Yb(I)
1180    NEXT I
1190    GOTO 290
1200    !
1210    !*****
1220    !
1230    PRINT "ENTER      A,B,GAMMA,X,YB,YT,YW,ALPH,HT"
1240    PRINT "ENTER      , ,KN/M3,M, M, M, M,DEG ,M"
1250    RETURN
1260    PRINT "SLICE NUMBER",I
1270    INPUT A(I),B(I),Ga(I),X(I),Yb(I),Yt(I),Yw(I),Alph(I),Ht(I)
1280    PRINT A(I),B(I),Ga(I),X(I),Yb(I),Yt(I),Yw(I),Alph(I),Ht(I)
1290    RETURN
1300    !
1310    !*****
1320    !
1330    T=0
1340    R=0
1350    FOR I=1 TO N
1360        G=S(I)^B(I)*(A(I))*TAN(P(I))/F
1370        T=T+((W(I)/(L(I)*COS(F(I))))-U(I)-G-(Delx(I)/(L(I)*COS(F(I)))))^B(I)

```

```

)) *A(I) *L(I) * (1/COS(P(I)))
1380      R=R+(W(I)-Delk(I))*TAN(P(I))
1390      NEXT I
1400      F1=F
1410      F=T/R
1420      Test=0
1430      FOR I=1 TO N
1440          IF (ABS(F/Fb-1)<.0001) AND (ABS(Sa(I)/S(I)-1)<.001) THEN Test=Test+
1
1450      NEXT I
1460      IF Test=N THEN 980
1470      IF ABS(F1/F-1)>.0001 THEN 1330
1480      IF ABS(F/Fa-1)<.0001 THEN 600
1490      IF ABS(F/Fa-1)>.0001 THEN 810
1500      RETURN
1510      END
1520 !*****

```

